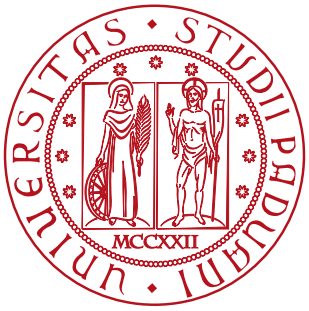

UNIVERSITÀ DEGLI STUDI DI PADOVA

DIPARTIMENTO DI FISICA E ASTRONOMIA "GALILEO GALILEI"

Corso di Laurea Magistrale in Fisica

TESI DI LAUREA MAGISTRALE

Probing gravity at the energy scale of inflation via primordial non-Gaussianity

Laureando

Domenico Matteo Bianco

Relatore

Prof. Nicola Bartolo

Co-relatore

Prof. Sabino Matarrese

Anno Accademico 2015-2016

Abstract

In this thesis, we review the standard inflationary paradigm and study some inflationary models among the so-called α-attractors. These models arise in the context of supergravity theories and they are related to Starobinsky inflationary model which was developed within a modified theory of gravity. Since their birth in 2013, they have experienced an increasingly interest among cosmologists thanks to the latest *Planck* satellite's results.

Our main concern is the study of the inflationary dynamics and observational predictions, such as primordial non-Gaussianity, of some α-attractor models. First, we focus on single-field models. We study the predictions of the α-attractors and the reasons underneath their universal behaviour. In particular, we analyse the acceptable initial conditions that lead to an inflationary era for the so-called T-models. Secondly, we focus on two-field α-attractor models. We analyse their background dynamics and their predictions, especially for what concern mechanisms that can produce large non-Gaussianities. We will make use of the *in-in* formalism and the δN formalism to compute the primordial non-Gaussianities.

We show that, in some of the models analysed, a relevant level of primordial non-Gaussianities can be produced via different mechanisms. For the two-field models, it can be generated thanks to the non-canonical kinetic term of one of the fields, to interactions between the fields described by the potential or to the α parameter in the Lagrangian of α-attractors.

To my parents

Contents

Introduction

Our thirst for knowledge and comprehension of Nature is as ancient as humanity. Since the first man has wondered about physical phenomena, the flux of questions and answers has never arrested. Even if humankind has stared at the sky for thousands of years, only recently cosmology has become a quantitative and predictive branch of science and has entered into a high precision era. The fundamental revolutions in this field were Heliocentrism (Nicolaus Copernicus, Johannes Kepler and Galileo Galilei, 16^{th}-17^{th} centuries), general relativity (Albert Einstein, 1915), the expansion of the Universe (Georges Lemaître and Edwin Hubble, 1927), the discovery of the Cosmic Microwave Background (Arno Penzias and Robert Wilson, 1964), the theory of inflation (Guth, 1981) and the ΛCDM model (late 90s). All these are milestones along our search for answers about the Universe.

Before the twentieth century, our knowledge of the Universe was very limited. Many theories were proposed during the centuries, but they were mainly speculations and were not based on precise measurements. Some beliefs withstood during the epochs thanks to the *ipse dixit*. There are some emblematic examples of this antiscientific prejudice, here we mention only the Geocentric model (two thousand years) and the Steady State theory (supported by Einstein for a period). However, nowadays cosmology is an observationally well-supported and predictive science. Our understanding of the Universe is on the right road and more precise measurements will be able to confirm or falsify the currently accepted ΛCDM model.

One of the main elements of the ΛCDM model is the theory of cosmological inflation. Inflation is a period of accelerated expansion in the early history of the Universe. It explains why our Universe looks the same in every direction and for every observer. In addition to this, it gives the proper initial conditions for the subsequent evolution of the Universe. In particular, it produced the small density fluctuations that became galaxies and clusters of galaxies, namely the largest structures of our Universe, and that gave rise to the temperature anisotropies and polarization of the Cosmic Microwave Background. Without inflation, some questions would be very difficult (if not impossible) to answer, as we will see. Although many properties of the inflationary mechanism are unknown, it is nonetheless the observationally best supported theory.

Cosmological inflation is the main subject of this thesis. In particular, in this work we will study some recently proposed models of inflation: α-attractors. These models arise in the context of supergravity theories and posses some peculiar properties that make them very interesting among all the possible inflationary mechanisms. Let us mention only one of these properties. These models are named α-attractors because they have a parameter α that affects their predictions. In a certain sense, they can parametrize the predictions of other inflationary models. Furthermore, the predictions of α-attractors are in perfect agreement with observations.

On the other hand, there are many different models of inflation and only a part of them has been ruled out by observations. Therefore, it is of fundamental importance to find measurable quantities capable to discern among them (for example, primordial non-Gaussianities).

In this thesis, we will review some textbook notions about modern cosmology and the standard theory of inflation. In particular, we will analyse in detail some models with one or two scalar fields driving the accelerated expansion of the early Universe. Their study will be usually split into three steps. First, we will study the background dynamics of the fields with special regard for initial conditions leading to an inflationary epoch. After this, we will focus on small perturbations with respect to the background. The second step concerns the analysis of the power spectrum, i.e. the two-point correlation function. Finally, we will examine the bispectrum, i.e. the three-point correlation function. The importance of bispectrum have significantly increased during the last ten years, since the era of precision measurements of the Cosmic Microwave Background begun. In the following, we will describe why the bispectrum is one of the most appropriate probes to distinguish among different inflationary theories.

We will try to generate large, i.e. observable, non-Gaussianities in the studied inflationary models. We will show that, in some of the two-field models, a relevant level of primordial non-Gaussianities can be produced via different mechanisms. Indeed, it can be generated thanks to the non-canonical kinetic term of one of the fields, to interactions between the fields or to the α parameter in the Lagrangian of α-attractors.

Outline of the thesis

The following is the road map of the thesis.

- Chapter 1 contains basic material about inflation which will be useful for the following discussion. We discuss the importance of inflation in modern cosmology and its merits. We describe the simplest mechanism that relies on a single scalar field and study some examples.

- In chapter 2, we review the theory of cosmological perturbations. We describe what is a gauge transformation for cosmological perturbations and how the latter change according to different gauge choices. We perturb the metric tensor and the energy-momentum tensor and describe the Scalar-Vector-Tensor decomposition. We report the perturbed Einstein equations and the perturbed equations that follow from the continuity equation for the energy momentum tensor. Finally, we define some gauge-invariant quantities frequently used in cosmology.

- In chapter 3, we define non-Gaussianities of cosmological perturbations and explain how to characterize their properties. Then, we introduce the concept of bispectrum (i.e. the Fourier counterpart of the three-point correlation function) and two techniques developed for its computation, the *in-in* formalism and the δN formalism. Finally, we explain why cosmologists are currently so interested in non-Gaussianities.

- Chapter 4 describes one of the possible generalization of the standard inflationary mechanism. We consider an inflationary period driven by two scalar fields with a generic field space metric. In particular, we present the mathematical formalism best suited for this generalization.

- In chapter 5, we introduce the reader to α-attractor models of inflation. These models were discovered a few years ago but they have become very popular after the release of *Planck* satellite results in 2013. We describe how these models arise from a broken conformal symmetry and study in detail the dynamics and initial conditions for a single-field model. Finally, we discuss the generalization of these models to the multifield case. In particular, we will focus on the two-field models that will be studied in the following chapters.

- Chapter 6 contains expressions useful for calculating cosmological correlators. We will analyse the two-point and three-point correlation functions of the inflationary perturbations and their lowest order contributions in the *in-in* expansion.

- In chapter 7, we apply all the machinery and techniques developed in the previous chapters. We study the background dynamics of the two-field α-attractor model introduced in chapter 5. We derive the Hamiltonian from the Lagrangian of this system, perturb the equation of motion and solve the equations for the free mode functions. To sum up, we get ready to apply the *in-in* formalism. In the last sections, we study two simple but instructive trajectories.

- In chapter 8, we study two other examples of the two-field aforementioned model with more complex potential terms than that considered in the previous chapter. We study extensively the background dynamics. Then, we approach the computations of non-Gaussianities using the *in-in* formalism. Finally, we apply the δN formalism to study the non-Gaussianities produced by one of these models.

Notation

Planck mass is defined as

$$m_{Pl}^2 = \frac{\hbar c}{G}\,,$$

where G stands for Newton gravitational constant, and the reduced Planck mass as

$$M_{Pl}^2 = \frac{\hbar c}{8\pi G}\,.$$

Our metric signature is $(-1,+1,+1,+1)$. Let $g_{\mu\nu}$ denote the metric and g its determinant. We denote covariant derivatives with ∇_μ or ";" and partial derivatives with ∂_μ or ",". We adopt the Einstein convention so that repeated indices are implicitly summed over. Greek letters as indices take values among $\{0,1,2,3\}$ and lowercase Latin letters are reserved for spatial indices $\{1,2,3\}$. We use the same symbol for the norm of a vector and for that of a four-vector, $k^2 = k^\mu k_\mu$

and $k^2 = k^i k_i$, but there is no real possibility to misunderstand an equation. We denote vectors with boldface.

In this thesis, if not stated differently, we usually adopt natural units

$$\hbar \equiv c \equiv 1\,,$$

and in some chapters we will also set $M_{Pl} \equiv 1$.

Chapter 1

The inflationary paradigm

"Invest in inflation. It's the only thing going up."

Will Rogers

In this chapter we will review the classical inflationary mechanism which relies on a single scalar field that drives an exponential expansion of the Universe at very early times (before primordial nucleosynthesis). Many cosmology books discuss this topic in a pedagogical way, we cite Liddle and Lyth's *Cosmological inflation and large-scale structure* [1] because our treatment follows the authors' approach which is focused on the generation of cosmological perturbations. Another classical book is Kolb and Turner's *The early universe* [2]. Finally, we mention the review written by A.R. Liddle [3] and the one by D. Langlois [4].

In section 1.1, we will review the state of the art of modern cosmology. We will describe the currently accepted model of our Universe and understand the reasons behind the introduction of the theory of inflation. In section 1.2, we will remember some basic ideas of modern cosmology, in particular the Friedmann-Robertson-Walker solution. In section 1.3, we will describe the inflationary mechanism and derive the necessary conditions for an accelerated expansion. Furthermore, we will review the standard inflationary model with a single scalar field driving inflation. In section 1.4, we will introduce some concepts useful to describe the casual structure of spacetime and the definition of efolding. The following sections 1.5 and 1.6 are focused on cosmological perturbations originated during inflation. In particular, we will see how inflation seeds the formation of structures in the universe and what are the statistical properties of these fluctuations. In section 1.7, we will discuss how gravitational waves are produced during inflation and their observable predictions. Finally, in the last section 1.8, some examples of inflationary mechanisms will be explored.

1.1 A glimpse into modern cosmology

Cosmology is as old as humankind, but it has become a high precision science from an observational point of view only in the last decades. The current standard theory of our Universe is the so-called ΛCDM model. Although its youth (it was born only in the second part of the

Parameter	Value	Definition
H_0	$67.27 \pm 0.66\ \mathrm{km\,s^{-1}\,Mpc^{-1}}$	Current expansion rate (1.8b)
$\Omega_b h^2$	0.02225 ± 0.00016	Relative baryon density
$\Omega_c h^2$	0.1198 ± 0.0015	Relative dark matter density
Ω_m	0.3156 ± 0.0091	Relative matter density
Ω_K	0.0008 ± 0.0040	Curvature parameter
$\sum m_\nu$	< 0.194 eV	Sum of neutrino masses
w	$-1.019^{+0.075}_{-0.080}$	Dark energy equation of state (1.11)
n_s	0.9645 ± 0.0049	Scalar spectral index (1.75)
$r_{0.002}$	< 0.10	Tensor-to-scalar ratio (1.93)
$dn_s/d\ln k$	-0.002 ± 0.013	Running of scalar spectral index (1.78)
$\ln(10^{10} A_s)$	3.094 ± 0.034	Scalar power spectrum amplitude (1.75)

Table 1.1: Main cosmological parameters. If the units of measure are not given, the parameter is dimensionless. In particular, "primordial" (inflationary) cosmological parameters n_s, $dn_s/d\ln k$ and $\ln(10^{10} A_s)$ are all measured at the pivot scale $k_0 = 0.05\ \mathrm{Mpc}^{-1}$; $r_{0.002}$ is measured at $k = 0.002\ \mathrm{Mpc}^{-1}$. The dimensionless parameter h is defined such as $H_0 = 100h\,\mathrm{km\,s^{-1}\,Mpc^{-1}}$. All relative densities are evaluated today. All values are latest 2015 *Planck* results [5, 6].

nineties), it is extremely predictive, observationally robust and sufficiently explanatory. It has been tested with increasing accuracy for twenty years and nowadays it can be considered our best effort to describe the Universe.

The ΛCDM model assumes that General Relativity describes gravity on very large scales and it can explain the present state of the Universe and the evolution that led to this. In particular, it describes the expansion of the Universe discovered by E. Hubble in 1929. It predicts the relative primordial abundances of the elements. It describes how the largest structures observed in the Universe, such as galaxies and clusters of galaxies, were born and their growth. To make a long story short, it describes 13.8 billion years of history apart for a tiny fraction of a second.

The model assumes that the Universe is made of baryons (i.e. ordinary matter as protons and electrons), photons, neutrinos, dark matter and dark energy. Indeed, CDM stands for cold dark matter. Dark matter is an important ingredient because it affects the growth and evolution of structures in the Universe. Dark matter is dark because it does not interact electromagnetically with baryons and hence it can be observed only indirectly through its gravitational effects. Dark energy acts like a cosmological constant Λ driving the accelerated expansion of the Universe at the present epoch. We do not know what dark energy is and thus we call it dark. Since the Universe expands, the densities of its components are diluted over time. Nowadays, the mass of our Universe consists of 4% hydrogen and helium, 0.5% neutrinos, 25% dark matter and 70% dark energy. The most important parameters of the ΛCDM theory are reported in table 1.1.

Inflation is a significant element of the standard cosmological model. Inflation is a period of accelerated expansion in the early history of the Universe. Indeed, it is the oldest period

we know (or think we know) about. Inflation is thought to have started 10^{-36} s after the Big Bang and have ended at about 10^{-33} s. In this infinitesimal time, the Universe grew by a factor of 10^{27}, at least[1]. This expansion affected the subsequent evolution of the Universe since it provided de facto its initial conditions, as we will explain extensively below.

Thanks to its elegance and simplicity, the theory of inflation rapidly became very attractive for cosmologists. One of the first proposals for inflation is the one by Alan Guth in 1981 [7] in order to solve some long-standing problems [8–13] that afflicted the Hot Big Bang theory, e.g. the so-called horizon (or homogeneity), flatness, smoothness and monopole problems. Through inflation, the Universe becomes naturally flat, homogeneous and isotropic, just as we observe it today.

During the seventies, cosmologists were worried about the singularity of our Universe. Among all the possible universes compatible with the Laws of Physics, our universe is nearly flat, homogeneous and isotropic on large scales. In addition to this, moving back in time, our Universe should have been indistinguishable from a flat one. The flatness problem can be solved assuming that the initial curvature was precisely null. Similarly, in order to solve the horizon problem, one should imagine at least a million causally disconnected patches that started their evolution exactly in the same physical conditions, in particular at the same temperature. Postulating all this is possible, but, without any physical principle underlying these symmetries, it is hardly attractive. Therefore the particular initial conditions chosen by our Universe appeared extremely unlikely. Physicists have learned (over the centuries) that invoking fine-tuning is as easy as misleading. Inflation can solve the aforementioned issues through a dynamical mechanism. For this reason, inflation soon became very popular, even if it was affected by its own problems. Later on, many different mechanisms were proposed and the basic theory was modified and refined.

Over the course of the years the importance of inflation for cosmologists has increased even more because it also provides a theory for large scale structure formation starting from quantum fluctuations. Nowadays this is the most important property of inflation and studying large scale structure is a way to test inflation. After all, inflation provided the initial conditions of our Universe and influenced all its evolution in spite of the inflationary shortness. Thanks to inflation, very small scales are stretched to such very large ones that they leave the quantum realm and reach the classical reign of General Relativity. Thus, observing the structure of the Universe, one is staring at the consequences of true quantum phenomena. In addition to this, inflation produces ripples in the spacetime fabric. The latter are the so-called primordial gravitational waves and they constitute an active area of research.

Nowadays all observational data supports the theory of inflation (e.g., see [5, 6, 14]), but its development is not over. During the years, the experimental constraints on inflation have became more tight allowing cosmologists to restrict the number of realistic models (see, e.g., figure 1.2).

Finally, let us briefly remember that alternatives to inflation exist. In recent years, many

[1] As if a bacterium (10^{-6} m) became as big as a galaxy (10^{21} m).

attempts were made but, until now, inflation is the most promising, theoretically robust and observationally supported scenario even if many questions remain unanswered. The most famous alternative is the ekpyrotic scenario. We refer to [15] (and references therein) for an introduction to these theories.

Currently, many aspects of the ΛCDM model constitute active areas of research. More accurate observations and more stringent constraints are obtained from year to year, and they will possibly detect deviations from the standard model. Here we cite only two of the biggest open questions about ΛCDM. Nowadays, dark matter and dark energy are puzzling cosmologists. They know some of their properties but they cannot say what they really are. Secondly, even if inflation is a well established theory, we have had no direct evidence of its existence until now and we do not know the underlying particle physics theory. However, we do know that the ΛCDM model (including inflationary initial conditions) works very well.

1.2 The Friedmann-Robertson-Walker Universe

On large scales (greater than 100 Mpc) our Universe is homogeneous and isotropic with very good approximation. This experimental fact is in accordance with the so-called Cosmological Principle: our Universe looks the same in all directions for all (comoving) observes on large scales. This observation leads to a simplification of the Einstein equations which describe how matter and spacetime geometry interact and eventually the evolution of the Universe.

Einstein field equations can be written in the form

$$R_{\mu\nu} - \frac{1}{2} g_{\mu\nu} R = 8\pi G\, T_{\mu\nu} - g_{\mu\nu}\Lambda\,, \tag{1.1}$$

where $g_{\mu\nu}$ is the metric of spacetime, $R_{\mu\nu}$ is the Ricci tensor, R is the Ricci scalar, $T_{\mu\nu}$ is the energy-momentum tensor and Λ is a constant (the so-called *cosmological constant*). These are 10 coupled non-linear second order partial differential equations. As such, they are very difficult to solve in general, and only a few analytical solutions are known. Einstein equations can be derived by varying the Einstein-Hilbert action

$$S_{\mathrm{HE}} = \frac{1}{8\pi G} \int d^4x \sqrt{-g} \left(\frac{R}{2} - \Lambda \right), \tag{1.2}$$

with respect to the tensor metric $g_{\mu\nu}$. On one hand, given the matter-energy content and proper initial or boundary conditions, Einstein equations can be solved for the metric $g_{\mu\nu}$. On the other hand, if one gives an ansatz for the metric, Einstein equations can be solved for the matter components. In the following we will assume that there exists only one matter component, the extension to many components being trivial. In addition, we assume that any component that constitutes the Universe is a perfect fluid and hence its energy-momentum tensor is given by

$$T_{\mu\nu} = (\rho + P) u_\mu u_\nu + P g_{\mu\nu}\,, \tag{1.3}$$

where u_μ is the four-velocity of the fluid, ρ is its energy density and P is its pressure.

In a Friedmann-Robertson-Walker (FRW) universe the spatial metric is homogeneous and isotropic (i.e. is maximally symmetric). Its line element may be written in comoving polar coordinates as

$$ds^2 = -dt^2 + a^2(t)\left(\frac{dr^2}{1-Kr^2} + r^2\left(d\theta^2 + \sin^2\theta d\phi^2\right)\right), \tag{1.4}$$

where $a(t)$ is the scale factor and $K = \{-1, 0, +1\}$ is the spatial curvature of the universe. Consider an observer at rest at a fixed point (t, r, θ, ϕ). This observer will remain always at rest regardless of the expansion of the Universe. Such an observer is called *comoving* observer. Physical distances are given by $\mathbf{x} = a(t)\mathbf{r}$. Hence, the physical separation between comoving particles scales as $a(t)$ and their momenta scale, or redshift, as a^{-1}. A photon emitted by a distant source suffers a redshift

$$1 + z = \frac{a_0}{a(t)}\,, \tag{1.5}$$

where a_0 is the scale factor at the moment of observation and $a(t)$ that at the time of emission. The Cosmic Microwave Background was emitted at $z \simeq 1100$, i.e. when the Universe was 1100 times smaller.

The flat FRW metric is given by

$$ds^2 = -dt^2 + a^2(t)\delta_{ij}dx^i dx^j = a^2(\tau)\left(-d\tau^2 + \delta_{ij}dx^i dx^j\right), \tag{1.6}$$

where in the second line we have used the definition of conformal time

$$d\tau = \frac{dt}{a(t)}\,. \tag{1.7}$$

Some useful formulas relating cosmic time t to conformal time τ are reported in appendix A. We always assume that the universe is flat (except in equation (1.8)) for reasons that will be explained in section 1.3. Notice that this metric looks like Minkowski one except for the scale factor that describes the expansion of the universe (see appendix B about conformal transformations).

The so-called Friedmann equations (for a homogeneous and isotropic universe) follow directly from Einstein equations and are usually written in the form

$$\frac{\ddot{a}}{a} = -\frac{4\pi G}{3}(\rho + 3P)\,, \tag{1.8a}$$

$$H^2 = \frac{8\pi G}{3}\rho - \frac{K}{a^2}\,, \tag{1.8b}$$

where the expansion rate H is defined as

$$H \equiv \frac{\dot{a}}{a}\,. \tag{1.9}$$

Often, it is useful the continuity equation

$$\dot{\rho} + 3H(\rho + P) = 0\,, \tag{1.10}$$

that follows from the continuity equation for the energy-momentum tensor $\nabla^\mu T_{\mu\nu} = 0$. Equations (1.8) and (1.10) describe the background evolution of a single-component universe. Notice

that we have said "background", that means that we are assuming homogeneity and isotropy. The former equations are not independent (only two of them are) and contain the three unknowns $a(t)$, $\rho(t)$ and $P(t)$, so we should supplement them with another one. It is customary to introduce an equation of state

$$P = w\rho, \tag{1.11}$$

where w is a constant dependent on the type of fluid studied (occasionally more complex equations can be considered). For non-relativistic matter, called dust or simply matter, $w = 0$; for radiation or relativistic matter $w = 1/3$; for a cosmological constant $w = -1$.

If the expansion of a single-component universe is accelerated $\ddot{a} > 0$, then it is simple to prove from equation (1.8a) that $w < -1/3$ for this component. Inflation is a period of accelerated expansion and then it is necessary to find a component with $w < -1/3$. In section 1.3, we will see that a scalar field can drive inflation.

Solving Friedmann equations for a single component of the universe, it is possible to obtain the relation

$$\rho \propto a^{-3(1+w)}. \tag{1.12}$$

Note that ρ is constant for a cosmological constant ($w = -1$). Therefore, its energy density does not decrease due to the expansion of the universe.

1.2.1 The de Sitter universe

The de Sitter universe has no matter or radiation content but has a positive cosmological constant driving its expansion. For a cosmological constant Λ, the equation of state (1.11) reads

$$\rho_\Lambda = \frac{\Lambda}{8\pi G} = -P_\Lambda\,, \tag{1.13}$$

and from the Friedmann equations (1.8) it is straightforward to derive

$$H^2 = \frac{\Lambda}{3}\,, \tag{1.14a}$$

$$a(t) \propto e^{Ht}. \tag{1.14b}$$

The energy-momentum tensor for a cosmological constant is $T^\Lambda_{\mu\nu} = -\Lambda g_{\mu\nu}$. On the other hand, it can be shown that the expectation value on the vacuum state of the energy-momentum tensor of some matter field is given by $\langle 0|\, T_{\mu\nu}\, |0\rangle = -\langle\rho\rangle\, g_{\mu\nu}$, so that the cosmological constant can be interpreted as the vacuum energy.

It is worth underlining the properties of the de Sitter universe. First, the expansion is exponential and the expansion rate H is constant. Secondly, expansion is driven by the vacuum energy associated to the cosmological constant that possesses negative pressure. Finally, the cosmological constant is the only component of this universe. Similar conditions to these should be guaranteed in order to sustain an inflationary period, as we are going to explain in section 1.3.

1.3 Single-field inflation

We have just pointed out that we need a component with negative pressure to obtain inflation, and specifically with equation of state $w < -1/3$ (see equation (1.8a)). Under some assumptions, a scalar field can drive the accelerated expansion in the early universe (such a scalar field is usually called *inflaton*). In principle, vector or tensor fields are possible candidates, but there are some subtleties because they fix a preferred direction in space. Nevertheless, a scalar field is the simplest choice. In addition to this, scalar field models are sufficiently predictive and consistent with observations, so they constitute a natural starting point.

A scalar field $\varphi(t, \mathbf{x})$ is described through the Lagrangian density

$$\mathcal{L} = -\frac{1}{2} g^{\mu\nu} \varphi_{,\mu} \varphi_{,\nu} - V(\varphi), \tag{1.15}$$

where $V(\varphi)$ is the potential associated to φ and usually contains a quadratic term in φ (the mass term). It is convenient to split the field into two parts

$$\varphi(t, \mathbf{x}) = \varphi_0(t) + \delta\varphi(t, \mathbf{x}), \tag{1.16}$$

where $\varphi_0(t)$ is the vacuum expectation value and it represents the classical solution on FRW universe and $\delta\varphi(t, \mathbf{x})$ is the perturbation of the field with respect to it. Note that $\varphi_0(t)$ depends only on time due to isotropy and homogeneity. The dynamics of the field is dominated by that of the background field since perturbations are assumed small.

The energy-momentum tensor for φ is [16]

$$T_{\mu\nu} = \varphi_{,\mu} \varphi_{,\nu} - \frac{1}{2} g_{\mu\nu} \varphi_{,\alpha} \varphi^{,\alpha} - g_{\mu\nu} V(\varphi). \tag{1.17}$$

Its energy density and pressure are respectively given by

$$\rho_\varphi = \frac{1}{2}\dot{\varphi}^2 + V(\varphi), \tag{1.18}$$

$$P_\varphi = \frac{1}{2}\dot{\varphi}^2 - V(\varphi). \tag{1.19}$$

More details about the energy-momentum tensor of a scalar field will be given in section 2.4.1.

As we said, inflation is a period of accelerated expansion in the early history of Universe. Therefore, it is characterized by

$$\ddot{a} > 0, \tag{1.20}$$

or equivalently by $w < -1/3$. A scalar field can be the inflaton if

$$\frac{1}{2}\dot{\varphi}^2 \ll V(\varphi), \tag{1.21}$$

so that $P_\varphi \simeq -\rho_\varphi$ and the expansion is nearly de Sitter. In order to satisfy the previous condition the potential $V(\varphi)$ should be sufficiently flat so that the velocity $\dot{\varphi}$ remains small; large deviations from flatness could lead inflation to an early end. The previous requirement belongs to the so-called *slow-roll* conditions, which ensure that inflation lasts for a sufficiently

long time. If inflation starts, all components different from the inflaton will become negligible in a few expansion time. In fact, equation (1.12) implies that the energy density of a component with $w \neq -1$ will be exponentially suppressed during inflation. Notice that the same reasoning applies for a non-zero primordial curvature of the universe since it is suppressed by a^{-2} into Friedmann equation (1.8b). This behaviour of inflation is very important since it allows us to neglect all the other components and to focus only on the dynamics of the inflaton. In the slow-roll approximation, equation (1.21) becomes

$$H^2 = \frac{8\pi G}{3} V(\varphi_0), \tag{1.22}$$

where we have neglected the curvature term due to the previous considerations.

The Euler-Lagrange equation associated to Lagrangian (1.15) reads

$$\ddot{\varphi} + 3H\dot{\varphi} - \frac{1}{a^2}\nabla^2\varphi = -\frac{dV}{d\varphi}\,, \tag{1.23}$$

that is the equation of motion for the field φ. From this, it is trivial to obtain the equation of motion for the background field

$$\ddot{\varphi}_0 + 3H\dot{\varphi}_0 = -\frac{dV}{d\varphi}(\varphi_0)\,. \tag{1.24}$$

Note that the term $3H\dot{\varphi}$ is a friction term due to the expansion of the universe. Since inflation should last for a sufficiently long period (see the following section), the potential should be sufficiently flat, i.e. $V' \ll V$ and $V'' \ll V$. The slow-roll condition (1.21) implies that $V' \ll V$. Thanks to this, the asymptotic solution of equation (1.24) is given by

$$\dot{\varphi} \simeq -\frac{V'(\varphi_0)}{3H}\,. \tag{1.25}$$

Differentiating the previous equation with respect to time, we obtain

$$\ddot{\varphi} \simeq -\frac{V''(\varphi_0)\dot{\varphi}}{3H}\,. \tag{1.26}$$

Using the flatness condition $V'' \ll V$ and equation (1.22), we obtain the constraint $\ddot{\varphi}_0 \ll V'$. Finally, the equations which describe inflation, in the slow-roll approximation, read

$$3H\dot{\varphi}_0 = -V'(\varphi_0), \tag{1.27a}$$

$$H^2 = \frac{8\pi G}{3} V(\varphi_0)\,. \tag{1.27b}$$

Notice that we have reduced a second order differential equation (1.24) to a first order one thanks to the slow-roll condition (1.21). This reduction is fundamental to obtain an attractor behaviour, namely that a wide range of initial conditions leads to the same inflationary dynamics and predictions. The existence of attractor solutions is an ingenious desirable way to avoid fine-tuning. The previous equations hold also for φ if we neglect small scales (and hence the Laplacian term in (1.23) is negligible).

Now we are going to introduce two slow-roll parameters. The first one is

$$\varepsilon \equiv -\frac{\dot{H}}{H^2} \simeq \frac{1}{16\pi G}\left(\frac{V'}{V}\right)^2, \tag{1.28}$$

and the second one is

$$\eta \equiv \frac{1}{3}\frac{V''}{H^2} \simeq \frac{1}{8\pi G}\frac{V''}{V}, \tag{1.29}$$

where the approximated equalities are valid in the slow-roll limit. Slow-roll conditions are satisfied if $\varepsilon \ll 1$ and $|\eta| \ll 1$. The former conditions make clear what flat potential means: the flatness is measured with respect to the height of the potential.

Inflation occurs if and only if $\varepsilon < 1$ and it ends at $\varepsilon = 1$. Indeed,

$$\frac{\ddot{a}}{a} = H^2 + \dot{H} = H^2(1-\varepsilon), \tag{1.30}$$

where we have used the definitions of H and ε. Therefore, $\ddot{a} > 0$ implies that $\varepsilon < 1$. Substituting equation (1.8a) into the previous one, we obtain

$$\dot{H} = -4\pi G\dot{\varphi}_0^2. \tag{1.31}$$

Hence, the slow-roll parameter ε (1.28) can be rewritten as

$$\varepsilon \simeq \frac{3}{2}\frac{\dot{\varphi}_0^2}{V}, \tag{1.32}$$

i.e. the ratio between the kinetic and the potential energy of the field φ.

The inflaton field rolls slowly down the potential towards a minimum. As we have seen, inflation ends when slow-roll conditions are no more satisfied and this usually happens before inflaton reaches the minimum. Typically, inflaton oscillates around the minimum decaying into particles [17–20]. This phase is known as *reheating* since the resulting particles thermalize and reheat the universe, thereby commencing the radiation dominated epoch in the standard Hot Big Bang model. Be aware that a period of reheating is necessary since the huge expansion due to inflation cools down the universe ($T \propto a^{-1}$ during radiation domination) while nucleosynthesis occurs at a temperature $T \sim 1$ MeV (see e.g. [2, 21]).

1.4 Horizons and causality

The greatest comoving distance from which an observer at time t can receive light signals is given by

$$d_P = \int_0^t \frac{dt}{a(t)}, \tag{1.33}$$

where we have assumed that the Big Bang happened at $t = 0$. This distance is called *comoving particle horizon* and it quantifies the extension of the causal region for the observer. Notice that all the worldlines of physical entities having interacted with the observer should have crossed his past light cone. Two observers separated by a distance greater than $2d_P$ could not have been in causal contact but, maybe, they will be in the future.

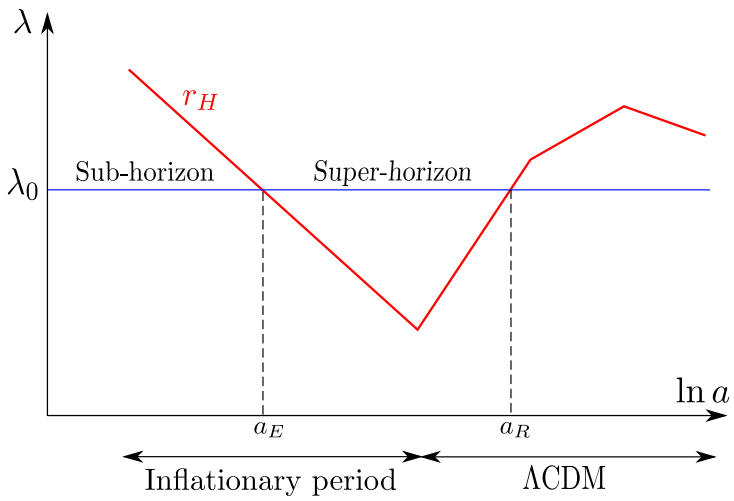

Figure 1.1: Evolution of the comoving Hubble radius r_H (1.34) over time. Comoving scales are plotted on the y-axis, time is measured in units of $\ln a$. Let us focus on a generic scale λ_0. During inflation this scale is well within the horizon (and so microphysical processes may affect it). At a_E, Hubble radius becomes smaller than the scale and we say that the scale crosses the horizon. From a_E to a_R the scale is said to be super-horizon and it is not influenced by microphysics. Later, the scale re-enters the horizon after the end of inflation. Although this picture is only a sketch, notice that the slope of r_H changes two times after the end of inflation. The first one occurred at matter-radiation equality, the second one when the cosmological constant started to dominate over the other components of the Universe.

Another useful quantity related to causality is the *comoving Hubble radius*. It is defined as

$$r_H \equiv \frac{1}{aH}\,, \tag{1.34}$$

and it expresses the typical scale over which particles are causally connected in the course of one expansion time $t_H = H^{-1}$. This concept is rather different from the particle horizon. In fact, if we compare the separation of two observers with the Hubble radius, we can say whether *now* (i.e. within one expansion time) they are in causal contact. The condition $\ddot{a} > 0$ and the Friedmann equations (1.8) imply that $\dot{r}_H < 0$ during inflation. Figure 1.1 is a helpful pictorial representation to have in mind.

Sometimes it is convenient to measure time during inflation with the number of e-foldings

$$N \equiv \int_t^{t_f} H\, dt'\,, \tag{1.35}$$

where t_f is the end of inflation and t is a generic instant of time. In the slow-roll approximation, it is straightforward to prove that

$$N = \int_{\varphi(t)}^{\varphi(t_f)} \frac{H}{\dot{\varphi}} d\varphi \simeq -8\pi G \int_{\varphi(t)}^{\varphi(t_f)} \frac{V}{V'} d\varphi\,. \tag{1.36}$$

Inflation must occur for at least 60 e-foldings in order to solve the aforementioned horizon and flatness problems (for example, see [6, 22]). Scales of cosmological interest range from 1 Mpc to 10 Gpc and then they cross the horizon approximately in 9 e-foldings.

1.5 Cosmological perturbations

Nowadays, the greatest quality of the inflationary theory is its capacity to seed the formation of structures in the Universe. In this section we will perturb only the scalar field and not the metric (which will be perturbed in chapter 2). Although being simple, this case is nonetheless instructive.

As previously done, we can split the field in two terms,

$$\varphi(t,\mathbf{x}) = \varphi_0(t) + \delta\varphi(t,\mathbf{x})\,. \tag{1.37}$$

The first one φ_0 obeys the background equations of motion and the second one represents a little perturbation away from the background solution.

After performing a Fourier transform of the fields (notice that $\mathbf{k}$ is a comoving wavenumber and its modulus is $k = 2\pi/\lambda$)

$$\varphi_I(t,\mathbf{x}) = \int \frac{d^3k}{(2\pi)^3} e^{i\mathbf{k}\cdot\mathbf{x}} \varphi_I(t,\mathbf{k})\,, \tag{1.38}$$

the equations of motion for φ_0 and $\delta\varphi$ become respectively

$$\ddot{\varphi}_0 + 3H\dot{\varphi}_0 = -V'(\varphi_0)\,, \tag{1.39}$$

$$\ddot{\delta\varphi} + 3H\dot{\delta\varphi} + \frac{k^2}{a^2}\delta\varphi = -V''(\varphi_0)\delta\varphi\,. \tag{1.40}$$

Plane waves have been used to expand the fields because we have assumed that the background spacetime is a spatially flat FRW universe.

Deriving equation (1.39) with respect to time leads to

$$(\dot{\varphi}_0)^{\cdot\cdot} + 3H(\dot{\varphi}_0)^{\cdot} = -V''\dot{\varphi}_0\,, \tag{1.41}$$

which looks like the previous equation for $\delta\varphi$. In the limit of large scales ($k^2 \ll a^2H^2$ or $\lambda \gg r_H$) and $t \gg H^{-1}$, equations (1.40) and (1.41) are not independent and the solutions are related by

$$\delta\varphi(t,\mathbf{x}) = -\delta t(\mathbf{x})\dot{\varphi}_0(t)\,. \tag{1.42}$$

This relation implies

$$\varphi(t,\mathbf{x}) = \varphi_0(t - \delta t(\mathbf{x}))\,, \tag{1.43}$$

which shows how a little perturbation introduces a time shift in the evolution of the field φ with respect to the background trajectory. This means that different regions in the universe go through the same history but at slightly different times. For concreteness, let us consider two regions $\mathcal{R}_1$ and $\mathcal{R}_2$ in which the inflaton takes constant values $\varphi_1 \neq \varphi_2$ at a certain time t_0. This implies that the potential energy is different in the two regions and hence, due to equations (1.27), they experience a different expansion. Through this mechanism, regions with different energy density can emerge in the universe, leading eventually to structure formation.

Let us briefly recap how inflation seeded structures in the Universe. First, quantum fluctuations produced perturbations in the inflaton field. Inflation made the wavelength of these

local perturbations grew exponentially reaching sizes of order of cosmological scales. After the end of inflation, inflaton decayed into matter and radiation transferring its fluctuations to them. Finally, density perturbations evolved driven by gravity.

Structure formation can occur via gravitational instability if there are small pre-existing fluctuations on relevant physical scales (e.g., the typical galaxy scale $\sim$ 1 Mpc). However, in the standard Big Bang model, these small perturbations have to be put in by hand, because it is impossible to produce fluctuations on any length scales larger than the horizon size (see figure 1.1). Inflation is able to provide a mechanism to generate both density perturbations and gravitational waves on large scales. Indeed, during inflation the comoving Hubble horizon decreases with time and quantum fluctuations can become classical on superhorizon scales.

1.5.1 Qualitative behaviour

Consider equation (1.40) without the potential term (in this case the field is said to be massless since the second derivative of the potential is related to the mass of the field),

$$\ddot{\delta\varphi} + 3H\dot{\delta\varphi} + \frac{k^2}{a^2}\delta\varphi = 0\,. \tag{1.44}$$

There are two limiting cases: $k \gg aH$ (sub-horizon scales) and $k \ll aH$ (super-horizon scales).

In the sub-horizon regime, the physical length is much smaller than the Hubble radius and the previous equation reduces to

$$\ddot{\delta\varphi} + \frac{k^2}{a^2}\delta\varphi = 0\,, \tag{1.45}$$

that is the equation of a free harmonic oscillator with a time-dependent frequency. This is a predictable result. The perturbations of the field oscillate due to vacuum quantum fluctuations. Obviously, quantum fluctuations can act only on very small scales and, on such scales, spacetime looks like Minkowski thanks to the Equivalence Principle. Notice that $H \ll ka^{-1}$ is equivalent to neglect the expansion of the universe and this is possible only on sufficiently small regions.

In the super-horizon regime $k \ll aH$, the physical length of the perturbations is larger than the Hubble radius and we get

$$\ddot{\delta\varphi} + 3H\dot{\delta\varphi} = 0\,. \tag{1.46}$$

This equation has two solutions, one is a constant and the other has a decaying amplitude. After a few Hubble times the decaying solution becomes negligible and only the constant one survives. Therefore, perturbations freeze on super-horizon scales. The reason is that there are no physical processes that can affect such scales due to causality. Quantum effects can only act on scales within the horizon and hence perturbations will remain nearly constant after they exit off it. This behaviour is particularly important since, after horizon crossing, perturbations do not evolve until they re-enter and this simplifies the study of structure formation.

1.5.2 Quasi-de Sitter expansion with a light inflaton

In this paragraph, we will solve equation (1.40) in a simple case. First of all, we rewrite that equation using conformal time in momentum space obtaining

$$\delta\varphi'' + 2\mathcal{H}\delta\varphi' + k^2\delta\varphi = -a^2\frac{\partial^2 V}{\partial\varphi^2}\delta\varphi\,, \tag{1.47}$$

where

$$\mathcal{H} \equiv \frac{a'}{a}\,. \tag{1.48}$$

Let us introduce a new rescaled field $\widehat{\delta\varphi} \equiv a\delta\varphi$ and quantize this one the with second quantization formalism, that is

$$\widehat{\delta\varphi}(\tau,\mathbf{x}) = \int \frac{d^3k}{(2\pi)^3}\left(u_k(\tau)a_{\mathbf{k}}e^{i\mathbf{k}\cdot\mathbf{x}} + u_k^*(\tau)a^\dagger_{-\mathbf{k}}e^{-i\mathbf{k}\cdot\mathbf{x}}\right), \tag{1.49}$$

where the annihilation $a_{\mathbf{k}}$ and creation $a^\dagger_{\mathbf{k}}$ operators satisfy the usual commutation relations

$$[a_{\mathbf{k}}, a^\dagger_{\mathbf{k}'}] = (2\pi)^3\delta^3(\mathbf{k}-\mathbf{k}')\hbar, \tag{1.50a}$$

$$[a_{\mathbf{k}}, a_{\mathbf{k}'}] = [a^\dagger_{\mathbf{k}}, a^\dagger_{\mathbf{k}'}] = 0\,. \tag{1.50b}$$

The functions $u_k(\tau)$, called *mode functions*, satisfy the normalization condition

$$u_k^* u_k' - u_k u_k^{*\prime} = -i\,. \tag{1.51}$$

If spacetime is flat, the mode functions assume the customary expression of relativistic Quantum Field Theory, that is

$$u_k(\tau) = \frac{e^{-ik\tau}}{\sqrt{2\omega_k}}\,, \tag{1.52}$$

where $\omega_k^2 \equiv k^2 + m^2$. The Equivalence Principle guarantees that inside small enough regions or for very early times, the mode functions should have this form. The last requirement is equivalent to a specific vacuum choice, also known as Bunch-Davies vacuum.

The equation (1.47) rewritten in terms of the mode functions reads

$$u_k'' + \left(k^2 - \frac{a''}{a} + a^2\frac{\partial^2 V}{\partial\varphi^2}\right)u_k = 0\,, \tag{1.53}$$

that is the equation of motion for a harmonic oscillator with time-dependent frequency. If expansion is quasi-de Sitter,

$$\frac{a''}{a} = \mathcal{H}^2 + \mathcal{H}' \simeq \frac{2}{\tau^2}\left(1 + \frac{3}{2}\varepsilon\right), \tag{1.54}$$

at first order in the slow-roll parameters. Notice that at zeroth order

$$\tau \simeq -\frac{1}{aH}\,, \tag{1.55}$$

hence the sub-horizon limit reads $-k\tau \to 0$. Moreover, it is easy to show that

$$a^2\frac{\partial^2 V}{\partial\varphi^2} = \frac{3\eta}{\tau^2}\,, \tag{1.56}$$

where the slow-roll condition $|\eta| \ll 1$ implies that the field φ is a very light field. The latest expressions allow us to rewrite equation (1.53) as

$$u_k'' + \left(k^2 - \frac{\nu^2 - \frac{1}{4}}{\tau^2}\right) u_k = 0\,, \tag{1.57}$$

where

$$\nu^2 \equiv \frac{9}{4} + 3\varepsilon - 3\eta\,. \tag{1.58}$$

Equation (1.57) is the well-known Bessel equation of order ν. The general solution is given by a superposition of two independent solutions (the Hankel functions of the first and second kind) and it can be written as

$$u_k(\tau) = \sqrt{-\tau}\Big(c_1(k) H_\nu^{(1)}(-k\tau) + c_2(k) H_\nu^{(2)}(-k\tau)\Big), \tag{1.59}$$

where c_1 and c_2 are two arbitrary functions of the momentum that can be fixed imposing boundary conditions. For what concern cosmological perturbations, an appropriate requirement is that $u_k(\tau) \to e^{-ik\tau}$ for $-k\tau \gg 1$, which corresponds to choose the Bunch-Davies vacuum.

The asymptotic behaviour of the Hankel functions is given by

$$H_\nu^{(1)}(x) \underset{x\to 0}{\sim} \sqrt{\frac{2}{\pi x}} e^{i(x - \frac{\pi}{2}\nu - \frac{\pi}{4})} + e^{i(x - \frac{\pi}{2}\nu + \frac{\pi}{4})} \frac{\nu^2 - \frac{1}{4}}{x\sqrt{2\pi x}}\,, \tag{1.60}$$

$$H_\nu^{(1)}(x) \underset{x\to -\infty}{\sim} -i\frac{2^\nu \Gamma(\nu)}{\pi} x^{-\nu} - i\frac{2^{\nu-2}\Gamma(\nu)}{\pi(\nu-1)} x^{2-\nu} + \left(-i\frac{\cos(\pi\nu)\Gamma(-\nu)}{2^\nu \pi} + \frac{1}{2^\nu \Gamma(\nu+1)}\right) x^\nu, \tag{1.61}$$

and they are related by

$$H_\nu^{(2)} = H_\nu^{(1)*}. \tag{1.62}$$

Using the latest equations, it is not difficult to show that $c_2(k) = 0$ and

$$c_1(k) = \frac{\sqrt{\pi}}{2} e^{i\left(\nu + \frac{1}{2}\right)\frac{\pi}{2}}, \tag{1.63}$$

assuming Bunch-Davies vacuum for $-k\tau \gg 1$. Thus the mode function takes the form

$$u_k(\tau) = \frac{\sqrt{\pi}}{2} e^{i\left(\nu + \frac{1}{2}\right)\frac{\pi}{2}} \sqrt{-\tau}\, H_\nu^{(1)}(-k\tau)\,, \tag{1.64}$$

and the field perturbation

$$\delta\varphi_k(\tau) = \frac{\sqrt{\pi}}{2} e^{i\left(\nu + \frac{1}{2}\right)\frac{\pi}{2}} (-\tau)^{\frac{3}{2}} H\, H_\nu^{(1)}(-k\tau)\,. \tag{1.65}$$

The modulus of the field perturbation on super-horizon scales can be rewritten as

$$|\delta\varphi_k(\tau)| = \frac{H}{\sqrt{2k^3}} \left(\frac{k}{aH}\right)^{\frac{3}{2} - \nu}. \tag{1.66}$$

Since $\nu \simeq 3/2$ (deviations are of order of slow-roll parameters and then small by definition), the amplitude of a given perturbation with wavenumber k is proportional to the expansion rate H which is nearly constant during inflation.

1.6 Power spectrum

Let $\delta(t, \mathbf{x})$ be a fluctuation of a field (for example you may think about $\delta\varphi$) around the FRW background. The two-point correlation function is

$$\xi(r) = \langle \delta(t, \mathbf{x} + \mathbf{r})\, \delta(t, \mathbf{x}) \rangle \,, \tag{1.67}$$

where the mean is performed on the statistical ensemble, and it represents the probability of finding a fluctuation at a distance r from another fluctuation.

If (statistical) homogeneity and isotropy hold, then in Fourier space it can be shown that

$$\langle \delta_{\mathbf{k}} \delta_{\mathbf{k}'} \rangle = (2\pi)^3 \delta(\mathbf{k} + \mathbf{k}') P(k) \,, \tag{1.68}$$

where $P(k)$ is called power spectrum. We will consider the former equation as the definition of the power spectrum. The variance of fluctuations' distribution is

$$\sigma^2 = \langle \delta^2(t, \mathbf{x}) \rangle = \frac{1}{2\pi^2} \int_0^{+\infty} \frac{dk}{k} k^3 P(k) \equiv \int_0^{+\infty} \frac{dk}{k} \mathcal{P}(k) \,, \tag{1.69}$$

where in the last equality we have defined the adimensional power spectrum $\mathcal{P}(k)$.

Starting from the definition (1.68) and using (1.66), the power spectrum for single-field inflation is

$$P_{\delta\varphi} = \frac{H^2}{2k^3} \left(\frac{k}{aH} \right)^{3-2\nu} , \tag{1.70}$$

and the adimensional power spectrum is

$$\mathcal{P}_{\delta\varphi} = \left(\frac{H}{2\pi} \right)^2 \left(\frac{k}{aH} \right)^{3-2\nu} . \tag{1.71}$$

Inflaton perturbations cannot be directly observed since inflaton decayed into particles. Plus, the perturbations are nearly frozen on superhorizon scales. For these reasons, it is convenient to introduce the comoving curvature perturbation

$$\mathcal{R} \simeq -H \frac{\delta\varphi}{\dot{\varphi}} \,. \tag{1.72}$$

This quantity has two merits: it is gauge-invariant and conserved on superhorizon scales. More details will be given in the following chapter. For what concerns us now, it is sufficient to say that the measurable adimensional power spectrum of $\mathcal{R}$ has the form

$$\mathcal{P}_{\mathcal{R}} = \left(\frac{H^2}{2\pi\dot{\varphi}} \right)^2 \left(\frac{k}{aH} \right)^{3-2\nu} . \tag{1.73}$$

The scalar spectral index n_s is defined as

$$n_s - 1 = \frac{d \ln \mathcal{P}(k)}{d \ln k} \,, \tag{1.74}$$

and it describes the shape (scale-dependence) of perturbations. If the spectral index is a constant, then the adimensional power spectrum turns out to follow a simple power law

$$\mathcal{P}(k) = \mathcal{P}(k_0)\left(\frac{k}{k_0}\right)^{n_s-1}, \tag{1.75}$$

where k_0 is a pivot scale. If $n_s = 1$, the spectrum is said to be scale-invariant corresponding to the so-called Harrison-Zel'dovich spectrum [23, 24]. More precisely, a power spectrum is scale-invariant if

$$\langle \delta_{\lambda\mathbf{k}} \delta_{\lambda\mathbf{k}'} \rangle = \langle \delta_{\mathbf{k}} \delta_{\mathbf{k}'} \rangle, \tag{1.76}$$

where λ is a rescaling factor[2]. Then, using the property $\delta^3(\lambda(\mathbf{k}+\mathbf{k}')) = \lambda^{-3}\delta^3(\mathbf{k}+\mathbf{k}')$, a scale-invariant power spectrum must obey

$$P(k) \propto \frac{1}{k^3}\,. \tag{1.77}$$

It is worth noticing that, for a scale-invariant spectrum, fluctuations are not constant on all scales k (this spectrum is called *white noise*). Indeed, the power spectrum scales as k^{-3} because the amplitude of fluctuations should be defined with respect to some physical length. This scale is provided by the Hubble radius (or by the particle horizon) which is not constant over time. In addition to the spectral index n_s it is usually measured its running, which is defined as

$$\frac{dn_s}{d\ln k}\,. \tag{1.78}$$

From equation (1.73), the scalar spectral index is simply given by

$$n_s - 1 = 3 - 2\nu\,. \tag{1.79}$$

Note that $n_s \simeq 1$ since $\nu \simeq 3/2$ and then the power spectrum is nearly scale-invariant for single-field inflation and deviations from scale invariance are of order of the slow-roll parameters. *Planck* satellite has recently measured $n_s = 0.9645 \pm 0.0049$ [6], thus scale invariance is ruled out by more than 5σ. Interestingly enough, the primordial power spectrum has a red tilt ($n_s - 1 < 0$). This agreement between observations and predictions is one of the most striking successes of single-field slow-roll inflation. Let us stress this important fact. Until now, we have not made any assumption on the particular form of the potential apart for flatness. Hence, a *nearly* scale-invariant power spectrum is a common prediction of all single-field models if the slow-roll conditions are satisfied.

Let us conclude this section with a comment. Notice that ν (1.58) can become imaginary if the field φ is sufficiently massive. In fact, $\eta \simeq m_\varphi^2(3H^2)^{-1}$ and ν is imaginary if $m_\varphi \gtrsim \frac{3}{2}H$. In this case, fluctuations of the scalar field remain in the vacuum state and do not produce perturbations on physically relevant scales. Indeed, the amplitude of the power spectrum is damped exponentially as $\exp\left(-2m_\varphi^2 H^{-1}\right)$ and the spectral index $n_s = 4$ [25].

[2]The rescaling is usually defined in coordinate space as $\mathbf{x} \to \lambda\mathbf{x}$, but it can obviously transferred to momentum space as $\mathbf{k} \to \lambda^{-1}\mathbf{k}$.

1.7 Primordial gravitational waves

Quantum fluctuations affect the metric as well as scalar fields. Gravity waves (i.e. the tensor metric perturbations) are not coupled to the energy density (as we will see in the next chapter) and hence they cannot affect the large-scale structure of the Universe. However, primordial gravitational waves affect the Cosmic Microwave Background (CMB) pattern of anisotropies (in particular the so-called B-modes) and, if they will be observed, they would be one of the most important sources of information about inflation. They can shed light on the inflationary mechanism without passing through matter perturbations that are more difficult to characterize since they evolve after the end of inflation. On the other hand, the imprint of primordial gravitational waves on the CMB was so dim that they have not been observed until now.

Considering tensor perturbations of the metric (i.e. neglecting the so-called scalar and vector metric perturbations, see chapter 2), these can be seen as ripples of the FRW background

$$ds^2 = a^2\Big(-d\tau^2 + (\delta_{ij} + h_{ij})dx^i dx^j\Big), \tag{1.80}$$

where $|h_{ij}| \ll 1$. The tensor h_{ij} has two physical degrees of freedom, or polarizations, and they are usually indicated as $\lambda = +, \times$. The metric $g_{\mu\nu}$ has ten degrees of freedom since it is a symmetric tensor in four dimensions, but the gauge fixing imposes four conditions. The perturbation h_{ij} has only two degrees of freedom since it is symmetric, traceless $h_{ii} = 0$ and divergenceless $\partial^i h_{ij} = 0$. The metric perturbation can be written in Fourier space as

$$h_{ij}(\tau, \mathbf{x}) = \sum_{\lambda=+,\times} \int \frac{d^3k}{(2\pi)^3} e^{i\mathbf{k}\cdot\mathbf{x}} \epsilon_{ij}^{\lambda}(\tau, \mathbf{k}) h_\lambda(\mathbf{k}), \tag{1.81}$$

where the polarization tensors ϵ_{ij}^{λ} satisfy

$$\epsilon_{ij}^{\lambda} = \epsilon_{ji}^{\lambda}, \tag{1.82}$$

$$k^i \epsilon_{ij}^{\lambda} = 0, \tag{1.83}$$

$$\epsilon_{ii}^{\lambda} = 0, \tag{1.84}$$

$$\epsilon_{ij}^{\lambda}(\tau, -\mathbf{k}) = \epsilon_{ij}^{\lambda\,*}(\tau, \mathbf{k}), \tag{1.85}$$

$$\sum_{\lambda} \epsilon_{ij}^{\lambda}\, \epsilon_{ij}^{\lambda\,*} = 4. \tag{1.86}$$

The equation of motion for the components of h_{ij} reads[3]

$$h_\lambda'' + 2\mathcal{H} h_\lambda' + \frac{k^2}{a^2} h_\lambda = 0, \tag{1.87}$$

that has the same form of equation (1.47) valid for a massless field. Gravitons are massless as well as photons since they both propagate at the speed of light. In fact the equation of motion for the two polarization states is the same as that for the perturbations of a massless scalar field (1.44). Therefore, we can simply adapt the previous results of the massless case.

[3]This equation is valid during inflation if the fields that drive it have vanishing anisotropic stress. This happens e.g. when the fields are scalar and minimally coupled to gravity.

On superhorizon scales, fluctuations are nearly frozen and hence their amplitude reads

$$|h_\lambda| = \sqrt{32\pi G}\frac{H}{\sqrt{2k^3}}\left(\frac{k}{aH}\right)^{\frac{3}{2}-\nu_T} . \tag{1.88}$$

Notice the dimensional factor absent for scalar perturbations (1.66). The difference consists in the fact that the metric perturbations are adimensional, but the scalar perturbations have dimension of mass $[\delta\varphi] = [M]$.

The adimensional power spectrum on scales larger than the horizon is

$$\mathcal{P}_T(k) = \frac{k^3}{2\pi^2}\sum_\lambda |h_\lambda| = \frac{64}{m_{Pl}^2}\left(\frac{H}{2\pi}\right)^2\left(\frac{k}{aH}\right)^{3-2\nu_T} . \tag{1.89}$$

The spectral index for tensor perturbations is defined as

$$n_T \equiv \frac{d\ln\mathcal{P}_T}{d\ln k} , \tag{1.90}$$

and then the power spectrum can be written as

$$\mathcal{P}_T(k) = A_T^2\left(\frac{k}{aH}\right)^{n_T} , \tag{1.91}$$

where

$$n_T = 3 - 2\nu_T = -2\varepsilon . \tag{1.92}$$

The tensor power spectrum is almost scale-invariant, as the scalar one. The amplitude A_T depends only on H (which is nearly constant during inflation).

The tensor-to-scalar ratio r is defined as

$$r \equiv \frac{\mathcal{P}_T}{\mathcal{P}_\mathcal{R}} , \tag{1.93}$$

and it equals to

$$r = 16\varepsilon = -8n_T . \tag{1.94}$$

This is a significant consistency relation since it holds for *any* single-field model of slow-roll inflation. In practice, primordial gravitational waves have not yet been observed and thus experiments can provide an upper limit on r usually assuming the validity of the consistency relation. The best current limit $r < 0.09$ (95% CL) was obtained by a joint analysis of *Planck*, BICEP2, *Keck Array* and other data [26].

The importance of the primordial gravitational waves relies on the fact that their amplitude is directly related to the energy scale of inflation $V^{1/4}$. From the expressions of the adimensional power spectra $\mathcal{P}_\mathcal{R}$ (1.73) and $\mathcal{P}_T$ (1.89), one can show that the energy scale of inflation is

$$V^{1/4} \simeq 4.4\cdot 10^{-3}\, M_{Pl}\left(\frac{r}{0.01}\right)^{\frac{1}{4}} , \tag{1.95}$$

where the value of the reduced Planck mass is $M_{Pl} = 2.435\cdot 10^{18}\,\text{GeV}$. Using the just mentioned observational constraint on r, the energy scale of inflation is lower than $2\cdot 10^{16}\,\text{GeV}$. This is the typical scale of Grand Unification Theories (GUT).

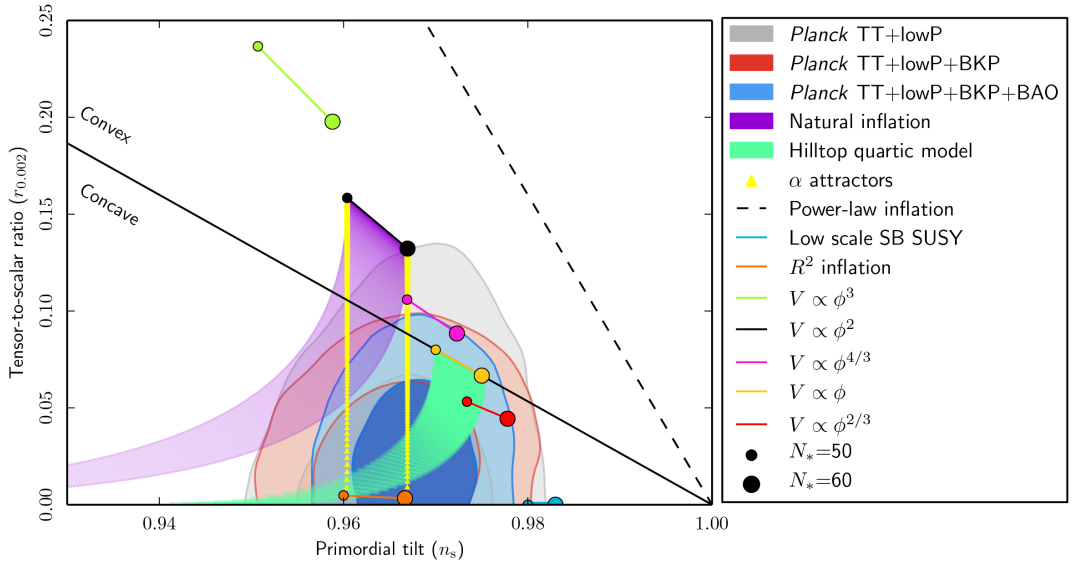

Figure 1.2: 2015 observational results by *Planck* satellite on the $r - n_s$ plane. The confidence regions (68% and 95% CL) are compared with the theoretical predictions of some models of inflation. Notice that some simple monomial power-law potentials (like ϕ^3) are excluded by observations. R^2 (or Starobinsky) predictions lie exactly at the centre of the coloured spot. The models named α-attractors can parametrize efficiently the observationally constrained region (we will discuss this behaviour extensively in chapter 5). The confidence regions are drawn along with *Planck* 2013 ones. Picture taken from [6].

1.8 Classification and examples

Since inflation was born, many models were proposed in order to explain the inflationary mechanism. They differ in the kind of potential and in the underlying particle physics theory. Some of them are nowadays excluded by observations, others have survived until now [6]. Here we will review the most interesting models for our discussion. Current observational constraints compared with the predictions of some models are depicted in figure 1.2.

The difference between single-field slow-roll inflationary mechanisms relies on the form of the potential term. This term can be characterized by two parameters [27]: the height Λ^4 of the potential, related to vacuum energy during inflation, and a width μ corresponding to the field excursion $\Delta\varphi = \varphi_{end} - \varphi_{init}$. The potential can thus be written in the general fashion

$$V(\varphi) = \Lambda^4 f\left(\frac{\varphi}{\mu}\right), \tag{1.96}$$

where the typical scales Λ^4 and μ have been emphasized.

Inflationary models are classified via their predictions in the $r - n_s$ plane. Since r (1.94) and n_s (1.79) depend on the slow-roll parameters ε and η, different regions in the $r - n_s$ plane can be parametrized via the slow-roll parameters, as in the following.

- Large-field models are defined in the region $0 < \eta < 2\varepsilon$. The field is initially displaced from

the minimum of the potential by an amount of order of the Planck mass. Typical examples are the monomial potentials $V(\varphi) = \Lambda^4 (\varphi/\mu)^p$ and exponential ones $V(\varphi) = \Lambda^4 \exp(\varphi/\mu)$.

- Small-field models cover the area $\eta < 0$. The field usually starts near the origin and rolls down the potential toward a minimum. Typical potentials of these models have the structure $V(\varphi) = \Lambda^4 [1 - (\varphi/\mu)^p]$.
- Hybrid models lie in the region $\eta > 2\varepsilon$. The inflaton rolls down the potential towards a minimum with non-zero vacuum energy. A second field is responsible for the end of inflation. The potential has the characteristic form $V(\varphi) = \Lambda^4 [1 + (\varphi/\mu)^p]$.

1.8.1 Monomial potential

The simplest potential giving inflation is

$$V(\varphi) = \frac{\lambda}{M_{Pl}^{n-4}} \varphi^n, \tag{1.97}$$

where n is a positive (usually even) integer and λ is a dimensionless coupling constant. This monomial potential is of large-field type and it is a generalization of the simplest potential giving inflation $V(\varphi) = \frac{1}{2} m^2 \varphi^2$ [13].

The slow-roll parameters (1.28) and (1.29) are

$$\varepsilon = \frac{n^2}{2} \frac{M_{Pl}^2}{\varphi^2}\,, \tag{1.98a}$$

$$\eta = n(n-1) \frac{M_{Pl}^2}{\varphi^2}\,. \tag{1.98b}$$

Inflation starts from $\varphi(0) \gg M_{Pl}$ and it ends when $\varepsilon = 1$, that is $\varphi(t_{end}) \simeq \alpha M_{Pl}$. From equation (1.36) (which holds only during slow-roll), we get

$$\varphi(N) = M_{Pl} \sqrt{2nN}\,, \tag{1.99}$$

where N is the number of e-folds till the end of inflation at which the observable scales cross the horizon during inflation. The predictions of this model are

$$n_s = 1 - \frac{2+n}{2N}\,, \tag{1.100a}$$

$$r = \frac{4n}{N}\,. \tag{1.100b}$$

These predictions are determined by the number of e-folds of inflation N and by the exponent n. Notice that, even if $\Delta\varphi \gg M_{Pl}$, one should not expect quantum gravity effects. Indeed, they may appear if $V(\varphi) \gtrsim M_{Pl}^4$.

1.8.2 Power-law inflation

Power-law inflation [28] has the potential

$$V(\varphi) = V_0 \exp\left(-\sqrt{\frac{2}{p}} \frac{\varphi}{M_{Pl}} \right), \tag{1.101}$$

and it has an exact analytical solution for the inflationary dynamics. The slow-roll parameters (1.28) and (1.29) are given by

$$\varepsilon = \frac{1}{p}\,, \tag{1.102a}$$

$$\eta = \frac{2}{p}\,, \tag{1.102b}$$

and the predictions are

$$n_s = 1 - \frac{2}{p}\,, \tag{1.103a}$$

$$r = \frac{16}{p}\,. \tag{1.103b}$$

The predictions depend on the parameter p and they are subjected to the relation

$$r = 8(1 - n_s)\,. \tag{1.104}$$

The predictions of power-law inflation can be recovered in the limit $n \to +\infty$ for the monomial potential (1.97). Notice that ε and η are constant and then inflation never ends in this model. Hence, this model should be modified in order for inflation to come to an end.

Let us make a remark. If there are n observable predictions that depend on k parameters, then there should be $n - k$ consistency relations. Their usefulness should be manifest. If we have n independent measurements of the predictions, we can use the consistency relations to distinguish between models. Otherwise, if we have less than n independent measures, the consistency relations can be used to infer the missing ones.

1.8.3 Starobinsky inflation

The original inflationary model studied by A. Starobinsky [9] contains an action with higher powers and derivatives of the Ricci curvature. This model arises in the context of generalization of Einstein gravity [29] and supergravity [30–32]. Recently, it has also been reinterpreted in terms of spontaneously breaking of conformal symmetry [33], as we will see extensively in chapter 5.

Consider the action

$$S = \frac{M_{Pl}^2}{2}\int d^4x\,\sqrt{-g}\left(R + \frac{R^2}{6M^2}\right), \tag{1.105}$$

where M is a constant with dimension of mass[4]. As a generalization of Einstein gravity, this is the simplest possibility one could imagine. Surprisingly, this model can lead to inflation without the presence of an explicit scalar field in this action. Indeed, gravity itself drives the exponential expansion. Thanks to a conformal transformation, the action can be rewritten removing the non-canonical gravitational term R^2 with the introduction of a scalar field (B. Whitt was the first to show this equivalence [34]).

The equations of motion for the metric are

$$\left(g_{\mu\nu}\,\Box - \nabla_\mu\nabla_\nu + R_{\mu\nu}\right)\left(1 + \frac{R}{3M^2}\right) - \frac{1}{2}\left(R + \frac{R^2}{6M^2}\right)g_{\mu\nu} = 0\,, \tag{1.106}$$

[4]The action S is dimensionless, d^4x has dimensions of $[M^{-4}]$ and then R has dimensions of $[M^2]$

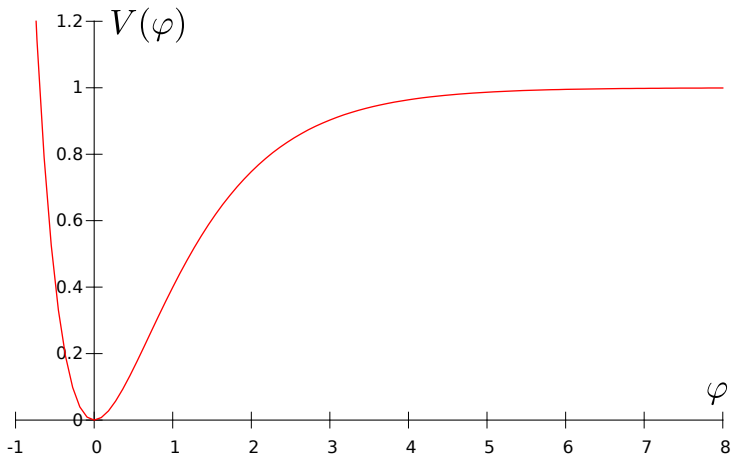

Figure 1.3: Starobinsky potential (1.111). For a scalar field φ, $[\varphi] = [M]$ in natural units. The values that the field assumes are measured in units of M_{Pl} so that $\varphi = 1$ stands for $\varphi = M_{Pl}$. Notice that inflation occurs on the plateau, i.e. for $\varphi \gg 1$.

which can be obtained varying the action with respect to the metric. The trace is given by

$$\Box R - M^2 R = 0\,. \tag{1.107}$$

Notice that these are fourth order equations with respect to covariant derivatives.

After the conformal transformation (see appendix B)

$$g_{\mu\nu} \mapsto \widetilde{g}_{\mu\nu} = \left(1 + \frac{\Phi}{3M^2}\right) g_{\mu\nu}\,, \tag{1.108}$$

and the redefinition

$$\varphi = \sqrt{\frac{3}{2}} \log\left(1 + \frac{\Phi}{3M^2}\right), \tag{1.109}$$

the action becomes

$$S = \frac{1}{2}\int d^4x\,\sqrt{-\widetilde{g}}\left[\widetilde{R} - \frac{1}{2}\partial_\mu\varphi\partial^\mu\varphi - \frac{3}{4}M^2\left(1 - e^{-\sqrt{\frac{2}{3}}\varphi}\right)^2\right], \tag{1.110}$$

where we have fixed $M_{Pl} \equiv 1$ (and we will assume this from now on except occasionally). This procedure is more general. Actually, it can be shown that a theory with the Lagrangian density $\sqrt{-g}f(R)$, where f is an arbitrary function of the Ricci curvature, is equivalent (in the so-called Einstein frame) to a theory with the standard gravity sector and a scalar field. This transition allows one to write second order equations of motion instead of higher order ones regardless of the function $f(R)$.

The potential for Starobinsky model is

$$V(\varphi) = \frac{3}{4}M^2\left(1 - e^{-\sqrt{\frac{2}{3}}\varphi}\right)^2, \tag{1.111}$$

and it is represented in figure 1.3. The slow-roll parameters (1.28) and (1.29) are

$$\varepsilon = \frac{4}{3}\left(e^{\sqrt{\frac{2}{3}}\varphi} - 1\right)^{-2}, \tag{1.112a}$$

$$\eta = -\frac{4}{3}\left(e^{\sqrt{\frac{2}{3}}\varphi} - 2\right)\left(e^{\sqrt{\frac{2}{3}}\varphi} - 1\right)^{-2}. \tag{1.112b}$$

The number of e-folds (1.36) is given by

$$N = \frac{3}{4}\left(e^{\sqrt{\frac{2}{3}}\varphi(N)} - e^{\sqrt{\frac{2}{3}}\varphi(0)}\right) + \frac{\sqrt{6}}{4}\big(\varphi(0) - \varphi(N)\big)\,. \tag{1.113}$$

Hitherto, all expressions are exact. On the other hand, inflation occurs for $\varphi \gg 1$ and it ends when $\varphi \sim 1$ (this condition is obtained imposing $\varepsilon = 1$). Therefore, we have $\varphi(N) \gg 1$ and $\varphi(0) \sim 1$ and hence we can approximate

$$N \simeq \frac{3}{4}e^{\sqrt{\frac{2}{3}}\varphi(N)}, \tag{1.114}$$

where the error is of order of few e-folds (they can be neglected since $N \sim 60$). Thanks to this approximation, the slow-roll parameters can be rewritten in the form

$$\varepsilon = \frac{4}{3}e^{-2\sqrt{\frac{2}{3}}\varphi} = \frac{3}{4N^2}\,, \tag{1.115a}$$

$$\eta = -\frac{4}{3}e^{-\sqrt{\frac{2}{3}}\varphi} = -\frac{1}{N}\,. \tag{1.115b}$$

Thus, the predictions of this model are given by

$$n_s = 1 - \frac{2}{N}\,, \tag{1.116a}$$

$$r = \frac{12}{N^2}\,, \tag{1.116b}$$

at lowest order in N^{-1}. If $N \simeq 60$, these predictions are so in agreement with latest *Planck* satellite results [6], reported in table 1.1, that the Bayesian evidence is calculated with respect to Starobinsky model (see figure 1.2).

Chapter 2

Cosmological perturbation theory

> "Space is certainly something more complicated than the average person would probably realize. Space is not just an empty background in which things happen."
>
> Alan Guth

Perturbation theory is widely used in physics because of its naturalness when dealing with complicated problems. Indeed, when a problem is too difficult to solve exactly (both analytically or numerically), one solves a simplified version of the problem without the complications. Then, one suppose that the complications introduce little perturbations on the background solution and expand the complete solution in powers of the perturbations. Through this procedure, one can obtain an approximated solution of the otherwise unsolvable initial problem. The applications of perturbation theory range from Hamiltonian mechanics to quantum physics.

In cosmology, studying perturbations is a task of fundamental importance since we know that our Universe is nearly homogeneous and isotropic. Hence, it is natural to consider the FRW universe as the background solution. Notice that the adverb "nearly" is what distinguishes a boring model of universe from a tantalizing one. Furthermore, remember that gravity is described through Einstein equations that are coupled and, also because of this, very difficult to solve. Perturbation theory allows us to tackle the problem and simplify our analysis.

An indicator of the significance of perturbation theory in cosmology is the number (almost countless[1]) of articles written about it. A very good and complete review was written by K.A. Malik and D. Wands [16] (other reviews worth citing are [35,36]). The enthusiast reader may give a look at [37] for one of the first articles on the subject, [38] about gauge transformations, [39,40] about perturbations produced in single-field inflation, [41,42] about perturbations in multi-field inflation and [43–45] about curvature and isocurvature perturbations.

In section 2.1, we will review the basic concepts of cosmological perturbation theory. In particular, we will introduce the reader to the concepts of coordinate choice and gauge transformation. In section (2.2), we will decompose a generic quantity into scalars, vectors and tensors defined with respect to the adopted coordinates. In the following two sections 2.3 and 2.4, we

[1] As an example, K.A. Malik and D. Wands cited 178 papers in their review [16] .

will perturb explicitly the metric and the energy momentum tensor. Specifically, we will report their unperturbed expressions and the linear order perturbations. Section 2.5 contains the main gauges employed in cosmology. In section 2.6, we will build gauge-invariant quantities and explain when it is convenient to work with them. In section 2.7, we will collect the most significant perturbed equations obtained perturbing Einstein equations and the continuity equation for the energy-momentum tensor. Finally, in section 2.8, we will explain the difference between adiabatic and entropy perturbations and why this distinction is made.

2.1 The universe as a manifold

The solution of Einstein equations for a homogeneous and isotropic universe is given by the Friedmann-Robertson-Walker solution (see section 1.2 for the case of single-component universe); we use the adjectives background and unperturbed when referring to it. Since our Universe is with good approximation homogeneous and isotropic, we expect that deviations from the unperturbed solution will be small. This is the basic idea underneath perturbation theory around some well known background solution.

The unperturbed universe is merely described by a manifold $\mathcal{M}_0$ with flat FRW metric. All tensor quantities defined on[2] $\mathcal{M}_0$ should reflect the property of homogeneity and isotropy (for example a scalar field depends only on time and does not on space coordinates). On the other hand, the real universe is described by a manifold $\mathcal{M}$ that resembles $\mathcal{M}_0$ but has some inhomogeneities. We expect that the metric $g_{\mu\nu}$ on $\mathcal{M}$ is related to the metric $\bar{g}_{\mu\nu}$ of $\mathcal{M}_0$ in the following manner

$$g_{\mu\nu} = \bar{g}_{\mu\nu} + \delta g_{\mu\nu}\,, \tag{2.1}$$

where $\delta g_{\mu\nu}$ is a small perturbation. All troubles appearing in general relativity perturbation theory are related with the meaning of the word "small". In fact, general relativity is invariant under generic changes of coordinates (i.e. diffeomorphisms between manifolds) and then a small perturbation for one observer may not be negligible for a second one. The freedom of fixing the coordinates is a virtue and a vice of general relativity. It is a virtue because we can select the best suited coordinates for the problem we are dealing with. However, it has the drawback that equations may look different for two observers and that inhomogeneities can have unphysical observer-dependent artefacts. Let us remark that general relativity equations are covariant, i.e. manifestly coordinate independent, but the procedure of splitting a tensor into background plus perturbation depends on the coordinate choice. In the following we will try to face this issue.

First of all, we need some basic definitions. A diffeomorphism

$$\varphi_\lambda : \mathcal{M}_0 \to \mathcal{M}\,, \tag{2.2}$$

that relates the background and the physical manifolds, is called *gauge*[3] (see figure 2.1). The

[2]Strictly speaking a tensor is defined on the tangent bundle of a manifold or an appropriate space build up from tangent bundles.

[3]Notice that gauge is an overused term in physics and that it has different meanings not necessarily correlated.

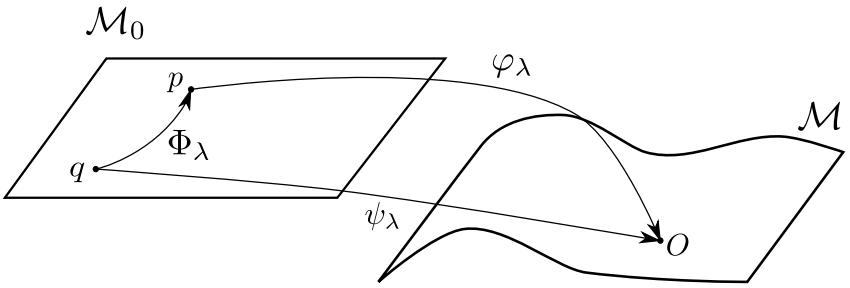

Figure 2.1: The background manifold $\mathcal{M}_0$ and the physical manifold $\mathcal{M}$ linked through two gauges φ_λ and ψ_λ.

procedure of gauge fixing is not unique. Once the gauge is fixed, we can relate quantities defined on $\mathcal{M}_0$ to their corresponding ones defined on $\mathcal{M}$.

A *coordinate system* is a map that assigns a point on $\mathcal{M}_0$ to a point of $\mathbb{R}^4$. In differential geometry jargon, a coordinate system is a collection of compatible charts (also known as atlas). In cosmology, we assume that spacetime is smooth and mathematically well-behaved such that it can be covered with only one chart. A coordinate system specifies a foliation of spacetime (slicing) into spacelike hypersurfaces of constant time. Spatial coordinates are defined on each of these slices (threading). It is of primary importance to remember that a gauge is not a coordinate choice.

Since the gauge choice is not mandatory, we can fix a second gauge ψ_λ between the two manifolds. Let us consider a point $O \in \mathcal{M}$. Thus, there should exist two points p and q on $\mathcal{M}_0$ such that $\varphi_\lambda(p) = \psi_\lambda(q) = O$. Therefore, it is natural to define the map $\Phi_\lambda(q) \equiv \varphi_\lambda^{-1}(\psi_\lambda(q)) = p$, which is a bijective function between points of $\mathcal{M}_0$. The map Φ_λ is named *gauge transformation*. Observe that a gauge transformation does not change the coordinate system fixed on $\mathcal{M}_0$, but it concerns only the points.

Having defined a coordinate system x^μ on $\mathcal{M}_0$, a coordinate system y^μ is fixed on $\mathcal{M}$ through the gauge. If the gauge is changed, a new coordinate system $\widetilde{y}^\mu$ will be fixed on $\mathcal{M}$. Relating the coordinate systems y^μ and $\widetilde{y}^\mu$ is the base of the so called "passive approach"[4].

Now we need to characterize a coordinate transformation, that is a transformation between two systems of coordinates. Let us define a smooth vector field ξ^μ on $\mathcal{M}$. The vector field sets a foliation of $\mathcal{M}$ through its integral curves χ^μ such as

$$\frac{d\chi^\mu(\lambda)}{d\lambda} = \xi^\mu(\chi(\lambda)). \tag{2.3}$$

In order to interpret the field ξ^μ as an infinitesimal coordinate displacement, we fix the initial condition $\chi^\mu(0) = y^\mu$ and let $\chi^\mu(1) = \widetilde{y}^\mu$. It is possible to obtain a finite coordinate transformation between y^μ and $\widetilde{y}^\mu$ through exponentiation

$$\widetilde{y}^\mu = \chi^\mu(1) = \mathrm{e}^{\xi^\alpha \partial_\alpha} y^\mu, \tag{2.4}$$

[4]Honestly, one can deal with the issue of gauge changing through two approaches, the "active" and the "passive" ones. The "active" considers the gauge transformation as a map between points of $\mathcal{M}_0$. We consider only one approach in order not to be verbose.

but, for our purposes, it is sufficient to consider only the first order expansion

$$\widetilde{y}^\mu = y^\mu + \xi^\mu + \mathcal{O}(\xi^2). \tag{2.5}$$

If we let λ vary, we can parametrize generic new coordinates $\widetilde{y}^\mu(\lambda)$ in terms of λ. The generalization is trivial and leads to

$$\widetilde{y}^\mu(\lambda) = \mathrm{e}^{\lambda\xi^\alpha\partial_\alpha} y^\mu = y^\mu + \lambda\xi^\mu + \mathcal{O}(\xi^2). \tag{2.6}$$

Consider two points O and $\widetilde{O}$ on $\mathcal{M}$ having the same coordinate y_0^μ in the two systems, namely $y^\mu(O) = \widetilde{y}^\mu(\widetilde{O}) = y_0^\mu$. We want to relate the value of a tensor field $\widetilde{T}_{\widetilde{O}}$ expressed in the coordinate system $\widetilde{y}^\mu$ in terms of the tensor T_O and its derivatives in the coordinate system y^μ. In differential geometry the solution is well-known, and tensors are related by the Lie derivative $\mathcal{L}$ along the flux of ξ^μ,

$$\widetilde{T}(y_0) = \left(\mathrm{e}^{\mathcal{L}_\xi} T\right)(y_0) \tag{2.7}$$

$$= T(y_0) + \mathcal{L}_\xi T(y_0) + \mathcal{O}(\xi^2). \tag{2.8}$$

Notice that the transformed tensor $\widetilde{T}$ and the initial tensor T are both evaluated at the same coordinate. Recalling that a gauge transformation is equivalent to a coordinate change on $\mathcal{M}$, we have understood how to relate tensors in different gauges. In particular, a gauge transformation is completely determined by the four-vector ξ^μ and hence it is associated to four degrees of freedom. Then the procedure of gauge fixing can be seen also as a constraint to impose on the components of tensors.

In cosmology, every tensor A can be split into a homogeneous part and a perturbation

$$A(\tau, \mathbf{y}) = \bar{A}(\tau) + \delta A(\tau, \mathbf{y}). \tag{2.9}$$

Under a gauge transformation

$$\delta A \mapsto \widetilde{\delta A} = \widetilde{A} - \bar{A} = \delta A + \mathcal{L}_\xi \bar{A} + \mathcal{O}(\xi^2). \tag{2.10}$$

Previous equation is fundamental since it relates perturbations defined in different gauges. Having set the gauge, the perturbation δA is fixed. Since a gauge transformation can be seen as a change of coordinate on $\mathcal{M}$ via (2.6), the perturbation can be expanded in powers of λ as

$$\delta A = \sum_{n=1}^{+\infty} \frac{\lambda^n}{n!} \delta A^{(n)}. \tag{2.11}$$

Notice that $\delta A^{(0)} = 0$ because the background is unperturbed by definition. In the following, we will retain only linear terms.

Starting from the definition of Lie derivative

$$\mathcal{L}_\xi A = \lim_{\lambda\to 0} \frac{A(\widetilde{y}) - \widetilde{A}(\widetilde{y})}{\lambda}, \tag{2.12}$$

it can be shown that it acts on a scalar S, a vector V^μ and a tensor $G^{\mu\nu}$ as

$$\mathcal{L}_\xi S = \xi^\alpha \partial_\alpha S, \tag{2.13a}$$
$$\mathcal{L}_\xi V^\mu = \xi^\alpha \partial_\alpha V^\mu - V^\alpha \xi_\alpha \xi^\mu, \tag{2.13b}$$
$$\mathcal{L}_\xi V_\mu = \xi^\alpha \partial_\alpha V_\mu + V^\alpha \xi_\alpha \xi_\mu, \tag{2.13c}$$
$$\mathcal{L}_\xi G^{\mu\nu} = \xi^\alpha \partial_\alpha G^{\mu\nu} - G^{\mu\alpha}\partial_\alpha \xi^\nu - G^{\alpha\nu}\partial_\alpha \xi^\mu, \tag{2.13d}$$
$$\mathcal{L}_\xi G_{\mu\nu} = \xi^\alpha \partial_\alpha G_{\mu\nu} + G_{\mu\alpha}\partial_\nu \xi^\alpha + G_{\alpha\nu}\partial_\mu \xi^\alpha. \tag{2.13e}$$

These equations set the transformation properties of scalars, vectors and tensors under a change of coordinates.

2.2 SVT decomposition

In the previous section, four-dimensional spacetime has been foliated through spacelike hypersurfaces of constant time. The natural continuation of this procedure is the Scalar-Vector-Tensor decomposition of spatial quantities (first introduced by Bardeen [46]). The idea behind is very simple, so let us start with an example. Consider a four-vector

$$a^\mu = (a^0, a^i), \tag{2.14}$$

the vector a^i can be split into a divergenceless and an irrotational term

$$a^i = \partial^i a_\parallel + a^i_\perp, \tag{2.15}$$

where $\partial_i a^i_\perp = 0$. This split resembles the well-known distinction between longitudinal electric and solenoidal magnetic fields. We say that $a_\parallel$ is a scalar and $a^i_\perp$ is a vector under spatial transformations (i.e. rotations and translations since the background metric is flat FRW).

The importance of the SVT decomposition is that equations regarding different types of perturbations decouple at linear order. This means that one can solve equations for scalars separately from those for vectors and tensors. At higher orders this is no longer true and equations become coupled [38]. The SVT decomposition is based on Helmoltz theorem. In representation theory, this corresponds to decomposing perturbations under the group of spatial rotations. Scalar perturbations have spin 0, vector ones have spin 1 and tensors have spin 2.

The coordinate transformations affect the aforementioned split between spatial and temporal components. Thus we need to deduce the transformation laws of these quantities under an infinitesimal coordinate transformation (2.6). First, it is useful to decompose the coordinate displacement ξ^μ of equation (2.6) as

$$\xi^0 = \alpha, \tag{2.16a}$$
$$\xi^i = \partial^i \beta + \gamma^i, \tag{2.16b}$$

where $\partial_i \gamma^i = 0$.

Let us start with a four-scalar $\rho = \bar{\rho} + \delta\rho$. The perturbation transforms under a coordinate change as

$$\widetilde{\delta\rho} = \delta\rho + \alpha\rho', \tag{2.17}$$

according to equations (2.10) and (2.13). A four-vector $u_\mu + \delta u_\mu$ transforms as

$$\widetilde{\delta u_\mu} = \delta u_\mu + \alpha u_\mu' + \partial_\mu \xi^\nu u_\nu \,. \tag{2.18}$$

Finally, tensors are gauge-invariant at first order, but they are not at higher orders.

In the following, we will refer to tensor quantities defined on $\mathcal{M}_0$ as four-tensors and to the spatial tensor quantities, defined via the SVT decomposition, simply as tensors.

2.3 Metric tensor

Before perturbing the metric, let us focus on the background metric, that is the flat FRW metric. The line element of this metric is given in conformal time by

$$ds^2 = a^2(\tau)\left(-d\tau^2 + \delta_{ij}dx^i dx^j\right). \tag{2.19}$$

The only non-zero Christoffel symbols are given by

$$\Gamma^0_{00} = \mathcal{H}\,, \tag{2.20a}$$
$$\Gamma^0_{ij} = \mathcal{H}\delta_{ij}\,, \tag{2.20b}$$
$$\Gamma^i_{0j} = \mathcal{H}\delta^i_{\ j}\,, \tag{2.20c}$$

where $\mathcal{H} \equiv a'/a$ and the prime denotes the derivative with respect to conformal time. The components of the Ricci tensor are

$$R_{00} = -3\mathcal{H}'\,, \tag{2.21a}$$
$$R_{ij} = (2\mathcal{H}^2 + \mathcal{H}')\delta_{ij}\,. \tag{2.21b}$$

Finally, the Ricci scalar is

$$R = \frac{6\mathcal{H}^2 + 6\mathcal{H}'}{a^2}\,. \tag{2.22}$$

Applying what previously explained, the metric can be split into

$$g_{\mu\nu}(\tau, \mathbf{x}) = \bar{g}_{\mu\nu}(\tau) + \delta g_{\mu\nu}(\tau, \mathbf{x})\,, \tag{2.23}$$

where the background flat FRW metric $\bar{g}_{\mu\nu}(\tau)$ is defined in equation (2.19). We decompose the metric perturbations into different terms, according to their transformation properties under spatial symmetries of the background. We only consider first order terms, being the generalization beyond our interests.

The perturbed line element of the flat FRW background can be written as

$$ds^2 = a^2(\tau)\left[-\left(1+2\phi\right)d\tau^2 + 2B_i d\tau dx^i + \left(\delta_{ij} + 2C_{ij}\right)dx^i dx^j\right], \tag{2.24}$$

where

$$B_i = \partial_i B - S_i\,, \tag{2.25}$$

$$C_{ij} = -\psi\delta_{ij} + \frac{1}{2}h_{ij} + \partial_i\partial_j E + \partial_{(i}F_{j)}\,, \tag{2.26}$$

and the previous quantities satisfy the constraints

$$\partial_i S^i = 0\,, \tag{2.27a}$$

$$\partial_i F^i = 0\,, \tag{2.27b}$$

$$h_{ii} = 0\,, \tag{2.27c}$$

$$\partial^i h_{ij} = 0\,. \tag{2.27d}$$

The perturbed metric depends on four scalars (ϕ, ψ, B, E), two vectors (S_i, F_i) and one tensor (h_{ij}). One scalar counts for one degree of freedom, one vector counts for two being divergenceless and one tensor counts for two since it is symmetric, divergenceless and traceless. Overall, they constitute ten degrees of freedom as one should expect because the metric itself has ten degrees of freedom. The gauge fixing procedure impose four additional constraints and thus only six degrees of freedom remain unbounded. Note that the comoving background spatial metric δ_{ij} is used to raise and lower spatial indices of vectors and tensors. If we used the perturbed metric to raise the indices, we would introduce second order terms, but we are studying only linear perturbations.

The contravariant metric can be deduced solving the constraint

$$g^{\mu\nu}g_{\nu\rho} = \delta^{\mu}{}_{\rho}\,, \tag{2.28}$$

which gives

$$g^{00} = -\frac{1}{a^2}\big(1 - 2\phi\big), \tag{2.29a}$$

$$g^{0i} = \frac{1}{a^2}B^i\,, \tag{2.29b}$$

$$g^{ij} = \frac{1}{a^2}\big(\delta^{ij} - 2C^{ij}\big). \tag{2.29c}$$

The transformations of the metric perturbations under a change of coordinates are given by (at first order)

$$\widetilde{\phi} = \phi + \mathcal{H}\alpha + \alpha'\,, \tag{2.30a}$$

$$\widetilde{\psi} = \psi - \mathcal{H}\alpha\,, \tag{2.30b}$$

$$\widetilde{B} = B - \alpha + \beta'\,, \tag{2.30c}$$

$$\widetilde{E} = E + \beta\,, \tag{2.30d}$$

for scalar quantities,

$$\widetilde{S}^i = S^i - \gamma^{i\prime}\,, \tag{2.31a}$$

$$\widetilde{F}^i = F^i + \gamma^i\,, \tag{2.31b}$$

for vectors and

$$\widetilde{h}_{ij} = h_{ij}\,, \tag{2.32}$$

for the tensor perturbation.

Some caution must be used. The variables introduced to characterize the perturbed metric are not defined in an unique way. Different conventions exist and we follow Mukhanov's notation [35] because the metric perturbation ψ can be interpreted as the intrinsic scalar curvature of spatial hypersurfaces.

The perturbed metric defines a time-like vector field

$$n_\mu \propto \frac{\partial \tau}{\partial x^\mu}\,, \tag{2.33}$$

which is orthogonal to hypersurfaces of constant τ. This vector field can be normalized imposing the constraint $n_\mu n^\mu = -1$. Its covariant derivative can be decomposed as

$$n_{\mu;\nu} = \frac{\theta}{3}\mathcal{P}_{\mu\nu} + \sigma_{\mu\nu} + \omega_{\mu\nu} - a_\mu n_\nu\,, \tag{2.34}$$

where $\mathcal{P}_{\mu\nu} \equiv g_{\mu\nu} + n_\mu n_\nu$ is the projection tensor orthogonal to n^μ, $\theta \equiv n^\mu{}_{;\mu} = 3H$ is the overall expansion rate,

$$\sigma_{\mu\nu} \equiv \frac{1}{2}\mathcal{P}_\mu{}^\alpha \mathcal{P}_\nu{}^\beta (n_{\alpha;\beta} + n_{\beta;\alpha}) - \frac{\theta}{3}\mathcal{P}_{\mu\nu} \tag{2.35}$$

is the symmetric and trace-free shear,

$$\omega_{\mu\nu} \equiv \frac{1}{2}\mathcal{P}_\mu{}^\alpha \mathcal{P}_\nu{}^\beta (n_{\alpha;\beta} - n_{\beta;\alpha}) \tag{2.36}$$

is the antisymmetric vorticity and $a_\mu \equiv n_{\mu;\nu}\, n^\nu$ is the acceleration. These quantities are named in such a way because they coincide with their Newtonian counterparts in fluid dynamics on spatial hypersurfaces. A similar decomposition can be performed for any time-like vector.

The scalar part of the shear is given by

$$\sigma^S_{ij} = \left(\partial_i\partial_j - \frac{1}{3}\delta_{ij}\nabla^2\right) a\sigma\,, \tag{2.37}$$

where

$$\sigma \equiv E' - B\,. \tag{2.38}$$

Its vector part is given by

$$\sigma^V_{ij} = a\left(F'_{(i,j)} - B_{(i,j)}\right), \tag{2.39}$$

and its tensor part by

$$\sigma^T_{ij} = \frac{a}{2}h'_{ij}\,. \tag{2.40}$$

The acceleration is given by $a_i = \phi_{,i}$, as in Newtonian mechanics. Finally, the expansion rate is

$$\theta = \frac{3}{a}\left(\mathcal{H} - \mathcal{H}\phi - \psi' + \frac{1}{3}\nabla^2\sigma\right). \tag{2.41}$$

2.4 Energy-momentum tensor

The matter perturbations affect the metric ones through Einstein equations. So we need to perturb the stress-energy tensor in order to get a consistent set of equations for the perturbed universe.

The stress-energy tensor for a fluid is given by [16]

$$T_{\mu\nu} = (\rho + P)u_\mu u_\nu + P g_{\mu\nu} + \pi_{\mu\nu}\,, \tag{2.42}$$

where ρ is the energy density of the fluid, P its pressure, $\pi_{\mu\nu}$ is the anisotropic stress tensor and

$$u^\mu = \frac{dx^\mu}{d\tau} \tag{2.43}$$

is its four-velocity that satisfies the constraint $u^\mu u_\mu = -1$. The anisotropic stress is subject to the conditions $\pi_{\mu\nu}u^\nu = 0$ and $\pi^\mu{}_\mu = 0$. The anisotropic stress vanishes for a perfect fluid and for minimally coupled to gravity scalar fields. The spatial part of the anisotropic stress can be decomposed into

$$\pi_{ij} = a^2\left(\Pi_{,ij} - \frac{1}{3}\delta_{ij}\nabla^2\Pi + \Pi_{(i,j)} + \Pi_{ij}\right), \tag{2.44}$$

where Π is a trace-free scalar, Π_i is a vector and Π_{ij} is a tensor.

Again, we split the energy density and the pressure into a background part and a small perturbation,

$$\rho = \bar{\rho} + \delta\rho, \tag{2.45a}$$

$$P = \bar{P} + \delta P. \tag{2.45b}$$

The four-velocity can be written as

$$u^\mu = \frac{1}{a}\left(\delta^\mu{}_0 + v^\mu\right). \tag{2.46}$$

From the constraint $u^\mu u_\mu = -1$, one can obtain

$$u^0 = \frac{1}{a}\left(1 - \phi\right), \tag{2.47}$$

$$u^i = \frac{1}{a}v^i. \tag{2.48}$$

The background components of the stress-energy tensor are given by

$$T^0{}_0 = -\bar{\rho}, \tag{2.49a}$$

$$T^0{}_i = 0\,, \tag{2.49b}$$

$$T^i{}_j = \delta^i{}_j\bar{P}, \tag{2.49c}$$

and the first order perturbations by

$$\delta T^0{}_0 = -\delta\rho, \tag{2.50a}$$

$$\delta T^0{}_i = \left(\bar{\rho} + \bar{P}\right)\left(v_i + B_i\right), \tag{2.50b}$$

$$\delta T^i{}_j = \delta P\,\delta^i{}_j + \frac{1}{a^2}\,\pi^i{}_j. \tag{2.50c}$$

2.4.1 Single scalar field

The action for a minimally coupled scalar field φ is given by

$$S = \int d^4x\sqrt{-g}\left(\frac{R}{2} + \mathcal{L}_\varphi\right), \tag{2.51}$$

where

$$\mathcal{L}_\varphi = -\frac{1}{2}g_{\mu\nu}\partial^\mu\varphi\partial^\nu\varphi - V(\varphi). \tag{2.52}$$

The energy momentum tensor is defined as

$$T_{\mu\nu} \equiv -\frac{2}{\sqrt{-g}}\frac{\delta S_\varphi}{\delta g^{\mu\nu}}. \tag{2.53}$$

The variation of the action is given by

$$\begin{aligned}\delta S_\varphi &= \int d^4x\left(\delta\sqrt{-g}\,\mathcal{L}_\varphi + \sqrt{-g}\,\delta\mathcal{L}_\varphi\right)\\ &= \int d^4x\sqrt{-g}\left(-\frac{1}{2}\partial_\mu\varphi\partial_\nu\varphi - \frac{1}{2}\mathcal{L}_\varphi g_{\mu\nu}\right)\delta g^{\mu\nu},\end{aligned} \tag{2.54}$$

where we have made use of

$$\delta\sqrt{-g} = -\frac{1}{2}\sqrt{-g}\,g_{\mu\nu}\delta g^{\mu\nu}. \tag{2.55}$$

Then, the energy-momentum tensor reads

$$\begin{aligned}T_{\mu\nu} &= \partial_\mu\varphi\partial_\nu\varphi + g_{\mu\nu}\mathcal{L}_\varphi\\ &= \partial_\mu\varphi\partial_\nu\varphi - \frac{1}{2}g_{\mu\nu}\partial_\alpha\varphi\partial^\alpha\varphi - g_{\mu\nu}V(\varphi).\end{aligned} \tag{2.56}$$

Comparing this expression with that of the stress-energy tensor (2.42) for a perfect fluid (i.e. $\pi_{\mu\nu} = 0$), one can identify

$$\rho = -\frac{1}{2}g^{\mu\nu}\partial_\mu\varphi\partial_\nu\varphi + V, \tag{2.57a}$$

$$P = -\frac{1}{2}g^{\mu\nu}\partial_\mu\varphi\partial_\nu\varphi - V, \tag{2.57b}$$

$$u_\mu = \frac{\partial_\mu\varphi}{\sqrt{g^{\alpha\beta}\partial_\alpha\varphi\partial_\beta\varphi}}, \tag{2.57c}$$

respectively with the energy density, the pressure and the four-velocity of the scalar field.

After having perturbed the field $\varphi(\tau, \mathbf{x}) = \bar{\varphi}(\tau) + \delta\varphi(\tau, \mathbf{x})$, the perturbed components of the stress-energy tensor for a scalar field are given by

$$T^0{}_0 = -\frac{1}{2a^2}\bar{\varphi}'^2 - V(\bar{\varphi}) + \frac{1}{a^2}\bar{\varphi}'(\phi\bar{\varphi}' - \delta\varphi') - V_{,\varphi}\delta\varphi, \tag{2.58a}$$

$$T^0{}_i = -\frac{1}{a^2}\bar{\varphi}'\,\partial_i\delta\varphi, \tag{2.58b}$$

$$T^i{}_j = \left(\frac{1}{2a^2}\bar{\varphi}'^2 - V(\bar{\varphi}) - V_{,\varphi}\delta\varphi + \frac{1}{a^2}\bar{\varphi}'(\delta\varphi' - \phi\bar{\varphi}')\right)\delta^i{}_j. \tag{2.58c}$$

At first order, scalar fields cannot affect vector or tensor perturbations of the metric.

2.5 Gauges

In cosmology different gauges can be fixed. As we have seen, there are no reasons to prefer a particular gauge than another, except for convenience in calculations or for the interpretation of the results. A gauge is chosen once the components of ξ^μ are fixed. Alternatively, one can fix the components of the metric (or other quantities) and hence fix the gauge through equations (2.30) and (2.31).

- **Longitudinal gauge.** Longitudinal gauge is also known as Newtonian or orthogonal zero-shear gauge. It is defined by the constraints

$$\widetilde{E} = 0\,, \tag{2.59a}$$

$$\widetilde{B} = 0\,. \tag{2.59b}$$

  In this gauge, equations are usually rather simple since the hypersurfaces of constant time are orthogonal to the worldlines of observers at rest in the spatial coordinates (since $B = 0$).

- **Spatially flat gauge.** Spatially flat gauge is defined through the constraints

$$\widetilde{\psi} = 0\,, \tag{2.60a}$$

$$\widetilde{E} = 0\,, \tag{2.60b}$$

$$\widetilde{F}_i = 0\,. \tag{2.60c}$$

  In this gauge, the spatial metric induced on spatial hypersurfaces has no scalar or vector perturbations. The perturbations of scalar quantities are gauge-invariant in this gauge. This gauge is chosen when we need to focus on the inflaton perturbations rather than the perturbations of the metric.

- **Synchronous gauge.** Synchronous gauge is defined through the constraints

$$\widetilde{\phi} = 0\,, \tag{2.61a}$$

$$\widetilde{B}_i = 0\,. \tag{2.61b}$$

  In this gauge, the proper time for observers at fixed spatial coordinates coincides with cosmic time. This simplifies the equations of motion since proper time can be used instead of cosmic time.

- **Comoving orthogonal gauge.** The comoving orthogonal gauge is defined by choosing spatial coordinates such that the fluid is seen at rest, i.e.

$$\widetilde{v}_i = 0\,. \tag{2.62}$$

- **Uniform density gauge.** In the uniform density gauge, the universe is foliated by uniform density

$$\widetilde{\delta\rho} = 0 \tag{2.63}$$

  hypersurfaces.

2.6 Gauge-invariant quantities

Gauge-invariant variables are very useful since they do not depend on the gauge choice. Observable quantities are gauge-invariant since, once a measurement has been performed, the result is unambiguous and it cannot depend on which coordinates the observer wants to employ. Notice that there exist quantities that are gauge-invariant at some order in perturbation theory but are not gauge-invariant strictly speaking (for example, the tensor perturbation h_{ij} of the metric). Combining gauge-dependent quantities it is possible to construct gauge-invariant variables. Furthermore, infinite gauge-invariant quantities exist since any combination of gauge-invariant quantities will obviously be gauge-invariant.

The variables

$$\Phi = \phi + \mathcal{H}(B - E') + (B - E')', \tag{2.64}$$

$$\Psi = \psi - \mathcal{H}(B - E'), \tag{2.65}$$

are gauge-invariant as can be demonstrated from the transformation equations (2.30). These variables were introduced by Bardeen [46]. These are the simplest gauge-invariant quantities derived from the metric, other possibilities are more complex. A gauge invariant vector is

$$\hat{\Phi}_i = F_i' + S_i, \tag{2.66}$$

and a tensor is simply given by h_{ij}.

Eventually, there are two approaches to make calculations. One can fix the gauge and compute all the quantities in this gauge. Alternatively, one can rely only on gauge-invariant quantities. Both options have advantages and drawbacks. Fixing the gauge can simplify calculations but it can introduce gauge artefacts, i.e. unphysical terms. On the other hand, using only gauge-invariant quantities might be more complex but they are certainly physical.

2.6.1 Comoving curvature perturbation

The intrinsic spatial curvature on constant time hypersurfaces is given by

$$R^{(3)} = \frac{4}{a^2}\nabla^2\psi. \tag{2.67}$$

However, the curvature perturbation ψ is not gauge-invariant (as can be inferred from (2.30b)).

Consider the *comoving slicing* in which the constant time hypersurfaces are orthogonal to the worldlines of comoving observers. During inflation, they measure $\delta\varphi_{com} = 0$. Since $\delta\varphi$ transforms as $\widetilde{\delta\varphi} = \delta\varphi - \bar{\varphi}'\delta\tau$,

$$\delta\tau = \frac{\delta\varphi}{\bar{\varphi}'} = \alpha \tag{2.68}$$

is the time shift necessary to go from a slice with generic $\delta\varphi$ to a slice with $\delta\varphi_{com} = 0$. Hence, the quantity

$$\mathcal{R} \equiv \psi + \mathcal{H}\frac{\delta\varphi}{\bar{\varphi}'}, \tag{2.69}$$

called comoving curvature perturbation, is gauge-invariant by construction. It represents the gravitational potential on comoving hypersurfaces where $\delta\varphi = 0$, that is $\mathcal{R}|_{\delta\varphi=0} = \psi$.

2.6.2 Uniform energy density slicing

The choice of the slicing is arbitrary, so let us consider a different possibility from the comoving slicing. The slicing with null energy density perturbation $\delta\rho = 0$ is called uniform energy density slicing. The time-displacement $\delta\tau = \delta\rho/\bar{\rho}' = \alpha$ allows to switch from a generic slice to one with $\delta\rho_{unif} = 0$. Therefore, the quantity

$$\zeta \equiv -\psi - \mathcal{H}\frac{\delta\rho}{\bar{\rho}'} \tag{2.70}$$

is gauge-invariant. It represents the gravitational potential on slices of uniform energy density, that is $\zeta|_{\delta\rho=0} = -\psi$.

Using the continuity equation

$$\bar{\rho}' + 3\mathcal{H}(\bar{\rho} + \bar{P}) = 0\,, \tag{2.71}$$

the curvature ζ can be rewritten as

$$\zeta = -\psi + \frac{\delta\rho}{3(\bar{\rho} + \bar{P})}\,. \tag{2.72}$$

During inflation $\bar{\rho} + \bar{P} = a^{-2}\,\bar{\varphi}'^2$ and the perturbation $\delta\varphi$ is frozen on superhorizon scales. Furthermore, $\delta\rho \simeq -3\mathcal{H}a^{-1}\,\bar{\varphi}'\delta\varphi$ in the slow-roll approximation. Hence,

$$\zeta = -\psi - \mathcal{H}\frac{\delta\varphi}{\bar{\varphi}'} = -\mathcal{R}\,. \tag{2.73}$$

The curvature perturbation on uniform energy density slices ζ coincides with the comoving curvature perturbation $\mathcal{R}$ on superhorizon scales.

2.6.3 Sasaki-Mukhanov variable

In the spatially flat gauge, the curvature perturbation vanishes, $\psi_{flat} = 0$. It is easy to show that the quantity

$$Q \equiv \frac{\bar{\varphi}'}{\mathcal{H}}\mathcal{R} = \delta\varphi + \psi\frac{\bar{\varphi}'}{\mathcal{H}} \tag{2.74}$$

is gauge invariant. It is dubbed Sasaki-Mukhanov variable and it represents the inflaton perturbation on spatially flat slices, i.e. $Q|_{\psi=0} = \delta\varphi$.

2.7 Perturbed equations

2.7.1 Einstein equations

Einstein equations with $\Lambda = 0$ read

$$R_{\mu\nu} - \frac{1}{2}g_{\mu\nu}R = 8\pi G\,T_{\mu\nu}\,. \tag{2.75}$$

Using the previous results (in particular equations (2.21b), (2.22) and (2.42)), the non-vanishing components are

$$3\mathcal{H}^2 = 8\pi G a^2 \bar{\rho}, \tag{2.76a}$$

$$\big(\mathcal{H}^2 + 2\mathcal{H}'\big)\delta_{ij} = -8\pi G a^2 \bar{P}\delta_{ij}\,. \tag{2.76b}$$

It is trivial to show that the last equations coincide with Friedmann equations (1.8).

Einstein equations (2.75) can be perturbed using the previous definitions and results. The (00) equation is given by

$$3\mathcal{H}(\mathcal{H}\phi + \psi') - \nabla^2(\psi + \mathcal{H}\sigma) = -4\pi G a^2 \delta\rho. \tag{2.77}$$

The $(0i)$ equation is given by

$$\psi' + \mathcal{H}\phi = -4\pi G a^2(\bar{\rho} + \bar{P})V\,, \tag{2.78}$$

where

$$V \equiv v + B \tag{2.79}$$

is the total covariant velocity perturbation. The off-trace equation reads

$$\sigma' + 2\mathcal{H}\sigma + \psi - \phi = 8\pi G a^2 \Pi, \tag{2.80}$$

and the trace one is

$$\psi'' + 2\mathcal{H}\psi' + \mathcal{H}\phi' + \big(\mathcal{H}^2 + 2\mathcal{H}'\big)\phi = 4\pi G a^2 \left(\delta P + \frac{2}{3}\nabla^2\Pi\right). \tag{2.81}$$

Equations (2.77) and (2.78) can be restated in terms of the curvature perturbations (2.69) and (2.70) as

$$\Psi' + \mathcal{H}\Phi - \frac{\mathcal{H}' - \mathcal{H}^2}{\mathcal{H}}(\Psi + \zeta) - \frac{1}{3\mathcal{H}}\nabla^2\Psi = 0\,, \tag{2.82a}$$

$$\Psi' + \mathcal{H}\Phi + \frac{\mathcal{H}' - \mathcal{H}^2}{\mathcal{H}}(\mathcal{R} - \Psi) = 0\,. \tag{2.82b}$$

The last equations can be combined to give

$$\nabla^2\Psi = -3\big(\mathcal{H}' - \mathcal{H}^2\big)(\zeta + \mathcal{R})\,, \tag{2.83}$$

which is the gauge-invariant generalization of the Poisson equation in Newtonian gravity.

Equation (2.80) rewritten in the longitudinal gauge reads

$$\Psi - \Phi = 8\pi G a^2 \Pi, \tag{2.84}$$

which is a constraint equation for the variables Ψ and Φ. Notice that $\Psi = \Phi$ if the anisotropic stress Π vanishes.

2.7.2 Energy and momentum conservation

The continuity equation for the energy momentum tensor,

$$\nabla_\mu T^{\mu\nu} = 0\,, \tag{2.85}$$

implies the continuity equation (2.71) (the other components vanish). Perturbing this equation gives the evolution equations for the perturbed quantities, i.e.

$$\delta\rho' + 3\mathcal{H}(\delta\rho + \delta P) + (\rho + P)\left(\nabla^2(V+\sigma) - 3\psi'\right) = 0\,, \tag{2.86a}$$

$$V' + \left(1 - 3c_s^2\right)\mathcal{H}V + \phi + \frac{1}{\rho + P}\left(\delta P + \frac{2}{3}\nabla^2\Pi\right) = 0\,, \tag{2.86b}$$

where

$$c_s^2 \equiv \frac{P'}{\rho'} \tag{2.87}$$

is the adiabatic speed of sound.

2.8 Adiabatic and entropy perturbations

Let us consider a system composed by many fluids or fields labelled by capital letter indices. This is a natural circumstance since in our Universe different species (such as photons, baryons, neutrinos,...) coexist and others could have in the past.

Consider the energy density. In a n-component system, the energy perturbations can be split into an overall density perturbation and $n-1$ relative density perturbations between the components. The total density perturbation is gauge-dependent due to equation (2.17). However the difference between two perturbations $\delta\rho_I - \delta\rho_J$ can be made gauge-invariant easily defining the relative density perturbation as

$$\delta\rho_{IJ} = \delta\rho_I - \frac{\rho_I'}{\rho_J'}\delta\rho_J\,. \tag{2.88}$$

The quantity $\delta\rho_{IJ}$ corresponds to $\delta\rho_I$ on the surfaces of uniform density of the fluid J.

Adiabatic perturbations are perturbations in the total energy density. Conversely, *entropy perturbations* are fluctuations between the different components of the system that leave the total energy unperturbed. Thus, adiabatic perturbations affect the intrinsic spatial curvature, while entropy ones do not. For this reason, the adiabatic perturbations are also called curvature and the entropy ones are called isocurvature. The entropy perturbations can be sourced by the anisotropic stress or by the presence of more fluids.

In the n-component system, there are one adiabatic perturbation and $n-1$ entropy ones. For the adiabatic perturbations,

$$\frac{\delta\rho_I}{\rho_I'} = \frac{\delta\rho_J}{\rho_J'} = \delta\tau\,. \tag{2.89}$$

The adiabatic perturbations can be visualized as small displacement along the background trajectory[5]. Notice that a time-displacement has the same effect on all the components. Conversely,

[5]Consider a function $\rho(\tau)$. Then, $\delta(\rho(\tau)) = \rho'\delta\tau$.

for entropy perturbations,

$$\frac{\delta\rho_I}{\rho_I'} \neq \frac{\delta\rho_J}{\rho_J'}\,. \tag{2.90}$$

They are associated to perturbations off the background trajectory.

In order to characterize the two type of fluctuations, it is customary to introduce the gauge-invariant relative perturbation

$$S_{IJ} = 3\mathcal{H}\left(\frac{\delta\rho_J}{\rho_J'} - \frac{\delta\rho_I}{\rho_I'}\right) = 3\big(\zeta_I - \zeta_J\big), \tag{2.91}$$

where $\zeta_I \equiv -\psi - \mathcal{H}\delta\rho_I/\rho_I'$. Notice that $S_{IJ} = 0$ for adiabatic perturbations and it does not vanish for entropy perturbations.

2.8.1 Non-adiabatic pressure

For a generic fluid, its pressure is a function of two thermodynamic quantities. In cosmology, the energy density ρ and the entropy S are usually preferred among the others. Therefore, the fluctuations of the pressure $P(\rho, S)$ are given by

$$\delta P = \left.\frac{\partial P}{\partial\rho}\right|_S \delta\rho + \left.\frac{\partial P}{\partial S}\right|_\rho \delta S, \tag{2.92}$$

where

$$c_s^2 = \left.\frac{\partial P}{\partial\rho}\right|_S \tag{2.93}$$

is the (squared) sound of speed. Moreover,

$$\delta P_{ad} \equiv \frac{\partial P}{\partial\rho}\delta\rho, \tag{2.94}$$

$$\delta P_{nad} \equiv \frac{\partial P}{\partial S}\delta S, \tag{2.95}$$

are, respectively, the adiabatic and non-adiabatic pressure perturbations. The non-adiabatic pressure can be sourced only by entropy perturbations (and hence it is non-null for imperfect fluids or for a system composed by many components).

2.8.2 Conservation of ζ

Rewriting the conservation equation (2.86a) in terms of the curvature perturbation on uniform density slices ζ (2.70), we get

$$\zeta' = -\mathcal{H}\frac{\delta P_{nad}}{\rho + P} - \Sigma_V\,, \tag{2.96}$$

where

$$\Sigma_V \equiv \frac{1}{3}\nabla^2(V + \sigma)\,, \tag{2.97}$$

i.e. it is the divergence of the velocity in the longitudinal gauge. Therefore, the curvature perturbation ζ is constant for adiabatic perturbations when the scalar shear Σ_V is negligible

or on superhorizon scales (i.e. when the Laplacian can be neglected). Indeed, using the definition (2.70) of ζ and the Bardeen potential Ψ (2.65), the previous equation becomes

$$\frac{\Sigma_V}{\mathcal{H}} = \frac{1}{3\mathcal{H}^2}\nabla^2(\zeta + \Psi) + \frac{2\rho}{3(\rho + P)}\left(\frac{\nabla^2}{\mathcal{H}^2}\right)^2 \Psi\,. \tag{2.98}$$

Hence, ζ is constant for adiabatic perturbations on superhorizon scales $k \ll \mathcal{H}$. Thanks to this property, the curvature perturbation ζ is usually employed to characterize the primordial density perturbations on superhorizon scales.

Chapter 3

Primordial non-Gaussianities

> "Experimental confirmation of a prediction is merely a measurement. An experiment disproving a prediction is a discovery."
>
> Enrico Fermi

The role of Gaussian distribution in probability theory is so central that it is also called normal. The Gaussian distribution is ubiquitous and it describes many different experimental sets. Furthermore, the central limit theorem guarantees a privileged position to the Gaussian distribution. This theorem states that the set of a sufficiently large number of independent random variables is normally distributed. This explains partially why the Gaussian distribution is so universal. We could fill this page with examples of Gaussian distributed phenomena, but we recall just one of them central for our discussion. We want to remind that the ground state wave function of the quantum harmonic free oscillator is normally distributed. The importance of this example relies on the fact that, in the formalism of second quantization, a field is given by a superposition of operators related to the harmonic oscillator, as in (1.49). These operators create and destroy oscillation modes (i.e. quanta) of given energy. Therefore on a very simple consideration, we could expect that inflaton perturbations are (almost) Gaussian quantum fields.

Although many phenomena ranging from physics to economy can be described completely by this probability density function, Gaussian is not the whole story, as it will be shown. In fact, casual variables that look Gaussian at first sight may be characterized by some deviations from "normality". In this chapter, we will see how to characterize these deviations and the importance of non-Gaussianities in cosmology.

In section 3.1, the concept of Gaussian random field will be defined. In addition to this we will see how to describe a non-Gaussian distribution. In section 3.2, we will introduce the concept of bispectrum, which is analogous to that of power spectrum. In addition to this, we will see how to specify its properties. In the following two sections, we will introduce two standard techniques employed to calculate bispectra in cosmology. In section 3.3, we will review the in-in formalism following Weinberg's treatment [47] and, in 3.4, the so-called δN formalism. In the final section 3.5, we will discuss the importance of non-Gaussianities from an observational point of view. In particular, we will explain how they can distinguish among different inflationary

mechanisms.

In this chapter we will always consider primordial (i.e. generated during inflation) non-Gaussianities. We are not interested in post-inflationary production of non-Gaussianities. Indeed, any nonlinearity in the Universe can introduce non-Gaussianities into perturbations that were initially Gaussian. For more details see [48] and references therein. We refer to appendix C for the relationship between non-Gaussianities and the CMB anisotropies.

A complete review on cosmological primordial non-Gaussianities was written by N. Bartolo, E. Komatsu, S. Matarrese and A. Riotto [49]; a more recent one was written by X. Chen [50]. The latest observational results can be found in *Planck* collaboration's paper [48].

3.1 Non-Gaussian random fields

In this section, we will define what a Gaussian random field is and how we can characterize deviations from Gaussianity. Consider a real field $\phi(\mathbf{x})$, where $\mathbf{x}$ is a coordinate. Its Fourier transform is given by

$$\phi(\mathbf{x}) = \int \frac{d^3k}{(2\pi)^3}\phi(\mathbf{k})e^{i\mathbf{k}\cdot\mathbf{x}}, \tag{3.1}$$

where $\phi(\mathbf{k})$ can be parametrized introducing two real functions

$$\phi(\mathbf{k}) = a_{\mathbf{k}} + ib_{\mathbf{k}}\,. \tag{3.2}$$

Since the field is real, these functions should satisfy the conditions $a_{\mathbf{k}} = a_{-\mathbf{k}}$ and $b_{\mathbf{k}} = -b_{-\mathbf{k}}$. In addition, the amplitude of the field can be written as $|\phi(\mathbf{k})|^2 = a_{\mathbf{k}}^2 + b_{\mathbf{k}}^2$. Knowing the set of coefficients $(a_{\mathbf{k}}, b_{\mathbf{k}})$ is sufficient to completely characterize the field $\phi(\mathbf{x})$. Then, specifying the probability density functions (PDF) of $a_{\mathbf{k}}$ and $b_{\mathbf{k}}$ is equivalent to determine that of $\phi(\mathbf{x})$.

The field $\phi(\mathbf{x})$ is said to be a Gaussian random field if the functions $a_{\mathbf{k}}$ and $b_{\mathbf{k}}$ are drawn, for every $\mathbf{k}$, from the Gaussian distribution

$$\mathcal{P}(a_{\mathbf{k}}, b_{\mathbf{k}}) = \frac{1}{\pi\sigma_k^2}\exp\left(-\frac{a_{\mathbf{k}}^2 + b_{\mathbf{k}}}{\sigma_k^2}\right). \tag{3.3}$$

The latter equation fixes the probability density function of the pair $(a_{\mathbf{k}}, b_{\mathbf{k}})$ with given $\mathbf{k}$. Notice that the distribution has zero mean and its normalization condition reads

$$\int_{-\infty}^{+\infty} da_{\mathbf{k}} \int_{-\infty}^{+\infty} db_{\mathbf{k}} \frac{1}{\pi\sigma_k^2}\exp\left(-\frac{a_{\mathbf{k}}^2 + b_{\mathbf{k}}^2}{\sigma_k^2}\right) = 1\,. \tag{3.4}$$

In order to generalize the PDF (3.3) to the probability density function of the field $\phi(\mathbf{x})$, we should introduce the functional

$$\mathcal{P}[\phi(\mathbf{k})] = \frac{1}{\pi\sigma_k^2}\exp\left(-\frac{|\phi(\mathbf{k})|^2}{\sigma_k^2}\right). \tag{3.5}$$

Notice that, in general, the variance $\sigma_{\mathbf{k}}^2$ may depend on the direction, but we have assumed statistical isotropy and hence it is only a function of the modulus of the vector $\mathbf{k}$. The statistical

isotropy is a very good approximation in cosmology due to isotropy and homogeneity of the Universe.

Since we are dealing with a probability distribution, we are not interested in the value assumed by a field at a point, but rather in the probability that the field assumes that value (or better an interval of values) in a certain region. In addition to this, experiments deal with only one realization (the measured value) among all the possible ones. Thus, it is necessary to average over the ensemble of possible realizations in order to compare observations with predictions. The expectation value of an observable $Q[\phi(\mathbf{k})]$, functional of the field $\phi(\mathbf{k})$, is given by

$$\langle Q[\phi(\mathbf{k})]\rangle = \int \mathcal{D}\phi \; Q[\phi(\mathbf{k})]P[\phi(\mathbf{k})]\,, \tag{3.6}$$

where the integral is made over all possible field configurations in momentum space. The meaning of this expression should be clear, even not knowing path integral formalism. The expectation value of the observable $Q[\phi(\mathbf{k})]$ is obtained averaging (i.e. integrating) over all the possible values that it can assume. However these values may have different probability of being observed and hence they should be weighted[1] by the functional $P[\phi(\mathbf{k})]$.

If the PDF is a Gaussian like (3.3), the expectation value of Q is

$$\langle Q[\phi(\mathbf{k})]\rangle = \prod_{\mathbf{k}} \int da_{\mathbf{k}} \int db_{\mathbf{k}}\, Q[\phi(\mathbf{k})] \frac{1}{\pi\sigma_k^2} \exp\left(-\frac{a_{\mathbf{k}}^2 + b_{\mathbf{k}}^2}{\sigma_k^2}\right). \tag{3.7}$$

The integral over all configurations has become $\prod_{\mathbf{k}} \int da_{\mathbf{k}} \int db_{\mathbf{k}}$, since $a_{\mathbf{k}}$ and $b_{\mathbf{k}}$ parametrize the possible configurations. Despite its appearance, this formula is rather simple to use in calculations. For example, let us compute the expectation value of $Q[\phi(\mathbf{k})] = a_{\mathbf{p}} a_{\mathbf{p}'}$, that is

$$\begin{aligned}\langle a_{\mathbf{p}} a_{\mathbf{p}'}\rangle &= \prod_{\mathbf{k}} \int da_{\mathbf{k}} \int db_{\mathbf{k}}\, a_{\mathbf{p}} a_{\mathbf{p}'} \frac{1}{\pi\sigma_k^2} \exp\left(-\frac{a_{\mathbf{k}}^2 + b_{\mathbf{k}}^2}{\sigma_k^2}\right) \\ &= \frac{\sigma_p^2}{2}\delta^3(\mathbf{p}+\mathbf{p}')\,.\end{aligned} \tag{3.8}$$

To obtain this result, recall that $a_{\mathbf{k}} = a_{-\mathbf{k}}$ and that the integral on the real axis of an odd function is null (the Gaussian is an even function). Furthermore, notice that the integral over $b_{\mathbf{k}}$ is trivial. Thanks to this result, it is now easy to evaluate

$$\langle \phi(\mathbf{p})\phi(\mathbf{p}')\rangle = \langle a_{\mathbf{p}} a_{\mathbf{p}'}\rangle - \langle b_{\mathbf{p}} b_{\mathbf{p}'}\rangle = \sigma_p^2 \delta^3(\mathbf{p}+\mathbf{p}')\,, \tag{3.9}$$

where the cross terms vanish. This is an important result. The correlation function (in Fourier space) is related to the dispersion of the Gaussian distribution. Obviously, an analogous calculation can be performed in coordinate space. Last equation coincides exactly with (1.68) with the definition $\sigma_k^2 = (2\pi)^3 P(k)$. Notice that isotropy and homogeneity manifest themselves through the presence of the δ function.

[1]The expectation value of a function $f(x)$ of the random variable x is given by $\langle f(x)\rangle = \int dx f(x) P(x)$, where $P(x)$ is the probability density function of x.

Since the Gaussian PDF is even under parity, all odd expectation values vanish. Furthermore, all even expectation values can be written in terms of the two point correlation function[2]. For example, it is straightforward to show that

$$\langle\phi(\mathbf{p}_1)\phi(\mathbf{p}_2)\phi(\mathbf{p}_3)\rangle = 0,$$
$$\langle\phi(\mathbf{p}_1)\phi(\mathbf{p}_2)\phi(\mathbf{p}_3)\phi(\mathbf{p}_4)\rangle = \sigma^2_{p_1}\sigma^2_{p_3}\delta^3(\mathbf{p}_1+\mathbf{p}_2)\delta^3(\mathbf{p}_3+\mathbf{p}_4) + 2 \text{ permutations}.$$

This result should not be surprising. Notice that, in equation (3.5), we assumed that the mean value of the distribution is zero (and this can always be achieved through a shift of the casual variable). However, a Gaussian distribution is completely determined if one fixes the mean and the variance. Therefore, we expect that all the correlators can be written in terms of the mean and the variance.

If a distribution is non-Gaussian, the latest properties will be no more valid. In particular, the odd correlators do not vanish. There exists only a way to be Gaussian, but possibly infinite ways to be non-Gaussian. Hence, one needs in principle to know all the correlation functions in order to characterize an unknown distribution. Luckily, in cosmology, we know that primordial perturbations are very well approximated by a Gaussian distribution (so far there is no evidence of primordial non-Gaussianity since all data are in agreement with an underlying Gaussian PDF [48] for the initial seeds of structure formation) and hence we expect small deviations from it. Therefore, it is natural to study the lowest order odd correlators to identify promising markers of non-Gaussianities. The one-point correlation function is not significant since one can always shift the peak of the distribution to make it coincide with its mean. Thus, the lowest order correlator characterizing non-Gaussianities is the three-point correlation function, or *bispectrum*.

Finally, we consider an explicit example of non-Gaussian probability density function. Let us introduce a skewness parameter $S_k \ll 1$ into (3.3),

$$\mathcal{P}(a_{\mathbf{k}}, b_{\mathbf{k}}) = \frac{1}{\pi\sigma_k^2}\exp\left(-\frac{a_{\mathbf{k}}^2+b_{\mathbf{k}}^2}{\sigma_k^2}\right)\left(1+S_k\frac{a_{\mathbf{k}}}{\sigma_k}\right).$$

The first correlators are given by

$$\langle\phi(\mathbf{p})\rangle = \frac{\sqrt{\pi}}{2}\sigma_p S_p,$$
$$\langle\phi(\mathbf{p})\phi(\mathbf{p}')\rangle = \sigma_p^2\delta^3(\mathbf{p}+\mathbf{p}'),$$
$$\langle\phi(\mathbf{p})\phi(\mathbf{p})\phi(\mathbf{p})\rangle = S_p\sigma_p^4.$$

Notice that the power spectrum coincides with that of a Gaussian distribution, but the one and three-point functions are not null. In addition to this, notice that the three-point correlation function is given by the two-point correlation function squared.

[2]This is a well-known result in QFT for free theories. For example, see [51].

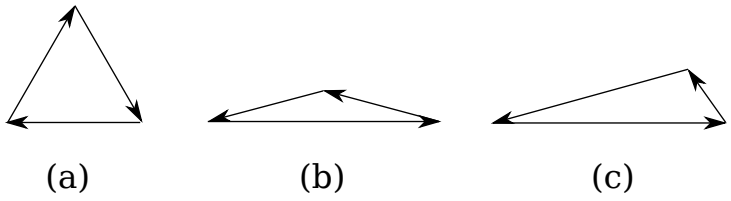

Figure 3.1: Possible momentum configurations: equilateral (a), folded (b) and squeezed (c).

3.2 Bispectrum: shape, running and amplitude

Non-Gaussianities are characterized, at lowest order, by the three-point correlation function, or equivalently by its Fourier transform, the bispectrum. Assuming as always homogeneity and isotropy, it can be proven that

$$\langle \delta_{\mathbf{k}_1} \delta_{\mathbf{k}_2} \delta_{\mathbf{k}_3} \rangle = (2\pi)^3 \delta^3(\mathbf{k}_1 + \mathbf{k}_2 + \mathbf{k}_3) B(k_1, k_2, k_3)\,, \tag{3.10}$$

where $B(k_1, k_2, k_3)$ is the bispectrum which depends only on the moduli of the momenta thanks to statistical isotropy. Notice that the Dirac delta forces the vectors $\mathbf{k}_i$ to form a triangle. The power spectrum depends only on one parameter: the amplitude of the scale considered. Conversely, the bispectrum is determined by three scales k_1, k_2 and k_3. Alternatively, in order to characterize the bispectrum, one can fix the overall momentum and two ratios between the momenta.

The bispectrum of the primordial curvature perturbation ζ (2.70) can be written in terms of the adimensional power spectrum evaluated at a fiducial scale k_0 introducing a dimensionless function $S(k_1, k_2, k_3)$,

$$B(k_1, k_2, k_3) = (2\pi)^4 \frac{S(k_1, k_2, k_3)}{(k_1 k_2 k_3)^2} \tilde{\mathcal{P}}_\zeta^2(k_0)\,. \tag{3.11}$$

Usually, the fiducial power spectrum is normalized such as $\tilde{\mathcal{P}}_\zeta = \tilde{\mathcal{P}}_\zeta(k_{Planck}) = 2.2 \cdot 10^{-9}$, where $k_{Planck} = 0.05\,\mathrm{Mpc}^{-1}$ [6]. If the bispectrum is scale-invariant, the function S is invariant under a rescaling of all the momenta. Different conventions are used in literature, but the plots of bispectra are usually based on S.

The dependence of $S(k_1, k_2, k_3)$ on the momenta is studied in two ways. If we fix the sum $K = \sum_i k_i$ and change the ratios k_2/k_1 and k_3/k_1, we are varying the *shape* of the bispectrum. Since the momenta are constrained to form a triangle, it is natural to study its shape and usually three types of shapes are inquired. The first one can be obtained if $k_1 \sim k_2 \sim k_3$ and it is known as "equilateral". If one of the momenta is almost equal to the sum of the others $k_1 \sim k_2 + k_3$, the shape is called "folded". Finally, if one momentum is negligible $k_1 \ll k_2 \sim k_3$ the shape is "squeezed" (or we say we are considering the so-called local limit). These shapes are represented in figure 3.1. If we keep the ratios of the momenta fixed and change the overall momentum K, we are studying the *running* of S. The shape is more valuable than running for bispectra that are nearly scale-invariant.

The amplitude, or *size*, of the bispectrum is denoted by the so-called non-linearity parameter

f_{NL} and it is defined through the matching limit

$$S(k_1, k_2, k_3) \xrightarrow{k_1=k_2=k_3} \frac{9}{10} f_{NL} \,. \tag{3.12}$$

The parameter f_{NL} can have a weak dependence on the overall momentum K which can be described by the index

$$n_{NG} - 1 \equiv \frac{d \ln f_{NL}}{d \ln K} \,, \tag{3.13}$$

in analogy with n_s and n_T.

Names have been given to different shapes of bispectra according to the dependence of S on the momenta. For the local bispectrum, S peaks at the squeezed triangle limit ($k_3 \ll k_1 = k_2$) as $\sim k_1/k_3$. The local bispectrum arises typically when non-Gaussianities are generated on super-horizon scales. The equilateral bispectrum peaks at the equilateral limit and the function S vanishes in the squeezed limit as $\sim k_3/k_1$. It is usually produced due to correlations between fluctuation modes of comparable wavelengths (i.e. the three perturbation modes mostly interact when they cross nearly simultaneously the cosmological horizon). The folded bispectrum reaches a maximum when $k_1 + k_2 \simeq k_3$. Let us also mention the so-called orthogonal bispectrum that generates a signal with a positive peak at the equilateral configuration and a negative peak at the folded configuration. For details on the various shapes we refer to [48–50, 52]

As an example, we consider the local bispectrum. The shape function of the local bispectrum has the form [53, 54]

$$S^{loc}(k_1, k_2, k_3) = \frac{3}{10} f_{NL}^{loc} \left(\frac{k_1^2}{k_2 k_3} + 2 \,\text{perm.} \right) . \tag{3.14}$$

In the squeezed limit $k_3 \ll k_1 \simeq k_2$, we obtain

$$\lim_{k_3 \ll k_1 \simeq k_2} S^{loc}(k_1, k_2, k_3) = \frac{3}{5} \frac{k_1}{k_3} f_{NL}^{loc} \,, \tag{3.15}$$

that has the aforementioned asymptotic behaviour. The prototypical example of a perturbation that can generate a bispectrum with the shape function S^{loc} is the local form of the Bardeen's gravitational potential Φ (2.64), that is [54–56]

$$\Phi(\mathbf{x}) = \Phi_L(\mathbf{x}) + f_{NL}^{loc} \left(\Phi_L^2(\mathbf{x}) - \langle \Phi_L^2(\mathbf{x}) \rangle \right) , \tag{3.16}$$

where $\Phi_L(\mathbf{x})$ is the linear Gaussian gravitational potential. The nonlinearity parameter f_{NL} represents the amplitude of a quadratic non-linear correction to Φ_L. The bispectrum is local since $\Phi_L(\mathbf{x})$ is always evaluated at the same position $\mathbf{x}$ into the previous expression.

3.3 The *in-in* formalism

The *in-in* formalism is a technique useful to calculate cosmological correlation functions generated during inflation. Historically, it was developed by J. Schwinger [57] and M. Keldysh [58] in the context of condensed matter. In cosmology, it was first used by R. Jordan [59] and became very popular recently since high precision data on CMB were available. Our treatment is based on Weinberg's one [47].

In cosmology, we deal with expectation values of operators written in terms of the field fluctuations. Let $\phi_a(\mathbf{x},t)$ be the fields and $\pi_\alpha(\mathbf{x},t)$ be their conjugate momenta (a labels different fields). Let Q be the operator we want to compute the expectation value. The operator Q is usually given by a combination of the field perturbations $\delta\phi_a$ and their perturbed conjugate momenta $\delta\pi_a$. Notice that the fluctuations may refer to scalar fields or metric perturbations. In the Heisenberg picture, the expectation value of Q is given by

$$\langle Q\rangle = \langle\Omega|\, Q(t)\,|\Omega\rangle\,, \tag{3.17}$$

where $|\Omega\rangle$ is the interacting theory vacuum state at the far past t_0 and t is generally the end of inflation. Note that the initial and final states are the same, conversely to Quantum Field Theory case. In fact, in Quantum Field Theory the most important observables are scattering amplitudes and particles are supposed not to be interacting in the far past and future. On the contrary, in cosmology we are interested in the expectation values of the fields at a fixed time and there is no evolution from one vacuum state in the past to one in the future.

The fields $\phi_a(\mathbf{x},t)$ and $\pi_\alpha(\mathbf{x},t)$ satisfy the usual equal-time commutation relations

$$[\phi_a(\mathbf{x},t),\pi_b(\mathbf{y},t)] = i\delta_{ab}\delta^3(\mathbf{x}-\mathbf{y})\,, \tag{3.18a}$$

$$[\phi_a(\mathbf{x},t),\phi_b(\mathbf{y},t)] = [\pi_a(\mathbf{x},t),\pi_b(\mathbf{y},t)] = 0\,. \tag{3.18b}$$

Their evolution is governed by Heisenberg equations

$$i\dot{\phi}_a(\mathbf{x},t) = [\phi_a(\mathbf{x},t),H]\,, \tag{3.19a}$$

$$i\dot{\pi}_a(\mathbf{x},t) = [\pi_a(\mathbf{x},t),H]\,, \tag{3.19b}$$

where

$$H[\phi,\pi] = \int d^3x\mathcal{H}[\phi,\pi] \tag{3.20}$$

is the Hamiltonian of the system which is a functional of the fields $\phi_a(\mathbf{x},t)$ and their conjugate momenta $\pi_a(\mathbf{x},t)$ (for brevity we have omitted the index a of the fields and their dependence on coordinates).

As usual in cosmology, the fields can be split into a background term and a fluctuation

$$\phi_a(\mathbf{x},t) = \bar{\phi}_a(t) + \delta\phi_a(\mathbf{x},t)\,, \tag{3.21a}$$

$$\pi_a(\mathbf{x},t) = \bar{\pi}_a(t) + \delta\pi_a(\mathbf{x},t)\,. \tag{3.21b}$$

Now comes the fundamental assumption regarding the fields. We suppose that the time-dependent background fields $\bar{\phi}_a(t)$ and $\bar{\pi}_a(t)$ are c-numbers and hence commute with the operators. The background evolution of the fields is governed by the equations of motion

$$\dot{\bar{\phi}}_a(t) = \frac{\partial\mathcal{H}}{\partial\bar{\pi}_a}\,, \tag{3.22a}$$

$$\dot{\bar{\pi}}_a(t) = -\frac{\partial\mathcal{H}}{\partial\bar{\phi}_a}\,. \tag{3.22b}$$

The commutation relations (3.18) become

$$[\delta\phi_a(\mathbf{x},t),\delta\pi_b(\mathbf{y},t)] = i\delta_{ab}\delta^3(\mathbf{x}-\mathbf{y}), \tag{3.23a}$$

$$[\delta\phi_a(\mathbf{x},t),\delta\phi_b(\mathbf{y},t)] = [\delta\pi_a(\mathbf{x},t),\delta\pi_b(\mathbf{y},t)] = 0. \tag{3.23b}$$

Since perturbations are small deviations from the classical trajectory, the Hamiltonian can be expanded as

$$H[\phi,\pi] = H[\bar{\phi},\bar{\pi}] + \sum_a \int d^3x \left(\frac{\partial\mathcal{H}}{\partial\bar{\phi}_a}\delta\phi_a + \frac{\partial\mathcal{H}}{\partial\bar{\pi}_a}\delta\pi_a\right) + \tilde{H}[\delta\phi,\delta\pi;t], \tag{3.24}$$

where $\tilde{H}$ collects all the higher order terms in perturbations. Inserting this expansion into the equations of motion (3.19) together with the split (3.21) and (3.22), we obtain the evolution equations of the perturbations

$$i\dot{\delta\phi}_a(\mathbf{x},t) = [\delta\phi_a(\mathbf{x},t),\tilde{H}], \tag{3.25a}$$

$$i\dot{\delta\pi}_a(\mathbf{x},t) = [\delta\pi_a(\mathbf{x},t),\tilde{H}]. \tag{3.25b}$$

As it is well known, the solutions can be written as

$$\delta\phi_a(\mathbf{x},t) = U^{-1}(t,t_0)\delta\phi_a(\mathbf{x},t_0)U(t,t_0), \tag{3.26a}$$

$$\delta\pi_a(\mathbf{x},t) = U^{-1}(t,t_0)\delta\pi_a(\mathbf{x},t_0)U(t,t_0), \tag{3.26b}$$

where the time evolution operator U satisfies

$$i\frac{d}{dt}U(t,t_0) = \tilde{H}[\delta\phi(t_0),\delta\pi(t_0);t]U(t,t_0), \tag{3.27}$$

with the initial condition $U(t_0,t_0) = 1$. Notice that we omitted to write the spatial dependence of the perturbed fields; from now on we will neglect to write it. Solving these equations is hard since $\tilde{H}$ contains interaction terms between the perturbations. In order to face this problem, the interaction picture can be introduced.

Let us decompose $\tilde{H}$ into

$$\tilde{H}[\delta\phi,\delta\pi;t] = H_0[\delta\phi,\delta\pi;t] + H_1[\delta\phi,\delta\pi;t], \tag{3.28}$$

where H_0 contains only kinematic terms, namely it does not contain interactions between perturbations as opposed to H_1. In order to account for the presence of interactions, we expand the operator U as a power series in H_1.

In the interaction picture, the equations of motion for the fields are

$$i\dot{\delta\phi}^I_a(\mathbf{x},t) = \left[\delta\phi^I_a(\mathbf{x},t), H_0[\delta\phi^I(t),\delta\pi^I(t);t]\right], \tag{3.29a}$$

$$i\dot{\delta\pi}^I_a(\mathbf{x},t) = \left[\delta\pi^I_a(\mathbf{x},t), H_0[\delta\phi^I(t),\delta\pi^I(t);t]\right], \tag{3.29b}$$

with the initial conditions

$$\delta\phi^I_a(t_0) = \delta\phi_a(t_0), \tag{3.30a}$$

$$\delta\pi^I_a(t_0) = \delta\pi_a(t_0). \tag{3.30b}$$

Notice that the interaction picture fields evolve as free fields satisfying linear wave equations. Obviously, difficulties are not eliminated as they are now involved in the evolution of the states. From equations (3.29) it follows that the time argument of $\delta\phi^I$ and $\delta\pi^I$ can be arbitrary and, in particular, we can choose

$$H_0[\delta\phi^I(t), \delta\pi^I(t); t] = H_0[\delta\phi(t_0), \delta\pi(t_0); t]. \tag{3.31}$$

The equations of motion (3.29) can be solved as done before introducing an unitary evolution operator U_0 such that

$$i\frac{d}{dt}U_0(t, t_0) = H_0[\delta\phi(t_0), \delta\pi(t_0); t]U_0(t, t_0), \tag{3.32}$$

with the initial condition $U_0(t_0, t_0) = 1$. Then, the interaction picture fields can be rewritten as

$$\delta\phi_a^I(\mathbf{x}, t) = U_0^{-1}(t, t_0)\delta\phi_a(\mathbf{x}, t_0)U_0(t, t_0), \tag{3.33a}$$
$$\delta\pi_a^I(\mathbf{x}, t) = U_0^{-1}(t, t_0)\delta\pi_a(\mathbf{x}, t_0)U_0(t, t_0). \tag{3.33b}$$

Combining equations (3.27) and (3.32), it is not difficult to show that

$$i\frac{d}{dt}\Big(U_0^{-1}(t, t_0)U(t, t_0)\Big) = U_0^{-1}(t, t_0)H_1[\delta\phi(t_0), \delta\pi(t_0); t]U(t, t_0). \tag{3.34}$$

Defining

$$F(t, t_0) \equiv U_0^{-1}(t, t_0)U(t, t_0), \tag{3.35}$$

and using equations (3.33), we get

$$i\frac{d}{dt}F(t, t_0) = H_I(t)F(t, t_0), \tag{3.36}$$

where we have defined

$$H_I(t) \equiv U_0(t, t_0)H_1[\delta\phi(t_0), \delta\pi(t_0); t]U_0^{-1}(t, t_0) = H_1[\delta\phi^I(t), \delta\pi^I(t); t], \tag{3.37}$$

i.e. the interaction Hamiltonian in the interaction picture. Notice that $F(t_0, t_0) = 1$. The solution of equation (3.36) is given by

$$F(t, t_0) = \mathrm{T}\exp\left(-i\int_{t_0}^{t} H_I(t)dt\right), \tag{3.38}$$

where T is the time-ordering operator. Finally, we build a time-evolution operator in the interaction picture. Let us come back to our original concern, that is the evaluation of the expectation value of an operator $Q[\delta\varphi(\mathbf{x}, t), \delta\pi(\mathbf{x}, t)]$. Applying the previous equalities, the interacting vacuum expectation value of Q is given by (omitting the spatial dependence of the fields)

$$\begin{aligned}
\langle Q\rangle &= \langle\Omega|\, Q[\delta\varphi(t), \delta\pi(t)]\,|\Omega\rangle \\
&= \langle\Omega|\, U^{-1}(t, t_0)\, Q[\delta\varphi(t_0), \delta\pi(t_0)]\, U(t, t_0)\,|\Omega\rangle \\
&= \langle\Omega|\, F^{-1}(t, t_0)U_0^{-1}(t, t_0)\, Q[\delta\varphi(t_0), \delta\pi(t_0)]\, U_0(t, t_0)F(t, t_0)\,|\Omega\rangle \\
&= \langle\Omega|\, F^{-1}(t, t_0)\, Q[\delta\varphi^I(t), \delta\pi^I(t)]\, F(t, t_0)\,|\Omega\rangle \\
&= \langle\Omega|\left[\bar{\mathrm{T}}\exp\left(i\int_{t_0}^{t} H_I(t)dt\right)\right] Q^I(t)\left[\mathrm{T}\exp\left(-i\int_{t_0}^{t} H_I(t)dt\right)\right]|\Omega\rangle,
\end{aligned} \tag{3.39}$$

where $\bar{\mathrm{T}}$ denotes anti-time-ordering. Notice that all the fields are written in the interaction picture since $H_I(t) = H_1[\delta\phi^I(t), \delta\pi^I(t); t]$ and $Q^I(t) = Q[\delta\phi^I(t), \delta\pi^I(t)]$. There is only one left issue to solve before applying this equation: how do we calculate the vacuum of the interacting theory? For example, in Quantum Field Theory this serious problem is avoided assuming that particles interact only for a finite time.

Since Q is a functional of cosmological perturbations, let us focus on a particular perturbation $\delta\phi^I(\mathbf{k}, t)$ expressed in Fourier space ($\mathbf{k}$ is a comoving wavelength). We can decompose this field using the mode functions $u(\mathbf{k}, t)$ as

$$\delta\phi^I(\mathbf{k}, t) = u(\mathbf{k}, t)a(\mathbf{k}) + u^*(-\mathbf{k}, t)a^\dagger(-\mathbf{k}), \tag{3.40}$$

where the annihilation a and creation $a^\dagger$ operators satisfy

$$[a(\mathbf{k}), a^\dagger(\mathbf{p})] = (2\pi)^3\delta^3(\mathbf{k} - \mathbf{p}), \tag{3.41}$$

$$[a(\mathbf{k}), a(\mathbf{p})] = [a^\dagger(\mathbf{k}), a^\dagger(\mathbf{p})] = 0, \tag{3.42}$$

and the mode functions satisfy the Wronskian condition

$$u(\mathbf{k}, t)\dot{u}^*(\mathbf{k}, t) - \text{c.c.} = i. \tag{3.43}$$

The mode functions are solutions of a second order differential equation and thus they are a linear superposition of two independent solutions. It is always[3] possible to find an early period during which the momentum of the mode is larger than the Hubble radius (i.e. it is sub-horizon) and to study the evolution over an interval shorter than a Hubble time. Under these assumptions, the equation of motion coincides with those in Minkowski space and the vacuum state is the Bunch-Davies vacuum. This vacuum state is annihilated by $a(\mathbf{k})$, that is $a(\mathbf{k})\,|0\rangle = 0$.

In equation (3.39), the vacuum of the interacting theory $|\Omega\rangle$ can be replaced [47] with the Bunch-Davies vacuum $|0\rangle$. The reason is the following. If each vertex of a diagram is connected only to other vertices, not to external lines, we have a vacuum fluctuation diagram. The identity

$$F^{-1}F = 1 \tag{3.44}$$

implies that there are not non-trivial vacuum fluctuations (unlike the case of ordinary Quantum Field Theory) since

$$\langle\Omega|\, F^{-1}F\,|\Omega\rangle = 1. \tag{3.45}$$

Hence, the vacuum of the interacting theory $|\Omega\rangle$ can be substituted with the Bunch-Davies vacuum $|0\rangle$ into equation (3.39).

Finally, the expectation value of the operator $Q(t)$ reads

$$\langle Q(t)\rangle = \langle 0|\left[\bar{\mathrm{T}}\exp\left(i\int_{t_0}^{t} H_I(t)dt\right)\right] Q^I(t)\left[\mathrm{T}\exp\left(-i\int_{t_0}^{t} H_I(t)dt\right)\right]|0\rangle. \tag{3.46}$$

[3]As long as field theory applies, this may not be true for a very early epoch. In addition to this, inflation should have occurred otherwise a scale would have become subhorizon only recently.

Expanding the exponentials, one can rewrite the previous expression as a series in powers of the interaction Hamiltonian H_I, that is

$$\langle Q(t)\rangle = \sum_{n=0}^{+\infty} \langle Q(t)\rangle^{(n)}\,, \tag{3.47}$$

where n refers to the number of interaction Hamiltonian into each term. It can be shown that the n-th order term of the previous expansion is given by [47]

$$\langle Q(t)\rangle^{(n)} = i^n \int_{t_0}^{t} dt_1 \int_{t_0}^{t_1} dt_2 \cdots \int_{t_0}^{t_{n-1}} dt_n \left\langle \Big[H^I(t_n), \Big[H^I(t_{n-1}), \dots \big[H^I(t_1), Q^I(t) \big] \Big] \Big] \right\rangle. \tag{3.48}$$

3.4 The δN formalism

The δN formalism [56, 60–62] is a powerful tool useful to calculate primordial power spectra and non-Gaussianity for superhorizon perturbations in multifield models. Such perturbations evolve classically because they are unaffected by microphysical processes. The δN formalism and the *in-in* formalism have the same predictions when they are both applicable, but the former is usually more convenient for computations.

Let us briefly remember what happens in single-field models. In the uniform density gauge, the curvature perturbation ζ (2.70) modifies the line element as

$$ds^2 = -dt^2 + e^{2\zeta} a^2(t) \delta_{ij} dx^i dx^j, \tag{3.49}$$

and it can be interpreted as a local rescaling of the scale factor. For superhorizon modes, ζ is frozen (non-adiabatic pressure is absent, see equation (2.96)). The superhorizon patches are casually disconnected and evolve independently (but in different ways since the perturbed scale factor depends on the position). This point of view is called "separate universe picture" [56, 63]. The difference between expansion rates of two zones can be characterized through the difference between their numbers of efoldings.

Let us have a look at the multifield case considering a set of scalar fields ϕ^I. We pick out an initial spatially flat hypersurface (both for the background and the perturbed manifold). This means there are no scalar perturbations of the spatial metric and all of them involve the scalar fields. We assume that the statistic of the fluctuations is known. On this slice, the studied modes should be superhorizon and we denote horizon-size patches with a coarse-grained comoving coordinate $\mathbf{x}$. We choose a final uniform density hypersurface, such that only the metric is perturbed (see figure 3.2).

The unperturbed fields $\bar{\phi}^I$ evolve classically to the unperturbed final slice during $N_0(\bar{\phi}^I)$ e-folds. The perturbed fields $\bar{\phi}^I + \delta\phi^I(\mathbf{x})$ evolve as well classically between the perturbed slices during $N(\bar{\phi}^I + \delta\phi^I)$ e-folds. The difference

$$\delta N = N(\bar{\phi}^I + \delta\phi^I) - N_0(\bar{\phi}^I) \tag{3.50}$$

equals the uniform-density curvature perturbation ζ (2.70) because of its definition [60, 61].

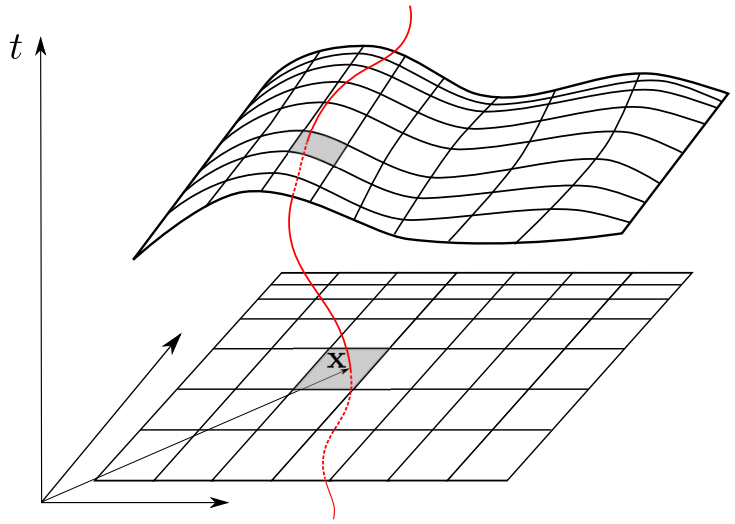

Figure 3.2: Separate universe picture in the δN formalism. Every patch should be thought as an independent universe, casually disconnected from the others. We depict the initial spatially flat slice and the final uniform density slice.

Being the fluctuations small, we can expand

$$\zeta = \delta N = N_{,I}\delta\phi^I + \frac{1}{2}N_{,IJ}\delta\phi^I\delta\phi^J + \mathcal{O}(\delta\phi^3)\,, \tag{3.51}$$

where we have made use of the shortened notation

$$N_{,I} \equiv \frac{\partial N}{\partial \phi^I}\,. \tag{3.52}$$

Notice that the curvature perturbation ζ and all the field perturbations $\delta\phi^I$ are evaluated at the same point in spacetime because we are considering superhorizon fluctuations.

Now it is straightforward to calculate power spectra and bispectra through

$$\langle\zeta(\mathbf{x}_1)\zeta(\mathbf{x}_2)\rangle = N_{,I}N_{,J}\langle\delta\phi^I(\mathbf{x}_1)\delta\phi^J(\mathbf{x}_2)\rangle\,, \tag{3.53}$$

$$\langle\zeta(\mathbf{x}_1)\zeta(\mathbf{x}_2)\zeta(\mathbf{x}_3)\rangle = \frac{1}{2}N_{,IJ}N_{,K}N_{,L}\langle\delta\phi^I(\mathbf{x}_1)\delta\phi^J(\mathbf{x}_1)\delta\phi^K(\mathbf{x}_2)\delta\phi^L(\mathbf{x}_3)\rangle + 2\text{ perm}\,, \tag{3.54}$$

where "2 perm" denotes the two remaining cyclic permutations over $(\mathbf{x}_1, \mathbf{x}_2, \mathbf{x}_3)$. The previous expressions for the two-point and three-point correlation functions are valid on superhorizon scales and they do not account for contributions originated at the horizon crossing (however these are usually negligible in multifield models). Typically, difficulties arise when the statistics of the perturbations $\delta\phi^I$ are not known and thus it is necessary to employ the quantum-mechanical *in-in* formalism.

In Fourier space,

$$\zeta(\mathbf{k}) = \delta N(\mathbf{k}) = N_{,I}\delta\phi^I(\mathbf{k}) + \frac{1}{2}N_{,IJ}\int\frac{d^3k'}{(2\pi)^3}\delta\phi^I(\mathbf{k}-\mathbf{k}')\delta\phi^J(\mathbf{k}')\,, \tag{3.55}$$

and hence the previous correlators become

$$\langle\zeta(\mathbf{k}_1)\zeta(\mathbf{k}_2)\rangle = N_{,I}N_{,J}\langle\delta\phi^I(\mathbf{k}_1)\delta\phi^J(\mathbf{k}_2)\rangle\,, \tag{3.56}$$

$$\langle\zeta(\mathbf{k}_1)\zeta(\mathbf{k}_2)\zeta(\mathbf{k}_3)\rangle = \frac{1}{2}N_{,IJ}N_{,K}N_{,L}\int\frac{d^3k'}{(2\pi)^3}\langle\delta\phi^I(\mathbf{k}_1-\mathbf{k}')\delta\phi^J(\mathbf{k}')\delta\phi^K(\mathbf{k}_2)\delta\phi^L(\mathbf{k}_3)\rangle + 2\text{ perm}\,. \tag{3.57}$$

As an application, let us consider a set of massless fields ϕ^I with Gaussian fluctuations. Starting from

$$\langle\zeta(\mathbf{k}_1)\zeta(\mathbf{k}_2)\rangle = N_{,I}N_{,J}\frac{H^2}{2k_1^3}(2\pi)^3\delta^3(\mathbf{k}_1+\mathbf{k}_2)\delta^{IJ} = (2\pi)^3\delta^3(\mathbf{k}_1+\mathbf{k}_2)P_\zeta\,, \tag{3.58}$$

the adimensional power spectrum is

$$\mathcal{P}_\zeta = \left(\frac{H}{2\pi}\right)^2(N_{,I})^2\,. \tag{3.59}$$

The three-point correlation function is

$$\begin{aligned}\langle\zeta(\mathbf{k}_1)\zeta(\mathbf{k}_2)\zeta(\mathbf{k}_3)\rangle &= (2\pi)^3\delta^3(\mathbf{k}_1+\mathbf{k}_2+\mathbf{k}_3)N_{,IJ}N_{,I}N_{,J}\frac{H^4}{4}\left(\frac{1}{k_1^3k_2^3}+2\text{ perm}\right)\\ &= (2\pi)^3\delta^3(\mathbf{k}_1+\mathbf{k}_2+\mathbf{k}_3)\frac{N_{,IJ}N_{,I}N_{,J}}{(N_{,L}^2)^2}\big(P(k_1)P(k_2)+2\text{ perm}\big),\end{aligned} \tag{3.60}$$

and then, according to the definition (3.11), the shape function is given by equation (3.14) and

$$f_{NL}^{loc} = \frac{5}{6}\frac{N_{,IJ}N_{,I}N_{,J}}{(N_{,L})^4}\,. \tag{3.61}$$

We have introduced the superscript *loc* to stress the fact that the non-Gaussianities are produced locally in field space. After Fourier transform, the non-Gaussianities become non-local in momentum space peaking at the squeezed limit, i.e. for $k_1 \ll k_2 \sim k_3$.

3.5 Non-Gaussianity as an experimental probe of inflation

The Cosmic Microwave Background provides us nowadays the most important laboratory to study the early Universe. Its main features are described in appendix C. In this section, we will assume that the reader is familiar with the following basic property of the CMB. The CMB is a blackbody radiation at a temperature of $T_0 = 2.725\,\mathrm{K}$ and originated almost 380 000 years after the Big Bang. It permeates all the space and it is nearly isotropic (the temperature anisotropies are of order$\Delta T/T_0 \sim 10^{-5}$). These small fluctuations keep track of those produced during inflation. Hence, studying the statistical properties of these fluctuations is equivalent to study the statistical properties of the perturbations produced by inflation since the latter are nearly frozen on superhorizon scales.

The power spectrum contains valuable information but it might not be sufficient to discern among single-field inflationary models (see figure 1.2) and among other inflationary models, e.g. between single- and multi-field models of inflation. On the other hand, different inflationary models predict different amplitudes, shapes, and scale dependence of the bispectrum. Therefore, the study of the bispectrum can be a very efficient tool to investigate inflationary mechanisms. Moreover, the primordial non-Gaussianity can distinguish models whose predictions for n_s are r are degenerate. Thanks to this, the non-Gaussianities constitute one of the most informative probes to test inflation [49, 50, 54, 56, 64, 65]. As such, they provide valuable information about physics at the energy scale of inflation.

A well-know result is that the amount of non-Gaussianity produced in standard[4] single-field inflation is of order of the slow-roll parameters [40, 66, 67]. Non-Gaussianities of this magnitude are undetectable through CMB and large-scale structure measurements [48]. On the other hand, if $f_{NL} \gg \mathcal{O}(\varepsilon, \eta)$ is detected, single-field inflation is ruled out and only other models are possible. In this hypothesis, the single-field standard model ought to be modified.

The *Planck* satellite has provided the tightest constraints up to now. They are [48] (68% CL statistical)

$$f_{NL}^{loc} = 0.8 \pm 5.0\,, \tag{3.62a}$$

$$f_{NL}^{equil} = -4 \pm 43\,, \tag{3.62b}$$

$$f_{NL}^{ortho} = -26 \pm 21\,. \tag{3.62c}$$

They are consistent with Gaussianity of the primordial perturbations, but there is still an ample gap to fill in to reach the single-field models' prediction of $f_{NL} \sim \mathcal{O}(\varepsilon, \eta)$. Notice that, improvements in the constraints on non-Gaussianity strongly limit the possible extensions to the standard paradigm, thus providing strong evidence into the mechanism that generated the cosmic structures.

In order to produce large non-Gaussianities, we should depart from the standard single-field mechanism and allow for modifications of its assumptions. Large non-Gaussianity can be produced by breaking the slow-roll conditions during inflation [68], using non-canonical kinetic terms [67, 69–71] or in multi-field inflationary models [72–78]. In what follows, we will describe briefly some mechanisms referring to the cited papers for detailed analysis.

In multi-field models, there is an additional (or more) light scalar field during inflation. The additional fields can have a role during inflation and drive the exponential expansion, these models are genuinely multi-field. Otherwise, the additional fields can remain subdominant with respect to the inflaton, but they can produce non-Gaussian entropy perturbations that can be transferred, possibly efficiently, to the curvature modes [72]. The super-horizon evolution of the fluctuations and the transfer to the curvature perturbation can generate large non-Gaussianities of the local type. For example, in the curvaton models [44, 79–81] the late-time decay of a non-inflationary scalar field produces curvature perturbations. If the fields different from the inflaton

[4]By standard, we mean inflation driven by a scalar field with canonical kinetic term, assuming the slow-roll conditions and working in the Bunch-Davies vacuum and in Einstein gravity.

have a mass $m \approx H$, the resulting non-Gaussianities have an intermediate shape between the local and the equilateral ones. This is the case of "quasi-single field" models of inflation [82].

Equilateral non-Gaussianities are generically produced in single-field models with a non-canonical kinetic term [83], which can also generate the orthogonal type [84]. These models are characterized by higher-derivative interactions in the Lagrangian. The correlation between the fluctuations is suppressed when one of the modes is on superhorizon scales, because the derivative terms are redshifted away, hence the bispectrum peaks when the three modes are of comparable wavelengths.

Single-field inflation cannot produce large local type non-Gaussianities and then they are a distinctive sign of multi-field inflation[5]. In addition to this, for single-field models there exists a consistency condition in the squeezed limit. This condition reads [66]

$$\langle \zeta(\mathbf{k}_1)\zeta(\mathbf{k}_2)\zeta(\mathbf{k}_3)\rangle \xrightarrow{k_3 \ll k_1 = k_2} (2\pi)^7 \frac{1}{4k_1^3 k_3^3}(1-n_s)\mathcal{P}(k_1)\mathcal{P}(k_3)\,. \tag{3.63}$$

Although this condition was originally obtained for single-field slow-roll inflation, the only needed assumption is the single field [67, 87]. At the end, this relationship is valid also for non-standard single-field models. Therefore, in the squeezed limit the (tree-level) bispectrum is determined by the power spectrum $\mathcal{P}(k)$ and the spectral index n_s. If the power spectrum is nearly scale invariant (as observed), $n_s - 1$ is of order of the slow-roll parameters and the non-Gaussianities are of the local type. However, single-field models cannot produce large non-Gaussianities of the local type. Therefore, a detection of a large (i.e. greater than slow-roll parameters) local non-Gaussianity in the squeezed limit with a (nearly) scale-invariant power spectrum can rule out all single-field inflationary models.

[5]There are some subtleties hidden in this statement. In fact, some single-fields models can be build *ad hoc* to produce local non-Gaussianities [85, 86].

Chapter 4

Two-field inflation

"Not only is the Universe stranger than we think,
it is stranger than we can think."

Werner Heisenberg

In this chapter we will discuss the formalism used to study multifield inflation, in particular we will consider the two-field case. Multifield inflation represents one of the possible generalizations of single-field inflation. It is fundamental to remember that the predictions of single-field models are in perfect agreement with the currently available data [6]. There is no experimental incentive to study more complex models. On the other hand, multifield models arise naturally in theory of supergravity and particle physics in which many scalar fields are usually involved. In addition, single-field models cannot produce any detectable non-Gaussianities despite multifield ones in which non-Gaussianities are usually generated with little effort.

However, the popular proverb "all that glitters ain't gold" could not be more appropriate to characterize multi-field inflation. Indeed, the introduction of many scalar fields makes the dynamics very intricate and full of possibilities. These models may be very sensitive to initial conditions so that the phase space may become highly non-trivial. Hence, some additional attention is needed studying these models.

Our discussion is mainly based on [88–90] because the authors' formalism can be used to deal with a generic multifield model of inflation. Many articles have been written about multi-field inflation with specific concerns. For example, the references [45, 60, 91–95] regard curvature and isocurvature perturbations and the computation of the power spectra. In addition to this, the references [73, 75, 90, 96–98] concern the non-Gaussianities produced in multi-field models and the bispectra.

In section 4.1, we will discuss the background dynamics of the inflaton. Specifically, we will introduce the kinematical basis whose usefulness will be manifest in the following sections. Section 4.2 will concern the generalization of the slow-roll conditions to multi-field case. In particular, we will introduce the slow-turn conditions in addition to the slow-roll ones. In section 4.3, we will distinguish between curvature and isocurvature perturbations and study their evolution equations. Sections 4.4 and 4.5 will be focused on to observable quantities such

as power spectra and spectral indices. Finally, in section 4.6, we will derive a condition in order to produce large non-Gaussianities using the δN formalism.

4.1 Background fields kinematics

We assume that inflation is driven by two scalar fields ϕ_1 and ϕ_2. Many of the following equations are valid also when there are more than two fields. However, we consider from the beginning the two-field case since in the following chapters we will study only two-field models.

We assume that the Lagrangian describing the inflaton fields has the form

$$S = \int d^4x\sqrt{-g}\left(\frac{R}{2} - \frac{1}{2}G_{IJ}\, g^{\mu\nu}\partial_\mu\phi^I\partial_\nu\phi^J - V(\phi_1,\phi_2)\right), \tag{4.1}$$

where $G_{IJ} = G_{IJ}(\phi_1,\phi_2)$ and capital Latin indices refer to field space ($I = \{1,2\}$). Notice that we allow the kinetic terms to be non-canonical (they are canonical if $G_{IJ} \equiv \delta_{IJ}$). In addition, notice that now we deal with two metrics: $g_{\mu\nu}$ is the metric in coordinate space and G_{IJ} is the one in field space.

Equations of motion follow from the variation of the action (4.1) with respect to the fields. This calculation is tedious but straightforward and the result in the FRW spacetime is [88]

$$\ddot{\phi}^I - \Gamma^I_{JK}\partial_\mu\phi^J\partial^\mu\phi^K + 3H\dot{\phi}^I + V^{,I} = 0\,, \tag{4.2}$$

where the connection coefficients (or Christoffel symbols) are defined as

$$\Gamma^I_{JK} = \frac{1}{2}G^{IL}\left(G_{LK,J} + G_{LJ,K} - G_{JK,L}\right). \tag{4.3}$$

It is worth noticing that the term with Christoffel symbols Γ^I_{JK} accounts for the non-trivial structure of field space. The non-trivial field metric introduces additional couplings between the fields into the equations of motion. The equation of motion for the background is simply

$$\ddot{\phi}^I + \Gamma^I_{JK}\dot{\phi}^J\dot{\phi}^K + 3H\dot{\phi}^I + V^{,I} = 0\,. \tag{4.4}$$

We define the covariant derivative along the flux of ϕ^I as

$$\mathcal{D}_t X^I = \dot{\phi}^J\nabla_J X^I = \dot{X}^I + \Gamma^I_{JK}X^J\dot{\phi}^K, \tag{4.5}$$

where "∇" denotes the derivative in field space.

The background density and pressure are respectively given by

$$\rho = \frac{1}{2}|\dot{\phi}|^2 + V\,, \tag{4.6a}$$

$$P = \frac{1}{2}|\dot{\phi}|^2 - V\,, \tag{4.6b}$$

where we have introduced the more compact notation

$$|\dot{\phi}|^2 = G_{IJ}\dot{\phi}^I\dot{\phi}^J. \tag{4.7}$$

Talking about notation, we use bold symbols to denote vectors in field space and ^{T} to denote transposition, so that the previous equation can be rewritten as

$$|\dot{\phi}|^2 = \dot{\boldsymbol{\phi}}^T \dot{\boldsymbol{\phi}}. \tag{4.8}$$

In multi-field models, Friedmann equation (1.8b) becomes

$$H^2 = \frac{1}{3}\left(\frac{1}{2}G_{IJ}\dot{\phi}^I\dot{\phi}^J + W\right). \tag{4.9}$$

Working with time t is not a convenient choice, it is better to employ the number of efoldings N defined as

$$N \equiv \int_{t_0}^{t} H\, dt', \tag{4.10}$$

where t_0 is the time at which initial conditions are given. Compare the last definition with the usual definition (1.35) given in chapter 1. Here we adopt this definition since we usually rewrite equations with respect to N in the sections in which we study the initial conditions for inflation[1]. Therefore, it is convenient to count the number of e-folds from the beginning of inflation and not from its end. Differentiating the previous equation, we obtain the relationship

$$dN = d(\ln a) = H dt. \tag{4.11}$$

In this chapter we will denote with a prime the derivative with respect to N.

Now we re-cast background equations using e-foldings. The Friedmann equation becomes

$$H^2 = \frac{V}{3-\varepsilon}, \tag{4.12}$$

and the background equation (4.4) takes the form

$$\mathcal{D}_N\boldsymbol{\phi}' + \big(3-\varepsilon\big)\big(\boldsymbol{\phi}' + \boldsymbol{\nabla}^T \ln V\big) = 0, \tag{4.13}$$

where the slow-roll parameter

$$\varepsilon \equiv -\frac{\dot{H}}{H^2} = -(\ln H)' = \frac{1}{2}|\phi'|^2 \tag{4.14}$$

is defined in the usual way (1.28). For convenience, we define the field-space vector

$$\boldsymbol{\eta} \equiv \mathcal{D}_N\boldsymbol{\phi}'. \tag{4.15}$$

The background dynamics in field space may be described in the basis formed by ϕ^1 and ϕ^2. Although this is a viable and legitimate choice, it is not the smartest and best suited for our purposes. In fact, it is convenient to work with the basis constituted by the normalized vector $e_\parallel$ along the direction of the field velocity and the vector $e_\perp$ orthogonal to it in the direction of $(\mathrm{I} - \mathbf{e}_\parallel\mathbf{e}_\parallel^T)\boldsymbol{\eta}$. The latter basis has the advantage that the curvature and isocurvature

[1] These sections are 5.6, 7.2 and 8.1.

perturbations are easily distinguishable. We denote the components of a vector $\mathbf{A}$ in the latter basis as

$$A_{\parallel} = \mathbf{e}_{\parallel} \cdot \mathbf{A}\,, \tag{4.16a}$$

$$A_{\perp} = \mathbf{e}_{\perp} \cdot \mathbf{A}\,, \tag{4.16b}$$

and the components of a matrix M in the following manner

$$\mathrm{M}_{\perp\parallel} = \mathbf{e}_{\perp} \cdot \mathrm{M}\mathbf{e}_{\parallel}\,. \tag{4.17}$$

The decomposition just performed allows us to characterize the trajectory in field space using a few quantities. The first one is simply the modulus of the velocity of the fields

$$v \equiv |\phi'|\,, \tag{4.18}$$

that is directly related to ε. The second one is the speed up rate

$$\frac{\eta_{\parallel}}{v} = (\ln v)'\,, \tag{4.19}$$

and it represents the logarithmic rate of change of v. The last one can be argued observing that the equations of motion for the basis vectors are

$$\mathcal{D}_N \mathbf{e}_{\parallel} = \frac{\eta_{\perp}}{v}\mathbf{e}_{\perp}\,, \tag{4.20}$$

$$\mathcal{D}_N \mathbf{e}_{\perp} = -\frac{\eta_{\perp}}{v}\mathbf{e}_{\parallel}\,. \tag{4.21}$$

Therefore, the quantity $\eta_{\perp}/v$ describes how fast the direction of the field trajectory is changing and we call it *turn rate*. Obviously, in single-field case, the turn rate is null since there is no direction for one field to turn into. Then, it is often useful to evaluate the ratio $\eta_{\perp}/\eta_{\parallel}$ which indicates the relative importance of multi-field to single-field behaviour.

4.2 Slow-roll and slow-turn

In this section, we generalize the slow-roll conditions to two-field inflation. In this case, the presence of the second field yields a more complex and richer dynamics than the single-field case. Indeed, slightly different initial conditions can lead to completely different trajectories. In some models there exists an attractor behaviour that simplifies the dynamics, but in others this does not happen and one has to study carefully the dependence on initial conditions.

Following [89], we introduce the slow-roll conditions

$$\varepsilon = \frac{1}{2}v^2 \ll 1\,, \tag{4.22}$$

$$\left|\frac{\eta_{\parallel}}{v}\right| \ll 1\,, \tag{4.23}$$

and the slow-turn condition

$$\frac{\eta_{\perp}}{v} \ll 1\,. \tag{4.24}$$

One can show that these conditions are equivalent to require that the potential is sufficiently flat and that the field slowly rolls down the potential. We will denote with SRST the combined slow-roll and slow-turn approximations.

At lowest order in the slow-roll parameters, the background equations read

$$H^2 = \frac{V}{3}\,, \tag{4.25a}$$

$$\boldsymbol{\phi}' = -\boldsymbol{\nabla}^T \ln V\,. \tag{4.25b}$$

Differentiating last equation, we get

$$\boldsymbol{\eta} = -\mathrm{M}\boldsymbol{\phi}' = \mathrm{M}\boldsymbol{\nabla}^T \ln V\,, \tag{4.26}$$

where the mass matrix M is defined as

$$\mathrm{M} \equiv \boldsymbol{\nabla}^T\boldsymbol{\nabla} \ln V\,. \tag{4.27}$$

The speed up rate is given by

$$\frac{\eta_\parallel}{v} = -M^{(1)}_{\parallel\parallel}, \tag{4.28}$$

and the turn rate is

$$\frac{\eta_\perp}{v} = -M^{(1)}_{\parallel\perp}, \tag{4.29}$$

where the superscript (1) denotes the lowest order expansion in the slow-roll parameters. The previous equations show that the background slow-roll dynamics is determined by the derivatives of $\ln V$.

4.3 Perturbed equations

We perturb the coordinate metric $g_{\mu\nu}$ as in (2.24) and consider only linear perturbations. We use gauge-invariant quantities in order to work only with physical quantities. In particular, we employ the Sasaki-Mukhanov variable generalized to the multi-field case, that is

$$\boldsymbol{\mathcal{Q}} \equiv \boldsymbol{\delta\phi} + \psi\boldsymbol{\phi}'. \tag{4.30}$$

This choice has the advantage that the equations of the field perturbations are decoupled from the (coordinate) metric perturbations, but not vice versa. Notice that the perturbations of the field metric are induced by that of the field.

The evolution equation for the field perturbations can be obtained perturbing the equation of motion (4.2). The result is [91]

$$\big(\mathcal{D}_t + 3H\big)\mathcal{D}_t\boldsymbol{\mathcal{Q}} + \left[\frac{k^2}{a^2} + \boldsymbol{\nabla}^T\boldsymbol{\nabla}V - \left(3 - \frac{\dot H}{H^2}\right)\dot{\boldsymbol{\phi}}\dot{\boldsymbol{\phi}}^T - \frac{1}{H}\Big((\mathcal{D}_t\dot{\boldsymbol{\phi}})\dot{\boldsymbol{\phi}}^T + \dot{\boldsymbol{\phi}}(\mathcal{D}_t\dot{\boldsymbol{\phi}}^T)\Big) - \mathbf{R}(\dot{\boldsymbol{\phi}},\dot{\boldsymbol{\phi}})\right]\boldsymbol{\mathcal{Q}} = 0\,, \tag{4.31}$$

where

$$\mathbf{R}^I{}_J(\dot{\boldsymbol{\phi}},\dot{\boldsymbol{\phi}}) = R^I{}_{KLJ}\dot\phi^K\dot\phi^L, \tag{4.32}$$

$$R^I{}_{KLJ} \equiv \Gamma^I_{JK,L} - \Gamma^I_{KL,J} + \Gamma^I_{LM}\Gamma^M_{KJ} - \Gamma^I_{JM}\Gamma^M_{KL}\,. \tag{4.33}$$

The Riemann curvature tensor $R^I{}_{KLJ}$ associated to G_{IJ} can be written in two dimensions as

$$R_{IKLJ} = \frac{R}{2}\left(G_{IL}G_{KJ} - G_{IJ}G_{KL}\right), \tag{4.34}$$

where R is the Ricci scalar. Substituting the last expression into (4.32) and using (4.14), we get

$$\mathbf{R}(\dot{\boldsymbol{\phi}}, \dot{\boldsymbol{\phi}}) = \frac{R}{2}H^2\Big(\boldsymbol{\phi}'\boldsymbol{\phi}'^T - 2\varepsilon \mathrm{I}\Big) = -\varepsilon H^2 R \mathbf{e}_\perp \mathbf{e}_\perp^T, \tag{4.35}$$

where in the last step we used the completeness of the basis $(\mathbf{e}_\perp, \mathbf{e}_\parallel)$. Equation (4.31) rewritten in terms of N reads

$$\frac{1}{3-\varepsilon}\mathcal{D}_N\mathcal{D}_N\boldsymbol{\mathcal{Q}} + \mathcal{D}_N\boldsymbol{\mathcal{Q}} + \frac{k^2}{a^2}\frac{\boldsymbol{\mathcal{Q}}}{V} + \left[\widetilde{\mathrm{M}} + \frac{\boldsymbol{\eta}\boldsymbol{\eta}^T}{(3-\varepsilon)^2}\right]\boldsymbol{\mathcal{Q}} = 0, \tag{4.36}$$

where the effective mass matrix $\widetilde{\mathrm{M}}$ is defined as

$$\widetilde{\mathrm{M}} \equiv \mathrm{M} + \frac{\varepsilon R}{3-\varepsilon}\mathbf{e}_\perp\mathbf{e}_\perp^T. \tag{4.37}$$

Notice that the second term is suppressed by the slow-roll parameter ε. Therefore, the evolution of the perturbations is determined mainly by the mass matrix M and secondly by the curvature of the field space plus a correction due to field acceleration $\boldsymbol{\eta}$, which is small during slow-roll. The matrix $\widetilde{\mathrm{M}}$ reduces to M when $R = 0$ (this is the case when the kinetic term is canonical). In the SRST limit, equation (4.36) becomes

$$\frac{1}{3-\varepsilon}\mathcal{D}_N\mathcal{D}_N\boldsymbol{\mathcal{Q}} + \mathcal{D}_N\boldsymbol{\mathcal{Q}} + \frac{k^2}{a^2}\frac{\boldsymbol{\mathcal{Q}}}{V} \simeq -\widetilde{\mathrm{M}}^{(1)}\boldsymbol{\mathcal{Q}}, \tag{4.38}$$

where

$$\widetilde{\mathrm{M}}^{(1)} = \mathrm{M} + \frac{\varepsilon}{3}R\mathbf{e}_\perp\mathbf{e}_\perp^T \tag{4.39}$$

is the first order approximation of $\widetilde{\mathrm{M}}$ in the slow-roll parameters and all the quantities should be taken at the same order for consistency. In the superhorizon limit $k \ll aH$, the evolution of the perturbations is governed by

$$\mathcal{D}_N\boldsymbol{\mathcal{Q}} \simeq -\widetilde{\mathrm{M}}^{(1)}\boldsymbol{\mathcal{Q}}, \tag{4.40}$$

which is similar to (4.26). In order to make the comparison more clear, let us rewrite equation (4.26) as

$$\mathcal{D}_N\boldsymbol{\phi}' = -\widetilde{\mathrm{M}}^{(1)}\boldsymbol{\phi}', \tag{4.41}$$

where we have used the fact that $\widetilde{\mathrm{M}}\boldsymbol{\phi}' = \mathrm{M}\boldsymbol{\phi}'$. This means that, at first order in the slow-roll parameters, the evolution of the background field $\boldsymbol{\phi}$ and that of the perturbation $\boldsymbol{\mathcal{Q}}$ is determined by $\widetilde{\mathrm{M}}$.

4.3.1 Adiabatic and entropy modes

Thanks to the rotation from the basis $(\mathbf{e}_1, \mathbf{e}_2)$ to $(\mathbf{e}_\parallel, \mathbf{e}_\perp)$, the modes naturally separate into the adiabatic and entropic components. Adiabatic modes are perturbations along the trajectory

and hence we denote them as $\mathcal{Q}_{\parallel} \equiv \mathbf{e}_{\parallel} \cdot \boldsymbol{\mathcal{Q}}$. Conversely, entropy modes are orthogonal to the trajectory and then we define $\mathcal{Q}_{\perp} \equiv \mathbf{e}_{\perp} \cdot \boldsymbol{\mathcal{Q}}$.

The evolution equation for adiabatic modes can be derived from the projection of equation (4.36) onto $\mathbf{e}_{\parallel}$. After some manipulations, the final result is [89]

$$\frac{1}{3-\varepsilon}\mathcal{Q}_{\parallel}'' + \mathcal{Q}_{\parallel}' + \left\{\frac{k^2}{a^2V} - \left(\frac{\eta_{\parallel}}{v}\right)\left[1 + \frac{1}{3-\varepsilon}\left(\ln\frac{\eta_{\parallel}}{v}\right)' + \frac{1}{3-\varepsilon}\left(\frac{\eta_{\parallel}}{v}\right)\right]\right\}\mathcal{Q}_{\parallel} = 2\left(\frac{\eta_{\perp}}{v}\right)\left\{\frac{1}{3-\varepsilon}\mathcal{Q}_{\perp}' + \left[1 + \frac{1}{3-\varepsilon}\left(\ln\frac{\eta_{\perp}}{v}\right)' + \frac{1}{3-\varepsilon}\left(\frac{\eta_{\parallel}}{v}\right)\right]\mathcal{Q}_{\perp}\right\}. \tag{4.42}$$

Hence, the evolution of the adiabatic perturbations is governed primarily by the speed up rate, the turn rate and the subhorizon term. Notice that adiabatic perturbations can be sourced by entropy ones if the turn rate is different from zero. If the turn rate vanishes, the adiabatic modes decouple from the entropy ones and the resulting equation is similar to that of single-field case.

In the superhorizon limit, the previous equation becomes

$$\left[1 + \frac{1}{3-\varepsilon}\mathcal{D}_N + \frac{2}{3-\varepsilon}\left(\frac{\eta_{\parallel}}{v}\right)\right]\left(\frac{\mathcal{Q}_{\parallel}}{v}\right)' = \left[1 + \frac{1}{3-\varepsilon}\mathcal{D}_N + \frac{2}{3-\varepsilon}\left(\frac{\eta_{\parallel}}{v}\right)\right]\left(2\frac{\eta_{\perp}}{v}\frac{\mathcal{Q}_{\perp}}{v}\right). \tag{4.43}$$

Setting the right-hand side of this equation to zero yields the associated homogeneous equation for $\mathcal{Q}_{\parallel}$. This homogeneous equation has two solutions: the growing and the decaying modes. The latter is heavily suppressed by the exponential expansion and hence it can be neglected with respect to the former. The growing mode is described by equation

$$\left(\frac{\mathcal{Q}_{\parallel}}{v}\right)' = 2\frac{\eta_{\perp}}{v}\frac{\mathcal{Q}_{\perp}}{v}, \tag{4.44}$$

or, equivalently, by

$$\mathcal{Q}_{\parallel}' = \frac{\eta_{\parallel}}{v}\mathcal{Q}_{\parallel} + 2\frac{\eta_{\perp}}{v}\mathcal{Q}_{\perp}, \tag{4.45}$$

where we have used $(\ln v)' = \eta_{\parallel}/v$. Hence, both the adiabatic and the entropy perturbations source the growing adiabatic mode on superhorizon scales. In addition to this, its evolution is governed by the speed up rate and the turn rate. In SRST limit, the adiabatic mode evolves slowly since the two rates are small. If $\eta_{\parallel}\,\mathcal{Q}_{\parallel} \gg \eta_{\perp}\,\mathcal{Q}_{\perp}$, the evolution is effectively single-field and the solution is $\mathcal{Q}_{\parallel} \propto v$. Otherwise, multi-field effects should be considered.

Again, projecting equation (4.36) onto $\mathbf{e}_{\perp}$ we obtain the evolution equation for entropy perturbations. This is given by [89]

$$\frac{1}{3-\varepsilon}\mathcal{Q}_{\perp}'' + \mathcal{Q}_{\perp}' + \left[\frac{k^2}{a^2V} + \mathrm{M}_{\perp\perp} + \frac{\varepsilon R}{3-\varepsilon} - 3\frac{1-\varepsilon}{(3-\varepsilon)^2}\left(\frac{\eta_{\perp}}{v}\right)^2\right]\mathcal{Q}_{\perp} = -\frac{2}{3-\varepsilon}\left(\frac{\eta_{\perp}}{v}\right)\left[\mathcal{Q}_{\parallel}' - \frac{\eta_{\parallel}}{v}\mathcal{Q}_{\parallel}\right]. \tag{4.46}$$

In contrast to the adiabatic modes, the evolution of the entropy modes is controlled by the subhorizon term, the turn rate, the speed up rate, $\mathrm{M}_{\perp\perp}$, ε and R. The field space curvature affects the entropy perturbations, but its contribution is suppressed by the slow-roll parameter ε. The turn rate anew tunes the sourcing of one mode by the other.

In the superhorizon limit, the last equation reads

$$\frac{1}{3-\varepsilon}\mathcal{Q}_\perp'' + \mathcal{Q}_\perp' = -\mu_\perp \mathcal{Q}_\perp\,, \tag{4.47}$$

where we have used equation (4.45) and defined the effective entropy mass as

$$\mu_\perp \equiv \mathrm{M}_{\perp\perp} + \frac{\varepsilon R}{3-\varepsilon} + \frac{9-\varepsilon}{(3-\varepsilon)^2}\left(\frac{\eta_\perp}{v}\right)^2. \tag{4.48}$$

Therefore, the entropy mode evolves independently from the adiabatic one in the superhorizon limit even if the field metric is not trivial. The terms $\mathrm{M}_{\perp\perp}$ and $\varepsilon R(3-\varepsilon)^{-1}$ can both enhance or suppress the entropy modes depending on their signs. Instead, the term with the turn rate squared is always positive in the SR limit and hence it always damps these modes; if $\eta_\perp/v \ll 1$, this produces a strong suppression. The term with the Ricci scalar is usually small in the slow-roll limit and it can become relevant during the end of inflation when $\varepsilon \sim 1$.

4.3.2 Curvature and isocurvature perturbations

Now, we want to relate the adiabatic and entropy perturbations to the comoving curvature and isocurvature perturbations. It can be shown [99] that the curvature perturbation $\mathcal{R}$, in the comoving gauge, during inflation is given by

$$\mathcal{R} = \frac{\mathcal{Q}_\parallel}{v}\,. \tag{4.49}$$

We define the isocurvature perturbation as

$$\mathcal{S} = \frac{\mathcal{Q}_\perp}{v}\,, \tag{4.50}$$

so that curvature and isocurvature power spectra have comparable magnitude at horizon exit.

In order to calculate these power spectra, we need the equation of motion for $\mathcal{R}$ and $\mathcal{S}$ on superhorizon scales. From equation (4.44) and the previous definitions, it is straightforward to get

$$\mathcal{R}' = 2\frac{\eta_\perp}{v}\mathcal{S}. \tag{4.51}$$

Hence, the evolution of the curvature perturbation depends only on the turn rate and on the isocurvature perturbation, but it is insensitive of ε and the speed up rate. Notice that, if there is no turning trajectory, the curvature perturbation $\mathcal{R}$ is conserved on superhorizon scales, as in single-field case. After integration, the solution of the last equation is

$$\mathcal{R} = \mathcal{R}_* + \int_{N_*}^{N} 2\frac{\eta_\perp}{v}\mathcal{S}\, d\widetilde{N}, \tag{4.52}$$

where "$*$" denotes the time of horizon exit.

Deriving equation (4.50) with respect to N and using (4.19), we obtain the equation for the evolution of the isocurvature perturbation, i.e.

$$\mathcal{S}' = \frac{1}{v}(v\mathcal{S})' - \frac{\eta_\parallel}{v}\mathcal{S} = \frac{1}{v}\left(\mathcal{Q}_\perp' - \frac{\eta_\parallel}{v}\mathcal{Q}_\perp\right). \tag{4.53}$$

The solution of this equation can be found if one knows the solution $\mathcal{Q}_\perp$ of (4.47). If this solution is not known, one can parametrize the evolution of isocurvature modes as

$$\mathcal{S}' = \beta \mathcal{S}, \tag{4.54}$$

following [93]. In the SRST approximation, at first order in the slow-roll parameters, it can be shown that

$$\beta^{(1)} = \widetilde{\mathrm{M}}^{(1)}_{\parallel\parallel} - \widetilde{\mathrm{M}}^{(1)}_{\perp\perp}. \tag{4.55}$$

The formal solution for the isocurvature perturbation is given by

$$\mathcal{S} = \mathcal{S}_* e^{\int_{N_*}^{N} \beta d\tilde{N}}, \tag{4.56}$$

where β can have an analytical or approximated expression. Thus, the sign of β determines whether the isocurvature mode is suppressed or enhanced.

Finally, we introduce an useful parametrization [93] of equations (4.51) and (4.53). The relationship between the curvature and isocurvature perturbations can be written as

$$\begin{pmatrix} \mathcal{R} \\ \mathcal{S} \end{pmatrix} = \begin{pmatrix} 1 & T_{\mathcal{RS}} \\ 0 & T_{\mathcal{SS}} \end{pmatrix} \begin{pmatrix} \mathcal{R}_* \\ \mathcal{S}_* \end{pmatrix}, \tag{4.57}$$

where the transfer functions $T_{\mathcal{RS}}$ and $T_{\mathcal{SS}}$ are defined as

$$T_{\mathcal{SS}}(t_*, t) = e^{\int_{t_*}^{t} \beta(\tilde{t}) H(\tilde{t}) d\tilde{t}}, \tag{4.58}$$

$$T_{\mathcal{RS}}(t_*, t) = \int_{t_*}^{t} 2 \frac{\eta_\perp}{v} T_{\mathcal{SS}}(t_*, \tilde{t}) H(\tilde{t}) d\tilde{t}. \tag{4.59}$$

This parametrization holds even after the end of inflation.

4.4 Power spectra

In this section we will solve the perturbation equation (4.36), obtain the expression of the mode functions and calculate the power spectra.

In order to solve equation (4.36), we follow the standard strategy discussed in section 1.5. Hence, we define the vector

$$\mathbf{q} \equiv a \boldsymbol{\mathcal{Q}}, \tag{4.60}$$

and use conformal time $d\tau = (aH)^{-1} dN$. After some algebra, equation (4.36) becomes

$$\mathcal{D}_\tau^2 \mathbf{q} + k^2 \mathbf{q} = (aH)^2 \left\{ (2-\varepsilon)\mathrm{I} - (3-\varepsilon)\left[\widetilde{\mathrm{M}} + \frac{\boldsymbol{\eta}\boldsymbol{\eta}^T}{(3-\varepsilon)^2} \right] \right\} \mathbf{q}. \tag{4.61}$$

An exact solution to this equation does not exist. On the other hand, we can solve it in different regimes and then match the solutions on the boundaries.

In the subhorizon limit $k \gg aH$, the right-hand side of equation (4.61) is negligible and this equation reduces to the Klein-Gordon equation apart for the second covariant derivative. In

order to solve this equation one should define an orthonormal basis parallel transported along the background trajectory [91]. Here, we do not provide further details. At the end, the solution is given by

$$\mathbf{q} = \frac{1}{\sqrt{k}}\left(\mathbf{a}(\mathbf{k})e^{-ik\tau} + \mathbf{a}^\dagger(-\mathbf{k})e^{ik\tau}\right), \tag{4.62}$$

where we have already quantized the fields introducing the destruction a_I and creation $a_I^\dagger$ operators for each field ϕ^I. They satisfy the usual commutation relations,

$$[a_I(\mathbf{k}), a_J^\dagger(\mathbf{k}')] = \delta_{IJ}\delta^3(\mathbf{k}-\mathbf{k}'), \tag{4.63a}$$

$$[a_I(\mathbf{k}), a_J(\mathbf{k}')] = [a_I^\dagger(\mathbf{k}), a_J^\dagger(\mathbf{k}')] = 0, \tag{4.63b}$$

and the annihilation condition $a_I(\mathbf{k})\,|0\rangle = 0$.

The second regime we consider is the time of horizon crossing, $k \sim aH$. Defining $x \equiv -k\tau$, to first-order in the slow-roll, we get

$$x \simeq (1+\varepsilon)\frac{k}{aH}\,. \tag{4.64}$$

Thanks to this equation, equation (4.61) in the SRST limit reads

$$\mathcal{D}_z^2\mathbf{q} + \mathbf{q} = \frac{1}{z^2}\left[2\mathrm{I} + 3\left(\varepsilon\mathrm{I} - \widetilde{\mathrm{M}}^{(1)}\right)\right]\mathbf{q}. \tag{4.65}$$

To solve this equation, we assume that the time variation of the term in square brackets can be neglected during horizon crossing. Then, the two modes can be decoupled through a rotation U that diagonalizes the effective mass matrix at horizon crossing. The rotation matrix can be parametrized as

$$\mathrm{U} = \begin{pmatrix} \cos\tilde{\theta} & -\sin\tilde{\theta} \\ \sin\tilde{\theta} & \cos\tilde{\theta} \end{pmatrix}, \tag{4.66}$$

and the diagonalized mass matrix is

$$\mathrm{U}^T\widetilde{\mathrm{M}}^{(1)}\mathrm{U} = \begin{pmatrix} m_+ & 0 \\ 0 & m_- \end{pmatrix}, \tag{4.67}$$

where

$$m_\pm = \frac{1}{2}\left[\mathrm{Tr}\big(\widetilde{\mathrm{M}}^{(1)}\big) \pm \sqrt{\big[\mathrm{Tr}\big(\widetilde{\mathrm{M}}^{(1)}\big)\big]^2 - 4\mathrm{Det}\big(\widetilde{\mathrm{M}}^{(1)}\big)}\,\right]. \tag{4.68}$$

The modes in the rotated basis $\tilde{\mathbf{q}} \equiv (\tilde{q}_+, \tilde{q}_-) = \mathrm{U}^T\mathbf{q}$ satisfy

$$\mathcal{D}_z^2\tilde{q}_\pm + \left[1 - \frac{1}{z^2}\left(\nu_\pm^2 - \frac{1}{4}\right)\right]\tilde{q}_\pm \simeq 0, \tag{4.69}$$

where

$$\nu_\pm \equiv \frac{3}{2} + \varepsilon - m_\pm, \tag{4.70}$$

and where we have supposed that the time variation of U along the trajectory is negligible during the period of horizon crossing. The last equation has the same form of (1.57) apart for the second covariant derivative along the trajectory. As previously done, one should define an

orthonormal basis parallel transported along the background trajectory [91]. The final solution is [89]

$$\tilde{q}_\pm = \sqrt{\frac{\pi z}{4k}}\Big[e^{i\frac{\pi}{2}(2+\varepsilon-m_\pm)}H^{(1)}_{\nu_\pm}(z)\tilde{a}_\pm(\mathbf{k}) + e^{-i\frac{\pi}{2}(2+\varepsilon-m_\pm)}H^{(2)}_{\nu_\pm}(z)\tilde{a}^\dagger_\pm(-\mathbf{k})\Big], \tag{4.71}$$

where $\tilde{\mathbf{a}} = \mathrm{U}^T\mathbf{a}$ and where the normalization have been fixed to match the subhorizon solution.

When the modes become superhorizon, the oscillatory behaviour disappears and the perturbations can grow or decay. Their evolution is described by the equations studied in the previous section.

We define the (dimensionless) power spectrum $\mathcal{P}_\mathcal{X}$ of a quantity $\mathcal{X}$ as

$$\langle\mathcal{X}(\mathbf{k})\mathcal{X}(\mathbf{k}')\rangle = (2\pi)^3\delta^3(\mathbf{k}+\mathbf{k}')\frac{2\pi^2\mathcal{P}_\mathcal{X}}{k^3}, \tag{4.72}$$

and the cross spectrum $\mathcal{C}_{\mathcal{X}\mathcal{Y}}$ of the quantities $\mathcal{X}$ and $\mathcal{Y}$ as

$$\langle\mathcal{X}(\mathbf{k})\mathcal{Y}(\mathbf{k}')\rangle = (2\pi)^3\delta^3(\mathbf{k}+\mathbf{k}')\frac{2\pi^2\mathcal{C}_{\mathcal{X}\mathcal{Y}}}{k^3}. \tag{4.73}$$

These definitions generalize to multifield case the definition of the adimensional power spectrum (1.69) in single-field inflation.

4.4.1 Horizon exit

To calculate the spectra of curvature and isocurvature perturbations at horizon exit, we should rotate the fluctuations in the decoupled basis. The curvature and isocurvature perturbations are related to that in the original basis through a rotation with angle θ such that $\tan\theta = \phi_2'/\phi_1'$. At the end, the curvature modes can be related to the decoupled ones by the combined rotation

$$\begin{pmatrix} a\mathcal{Q}_\parallel \\ a\mathcal{Q}_\perp \end{pmatrix} = \begin{pmatrix} \cos(\tilde{\theta}-\theta) & -\sin(\tilde{\theta}-\theta) \\ \sin(\tilde{\theta}-\theta) & \cos(\tilde{\theta}-\theta) \end{pmatrix}\begin{pmatrix} \tilde{q}_+ \\ \tilde{q}_- \end{pmatrix}, \tag{4.74}$$

where the rotation angle satisfies

$$\tan 2(\tilde{\theta}-\theta) = \frac{2\widetilde{\mathrm{M}}^{(1)}_{\parallel\perp}}{\widetilde{\mathrm{M}}^{(1)}_{\parallel\parallel} - \widetilde{\mathrm{M}}^{(1)}_{\perp\perp}}\,. \tag{4.75}$$

Finally, the power spectra at horizon exit are given by

$$\mathcal{P}_{\mathcal{R}*} = \left(\frac{H_*}{2\pi}\right)^2\frac{1}{2\varepsilon_*}\Big[1+2(C-1)\varepsilon - 2C\widetilde{\mathrm{M}}_{\parallel\parallel}\Big]_*, \tag{4.76a}$$

$$\mathcal{P}_{\mathcal{S}*} = \left(\frac{H_*}{2\pi}\right)^2\frac{1}{2\varepsilon_*}\Big[1+2(C-1)\varepsilon - 2C\widetilde{\mathrm{M}}_{\perp\perp}\Big]_*, \tag{4.76b}$$

$$\mathcal{C}_{\mathcal{R}\mathcal{S}*} = \left(\frac{H_*}{2\pi}\right)^2\frac{1}{2\varepsilon_*}\Big[-2C\widetilde{\mathrm{M}}_{\parallel\perp}\Big]_*, \tag{4.76c}$$

where $C \equiv 2-\ln 2-\gamma \simeq 0.7296$ and γ is the Euler-Mascheroni constant. Notice that the curvature and isocurvature spectra have comparable magnitude but the cross spectrum is suppressed

by the turn rate since $\eta_\perp/v \simeq -\widetilde{\mathrm{M}}^{(1)}_{\parallel\perp}$. Again, the turn rate determines the strength of sourcing between the modes. If the turn rate is null, then the curvature and isocurvature modes are not correlated at horizon exit and the decoupled basis coincides with the kinematical one.

The tensor spectrum, to first order in the slow-roll parameters, is

$$\mathcal{P}_{T_*} = 8\left(\frac{H_*}{2\pi}\right)^2\Big[1+2(C-1)\varepsilon\Big]_*\,, \tag{4.77}$$

and it is conserved for modes outside the horizon. The expression of the tensor spectrum is independent from the number of scalar fields.

4.4.2 End of inflation

The parametrization (4.57) can be used to relate the spectra at horizon crossing to that at the end of inflation. The spectra at the end of inflation can be expressed in terms of that at horizon crossing as

$$\mathcal{P}_\mathcal{R} = \mathcal{P}_{\mathcal{R}_*} + 2T_{\mathcal{RS}}\mathcal{C}_{\mathcal{RS}_*} + T^2_{\mathcal{RS}}\mathcal{P}_{\mathcal{S}_*}\,, \tag{4.78a}$$

$$\mathcal{P}_\mathcal{S} = T^2_{\mathcal{SS}}\mathcal{P}_{\mathcal{S}_*}\,, \tag{4.78b}$$

$$\mathcal{C}_{\mathcal{RS}} = T_{\mathcal{SS}}\mathcal{C}_{\mathcal{RS}_*} + T_{\mathcal{RS}}T_{\mathcal{SS}}\mathcal{P}_{\mathcal{S}_*}\,, \tag{4.78c}$$

where all left-hand sides are evaluated at the end of inflation. Using equations (4.76) and keeping only lowest order terms in the SRST approximation, the previous equations become

$$\mathcal{P}_\mathcal{R} = \left(\frac{H_*}{2\pi}\right)^2\frac{1}{2\varepsilon_*}\Big(1+T^2_{\mathcal{RS}}\Big)\,, \tag{4.79a}$$

$$\mathcal{P}_\mathcal{S} = \left(\frac{H_*}{2\pi}\right)^2\frac{1}{2\varepsilon_*}T^2_{\mathcal{SS}}\,, \tag{4.79b}$$

$$\mathcal{C}_{\mathcal{RS}} = \left(\frac{H_*}{2\pi}\right)^2\frac{1}{2\varepsilon_*}T_{\mathcal{RS}}T_{\mathcal{SS}}\,. \tag{4.79c}$$

All three spectra have the common factor $\left(\frac{H_*}{2\pi}\right)^2\frac{1}{2\varepsilon_*}$, but they are modulated by different transfer functions. In particular, the ratio $T_{\mathcal{SS}}/T_{\mathcal{RS}}$ governs the relative sizes of the spectra since it affects the sizes of the cross correlation and isocurvature spectra. The single-field case can be recovered setting $T_{\mathcal{SS}} = 0$, which also implies $T_{\mathcal{RS}} = 0$. If the turn rate is large, $T_{\mathcal{RS}} \geqslant \mathcal{O}(1)$ and $T_{\mathcal{SS}} \ll 1$, typically. This yields the hierarchy $\mathcal{P}_\mathcal{R} \gg \mathcal{C}_{\mathcal{RS}} \gg \mathcal{P}_\mathcal{S}$ and $\mathcal{P}_\mathcal{R} \gg \mathcal{P}_T$. On the other hand, if the turn rate is small, we expect $T_{\mathcal{RS}} \ll 1$ and $T_{\mathcal{SS}} \lesssim \mathcal{O}(1)$. In this limit, the curvature spectrum can be approximated with the single-field one and the other spectra are smaller, with their relative size depending on the ratio $T_{\mathcal{SS}}/T_{\mathcal{RS}}$.

4.5 Observables

From the expressions of the power spectra (4.79), we can calculate the spectral indices, the tensor-to-scalar ratio and the cross-correlation ratio. In this section, all quantities are evaluated at horizon crossing and hence we omit the subscript "$*$".

In order to express the spectral indices in a compact manner, it is convenient to introduce some quantities. First, let us define the correlation angle Δ_N as

$$\sin\Delta_N \equiv \frac{T_{\mathcal{RS}}}{\sqrt{1+T_{\mathcal{RS}}^2}}\,. \tag{4.80}$$

We use the subscript N because the correlation angle is the angle between $\mathbf{e}_\parallel$ and the gradient $\boldsymbol{\nabla} N$, that is $\mathbf{e}_\parallel \cdot \boldsymbol{\nabla} N \propto \cos\Delta_N$. For a generic multi-field model, the curvature spectrum is given by [91]

$$\mathcal{P}_{\mathcal{R}} = \left(\frac{H_*}{2\pi}\right)^2 |\boldsymbol{\nabla} N|^2, \tag{4.81}$$

which is the generalization of (3.59). Since $\boldsymbol{\phi}' \cdot \boldsymbol{\nabla} N = 1$, one can show that

$$\boldsymbol{\nabla}^T N = \frac{1}{\sqrt{2\varepsilon}}\left[\mathbf{e}_\parallel + T_{\mathcal{RS}}\mathbf{e}_\perp\right], \tag{4.82}$$

which follows from the comparison of expression (4.79a) with (4.81). Hence, Δ_N is really the angle between $\mathbf{e}_\parallel$ and $\boldsymbol{\nabla} N$. Secondly, we introduce a normalized vector $\mathbf{e}_N$ parallel to $\boldsymbol{\nabla}^T N$, that is

$$\mathbf{e}_N = \cos\Delta_N\,\mathbf{e}_\parallel + \sin\Delta_N\,\mathbf{e}_\perp\,. \tag{4.83}$$

We define the spectral index of a spectrum $\mathcal{P}_{\mathcal{X}}$ as

$$n_{\mathcal{X}} = \frac{d\ln\mathcal{P}_{\mathcal{X}}}{d\ln k}\,. \tag{4.84}$$

To first-order in the SRST limit, one can show that the spectral indices are given by [89]

$$n_{\mathcal{R}} = -2\varepsilon + 2\mathbf{e}_N^T\cdot\widetilde{\mathrm{M}}\mathbf{e}_N\,, \tag{4.85a}$$

$$n_{\mathcal{S}} = -2\varepsilon + 2\mathbf{e}_\perp^T\cdot\widetilde{\mathrm{M}}\mathbf{e}_\perp\,, \tag{4.85b}$$

$$n_{\mathcal{C}} = -2\varepsilon + 2\mathbf{e}_N^T\cdot\widetilde{\mathrm{M}}\mathbf{e}_\perp\arcsin\Delta_N\,, \tag{4.85c}$$

$$n_T = -2\varepsilon\,. \tag{4.85d}$$

Hence, deviations from scale invariance are determined by the slow-roll parameter ε and by the matrix $\widetilde{\mathrm{M}}$, which is affected by multi-field behaviour. Notice that the index $n_{\mathcal{R}}$ has not the same definition as n_s (1.74).

The tensor-to-scalar ratio is given by

$$r = 16\varepsilon\cos^2\Delta_N\,, \tag{4.86}$$

to first-order in SRST approximation. The cross-correlation ratio is given by

$$r_C \equiv \frac{\mathcal{C}_{\mathcal{RS}}}{\sqrt{\mathcal{P}_{\mathcal{R}}\mathcal{P}_{\mathcal{S}}}} = \sin\Delta_N\,, \tag{4.87}$$

to the same order.

Previously defined observables are related by the consistency relation

$$r = -8n_T\left(1-r_C^2\right), \tag{4.88}$$

which is the analogous of (1.94).

4.6 Non-Gaussianities

In this section we will compute the parameter f_{NL} using the δN formalism [90]. We consider the local shape since it is the dominant type present during multifield inflation. The curvature perturbation is given by [60, 62]

$$\mathcal{R} = \boldsymbol{\nabla} N \cdot \boldsymbol{\delta\phi}, \tag{4.89}$$

where $\boldsymbol{\delta\phi}$ is measured in the flat gauge and the gradient is evaluated at horizon exit. The generalization to non-trivial field space metric of equation (3.61) is given by [62]

$$f_{NL} = \frac{5}{6}\frac{\boldsymbol{\nabla}^I N\, \boldsymbol{\nabla}_I \boldsymbol{\nabla}^J N\, \boldsymbol{\nabla}_J N}{|\boldsymbol{\nabla} N|^4}. \tag{4.90}$$

Comparing equations (4.79a) and (4.81), we obtain

$$\boldsymbol{\nabla} N = \sqrt{\frac{1+T_{\mathcal{RS}}^2}{2\varepsilon_*}}\mathbf{e}_N = \frac{1}{\sqrt{2\varepsilon_*}\cos\Delta_N}\mathbf{e}_N\,. \tag{4.91}$$

Thanks to this expression, equation (4.90) becomes

$$f_{NL} = \frac{5}{6}\frac{\mathbf{e}_N^T \boldsymbol{\nabla}\boldsymbol{\nabla}^T N\, \mathbf{e}_N}{|\boldsymbol{\nabla} N|^2}. \tag{4.92}$$

Since $\mathbf{e}_N$ is normalized, we have $\mathbf{e}_N \cdot \mathbf{e}_N = 1$ and then $\boldsymbol{\nabla}\mathbf{e}_N \cdot \mathbf{e}_N = 0$. Therefore, we get

$$\boldsymbol{\nabla}\boldsymbol{\nabla}^T N\, \mathbf{e}_N = \boldsymbol{\nabla}|\boldsymbol{\nabla} N|, \tag{4.93}$$

which implies

$$\frac{\boldsymbol{\nabla}\boldsymbol{\nabla}^T N\, \mathbf{e}_N}{|\boldsymbol{\nabla} N|} = -\frac{\boldsymbol{\nabla}\varepsilon_*}{2\varepsilon_*} + \sin\Delta_N \cos\Delta_N\, \boldsymbol{\nabla} T_{\mathcal{RS}}\,, \tag{4.94}$$

where we have used the definition (4.80) and equation (4.91). Using equations (4.14) and (4.25b), one can show that

$$\boldsymbol{\nabla}\varepsilon = -\mathrm{M}\boldsymbol{\phi}'. \tag{4.95}$$

Substituting the last equation into the previous one, we find that

$$\frac{\boldsymbol{\nabla}\boldsymbol{\nabla}^T N\, \mathbf{e}_N}{|\boldsymbol{\nabla} N|^2} = \cos\Delta_N \left[\mathrm{M}^* \mathbf{e}_\parallel^* + \sqrt{2\varepsilon_*}\, \sin\Delta_N \cos\Delta_N\, \boldsymbol{\nabla} T_{\mathcal{RS}}\right]. \tag{4.96}$$

After the projection of this vector onto $\mathbf{e}_N$ and some manipulations, we get the final result [90]

$$\frac{6}{5} f_{NL} = \frac{1}{2}\big(n_{\mathcal{R}} - n_T\big)\cos^2\Delta_N + \Big[\mathrm{M}^*_{\parallel\perp} + \sqrt{2\varepsilon_*}\, \sin\Delta_N \cos\Delta_N \left(\mathbf{e}_\perp^* \cdot \boldsymbol{\nabla} T_{\mathcal{RS}}\right)\Big]\sin\Delta_N \cos\Delta_N\,. \tag{4.97}$$

As we have seen, observations constrain the indices $n_{\mathcal{R}}$ (4.85a) and n_T (4.85d) to be much less than unity. Furthermore, the turn rate $\eta_\perp/v \simeq -\mathrm{M}_{\parallel\perp}$ at horizon crossing should be less than unity in order not to spoil scale-invariance and break down the SRST approximation. Therefore, the magnitude of f_{NL} can exceed unity only if

$$\left|\sin^2\Delta_N \cos^2\Delta_N \left(\mathbf{e}_\perp^* \cdot \boldsymbol{\nabla} T_{\mathcal{RS}}\right)\right| \gtrsim \frac{1}{\sqrt{2\varepsilon_*}}\,. \tag{4.98}$$

Notice that ε is small at horizon exit and hence the right-hand side is greater than one. In order to satisfy this condition, obviously $\sin\Delta_N \neq 0$, i.e. the sourcing between modes should not vanish. In addition to this, the sourcing should be moderate to avoid $\sin^2\Delta_N \cos^2\Delta_N \ll 1$. Hence, in order to satisfy this condition, the term $\left(\mathbf{e}_\perp^* \cdot \boldsymbol{\nabla} T_{\mathcal{RS}}\right)$ should be large. This means that the sourcing $T_{\mathcal{RS}}$ of curvature modes by isocurvature ones should be sensitive to a shift perpendicular to the background trajectory. Physically speaking, two near trajectories must experience different sourcing and then small perturbations off the background trajectory have different dynamics.

Chapter 5

α-attractors

"In the absence of observers, our Universe is dead."

Andrei Linde

The so-called "α-attractor" models were born only recently but have experienced an increasingly interest among cosmologists due to their peculiarities and predictiveness. They were studied first by Andrei Linde and Renata Kallosh in 2013 in a series of papers [33, 100–102]. These models arise in the context of supergravity theories [103, 104] along with the attempt to build an inflationary mechanism in such theories [105–108]. Inflation is supposed to occur at high energies ($\sim 10^{16}\,\mathrm{GeV}$) and hence it is of fundamental importance to build a high-energy theory embedding the inflationary mechanism.

The birth of these models is quite interesting. In 2013, the data released by *Planck* [109] and by WMAP [110] pointed out that two models, the Starobinsky model [9] and the Higgs model [111], were in agreement with the latest measurements at that time (indeed, they are also in perfect agreement also with 2015 *Planck* results [6] represented in figure 1.2). This event was not read as a coincidence by cosmologists and the following deep research uncovered the existence of several classes of different models that share the same predictions. The first class discovered was conformal attractors [101, 102] which were soon generalized to α-attractors [103, 112]. Another class of models, dubbed ξ-attractors, describes inflation through a non-minimally coupled to gravity field [113–115]. In addition to those, there are models with two attractor points [116–118] that can parametrize large regions of the $r - n_s$ plane (in particular they cover the region fitting the experimental data).

In section 5.1, we will review the ideas on which α-attractors are based. Specifically, we will introduce the concept of spontaneously broken conformal symmetry. In the following two sections 5.2 and 5.3, two different classes of models (T-models and E-models) will be discussed along with their predictions. In section 5.4, we will understand why and to what extent predictions of these models are universal. In the following section 5.5, we will review the whole class of pole inflationary models and these will help us understand better the origin of the universality of α-attractor models. In section 5.6, we will analyse the initial conditions of T-models leading to inflation and their background dynamics. Finally, in section 5.7, we will describe the extension

of these models to the multi-field case which will be especially important for the last part of this thesis.

Our simulations of the background dynamics of the inflaton in chapters 5, 7 and 8 are based on the *Mathematica* code developed by M. Dias, J. Frazer and D. Seery [119] modified to fit our necessities.

5.1 Conformal invariance and conformal gauge

A conformal transformation is a local transformation of the metric

$$g_{\mu\nu}(x) \mapsto \widetilde{g}_{\mu\nu} = \Omega^2(x) g_{\mu\nu}(x), \tag{5.1}$$

where $\Omega(x)$ is a generic function of the coordinates. See appendix B for a brief review on conformal transformations.

Let us consider a simple but instructive toy model with two scalar fields ϕ and χ. Suppose the Lagrangian has the form [101]

$$\mathcal{L}_{toy} = \sqrt{-g}\left[\frac{1}{2}\partial_\mu\chi\partial^\mu\chi + \frac{\chi^2}{12}R - \frac{1}{2}\partial_\mu\phi\partial^\mu\phi - \frac{\phi^2}{12}R - \frac{\lambda}{4}\left(\phi^2-\chi^2\right)^2\right], \tag{5.2}$$

where λ is an adimensional constant. Notice that the kinetic term for χ has the wrong sign, but this is not a problem as it will be clear in the proceeding. The Lagrangian is locally conformal invariant under the transformations

$$\widetilde{g}_{\mu\nu} = e^{-2\sigma(x)} g_{\mu\nu}, \tag{5.3a}$$

$$\widetilde{\chi} = e^{\sigma(x)}\chi, \tag{5.3b}$$

$$\widetilde{\phi} = e^{\sigma(x)}\phi. \tag{5.3c}$$

It is also invariant under a $\mathrm{SO}(1,1)$ global symmetry that acts like a boost between the fields. The field χ is called "conformon".

Our theory is conformal invariant by construction and hence we are free to fix the degrees of freedom derived from this symmetry. This fixing procedure is called *gauge fixing*. Notice that the word *gauge* is overused in physics and has slightly different meaning according to the context (in particular, compare this gauge with that of chapter 2). The gauge fixing procedure is, as usual, not unique. For example, we can fix the so-called rapidity gauge[1] $\chi^2 - \phi^2 = 6M_{Pl}^2$ to remove χ,

$$\mathcal{L}_{toy} = \sqrt{-g}\left[\frac{R}{2} - \frac{1}{2}\left(\frac{6}{\phi^2+6}\right)\partial_\mu\phi\partial^\mu\phi - 9\lambda\right]. \tag{5.4}$$

[1]The name "rapidity" was chosen in analogy with the concept of rapidity in special relativity. The rapidity w is defined as $\tanh w = \beta$, where $\beta = v/c$ is the (adimensional) velocity, and it is useful for a geometric interpretation of Lorentz transformations. The Lorentz transformation between two frames of reference can be parametrized through rapidity and the reparametrized boost has the same form as a rotation, but with hyperbolic functions. The Lorentz factor turns out to be $\gamma \equiv (1-\beta^2)^{-1/2} = \cosh w$ and $\beta\gamma = \sinh w$. The parallelism between the rapidity gauge and rapidity in special relativity is the following. We can define $\chi/\sqrt{6} = \cosh(\varphi/\sqrt{6}) \equiv \gamma$ and $\phi/\sqrt{6} = \sinh(\varphi/\sqrt{6}) \equiv \gamma\beta$ and obtain $\tanh(\varphi/\sqrt{6}) = \beta$.

You can read that in the starting Lagrangian (5.2) there is not an explicit scale of mass. We have introduced the Planck mass only through the gauge fixing procedure. In order to obtain a canonical kinetic term, one can define a new field φ such that $\phi = \sqrt{6}\sinh\left(\varphi/\sqrt{6}\right)$. Then, the Lagrangian becomes

$$\mathcal{L}^E_{toy} = \sqrt{-g}\left[\frac{R}{2} - \frac{1}{2}\partial_\mu\varphi\partial^\mu\varphi - 9\lambda\right], \tag{5.5}$$

that is the Einstein frame Lagrangian for a massless scalar field φ and a cosmological constant 9λ. It is worth noticing that the new Lagrangian is not locally conformal invariant. Furthermore, the interaction terms like $\chi^2 R$ do not appear any more and we have restored Einstein theory of gravity. Alternatively, we could have parametrized the original fields as

$$\chi = \sqrt{6}\cosh\frac{\varphi}{\sqrt{6}}\,, \tag{5.6a}$$

$$\phi = \sqrt{6}\sinh\frac{\varphi}{\sqrt{6}}\,, \tag{5.6b}$$

so that the gauge fixing condition is automatically satisfied. With this parametrization we can obtain directly Lagrangian (5.5) from (5.2).

Another possible choice for the gauge is $\chi = \sqrt{6}$. In this case, the Lagrangian (5.2) becomes

$$\mathcal{L}^J_{toy} = \sqrt{-g}\left[\frac{R}{2}\left(1 - \frac{\phi^2}{6}\right) - \frac{1}{2}\partial_\mu\phi\partial^\mu\phi - \frac{\lambda}{4}(\phi^2 - 6)^2\right]. \tag{5.7}$$

Note that the Lagrangian is expressed in Jordan frame and that it exhibits a non-minimal coupling between ϕ and R. After having performed the conformal transformation

$$g_{\mu\nu} \to \left(1 - \frac{\phi^2}{6}\right)^{-1} g_{\mu\nu}\,, \tag{5.8}$$

the Lagrangian reads

$$\mathcal{L}_{toy} = \sqrt{-g}\left[\frac{R}{2} - \frac{1}{2}\left(1 - \frac{\phi^2}{6}\right)^{-2}\partial_\mu\phi\partial^\mu\phi - 9\lambda\right], \tag{5.9}$$

and a non-canonically normalized kinetic term appears. Notice that it has poles for $\phi = \pm\sqrt{6}$. In order to remove them, we should define a new field φ such that

$$\frac{d\varphi}{d\phi} = \left(1 - \frac{\phi^2}{6}\right)^{-1}, \tag{5.10}$$

and the resulting Lagrangian coincides with (5.5).

5.2 T-models

We can preserve conformal invariance and break $\mathrm{SO}(1,1)$ symmetry by introducing a function $F(\phi/\chi)$ into (5.2) [101],

$$\mathcal{L} = \sqrt{-g}\left[\frac{1}{2}\partial_\mu\chi\partial^\mu\chi + \frac{\chi^2}{12}R - \frac{1}{2}\partial_\mu\phi\partial^\mu\phi - \frac{\phi^2}{12}R - \frac{F(\phi/\chi)}{36}\left(\phi^2 - \chi^2\right)^2\right]. \tag{5.11}$$

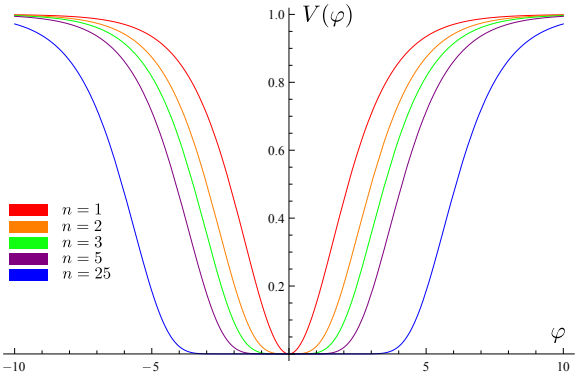

(a) Effects of the variation of n with $\alpha = 1$. Note that the potentials are very different for small values of φ, but they asymptotically coincide for $\varphi \to \infty$.

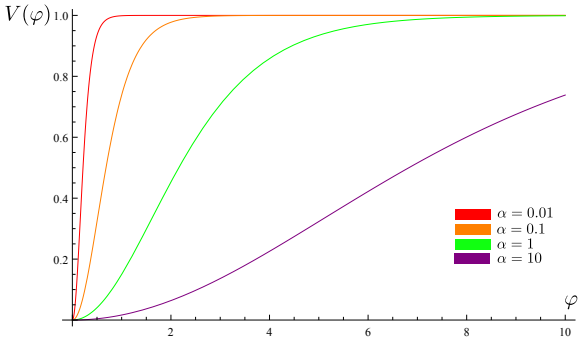

(b) Effects of the variation of α with $n = 1$. Notice the effects of the variation of α on the inflationary region (i.e. the plateau of the potential).

Figure 5.1: Examples of potentials (5.14) for T-models with $\lambda_n = 1$.

In the limit $F(\phi/\chi) \to$ const, we restore SO(1, 1) symmetry. After having fixed the gauge $\chi = \sqrt{6}$, our Lagrangian in Jordan frame becomes

$$\mathcal{L} = \sqrt{-g}\left[\frac{R}{2}\left(1 - \frac{\phi^2}{6}\right) - \frac{1}{2}\partial_\mu\phi\partial^\mu\phi - F\left(\frac{\phi}{\sqrt{6}}\right)\left(1 - \frac{\phi^2}{6}\right)^2\right]. \tag{5.12}$$

Notice the presence of an UV cutoff at $\phi = \sqrt{6}M_{Pl}$. This is due to the fact that, if the field exceeded the value $\sqrt{6}$ (in Planck units), then our theory would describe antigravity instead of gravity (due to the change of the sign in front of R). After the conformal transformation (5.8) and the introduction of a new field φ that satisfies (5.10), the starting Lagrangian (5.11) takes the form

$$\mathcal{L} = \sqrt{-g}\left[\frac{R}{2} - \frac{1}{2}\partial_\mu\varphi\partial^\mu\varphi - F\left(\tanh\frac{\varphi}{\sqrt{6\alpha}}\right)\right], \tag{5.13}$$

where we have introduced an adimensional parameter α that allows us to shift the UV cutoff [116]. Even if α allows us to parametrize a class of models and then its usefulness is obvious, we have cheated by introducing it in a reckless manner. To be honest, this parameter arises naturally in theory of supergravity and it is related to the Kähler curvature of the manifold. For our purposes, it is sufficient to think of α as a parameter influencing the UV cutoff[2]. We usually consider $\alpha = 1$, but it will be simple to reintroduce it. In fact, it is sufficient to rescale all the occurrences $\varphi/M_{Pl} \to \varphi/(\sqrt{\alpha}M_{Pl})$ (notice that the kinetic term of φ is not rescaled).

The hyperbolic tangent has the asymptotic behaviour $\tanh\varphi \to \pm 1$ in the limit $\varphi \to \pm\infty$ and then $F \to$ const in the same limit. The function $F(\phi/\chi)$ is arbitrary, therefore it is possible to mimic an arbitrary chaotic inflation potential. We point out that we can obtain a generic potential starting from a conformal theory with spontaneously broken conformal invariance. On the other hand, this procedure looks sometimes a little bit artificial. Indeed, to obtain the simple term φ^2 we need to choose $F(\tanh\frac{\varphi}{\sqrt{6}}) \sim (\tanh^{-1}\tanh\varphi)^2$. Alternatively, the function F may be thought as a deviation from an inflationary theory driven by a cosmological constant. Thus

[2]The interested reader may give a look at [112]

it is interesting to study the simplest case of monomial functions $F(\phi/\chi) = \lambda(\phi/\chi)^{2n}$. In this case the transformed potential of (5.13) has the form

$$V(\varphi) = \lambda_n \tanh^{2n}\left(\frac{\varphi}{\sqrt{6\alpha}}\right), \tag{5.14}$$

and these theories are known as T-models[3]. The potential for different values of n and α is represented in figure 5.1.

Inflation occurs in the limit $\varphi \gg 1$ where the potential is flat enough. In this limit, the potential is

$$V(\varphi) = \lambda\left(\frac{1-e^{-\sqrt{2/(3\alpha)}\varphi}}{1+e^{-\sqrt{2/(3\alpha)}\varphi}}\right)^{2n} = \lambda\left(1-4ne^{-\sqrt{\frac{2}{3\alpha}}\varphi}+\mathcal{O}\left(e^{-2\sqrt{\frac{2}{3\alpha}}\varphi}\right)\right). \tag{5.15}$$

Notice that deviations from flatness are exponentially suppressed in the limit $\varphi \gg 1$. Rewriting equation (1.36) in the form

$$\frac{d\varphi}{dN} = \frac{V'}{V} = n\sqrt{\frac{2}{3\alpha}}\left(\sinh\frac{\varphi}{\sqrt{6\alpha}}\cosh\frac{\varphi}{\sqrt{6\alpha}}\right)^{-1}, \tag{5.16}$$

and after integrating with respect to dN, we obtain the number of e-folds of inflation during slow-roll

$$N = \frac{3\alpha}{2n}\sinh^2\frac{\varphi(N)}{\sqrt{6\alpha}}. \tag{5.17}$$

The slow-roll parameters are given by

$$\varepsilon = \frac{1}{2}\left(\frac{V'}{V}\right)^2 = \frac{n^2}{3\alpha}\left(\sinh\frac{\varphi}{\sqrt{6\alpha}}\cosh\frac{\varphi}{\sqrt{6\alpha}}\right)^{-2}, \tag{5.18a}$$

$$\eta = \frac{V''}{V} = -\frac{2n}{3\alpha}\left(1-\frac{2n-1}{2}\sinh^{-2}\frac{\varphi}{\sqrt{6\alpha}}\right)\left(\cosh\frac{\varphi}{\sqrt{6\alpha}}\right)^{-2}, \tag{5.18b}$$

and it is immediate to calculate

$$n_s - 1 = 2\eta - 6\varepsilon = -\frac{8n}{3\alpha}\left(\sinh\sqrt{\frac{2}{3\alpha}}\varphi\right)^{-2}\left(n+\cosh\sqrt{\frac{2}{3\alpha}}\varphi\right), \tag{5.19a}$$

$$r = 16\varepsilon = \frac{16n^2}{3\alpha}\left(\sinh\frac{\varphi}{\sqrt{6\alpha}}\cosh\frac{\varphi}{\sqrt{6\alpha}}\right)^{-2}. \tag{5.19b}$$

After some algebra, one can obtain the relationship

$$r = \left(\frac{2n-1}{8n} - \frac{N}{6\alpha} - \frac{3}{8}\right)^{-1}(n_s - 1). \tag{5.20}$$

This equation relates the predictions of the α-attractor models in the $r - n_s$ plane. Varying α or n it is possible to have different predictions. The previous relationship is represented in

[3]There is an interesting bit of trivia about T-models' name. Although "T" can stand simply for the presence of the hyperbolic tangent, R. Kallosh and A. Linde in their pioneering work [101] assert that the name refers to Henry Ford's T-model. The reason of this analogy is the following. Like Ford's T-models were painted in any colour as long as it was black, inflationary T-models share the same predictions regardless of the particular form of the potential F.

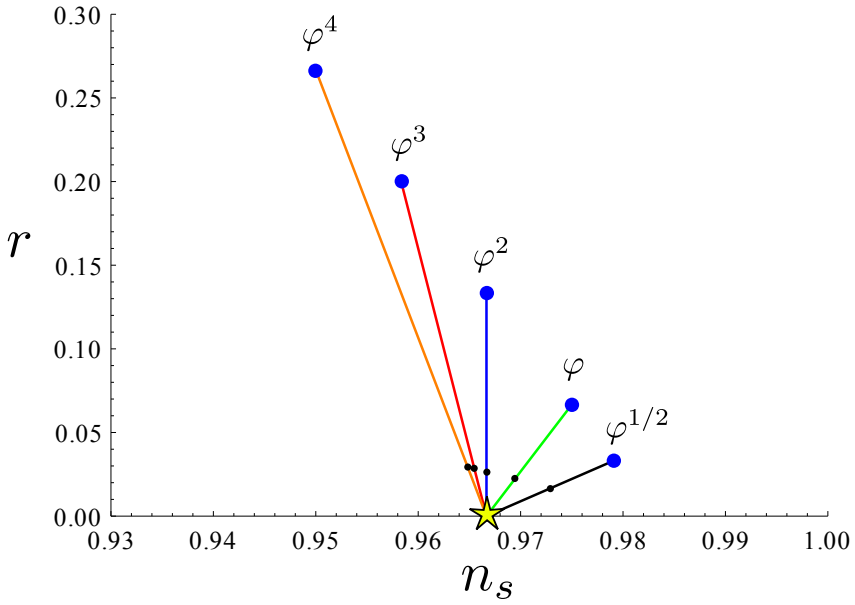

Figure 5.2: The $r - n_s$ plane for different potentials (5.14) with $2n = \frac{1}{2}, 1, 2, 3, 4$ for $N = 60$. This plot can be obtained from equation (5.20) with n and N fixed and varying α (notice that the full expressions for n_s (5.19a) and r (5.19b) should be used). The yellow star is the attractor point $(1 - 2/N, 0)$ for $\alpha \to 0$. Notice the fan-like structure of the predictions with different n. In the limit $\alpha \to \infty$, we recover the predictions $(1-(n+1)/N, 8n/N)$ of the monomial potential φ^{2n} (see equations (5.23) and section 1.8.1), which are represented by blue dots. Black dots correspond to $\alpha = 10$. The predictions of different potentials merge when $\alpha \lesssim 1$. *Planck* data constrain the value of α to $\alpha \lesssim 14$ [6]. Compare this plot with figure 1.2.

figure 5.2 for some values of n as a function of α. Notice the attractor point and the behaviour for different potentials (5.14) in the limit $\alpha \to 0$. The α-attractor models owe their name to this α-dependent behaviour.

If we consider the limit $\varphi \gg 1$, then we can approximate [101]

$$N \simeq \frac{3\alpha}{8n} e^{\sqrt{\frac{2}{3\alpha}}\varphi(N)}, \tag{5.21a}$$

$$\varepsilon \simeq \frac{3\alpha}{4N^2}, \tag{5.21b}$$

$$\eta \simeq -\frac{1}{N}, \tag{5.21c}$$

and the predictions reduce to

$$n_s - 1 \simeq -\frac{2}{N}, \tag{5.22a}$$

$$r \simeq \frac{12\alpha}{N^2}, \tag{5.22b}$$

at lowest order in $1/N$. Let us suppose that the observable window during inflation consists of 60 e-foldings, then the models predict $n_s = 0.967$ which is in perfect agreement with the latest *Planck* satellite result $n_s = 0.9645 \pm 0.0049$ [6]. At this point, the prediction may look both

accidental and of minor importance but this is only the tip of the iceberg among all interesting properties of α-attractors. Finally, notice that a variation of α corresponds to a change in r and that insofar we have only an upper limit $r < 0.09$ (95% CL) [26].

For $\alpha = 1$, the predictions coincide with that of the Starobinsky model (1.116) [9,34,120,121] and the Higgs inflation [111, 122] at leading order in $1/N$.

In the limit of large α, the predictions coincide with those of chaotic inflation (1.100) with potential $V \sim \varphi^{2n}$, that is [112, 116]

$$n_s - 1 = -\frac{n+1}{N}\,, \tag{5.23a}$$

$$r = \frac{8n}{N}\,. \tag{5.23b}$$

This behaviour is easy to understand looking at the expression for the inflaton potential (5.14) in the limit $\alpha \to \infty$.

5.3 E-models

Let us consider a Lagrangian [100]

$$\mathcal{L}_E = \sqrt{-g}\left[\frac{1}{2}\partial_\mu\chi\partial^\mu\chi + \frac{\chi^2}{12}R - \frac{1}{2}\partial_\mu\phi\partial^\mu\phi - \frac{\phi^2}{12}R - \frac{\lambda}{4}\phi^2(\phi-\chi)^2\right], \tag{5.24}$$

similar to (5.2) apart for the potential term. This Lagrangian is not symmetric under SO(1, 1) like (5.2), but it has the same conformal invariance. Fixing the rapidity gauge $\chi^2 - \phi^2 = 6$ and introducing the canonically normalized field φ (5.10) as previously done, the Lagrangian (5.24) becomes

$$\mathcal{L}_E = \sqrt{-g}\left[\frac{R}{2} - \frac{1}{2}\partial_\mu\varphi\partial^\mu\varphi - \frac{9\lambda}{4}\left(1 - e^{-\sqrt{\frac{2}{3}}\varphi}\right)^2\right], \tag{5.25}$$

which has the same form of that of Starobinsky model (1.111).

Alternatively, in order to obtain the previous Lagrangian, one can follow another approach starting from Lagrangian (5.11) [101]. Indeed, since the function F in (5.11) is completely arbitrary, we can investigate different possibilities apart for T-models. If we choose $F(\phi/\chi) \sim \frac{\phi^2}{(\phi+\chi)^2}$, fix the rapidity gauge and switch to Einstein frame, we obtain exactly the previous Lagrangian (5.25).

The parameter α can be introduced through the rescale $\varphi/M_{Pl} \to \varphi/(\sqrt{\alpha}M_{Pl})$. With α, the Lagrangian of E-models[4] looks like

$$\mathcal{L}_E = \sqrt{-g}\left[\frac{R}{2} - \frac{1}{2}\partial_\mu\varphi\partial^\mu\varphi - F\left(1 - e^{-\sqrt{\frac{2}{3\alpha}}\varphi}\right)\right]. \tag{5.26}$$

As previously done for T-models, the simplest potential has the monomial form

$$V(\varphi) = \left(1 - e^{-\sqrt{\frac{2}{3\alpha}}\varphi}\right)^{2n}, \tag{5.27}$$

[4]Here, "E" stands simply for exponential.

where n is a natural number. Notice that the potential of E-models is asymmetric, as opposed to that of T-models.

The equation of motion for the field φ during slow-roll can be written as

$$\frac{d\varphi}{dN} = \frac{V'}{V} = 2n\sqrt{\frac{2}{3\alpha}}\left(e^{\sqrt{\frac{2}{3\alpha}}\varphi} - 1\right)^{-1}, \tag{5.28}$$

and, after integration, we get

$$N = \frac{3\alpha}{4n}e^{\sqrt{\frac{2}{3\alpha}}\varphi(N)}, \tag{5.29}$$

which is valid for large N and it is analogous to (5.17). The slow-roll parameters are given by

$$\varepsilon = \frac{1}{2}\left(\frac{V'}{V}\right)^2 = \frac{1}{2}\left(\sqrt{\frac{3}{2}}\frac{\sqrt{\alpha}}{N}\right)^2 = \frac{3\alpha}{4N^2}\,, \tag{5.30a}$$

$$\eta = \left(\frac{V''}{V}\right) = -\frac{1}{N}\,, \tag{5.30b}$$

at lowest order in $1/N$ and where the expression of η is valid for $N \gg \alpha$. Hence, at least in the previous limit, the predictions of E-models coincide with that of T-models (5.22). If $\alpha = 1$, we recover the predictions of the Starobinsky model (1.116).

5.4 Universality of predictions

Conformal inflationary models share the same predictions regardless of the type of the starting potential. This behaviour is induced through the stretch of the potential passing from ϕ to $\sqrt{6}\tanh(\varphi/\sqrt{6})$. Remember that a sufficiently large flat region in the potential is an essential element in order to have an inflationary period. The procedure of conformal stretch allows us to build an entire class of potentials that could lead to inflation. Here we assume $\alpha = 1$ since a different value induces a rescaling of the field in the potential term and does not alter the characteristics that we are going to describe. Our discussion is partially based on [101].

Let us consider an instructive potential, $V(\phi) = \sin(8\phi)$ (there is nothing special neither in the choice of sine function nor in the value 8). If we stretch $\phi \to \sqrt{6}\tanh(\varphi/\sqrt{6})$ in this potential, we obtain a new potential with two horizontal asymptotes (see figure 5.3). Notice that the stretched potential $V(\varphi)$ possesses two flat regions, one for positive values of the field and the other one for negative values. The former has the perfect form for slow-roll inflation, while the latter cannot be a viable option.

Notice that the transformation $\phi \to \sqrt{6}\tanh(\varphi/\sqrt{6})$ leads to potentials $V(\varphi)$ that tend asymptotically to $V(\phi = \sqrt{6})$ since the hyperbolic tangent is exponentially pushed towards ± 1 as $\varphi \to \pm\infty$. In addition, this procedure is insensitive to the initial potential, in fact it could have any form and produce a stretched potential with an inflationary region. Since the asymptotic behaviour is determined merely by the growth of $V(\phi)$ near $\phi = \pm\sqrt{6}$, someone has fifty percent chance to get an inflationary region starting from an arbitrary potential. This procedure is the farthest one from fine-tuning one could imagine: with an arbitrary potential one could get an ideal inflationary region.

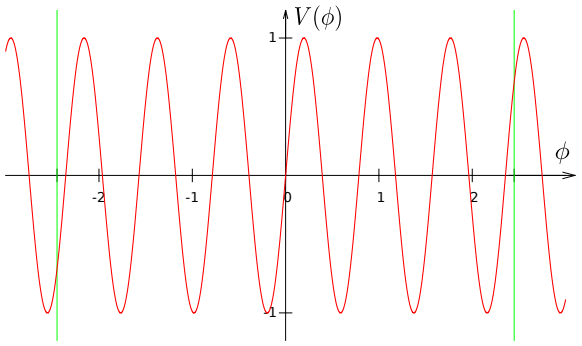

(a) Potential $V(\phi) = \sin(8\phi)$. Green vertical lines at $\phi = \pm\sqrt{6}$. Note that the sine has three peaks between 0 and $\sqrt{6}$.

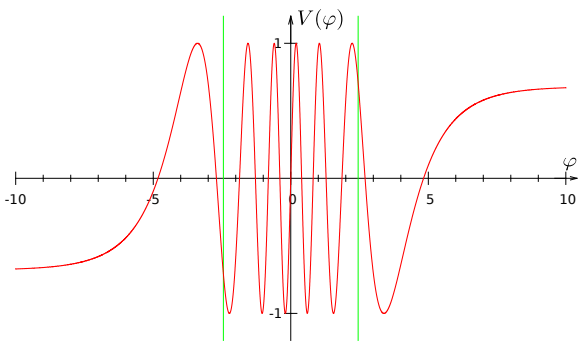

(b) Potential $V(\varphi) = \sin(8\sqrt{6}\tanh\frac{\varphi}{\sqrt{6}})$. Green vertical lines at $\varphi = \pm\sqrt{6}$. The asymptotic values are equal to $V(\phi = \pm\sqrt{6})$.

Figure 5.3: Notice that the asymptotic behaviour of $V(\varphi)$ depends on the values assumed by $V(\phi)$ at $\phi = \pm\sqrt{6}$. Note also that inflation can only occur in the right plateau in figure (b).

Intuitively, the reason why this stretch could produce an inflationary potential is clear. Anyway, we want to found our guess on the basis of an analytical investigation. Only two assumptions are necessary. First, we start from a potential $V(\phi)$ and perform the transformation

$$\phi(\varphi) = \sqrt{6}\tanh\frac{\varphi}{\sqrt{6}}\,. \tag{5.31}$$

Secondly, we suppose that inflation occurs for $\varphi \gg 1$. The derivative of the potential with respect to φ is given by

$$\frac{dV(\varphi(\phi))}{d\varphi} = \frac{dV}{d\phi}\frac{d\phi}{d\varphi} = \frac{dV}{d\phi}\frac{1}{\cosh^2\left(\varphi/\sqrt{6}\right)}\,. \tag{5.32}$$

Since inflation occurs for $\varphi \gg 1$, we can approximate $dV/d\phi$ with the value it assumes at $\phi = \sqrt{6}$ (from now on, we are only going to focus on this point); let us indicate it with V'_*. For the same reason, we approximate the potential $V(\phi)$ with V_*. The slow-roll parameter

$$\varepsilon \simeq \frac{1}{2}\left(\frac{dV}{d\varphi}\frac{1}{V}\right)^2 \simeq \frac{1}{2}\left(\frac{V'_*}{V_*}\frac{1}{\cosh^2\left(\varphi/\sqrt{6}\right)}\right)^2 \tag{5.33}$$

is very small due to the damping factor $\cosh^{-4}$. Remarkably, we have never made assumptions on the initial potential. Through the transformation $\phi \to \varphi$ the slow-roll parameter ε is suppressed without imposing any condition on the form of the potential. We expect that $\varepsilon \sim 1$ when $\varphi \sim \sqrt{6}$, but this is only a rough estimate since in this region the damping factor is absent while ε depends on the specific potential chosen.

The second derivative of the potential is given by

$$\frac{d^2V(\varphi(\phi))}{d\varphi^2} = \frac{d^2V}{d\phi^2}\left(\frac{d\phi}{d\varphi}\right)^2 + \frac{dV}{d\phi}\frac{d^2\phi}{d\varphi^2} \simeq V''_*\frac{1}{\cosh^4\left(\varphi/\sqrt{6}\right)} - \sqrt{\frac{2}{3}}V'_*\frac{\sinh\left(\varphi/\sqrt{6}\right)}{\cosh^3\left(\varphi/\sqrt{6}\right)}\,, \tag{5.34}$$

with the same approximations considered before. The slow-roll parameter

$$\eta = \frac{1}{V}\frac{d^2V}{d\varphi^2} \simeq \frac{V''_*}{V_*}\frac{1}{\cosh^4\left(\varphi/\sqrt{6}\right)} - \sqrt{\frac{2}{3}}\frac{V'_*}{V_*}\frac{\sinh\left(\varphi/\sqrt{6}\right)}{\cosh^3\left(\varphi/\sqrt{6}\right)} \tag{5.35}$$

tends exponentially to zero as $\varphi \to +\infty$. Again, we have not made any assumption on the behaviour of the potential and hence observations similar to the previous ones apply. Finally, it is clear that the particular form of the potential is important only at the end of inflation.

One question is still unanswered: to what extent are predictions of such models model-independent? Let us have a look in the neighbourhood of $\phi = \sqrt{6}$, which is a special value as we have explained. The Taylor expansion of $V(\phi)$ near $\phi = \sqrt{6}$ reads

$$V(\phi) = V_* + \sqrt{6}V'_* x + \frac{6}{2}V''_* x^2 + \dots , \tag{5.36}$$

where $x \equiv (\phi - \sqrt{6})/\sqrt{6} = \tanh \frac{\varphi}{\sqrt{6}} - 1$ and $V_* \equiv V(x = 0)$. When $\phi = \sqrt{6}$, we get $x = 0$ and $\varphi \to +\infty$. Because of this, we can approximate $\tanh(\varphi/\sqrt{6}) \simeq 1 - 2\exp(-\sqrt{2/3}\varphi)$ and hence $x \simeq -2\exp(-\sqrt{2/3}\varphi)$. Then the previous expansion with respect to φ reads

$$V(\varphi) = V_* - 2\sqrt{6}V'_* e^{-\sqrt{\frac{2}{3}}\varphi} + 12V''_* e^{-2\sqrt{\frac{2}{3}}\varphi} + \dots , \tag{5.37}$$

where $V_* \equiv V(x = 0) = V(\varphi \to \infty)$. Notice that all higher terms are exponentially suppressed. Then, if $V(\phi)$ has not a pathological behaviour, all the stretched potentials will look the same in the flat region.

The equation of motion for φ in the slow-roll approximation is given by

$$\frac{d\varphi}{dN} = \frac{1}{V}\frac{dV}{d\varphi} , \tag{5.38}$$

and it can be restated in terms of ϕ as

$$\frac{d\varphi}{dN} = \frac{1}{V}\frac{dV}{d\phi}\frac{d\phi}{d\varphi} \simeq \frac{V'_*}{V_*}\cosh^{-2}\frac{\varphi}{\sqrt{6}} . \tag{5.39}$$

We integrate this equation

$$\int_N^0 \frac{V'_*}{V_*} dN' = \int_{\varphi(N)}^{\varphi(0)} \cosh^2 \frac{\varphi}{\sqrt{6}}\, d\varphi \tag{5.40}$$

$$N\,\frac{V'_*}{V_*} = \frac{\varphi(N) - \varphi(0)}{2} + \frac{\sqrt{6}}{4}\left[\sinh\left(\sqrt{\frac{2}{3}}\varphi(N)\right) - \sinh\left(\sqrt{\frac{2}{3}}\varphi(0)\right)\right] , \tag{5.41}$$

where N denotes the number of e-folds till the end of inflation. In order to study this expression, it is convenient to make a plot varying the ratio V'_*/V_*, that is the only model-dependent term. Figure 5.4 captures the main features of this expression and we rely on its description for comments on the last equation. The main result from this analysis is that it is always possible to find an inflationary region of the stretched potential for a given initial potential $V(\phi)$. Notice that the exponentially stretch makes the specific expression of the potential nearly insignificant. Because of that, we can claim that the predictions of these models are universal.

Notice that the number of e-folds depends on the field roughly as $N \sim \sinh(\varphi/\sqrt{6})$ in the limit $\varphi \gg 1$. This dependence introduces a hierarchy for the slow-roll parameters. In fact, the slow-roll parameter ε (5.33) goes as $\varepsilon \sim N^{-2}$ and η (5.35) behaves as $\eta \sim N^{-1}$. This dependence is the same that we found in equations (5.21).

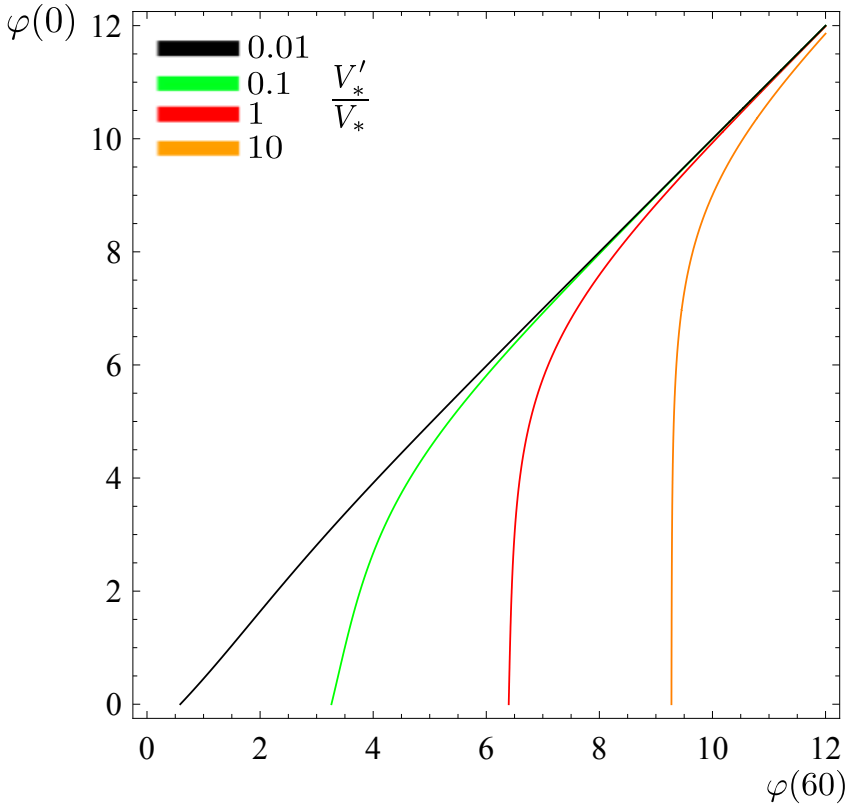

Figure 5.4: This plot tries to represent the most important properties of equation (5.41) which holds only during slow-roll. Some comments are in order hereby. The plot can be read as follows. If the field starts from $\varphi(60)$, then it will reach the value $\varphi(0)$ after 60 e-folds of inflation. Different ratios of V'_*/V_* are plotted according to the legend. Let us focus on the red line. If $\varphi(60) = 7$ then $\varphi(0) \sim 6$; after that, inflation is not over and we should add all the e-folds from $\varphi(0)$ to $\varphi \sim \sqrt{6}$. This initial value appears appropriate if we want inflation to last for at least 60 e-folds. For large initial values of $\varphi(60)$, 60 e-folds elapse so rapidly that $\varphi(0) \simeq \varphi(60)$ and hence in this region there are no obstacle for a sufficiently long inflation. Let us note that this behaviour is independent of the ratio V'_*/V_*. That ratio determines the possible initial conditions for an acceptable inflationary era. Indeed, increasing the ratio, translates to the right the acceptable initial values. This is obvious since, if the non-stretched potential has a high ratio V'_*/V_*, the field should start in a sufficiently flat region of the stretched potential, i.e. $\varphi \gg 1$. Decreasing the ratio flatten the function towards the straight line $\varphi(0) = \varphi(60)$ leading to trivial results (in the limit $V'_*/V_* \to 0$, the non-stretched potential is already sufficiently flat for inflation). At the end, the ratio V'_*/V_* has little importance; we can always find a suitable region of the stretched potential where inflation can occur. Let us conclude with a warning. Equation (5.41) holds only in the slow-roll limit; here we have not considered this issue. However it is simple to take care of this restriction with equation (5.33). For example, if $V'_*/V_* = 1$, then $\varepsilon \ll 1$ for $\varphi \gtrsim 2$.

Let us conclude this section with a rough estimate. Suppose that inflation ends exactly when

$$\varepsilon = \frac{1}{2}\varphi'^2 = 1\,, \tag{5.42}$$

then the final velocity is $|\varphi'| = \sqrt{2}$. Let us assume that afterwards the field moves with constant velocity (obviously this is a drastic approximation since the field is accelerating) and that $\varepsilon = 1$ for $\varphi \sim \sqrt{6}$, then the field will reach the value $\varphi = 0$ in less than 2 e-folds. These considerations are important after the end of inflation for the reheating phase.

5.5 Pole inflation and universality

In this section we are going to describe the class of pole inflationary models [123–125]. These models will help us comprehend the origin of the attractor behaviour behind α-attractors in a more general framework.

Consider a single-field Lagrangian for the field φ. Suppose that there is a point in field space where the kinetic term is singular (for example the Lagrangian (5.9) has this property). For convenience, we assume that this point is the origin $\varphi = 0$ of the field space. Thanks to these assumptions, the studied Lagrangian takes the form [124]

$$\mathcal{L} = \sqrt{-g}\left[-\frac{1}{2}\frac{a_p}{\phi^p}\partial_\mu\phi\partial^\mu\phi - V_0\Big(1 - \phi + \mathcal{O}\left(\phi^2\right)\Big)\right], \tag{5.43}$$

where $a_p > 0$ and we have expanded the potential about the origin since we assume that it is regular in this region.

The canonically normalized field φ can be obtained through the redefinition

$$\varphi = \frac{2\sqrt{a_p}}{p-2}\phi^{\frac{2-p}{2}} \tag{5.44}$$

if $p \neq 2$, or through

$$\varphi = -\sqrt{a_p}\log\phi \tag{5.45}$$

if $p = 2$. We notice, en passant, that a non-canonically normalized kinetic term of the form

$$-\frac{1}{2}f^{-2}(\phi)\partial_\mu\phi\partial^\mu\phi, \tag{5.46}$$

where $f(\phi)$ is a generic function, can be normalized defining a new field φ such as

$$\frac{d\phi}{d\varphi} = f(\phi)\,. \tag{5.47}$$

The inflaton potential is therefore

$$V(\varphi) = V_0\left(1 - \left(\frac{p-2}{2\sqrt{a_p}}\varphi\right)^{\frac{2}{2-p}} + \mathcal{O}\left(\varphi^2\right)\right) \tag{5.48}$$

if $p \neq 2$, or

$$V(\varphi) = V_0\left(1 - e^{-\frac{\varphi}{\sqrt{a_p}}} + \mathcal{O}\left(\varphi^2\right)\right) \tag{5.49}$$

if $p = 2$. The last expression should be familiar to the reader because it looks like (5.15).

Using equation (1.36) and after some algebra, the number of e-folds can be written as [124]

$$N = \frac{a_p}{p-1}\left(\frac{1}{\phi^{p-1}(N)} - \frac{1}{\phi^{p-1}(N_f)}\right), \tag{5.50}$$

where N_f is the total number of e-folds of inflation, $\phi(N_f) = (2a_p)^{\frac{1}{p}}$ and where we have retained only the leading order terms. Note that the number of e-foldings of inflation is completely determined by the order p of the pole and by the factor a_p. Right from the beginning, we have considered a simple pole, even if this was not mandatory. Indeed, nothing prevents us from expanding the field about the pole using Laurent series but, in the limit $N \gg 1$, one can assume that the only relevant pole is the lowest order one (this can be false if $a_p \gg 1$ for a given p).

The spectral index turns out to be

$$n_s - 1 = -\frac{p}{(p-1)N}\,, \tag{5.51}$$

and the tensor-to-scalar ratio is

$$r = \frac{8}{a_p}\left(\frac{a_p}{(p-1)N}\right)^{\frac{p}{p-1}}. \tag{5.52}$$

Hence, the spectral index depends only on the order of the pole. Instead, r depends also on the residue a_p, but this dependence becomes weak in the limit of large p. For $p = 2$, the predictions (5.22) of α-attractors are recovered. Hence, the presence of a second order pole is responsible for the attractor behaviour previously discussed. The stretching of the potential derives from the expansion (5.49). In fact, if the field $\varphi \gg 1$, the only non-suppressed term is V_0, that is the value of the potential at the pole $\phi = 0$.

5.6 T-models and initial conditions

In this section, we will analyse a single-field T-model and study its inflationary dynamics. In particular, we will study which initial conditions lead to an inflation that lasts at least $50 \div 70$ efoldings. This is a stringent condition to impose on the inflationary background solution together with the slow-roll conditions.

The Lagrangian of T-models on flat FRW is given by (5.13),

$$\mathcal{L} = a^3(t)\left(-\frac{1}{2}\partial_\mu\varphi\partial^\mu\varphi - V\left(\tanh\frac{\varphi}{\sqrt{6\alpha}}\right)\right). \tag{5.53}$$

We have seen that reasonable potentials are given by (5.14). With a little loss of generality, we fix the potential

$$V(\varphi) = \tanh^2\frac{\varphi}{\sqrt{6}}\,, \tag{5.54}$$

since other possibilities are similar to this case and the conclusions can be readily generalized to generic terms. In addition to this, we have fixed $\alpha = 1$. This potential is represented in figure 5.5a. At the end of this section, we will consider the generic potential (5.14).

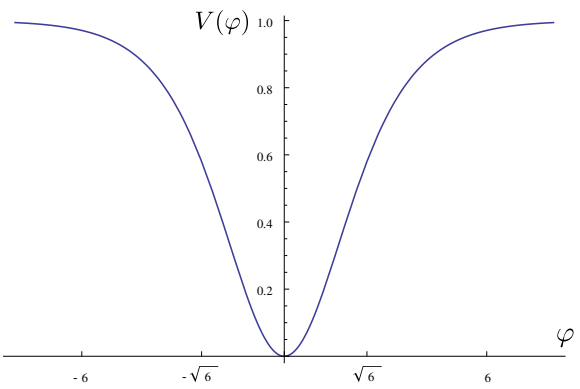

(a) Potential $V = \tanh^2(\varphi/\sqrt{6})$. Notice the flat region for $\varphi \gtrsim 6$.

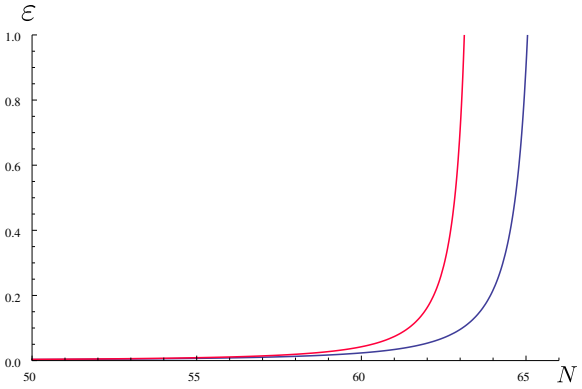

(b) Slow-roll parameter $\varepsilon(N)$ for $\varphi(0) = 6.3$ and $\varphi'(0) = 0$. Numerical solution (blue) compared with analytical approximation (red) obtained from equations (5.58) and (5.60).

Figure 5.5

It is convenient to face the problem using the number of e-folds instead of time in order to constrain easily the duration of inflation. Furthermore, it is convenient to define the number of e-folds as $dN = Hdt$ so that initial conditions are given at $N = 0$ (see definition (4.10)). This definition is particularly useful for numerical computations because one fixes the initial conditions and he does not know in advance when inflation will end. Notice that inflation can start some time later at $N = N_i$ and it ends after N_f e-folds of inflation.

The background equations of motion rewritten in terms of the number of e-folds N are[5]

$$\varphi'' + (3 - \varepsilon)\varphi' + (3 - \varepsilon)\frac{V'}{V} = 0, \tag{5.55a}$$

$$H^2 = \frac{V}{3 - \varepsilon}, \tag{5.55b}$$

where the prime denotes the derivative with respect to N and $\varepsilon = \frac{1}{2}\varphi'^2$. In figure 5.6, some trajectories are depicted considering the potential (5.54). Observe the relationship between the field excursion and the number of e-folds.

Notice that $|\varphi'| < \sqrt{6}$ due to equation (5.55b). The value $\sqrt{6}$ has nothing to do with that in the potential of α-attractors. Why is there a maximum velocity for the field? First of all, notice that N is an useful parameter to use in calculations but it is a rather dumb unity of measure for time. Let us consider a field φ and suppose that its potential vanishes. Then, Friedmann equation reads

$$H^2 = \frac{\dot{\varphi}^2}{6}. \tag{5.56}$$

The previous equation can be considered as a constraint on $\dot{\varphi}$ once H is fixed. Therefore, the maximum velocity allowed for a fixed H is $\dot{\varphi} = \sqrt{6}H$. Rewritten in terms of N, this maximum velocity reads $\varphi' = \sqrt{6}$. Finally, note that φ' is adimensional.

[5]These equations can be derived directly from the equations (1.24) and (1.8b) using the definition $dN = Hdt$. Alternatively, they can be deduced from equations (4.12) and (4.13) considering a one-dimensional field space.

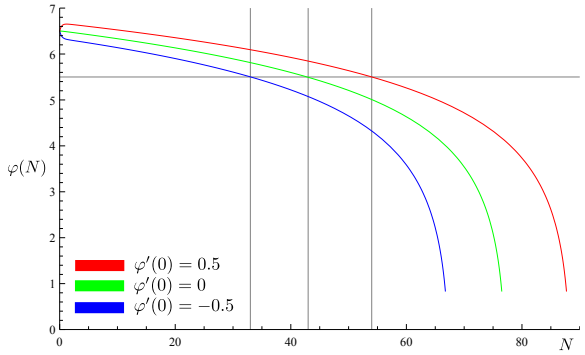

(a) Value of the field φ as a function of the number of e-folds N for three different trajectories. Notice that inflation ends ($\varepsilon = 1$) when $\varphi \simeq 0.8$.

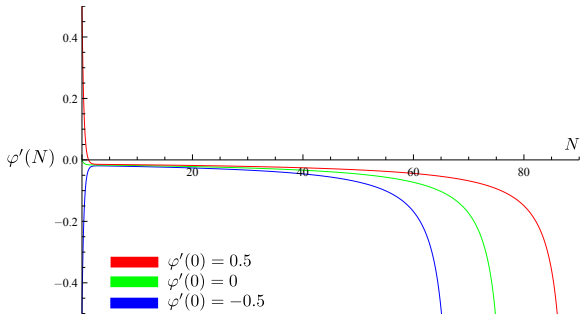

(b) Value of the field velocity φ' as a function of the number of e-folds N for the three trajectories shown in the left plot. Notice the initial suppression of the velocities (compare with figure 5.7a).

Figure 5.6: Trajectories for the potential (5.54) with initial condition $\varphi(0) = 6.5$ and different initial velocities $\varphi'(0)$. Inflation ends at $N_f \simeq 67$ if $\varphi'(0) = -0.5$, at $N_f \simeq 77$ if $\varphi'(0) = 0$ and at $N_f \simeq 88$ if $\varphi'(0) = 0.5$. It is interesting to calculate how many e-folds are necessary for the field φ to reach a certain value. As an example, let us consider the number of e-folds N_1 elapsed from $\varphi(0) = 6.5$ to $\varphi(N_1) = 5.5$. We obtain $N_1 \simeq 33$ (50% of the total number of e-folds N_f of inflation) for $\varphi'(0) = -0.5$, $N_1 \simeq 43$ (55% of N_f) for $\varphi'(0) = 0$ and $N_1 \simeq 54$ (60% of N_f) for $\varphi'(0) = 0.5$. The total field excursion $\varphi(0) - \varphi(N_f) \sim 6$ for all trajectories, however at least one half of the total number of e-folds elapsed for a field excursion $\varphi(0) - \varphi(N_1) = 1$.

In the slow-roll approximation, we get

$$\frac{d\varphi}{dN} = -\sqrt{\frac{2}{3}}\frac{1}{\cosh(\varphi/\sqrt{6})\sinh(\varphi/\sqrt{6})}\,. \tag{5.57}$$

The velocity of the field tends to zero if $\varphi \gg 1$. We can suppose that the field starts from rest since $\frac{1}{2}\varphi'^2 \ll 1$ in order to have slow-roll; our results will be just slightly modified introducing an initial velocity (afterwards we will discuss what happens if the initial velocity is not zero). Notice that the exponential suppression ceases in a neighbourhood of $\varphi \sim \sqrt{6}$ and there the field velocity can increase. The last equation can be integrated and the result is

$$\varphi(N) = \sqrt{6}\,\mathrm{arccosh}\sqrt{\cosh^2\left(\frac{\varphi(N_i)}{\sqrt{6}}\right) - \frac{2}{3}N}\,. \tag{5.58}$$

This equation holds only during the slow-roll period, therefore we need to estimate when slow-roll breaks down. Before doing this, let us calculate the second fundamental slow-roll parameter,

$$\eta = \frac{1 - 2\sinh^2(\varphi/\sqrt{6})}{9\cosh^2(\varphi/\sqrt{6})\sinh^2(\varphi/\sqrt{6})}\,. \tag{5.59}$$

In the limit $\varphi \gg 1$, it is exponentially suppressed and hence inflation can occur without any obstacle.

Let us suppose that equation (5.58) describes the trajectory of the field even after the slow-roll regime. Inflation ends when $\varepsilon = 1$, or else when $|\varphi'| = \sqrt{2}$. Given the previous assumption,

$$\frac{1}{2}\left(\sqrt{\frac{2}{3}}\frac{1}{\cosh(\varphi/\sqrt{6})\sinh(\varphi/\sqrt{6})}\right)^2 = 1 \tag{5.60}$$

when

$$\frac{1}{2}\sinh\sqrt{\frac{2}{3}}\varphi = \frac{\sqrt{3}}{3}, \tag{5.61}$$

and hence inflation ends at $\varphi(N_f) \simeq 1.2$. This is only a rough estimate since we have extrapolated it assuming slow-roll dynamics even when the field velocity is of order one. On the other hand, it is not necessary to know the exact value at which inflation ends. The reason is simple. As long as $\varphi \gtrsim \sqrt{6}$ inflaton is in the slow-roll regime. In proximity of $\varphi \sim \sqrt{6}$, the velocity of the field becomes of order unity and so it will reach the minimum of the potential in less than three e-folds even assuming a constant velocity (obviously the field is accelerating). Finally, inflation should have lasted at least for 50 e-folds before inflaton reaches the value $\varphi \sim \sqrt{6}$ and hence a few e-folds are negligible. In figure 5.5b the analytical approximation is compared with the numerical solution. The difference between the numerical simulation and the analytical approximation is evident only during the last 5 e-folds of inflation. Finally, the value $\varphi(N_f)$ can be obtained through numerical computations. For example, if $\varphi(N_i) = 6.5$, inflation ends when $\varphi \simeq 0.8$, as can be inferred from figure 5.6a.

It is interesting to notice that the initial velocity of the field may be of order unity as the velocity undergoes an initial damping period. Indeed, in the limit $\varphi >> 1$, equation (5.55a) reduces to

$$\varphi'' + \left(3 - \frac{1}{2}\varphi'^2\right)\varphi' = 0\,. \tag{5.62}$$

The solution of this equation can be found analytically with the method of the integrating factor. Let us solve first the equation

$$y' + Ay + By^3 = 0\,, \tag{5.63}$$

where A and B are constant and it has the same form of equation (5.62). Rewriting the last equation as

$$\frac{dy}{Ay + By^3} + dN = 0\,, \tag{5.64}$$

we need to find a function $\Phi(y, N)$ that can satisfy

$$\frac{d\Phi}{dy} = (Ay + By^3)^{-1}, \tag{5.65a}$$

$$\frac{d\Phi}{dN} = 1\,. \tag{5.65b}$$

These conditions lead to the solution

$$\Phi(y, N) = \frac{1}{A}\ln\left(\frac{y}{\sqrt{A + By^2}}\right) + N\,. \tag{5.66}$$

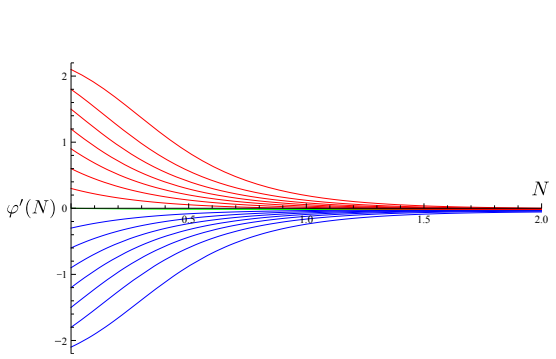

(a) Attractor behaviour of the system (5.55) with potential (5.54) and $\varphi(0) = 6.3$. Even with a high initial velocity $\varphi'(0)$, inflation starts. Notice that the attractor solution is reached in less than 2 e-folds and that the sign of the velocity does not matter. Even if slow-roll dynamics is very similar (see figure 5.6b), the solution with $\varphi'(0) = 2.1$ predicts $N_f \simeq 152$ and that with $\varphi'(0) = -2.1$ predicts $N_f \simeq 30$.

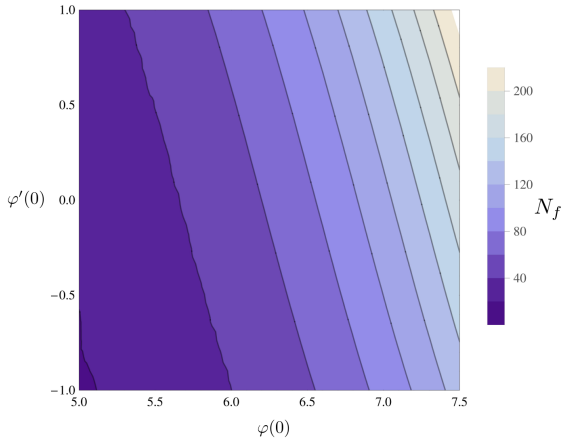

(b) Viable initial conditions. N_f is the total number of e-folds of inflation. Every coloured band corresponds to 20 e-folds. The tilts are caused by the initial velocity. If the initial velocity is negative $\varphi'(0) < 0$ (i.e. directed towards the minimum), then inflation lasts less than the opposite case.

Figure 5.7: Dynamics of inflaton described by equations (5.55) with potential (5.54).

At the end, the general solution of (5.63) is given by the curves $\Phi(y, N) = C$, where C is a constant, and hence

$$y(N) = \pm \sqrt{\frac{A}{\exp\Big\{2A(N-C)\Big\} - B}}\,. \tag{5.67}$$

Substituting the values $A = 3$ and $B = -\frac{1}{2}$ inferred from (5.62), we get the solution

$$\varphi'(N) = \pm\sqrt{6}\left[e^{6N}\left(\frac{6}{\varphi'^2(0)} - 1\right) + 1\right]^{-\frac{1}{2}}, \tag{5.68}$$

where we have restored the initial velocity[6]. Now the initial suppression is manifest and it is represented in figure 5.7a. Since the characteristic time is 1/3 e-folds, the suppression is very efficient and the velocity dropped in only one e-fold. After that, slow-roll inflation starts. The sign in front of the square root is determined by the sign of the initial velocity. Let us notice explicitly that this solution holds when V'/V is negligible, but the field is not necessarily slowly rolling (in fact this equation is particularly useful to study initial conditions). On the other hand, after the exponential suppression of the velocity, the field starts to slowly roll down driven by the potential. A region of the field space where initial conditions are acceptable is depicted in figure 5.7b along with the number of e-folds of inflation. Notice that the potential is so flat

[6]Notice that in equation (5.68) $\varphi'(0) \neq 0$. The solution of (5.62) with $\varphi'(0) = 0$ is simply given by $\varphi(N) \equiv \varphi(0)$. Notice that, in presence of a potential, the field could have a zero initial velocity and start rolling down.

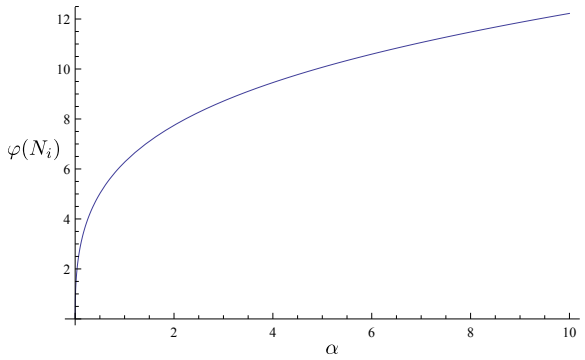

(a) Effect of the variation of α for the potential $V(\varphi) = \tanh^2\left(\varphi/\sqrt{6\alpha}\right)$.

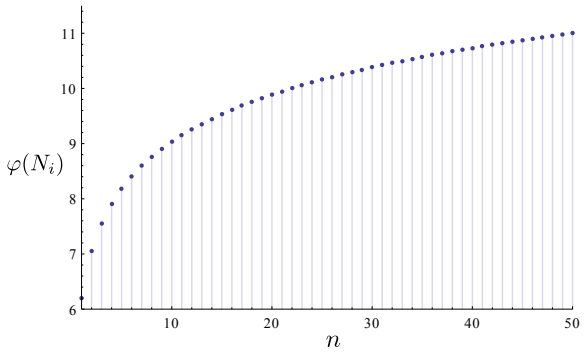

(b) Effect of the variation of n for the potential $V(\varphi) = \tanh^{2n}\left(\varphi/\sqrt{6}\right)$.

Figure 5.8: Drift of initial position $\varphi(N_i)$ described by equation (5.70) with $N_f = 60$ due to variation of α and n. If the initial position $\varphi(N_i)$ is greater than the value extrapolated from the plots, inflation lasts for more than 60 e-folds.

that shifting the initial position of the field from $\varphi(0) \sim 6$ to $\varphi(0) \sim 7.5$ increases by nearly a hundred the number of efoldings of inflation.

Before concluding this section, we consider the more general potential $V(\varphi) = \tanh^{2n}\frac{\varphi}{\sqrt{6\alpha}}$. Equation (5.58) becomes

$$\varphi(N) = \sqrt{6\alpha}\,\operatorname{arccosh}\sqrt{\cosh^2\left(\frac{\varphi(N_i)}{\sqrt{6\alpha}}\right) - \frac{2n}{3\alpha}N}\,. \tag{5.69}$$

The parameter α affects the region where inflation occurs and the value of the field at the end of inflation. Indeed, now we expect that inflation ends when $\varphi(N_f) \sim \sqrt{6\alpha}$. Suppose we want to estimate the initial configuration that leads to 60 e-folds of inflation. Previous equation can be inverted easily,

$$\varphi(N_i) \simeq \sqrt{6\alpha}\,\operatorname{arccosh}\sqrt{\cosh^2(1) + \frac{40n}{\alpha}}\,, \tag{5.70}$$

where we have supposed that equation (5.69) is valid until the end of inflation. The dependence on α is depicted in figure 5.8a and that on n in figure 5.8b. If the field starts to slow-roll with a higher initial position than $\varphi(N_i)$, inflation will last for more than 60 e-folds. These estimates are rather good even considering an initial velocity because it is rapidly suppressed during an initial transient. In addition to this, the field reaches the minimum in a few e-folds after $\varphi \sim \sqrt{6}$.

Finally, let us sum up the main results of this section. If the potential of our model is (5.54), inflation occurs for at least 60 e-folds if the initial position of the field is $\varphi(0) \gtrsim 6.3$ with a little dependence on the initial velocity (see figure 5.7). Notice that the ratio $V'_*/V_* = 0.82$ for the potential (5.54), and then one can compare the results of this section to those of section 5.4.

5.7 Two-field attractors

The Lagrangian (5.11) can be trivially extended [102] to include n fields ϕ_I together with the conformon field χ,

$$\mathcal{L} = \sqrt{-g}\left[\frac{1}{2}\partial_\mu\chi\partial^\mu\chi + \frac{\chi^2}{12}R - \frac{1}{2}\partial_\mu\phi_I\partial^\mu\phi_I - \frac{\phi_I^2}{12}R - \frac{W(\phi_I/\chi)}{36}\left(\chi^2-\phi_I^2\right)^2\right], \tag{5.71}$$

where a sum over I is implicit. This Lagrangian is locally conformal invariant and, in the limit $W \to$ const, it has also a global SO$(n,1)$ symmetry.

We are interested only in the two-field case, then $I = 1, 2$. Hence, the previous Lagrangian explicitly reads

$$\mathcal{L} = \sqrt{-g}\left[\frac{1}{2}\partial_\mu\chi\partial^\mu\chi + \frac{\chi^2}{12}R - \frac{1}{2}\partial_\mu\phi_1\partial^\mu\phi_1 - \frac{1}{2}\partial_\mu\phi_2\partial^\mu\phi_2 - \frac{\phi_1^2+\phi_2^2}{12}R - \frac{W(\phi_1/\chi,\phi_2/\chi)}{36}\left(\chi^2-\phi_1^2-\phi_2^2\right)^2\right], \tag{5.72}$$

Observing the form of this Lagrangian, it is natural to parametrize the fields as

$$\phi_1 = \rho\cos\theta\,, \tag{5.73a}$$

$$\phi_2 = \rho\sin\theta\,. \tag{5.73b}$$

Then we get

$$\mathcal{L} = \sqrt{-g}\left[\frac{\chi^2-\rho^2}{12}R + \frac{1}{2}\partial_\mu\chi\partial^\mu\chi - \frac{1}{2}\partial_\mu\rho\partial^\mu\rho - \frac{1}{2}\rho^2\partial_\mu\theta\partial^\mu\theta - \frac{\left(\chi^2-\rho^2\right)^2}{36}W\left(\frac{\rho}{\chi}\cos\theta, \frac{\rho}{\chi}\sin\theta\right)\right], \tag{5.74}$$

and we can fix the gauge $\chi^2 - \rho^2 = 6$ to obtain

$$\mathcal{L} = \sqrt{-g}\left[\frac{R}{2} - \frac{1}{2}\frac{\partial_\mu\rho\partial^\mu\rho}{1+\frac{\rho^2}{6}} - \frac{1}{2}\rho^2\partial_\mu\theta\partial^\mu\theta - W\left(\frac{\rho}{\sqrt{\rho^2+6}}\cos\theta, \frac{\rho}{\sqrt{\rho^2+6}}\sin\theta\right)\right]. \tag{5.75}$$

Since there is a non-canonically normalized kinetic term for ρ, we introduce a new field φ such that

$$\rho = \sqrt{6}\sinh\frac{\varphi}{\sqrt{6}}\,, \tag{5.76}$$

in order to get the Lagrangian

$$\mathcal{L} = \sqrt{-g}\left[\frac{R}{2} - \frac{1}{2}\partial_\mu\varphi\partial^\mu\varphi - 3\sinh^2\frac{\varphi}{\sqrt{6}}\,\partial_\mu\theta\partial^\mu\theta - W\left(\tanh\frac{\varphi}{\sqrt{6}}\cos\theta, \tanh\frac{\varphi}{\sqrt{6}}\sin\theta\right)\right]. \tag{5.77}$$

Note that now φ has a canonical kinetic term as opposed to θ. Furthermore it is impossible to obtain a standard kinetic term for θ since its redefinition involves the field φ and then a new non-canonical kinetic term for φ.

Before concluding, let us relate explicitly the dependence on the initial variables ϕ_1 and ϕ_2 of the potential W into Lagrangian (5.71) with that on ϕ and θ of the potential in (5.77). After the gauge fixing, the dependence on ϕ_1 and ϕ_2 of the original potential of Lagrangian (5.71) is given by

$$W = W\left(\frac{\phi_1}{\sqrt{6+\phi_1^2+\phi_2^2}}, \frac{\phi_2}{\sqrt{6+\phi_1^2+\phi_2^2}}\right) \equiv W(z_1, z_2)\,, \tag{5.78}$$

where in the last equality we have defined the variables z_1 and z_2. Passing from Lagrangian (5.71) to (5.77) corresponds to

$$z_1 \to \tanh \frac{\varphi}{\sqrt{6}} \cos\theta, \tag{5.79a}$$

$$z_2 \to \tanh \frac{\varphi}{\sqrt{6}} \sin\theta. \tag{5.79b}$$

Finally, let us rewrite for future convenience the full dependence of the potential W,

$$W\left(\tanh \frac{\varphi}{\sqrt{6}} \cos\theta\,,\, \tanh \frac{\varphi}{\sqrt{6}} \sin\theta\right). \tag{5.80}$$

Given this dependence, it is natural for the field φ to have a T-model-like potential (see equation (5.14)). Throughout chapters 7 and 8, we will analyse some models of two-field inflationary mechanisms described by Lagrangian (5.77). In particular, we will fix different potentials and analyse the background dynamics. In addition to this, we will study their predictions for non-Gaussianities.

Chapter 6

Two-field inflation and *in-in* formalism

> "Do not worry about your difficulties in Mathematics. I can assure you mine are still greater."
>
> Albert Einstein

In this chapter we will obtain explicit expressions for the correlators in a two-field theory using the *in-in* formalism [47, 57, 58, 66]. The treatment will be as general as possible and the results will be useful for the next chapters. In particular, after having fixed the Hamiltonian (section 6.1), we will compute the first correction to the power spectrum (section 6.2) and the lowest-order non-vanishing ones for the bispectrum (section 6.3).

6.1 Hamiltonian and correlators

In section 3.3, we have seen how to calculate the interacting vacuum expectation value of an operator Q. The master formula we have obtained is equation (3.46), that is

$$\langle Q(t)\rangle = \langle 0|\left[\bar{\mathrm{T}}\exp\left(i\int_{t_0}^{t} H_I(t)dt\right)\right]Q^I(t)\left[\mathrm{T}\exp\left(-i\int_{t_0}^{t} H_I(t)dt\right)\right]|0\rangle\,, \tag{6.1}$$

where T and $\bar{\mathrm{T}}$ are, respectively, the time-ordering and anti-time-ordering operators, H_I is the interaction Hamiltonian written in interaction picture and $|0\rangle$ is the vacuum of the free theory.

Suppose that the free theory is well-known and that H_I can be treated as a small perturbation. Hence, the previous expression can be expanded into powers of the interaction Hamiltonian (see equation (3.47)). The n-th order of this expansion is given by

$$\langle Q(t)\rangle^{(n)} = i^n\int_{t_0}^{t} dt_1\int_{t_0}^{t_1} dt_2\cdots\int_{t_0}^{t_{n-1}} dt_n\,\langle 0|\Big[H^I(t_n),\Big[H^I(t_{n-1}),\dots\big[H^I(t_1),Q^I(t)\big]\Big]\Big]|0\rangle\,. \tag{6.2}$$

This form is called commutator form due to the presence of nested commutators. However, one can expand the commutators and rearrange the integration variables in order to obtain a more compact expression. This is called factorized form. General formulae for nth order factorized

form expectation values exist [82], but they are not particularly illuminating, so we prefer to give only the lowest order expressions. These are given by

$$\langle Q(t)\rangle^{(1)} = -\,2\mathrm{Re}\left\{ i\int_{t_0}^{t}\langle H^I(t_1)Q^I(t)\rangle \right\}, \tag{6.3}$$

$$\langle Q(t)\rangle^{(2)} = \int_{t_0}^{t}dt_1\int_{t_0}^{t}dt_2\,\langle H^I(t_1)Q^I(t)H^I(t_2)\rangle - 2\mathrm{Re}\left\{\int_{t_0}^{t}dt_1\int_{t_0}^{t_1}dt_2\,\langle Q^I(t)H^I(t_1)H^I(t_2)\rangle\right\}. \tag{6.4}$$

They can be obtained just remembering that Q and H are observables and hence Hermitian operators.

In order to specify our theory, we should provide the Hamiltonian. We consider a theory with two scalar interacting fields φ and θ described by the action (4.1). We consider only the perturbations of the fields φ and θ and neglect perturbations of the metric. The interactions between the fields can be generated by the potential term or by the non-canonical kinetic term. We suppose that the background dynamics is known and that the perturbations are quantized in Fourier space as

$$\delta\varphi^I_{\mathbf{k}} = u_{\mathbf{k}}a_{\mathbf{k}} + u^*_{-\mathbf{k}}a^\dagger_{-\mathbf{k}}, \tag{6.5a}$$

$$\delta\theta^I_{\mathbf{k}} = v_{\mathbf{k}}b_{\mathbf{k}} + v^*_{-\mathbf{k}}b^\dagger_{-\mathbf{k}}, \tag{6.5b}$$

where the creation $(a^\dagger, b^\dagger)$ and annihilation (a, b) operators satisfy the commutation relations

$$[a_{\mathbf{k}}, a^\dagger_{\mathbf{k}'}] = (2\pi)^3\delta^3(\mathbf{k}-\mathbf{k}'), \tag{6.6a}$$

$$[a_{\mathbf{k}}, a_{\mathbf{k}'}] = [a^\dagger_{\mathbf{k}}, a^\dagger_{\mathbf{k}'}] = 0, \tag{6.6b}$$

$$[b_{\mathbf{k}}, b^\dagger_{\mathbf{k}'}] = (2\pi)^3\delta^3(\mathbf{k}-\mathbf{k}'), \tag{6.6c}$$

$$[b_{\mathbf{k}}, b_{\mathbf{k}'}] = [b^\dagger_{\mathbf{k}}, b^\dagger_{\mathbf{k}'}] = 0. \tag{6.6d}$$

We suppose that the explicit form of the mode functions $u_{\mathbf{k}}$ and $v_{\mathbf{k}}$ has been calculated from the equation of motion for the perturbations following from the free Hamiltonian. There are not other necessary assumptions. Suppose that the interaction terms of the Hamiltonian density have the structure

$$\mathcal{H}^{(2)}_{INT} = Z(\varphi,\theta,t)\,\delta\varphi\delta\theta, \tag{6.7}$$

$$\mathcal{H}^{(3)}_{INT} = A(\varphi,\theta,t)\,\delta\varphi^3 + B(\varphi,\theta,t)\,\delta\theta\delta\varphi^2 + C(\varphi,\theta,t)\,\delta\theta^2\delta\varphi + D(\varphi,\theta,t)\,\delta\theta^3, \tag{6.8}$$

where Z, A, B, C, D are generic functions of the background fields. Let us notice that e.g. the term $B(\varphi,\theta,t)\delta\theta\delta\varphi^2$ can be $B(\varphi,\theta,t)\dot{\delta\theta}\delta\varphi^2$ or $B(\varphi,\theta,t)\delta\theta\dot{\delta\varphi}^2$ or other possibilities with spatial derivatives, but we will consider only the term previously written because how to include derivatives will be soon evident. This structure has been chosen because the model that we will study in the next chapter has an Hamiltonian with this form. We made all these assumptions for future convenience. More specifically, in the following chapter we will study a two-field model of inflation described by the Lagrangian (5.77) (compare the previous form of the Hamiltonian with the Hamiltonian (7.38) associated with the two-field model (5.77)).

The term (6.7) can be expressed in Fourier space as

$$H^{(2)}(t) = \int d^3x \mathcal{H}^{(2)I}_{INT}(t,\mathbf{x}) = Z\int d^3x \int \frac{d^3k}{(2\pi)^3}\int \frac{d^3k'}{(2\pi)^3} e^{-i\mathbf{x}\cdot(\mathbf{k}+\mathbf{k}')}\delta\varphi^I_{\mathbf{k}}(t)\delta\theta^I_{\mathbf{k}'}(t)$$
$$= Z\int \frac{d^3k}{(2\pi)^3}\delta\varphi^I_{\mathbf{k}}(t)\delta\theta^I_{-\mathbf{k}}(t)\,. \tag{6.9}$$

The first contribution to (6.8) can be rewritten as

$$H^{(3)}_A(t) = \int d^3x \mathcal{H}^{(3)I}_A(t,\mathbf{x})$$
$$= A\int \frac{d^3k_1}{(2\pi)^3}\int \frac{d^3k_2}{(2\pi)^3}\delta\varphi^I_{\mathbf{k}_1}(t)\delta\varphi^I_{\mathbf{k}_2}(t)\delta\varphi^I_{-\mathbf{k}_1-\mathbf{k}_2}(t)\,, \tag{6.10}$$

and analogous expressions hold for the terms with couplings B, C, and D.

The non-zero contractions are given by

$$\overbrace{\delta\varphi^I_{\mathbf{k}}(t_1)\delta\varphi^I_{\mathbf{k}'}}(t_2) = (2\pi)^3\delta^3(\mathbf{k}+\mathbf{k}')\,u_{\mathbf{k}}(t_1)u^*_{\mathbf{k}}(t_2)\,, \tag{6.11}$$
$$\overbrace{\delta\theta^I_{\mathbf{k}}(t_1)\delta\theta^I_{\mathbf{k}'}}(t_2) = (2\pi)^3\delta^3(\mathbf{k}+\mathbf{k}')\,v_{\mathbf{k}}(t_1)v^*_{\mathbf{k}}(t_2)\,, \tag{6.12}$$

due to the commutation relations (6.6). Notice that one mode function appears always together with its conjugate since the only non-zero expectation values are that of an annihilation operator followed (on its right) by a creation operator.

Before concluding this paragraph, let us make a remark. Note that the interaction Hamiltonian has a symmetric form, then one can exchange the two fields $\varphi \leftrightarrow \theta$ in the upcoming formulas with the following identifications: $u_{\mathbf{k}} \leftrightarrow v_{\mathbf{k}}$, $A \leftrightarrow D$, $B \leftrightarrow C$. Thanks to this symmetry, we will calculate expectation values only for the field φ.

Finally, in the following we will omit for brevity the superscript "I" standing for interaction picture.

6.2 Power spectrum

In this section we will calculate the power spectrum $\langle\delta\varphi_{\mathbf{p}_1}(t)\delta\varphi_{\mathbf{p}_2}(t)\rangle$ at first-order in the expansion of the *in-in* formalism (we will for shortness and some abuse of notation indicate the power spectrum as the correlator $\langle\delta\varphi^2\rangle$).

The lowest order of the *in-in* expansion is simply given by

$$\langle\delta\varphi_{\mathbf{p}_1}(t)\delta\varphi_{\mathbf{p}_2}(t)\rangle^{(0)} = (2\pi)^3\delta^3(\mathbf{p}_1+\mathbf{p}_2)\,|u_{p_1}(t)|^2. \tag{6.13}$$

The expression for the first-order term reads

$$\langle\delta\varphi_{\mathbf{p}_1}(t)\delta\varphi_{\mathbf{p}_2}(t)\rangle^{(1)} = i\int_{t_0}^{t} dt_1 \left\langle\Big[H(t_1),\delta\varphi_{\mathbf{p}_1}(t)\delta\varphi_{\mathbf{p}_2}(t)\Big]\right\rangle$$
$$= 0\,, \tag{6.14}$$

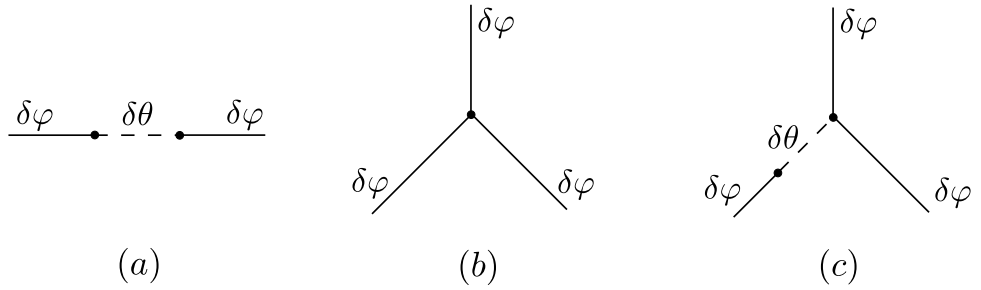

Figure 6.1: The diagrams for which a full computation is explained in the chapter. (a) is the representation of (6.17), (b) of (6.21) and (c) of (6.23).

since $H(t_1)$ can be neither $H^{(2)}$ (the fields cannot be contracted properly because there are three $\delta\varphi_{\mathbf{p}_i}$ and only one $\delta\theta$, and so all the possible contractions vanish) nor $H^{(3)}$ (there is surely a non-contracted field).

At second order, things become more complicated. The correction to the power spectrum is given by

$$\langle\delta\varphi_{\mathbf{p}_1}(t)\delta\varphi_{\mathbf{p}_2}(t)\rangle^{(2)} = i^2\int_{t_0}^{t}dt_1\int_{t_0}^{t_1}dt_2\,\Big\langle\Big[H(t_2),\big[H(t_1),\delta\varphi_{\mathbf{p}_1}(t)\delta\varphi_{\mathbf{p}_2}(t)\big]\Big]\Big\rangle \tag{6.15}$$

$$= \int_{t_0}^{t}dt_1\int_{t_0}^{t}dt_2\,\langle H(t_1)\delta\varphi^2 H(t_2)\rangle - 2\mathrm{Re}\left\{\int_{t_0}^{t}dt_1\int_{t_0}^{t_1}dt_2\,\langle\delta\varphi^2 H(t_1)H(t_2)\rangle\right\}, \tag{6.16}$$

where both the commutator and the factorized form are shown. The Hamiltonians can be both $H^{(2)}$ or both $H^{(3)}$. In the latter case, all fields are contracted if the Hamiltonians are AA, AC, BB, BD, CC, DD. We have introduced intentionally an obvious notation that does not require any further explanation (AA stands for a term with two $H_A^{(3)}$). The terms AA, AC, BB, BD, CC are loop diagrams, as one can easily prove. Finally, the term DD is not connected. Therefore, we consider the case in which both Hamiltonians are $H^{(2)}$. The associated diagram is represented in figure 6.1a.

Usually the factorized form is more convenient for analytical calculations since it involves fewer terms, but the commutator form is useful for numerical computations. Hence, we define

$$\begin{aligned}\langle\delta\varphi_{\mathbf{p}_1}(t)\delta\varphi_{\mathbf{p}_2}(t)\rangle^{(2)} &= \int_{t_0}^{t}dt_1\int_{t_0}^{t}dt_2\,\langle H^{(2)}(t_1)\delta\varphi^2 H^{(2)}(t_2)\rangle \\ &\quad - 2\mathrm{Re}\left\{\int_{t_0}^{t}dt_1\int_{t_0}^{t_1}dt_2\,\langle\delta\varphi^2 H^{(2)}(t_1)H^{(2)}(t_2)\rangle\right\} \\ &\equiv \langle\delta\varphi_{\mathbf{p}_1}(t)\delta\varphi_{\mathbf{p}_2}(t)\rangle_1^{(2)} + \langle\delta\varphi_{\mathbf{p}_1}(t)\delta\varphi_{\mathbf{p}_2}(t)\rangle_2^{(2)}\,,\end{aligned} \tag{6.17}$$

and we separately compute the two terms. The first one is given by

$$\begin{aligned}
\langle\delta\varphi_{\mathbf{p}_1}(t)\delta\varphi_{\mathbf{p}_2}(t)\rangle_1^{(2)} &= \int_{t_0}^{t}dt_1\int_{t_0}^{t}dt_2 Z(t_1)Z(t_2)\int\frac{d^3k_1}{(2\pi)^3}\int\frac{d^3k_2}{(2\pi)^3}\\
&\quad\langle\delta\varphi_{\mathbf{k}_1}(t_1)\delta\theta_{-\mathbf{k}_1}(t_1)\delta\varphi_{\mathbf{p}_1}(t)\delta\varphi_{\mathbf{p}_2}(t)\delta\varphi_{\mathbf{k}_2}(t_2)\delta\theta_{-\mathbf{k}_2}(t_2)\rangle\\
&= 2\int_{t_0}^{t}dt_1\int_{t_0}^{t}dt_2 Z(t_1)Z(t_2)\int\frac{d^3k_1}{(2\pi)^3}\int\frac{d^3k_2}{(2\pi)^3}\\
&\quad\left\{\overbrace{\delta\varphi_{\mathbf{k}_1}(t_1)\delta\theta_{-\mathbf{k}_1}(t_1)\delta\varphi_{\mathbf{p}_1}(t)\delta\varphi_{\mathbf{p}_2}(t)\delta\varphi_{\mathbf{k}_2}(t_2)\delta\theta_{-\mathbf{k}_2}(t_2)}\right\}\\
&= (2\pi)^3\delta^3(\mathbf{p}_1+\mathbf{p}_2)2\int_{t_0}^{t}dt_1\int_{t_0}^{t}dt_2 Z(t_1)Z(t_2)\\
&\quad\left\{u_{-\mathbf{p}_1}(t_1)u^*_{\mathbf{p}_1}(t)u_{\mathbf{p}_2}(t)u^*_{-\mathbf{p}_2}(t_2)v_{-\mathbf{p}_1}(t_1)v^*_{-\mathbf{p}_2}(t_2)\right\}\\
&= (2\pi)^3\delta^3(\mathbf{p}_1+\mathbf{p}_2)2u^*_{p_1}(t)u_{p_1}(t)\left|\int_{t_0}^{t}dt_1 Z(t_1)u_{p_1}(t_1)v_{p_1}(t_1)\right|^2,
\end{aligned}$$

where in the first line we have used equation (6.9), in the second line we have contracted the fields (notice that this is the only possibility that avoids disconnected diagrams), in the third we have used the expression (6.11) and integrated over $\mathbf{k}_1$ and $\mathbf{k}_2$ and in the last line we have rearranged the remaining factors. We have supposed that the background is homogeneous and isotropic and hence the mode functions depend only on the amplitudes of the momenta. The evaluation of the second term is similar to the previous one. The final result is

$$\begin{aligned}
\langle\delta\varphi_{\mathbf{p}_1}(t)\delta\varphi_{\mathbf{p}_2}(t)\rangle_2^{(2)} &= -4(2\pi)^3\delta^3(\mathbf{p}_1+\mathbf{p}_2)\\
&\quad\mathrm{Re}\left\{u_{p_1}(t)^2\int_{t_0}^{t}dt_1 Z(t_1)u^*_{p_1}(t_1)v_{p_1}(t_1)\int_{t_0}^{t_1}dt_2 Z(t_2)u^*_{p_1}(t_2)v^*_{p_1}(t_2)\right\}.
\end{aligned}\tag{6.18}$$

Finally, summing up the two previous results, we get

$$\begin{aligned}
\langle\delta\varphi_{\mathbf{p}_1}(t)\delta\varphi_{\mathbf{p}_2}(t)\rangle^{(2)} &= (2\pi)^3\delta^3(\mathbf{p}_1+\mathbf{p}_2)\left[2u^*_{p_1}(t)u_{p_1}(t)\left|\int_{t_0}^{t}dt_1 Z(t_1)u_{p_1}(t_1)v_{p_1}(t_1)\right|^2\right.\\
&\quad\left.-4\mathrm{Re}\left\{u_{p_1}(t)^2\int_{t_0}^{t}dt_1 Z(t_1)u^*_{p_1}(t_1)v_{p_1}(t_1)\int_{t_0}^{t_1}dt_2 Z(t_2)u^*_{p_1}(t_2)v^*_{p_1}(t_2)\right\}\right].
\end{aligned}\tag{6.19}$$

The dependence of Z on time may be explicit or through the background fields. Hence, one should integrate over the past history of the background fields. Furthermore, the time t, at which the correlator is evaluated, is usually chosen to be the end of inflation (since, e.g. later on the perturbations remain nearly constant in the standard scenario).

At third order, all connected diagrams contain loops. Indeed, there are two possibilities in order to have the correct number of contracted fields, two $H^{(3)}$ and one $H^{(2)}$ or three $H^{(2)}$.

The latter possibility does not produce any contribution since there is always a null contraction between $\delta\theta$ and $\delta\varphi$. In the other case we can proceed as follows. The interaction Hamiltonian $H^{(2)}$ contains one $\delta\theta$ and then the possibilities for the two $H^{(3)}$ are AB, AD, BC, CD. It is simple to show that all these are loop diagrams.

6.3 Bispectrum

The zeroth order of the correlator $\langle\delta\varphi^3\rangle$ vanishes since there is no way to contract properly the fields. The first-order is given by

$$\langle\delta\varphi_{\mathbf{p}_1}(t)\delta\varphi_{\mathbf{p}_2}(t)\delta\varphi_{\mathbf{p}_3}(t)\rangle^{(1)} = i\int_{t_0}^{t} dt_1\,\langle\big[H(t_1),\delta\varphi_{\mathbf{p}_1}(t)\delta\varphi_{\mathbf{p}_2}(t)\delta\varphi_{\mathbf{p}_3}(t)\big]\rangle\,. \tag{6.20}$$

Notice that H cannot be $H^{(2)}$. It can only be $H_A^{(3)}$ since other terms are non-connected diagrams or contain uncontracted fields. Then, one gets

$$\begin{aligned}\langle\delta\varphi^3(t)\rangle^{(1)} &= i\int_{t_0}^{t} dt_1\,\langle\big[H_A^{(3)}(t_1),\delta\varphi_{\mathbf{p}_1}(t)\delta\varphi_{\mathbf{p}_2}(t)\delta\varphi_{\mathbf{p}_3}(t)\big]\rangle \\ &= -12(2\pi)^3\delta^3(\mathbf{p}_1+\mathbf{p}_2+\mathbf{p}_3)\mathrm{Im}\left\{u_{p_1}^*(t)u_{p_2}^*(t)u_{p_3}^*(t)\int_{t_0}^{t} dt_1 A(t_1)u_{p_1}(t_1)u_{p_2}(t_1)u_{p_3}(t_1)\right\}.\end{aligned} \tag{6.21}$$

This is a self-interaction term for the field φ (see figure 6.1b). It can produce non-Gaussianities, but these are compensated by the metric perturbations [40, 66]. Accounting also for the next order of the bispectrum in the *in-in* formalism, terms that involve such interactions will appear.

The next order in the expansion of the bispectrum is

$$\langle\delta\varphi^3(t)\rangle^{(2)} = \int_{t_0}^{t} dt_1\int_{t_0}^{t} dt_2\,\langle H(t_1)\delta\varphi^3 H(t_2)\rangle - 2\mathrm{Re}\left\{\int_{t_0}^{t} dt_1\int_{t_0}^{t_1} dt_2\,\langle\delta\varphi^3 H(t_1)H(t_2)\rangle\right\}. \tag{6.22}$$

Notice that $H(t_1)$ and $H(t_2)$ cannot obviously be both $H^{(2)}$ or both $H^{(3)}$. Hence one of them should be $H^{(2)}$ and the other $H^{(3)}$. In addition to this, $H^{(3)}$ should contain at least one $\delta\theta$, since $H^{(2)}$ does. On the other hand, it can contain neither two $\delta\theta$, because otherwise there would be a null contraction between $\delta\varphi$ and $\delta\theta$, nor three $\delta\theta$, because these are disconnected diagrams. Therefore the only allowed term is $H_B^{(3)}$ (the corresponding diagram is represented in figure 6.1c). The final result is given by

$$\begin{aligned}\langle\delta\varphi^3(t)\rangle^{(2)} = 4(2\pi)^3\delta^3(\mathbf{p}_1+\mathbf{p}_2+\mathbf{p}_3)\mathrm{Re}\Bigg\{&\int_{t_0}^{t} dt_1\int_{t_0}^{t_1} dt_2 B(t_1)Z(t_2)v_{p_3}(t_1)v_{p_3}^*(t_2) \\ &\Big(u_{p_1}^*(t)u_{p_2}^*(t)u_{p_3}(t)u_{p_1}(t_1)u_{p_2}(t_1)u_{p_3}^*(t_2) + u_{p_1}(t)u_{p_2}(t)u_{p_3}^*(t)u_{p_1}^*(t_2)u_{p_2}^*(t_2)u_{p_3}(t_1) \\ &- u_{p_1}(t)u_{p_2}(t)u_{p_3}(t)u_{p_1}^*(t_2)u_{p_2}^*(t_2)u_{p_3}^*(t_1) - u_{p_1}(t)u_{p_2}(t)u_{p_3}(t)u_{p_1}^*(t_1)u_{p_2}^*(t_1)u_{p_3}^*(t_2)\Big) \\ &+ 5\text{ perm}\Bigg\},\end{aligned} \tag{6.23}$$

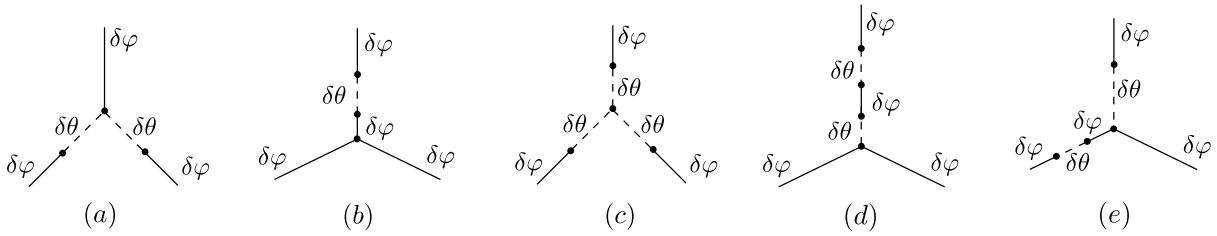

Figure 6.2: Diagrams associated to third and fourth-order contributions to bispectrum in the *in-in* expansion.

where "perm" denotes the possible permutations over the three momenta.

At third order, with three Hamiltonians, we have two possibilities: one of the Hamiltonian in the correlator is $H^{(3)}$ and the others are $H^{(2)}$ or all of them are $H^{(3)}$.

- $1H^{(3)}$: since $H^{(2)}$ contains one $\delta\theta$, $H^{(3)}$ can contain zero or two $\delta\theta$ and thus it can be $H_A^{(3)}$ or $H_C^{(3)}$. Both are acceptable possibilities.

- $3H^{(3)}$: the combinations leading to fields that are all contracted are AAA, AAC, ABB, ACC, ADD, BBC, CCC,CDD. The disconnected ones are CDD, ADD. The remaining diagrams contain loops.

The only connected diagrams with no loops, at third order, contain the bracket $\langle \delta\varphi^3 H_A^{(3)} H^{(2)} H^{(2)} \rangle$ or $\langle \delta\varphi^3 H_C^{(3)} H^{(2)} H^{(2)} \rangle$.

Finally, we consider what happens at fourth order. Again, we have two possibilities in order to have all fields contracted: one $H^{(3)}$ or three $H^{(3)}$ (being the other Hamiltonians $H^{(2)}$).

- $1H^{(3)}$: $H^{(3)}$ must contains an odd number of $\delta\theta$ since there are three $H^{(2)}$. Both the term B and D produce diagrams with no loops.

- $3H^{(3)}$: Studying all the possibilities is now rather tedious. It is surely convenient to reason "topologically" and try to draw a connected diagram with no loops and four vertices. The final answer is that such a diagram does not exist.

The third order and fourth order corrections with no loops to bispectrum are represented in figure 6.2.

So far, our discussion has been general. In cosmology, the correlators that we need to compute are related to the perturbations of the fields or the metric. In the following chapter, we will consider $\delta\varphi$ and $\delta\theta$ as perturbations of the scalar fields in a two-field inflationary model. However, using the curvature perturbation ζ (2.70) is a more convenient choice since ζ is gauge-invariant and it is conserved on superhorizon scales. In addition to this, the perturbations of the field $\delta\varphi$ are quantum fluctuations and we need to relate them with classical density perturbations.

Notice that all the correlators we have considered refers to the basis (φ, θ) of the field space. However, the curvature perturbation is the component of perturbations parallel to the background velocity. Therefore, the previous correlators are almost useless if we do not rotate this basis. Obviously the rotation matrix is local, i.e. it depends on the position of the background

trajectory. This rotation has been introduced before equation (4.74). In chapter 8 we will explicitly perform this rotation for the case we are interested in.

Chapter 7

Towards two-field inflationary models

> "In the beginning there were only probabilities. The Universe could only come into existence if someone observed it. It does not matter that the observers turned up several billion years later. The Universe exists because we are aware of it."
>
> Martin J. Rees

In chapter 5, we have seen how multi-field inflationary models arise in the context of supergravity with local conformal invariance. In this chapter, we will study in detail two examples of two-field models described by the Lagrangian (5.77). In particular, we will compute the power spectrum and the bispectrum of curvature perturbations and, eventually, we will try to understand what are the conditions under which observable non-Gaussianities can be generated.

In section 7.1, we will discuss the background dynamics of the fields keeping the treatment as general as possible. Furthermore, we will derive the equations of motion for the perturbations. In section 7.2, we will analyse the acceptable initial conditions for inflation studying the background equations. This section is the continuation of the previous one. In particular, we will see how each term into the background equations affects the dynamics of the fields. In the following section 7.3, we will apply the *in-in* formalism (introduced in section 3.3) to our model. We will derive the perturbed Hamiltonian and the mode functions following the prescriptions of this formalism. Section 7.4 regards slow-roll dynamics and the definition of slow-roll parameters when the kinetic term is non-canonical. We will focus on our model, but we will try to explain the general approach to build slow-roll parameters when dealing with non-canonical kinetic terms. In section 7.5, we will consider a simple example of trajectory, a circle in field space (following [82]), and study its predictions. Finally, in section 7.6, we will study another example of trajectory, a nearly straight one. These trajectories will be prototypical for the more general analysis of the following chapter.

7.1 A non-canonical kinetic term

Our starting point is the Lagrangian (5.77),

$$\mathcal{L} = \sqrt{-g}\Bigg[\frac{R}{2} - \frac{1}{2}\partial_\mu\varphi\partial^\mu\varphi - 3\sinh^2\frac{\varphi}{\sqrt{6}}\,\partial_\mu\theta\partial^\mu\theta - W\left(\tanh(\varphi/\sqrt{6})\cos\theta, \tanh(\varphi/\sqrt{6})\sin\theta\right)\Bigg], \tag{7.1}$$

where W is the potential term. Note that θ exhibits a non-canonical kinetic term. If we interpret the fields as classical variables, θ would be an angle and φ would be related to the radial distance from the origin in polar coordinates.

In order to be as general as possible within a Lagrangian of the type (7.1), we are going to focus on

$$\mathcal{L} = a^3(t)\Bigg[\frac{R}{2} - \frac{1}{2}\partial_\mu\varphi\partial^\mu\varphi - \frac{f(\varphi)}{2}\partial_\mu\theta\partial^\mu\theta - W(\varphi,\theta)\Bigg], \tag{7.2}$$

where we have defined

$$f(\varphi) \equiv 6\sinh^2\frac{\varphi}{\sqrt{6}}\,. \tag{7.3}$$

In this manner, the following equations can be generalized without effort to a different non-canonical kinetic term. In addition to this, we have assumed that the background spacetime is FRW. In spite of these redefinitions, we are interested in the model (7.1) and hence our considerations will refer to it, unless otherwise stated.

The field space metric is given by

$$G_{IJ} = \begin{pmatrix} 1 & 0 \\ 0 & f(\varphi) \end{pmatrix}. \tag{7.4}$$

Directly from this expression one can derive the Christoffel symbols (4.3),

$$\Gamma^{\varphi}_{\theta\theta} = -\frac{1}{2}f', \tag{7.5a}$$

$$\Gamma^{\theta}_{\varphi\theta} = \frac{1}{2}\frac{f'}{f}, \tag{7.5b}$$

the components of the Ricci tensor,

$$R_{\varphi\varphi} = \frac{f'^2 - 2ff''}{4f^2}, \tag{7.6a}$$

$$R_{\theta\theta} = \frac{f'^2 - 2ff''}{4f}, \tag{7.6b}$$

and the Ricci scalar,

$$R = \frac{f'^2 - 2ff''}{2f^2}. \tag{7.7}$$

Notice that, if f is given by equation (7.3), the Ricci scalar is a constant, $R = -1/3$.

The equations of motion for the fields are given by Euler-Lagrange equations (4.2),

$$\ddot{\varphi} + 3H\dot{\varphi} - \frac{1}{a^2}\nabla^2\varphi + W_\varphi + \frac{f'}{2}\partial_\mu\theta\partial^\mu\theta = 0, \tag{7.8}$$

$$\ddot{\theta} + 3H\dot{\theta} - \frac{1}{a^2}\nabla^2\theta + \frac{1}{f}W_\theta - \frac{f'}{f}\partial_\mu\varphi\partial^\mu\theta = 0, \tag{7.9}$$

where

$$W_\chi \equiv \frac{\partial W}{\partial \chi}\,. \tag{7.10}$$

The last terms on the l.h.s. in both equations come from the non-canonical kinetic term for θ. Notice that both the non-canonical kinetic term and the potential are responsible for interactions between the fields. The previous equations are decoupled if and only if the potential has the form $W = V(\varphi) + U(\theta)$ and $f \equiv$ const. From now on, we will denote the derivatives of the potential with respect to the fields without the comma for shortness.

As always, we split the fields into a background term and a perturbation as

$$\varphi(t, \mathbf{x}) = \varphi_0(t) + \delta\varphi(t, \mathbf{x})\,, \tag{7.11a}$$

$$\theta(t, \mathbf{x}) = \theta_0(t) + \delta\theta(t, \mathbf{x})\,. \tag{7.11b}$$

The background equations of motion follow straightforwardly from equations (7.8) and (7.9),

$$\ddot{\varphi}_0 + 3H\dot{\varphi}_0 - \frac{f'}{2}\dot{\theta}_0^2 + W_\varphi = 0\,, \tag{7.12}$$

$$\ddot{\theta}_0 + 3H\dot{\theta}_0 + \frac{f'}{f}\dot{\varphi}_0\dot{\theta}_0 + \frac{1}{f}W_\theta = 0\,. \tag{7.13}$$

The non-trivial field space metric introduces a new potential term $-\frac{f'}{2}\dot{\theta}_0^2$ dependent on the angular velocity $\dot{\theta}_0$ into the first equation. Notice that this term is always negative and hence it forces the field φ to accelerate. Conversely, in the second one, the non-trivial field space metric introduces the term $\frac{f'}{f}\dot{\varphi}_0\dot{\theta}_0$ dependent on $\dot{\varphi}_0$. The sign of this term depends on the sign of the velocity $\dot{\varphi}_0$ and hence it can accelerate or decelerate θ.

The first peculiarity of this model we want to point out is the presence of hyperbolic functions. Indeed, these functions can exponentially enhance or suppress some of the terms in the equations affecting the background dynamics. For example, the first derivative

$$f' = 2\sqrt{6}\sinh\frac{\varphi_0}{\sqrt{6}}\cosh\frac{\varphi_0}{\sqrt{6}} \tag{7.14}$$

can be very large if $\varphi_0 \gg \sqrt{6}$. On the other hand, the factor

$$\frac{f'}{f} = \sqrt{\frac{2}{3}}\frac{1}{\tanh(\varphi_0/\sqrt{6})} \tag{7.15}$$

is nearly constant in the same limit.

The Friedmann equation (4.9) reads

$$H^2 = \frac{1}{3}\Big(\frac{1}{2}\dot{\varphi}_0^2 + \frac{f}{2}\dot{\theta}_0^2 + W\Big), \tag{7.16}$$

since

$$\begin{aligned} \rho &= \frac{1}{2}\dot{\varphi}_0^2 + \frac{f}{2}\dot{\theta}_0^2 + W\,, \\ P &= \frac{1}{2}\dot{\varphi}_0^2 + \frac{f}{2}\dot{\theta}_0^2 - W\,. \end{aligned} \tag{7.17}$$

From now on, we will drop the subscript "0" that characterizes the background fields. The reader should be able anyway to interpret correctly all the following equations[1].

Equations for fluctuations can be derived perturbing equations (7.8) and (7.9). The result, up to second order, is

$$\ddot{\delta\varphi} + 3H\dot{\delta\varphi} - \frac{1}{a^2}\nabla^2\delta\varphi - \frac{\dot\theta^2}{2}\Big(f''\delta\varphi + \frac{1}{2}f'''\delta\varphi^2\Big) - f'\Big(\dot\theta\dot{\delta\theta} - \frac{1}{2}\partial_\mu\delta\theta\partial^\mu\delta\theta\Big) - f''\dot\theta\delta\varphi\dot{\delta\theta} + W_{\varphi\varphi}\delta\varphi + W_{\varphi\theta}\delta\theta + \frac{1}{2}W_{\varphi\varphi\varphi}\delta\varphi^2 + W_{\varphi\varphi\theta}\delta\varphi\delta\theta + \frac{1}{2}W_{\varphi\theta\theta}\delta\theta^2 = 0\,, \tag{7.18}$$

$$\ddot{\delta\theta} + 3H\dot{\delta\theta} - \frac{1}{a^2}\nabla^2\delta\theta + \frac{f'}{f}\Big(\dot\varphi\dot{\delta\theta} + \dot\theta\dot{\delta\varphi}\Big) - \frac{f'}{f}\partial_\mu\delta\varphi\partial^\mu\delta\theta + \left(\frac{f'}{f}\right)'\Big(\dot\varphi\dot\theta + \dot\theta\dot{\delta\varphi} + \dot\varphi\dot{\delta\theta}\Big)\delta\varphi + \left(\frac{f'}{f}\right)''\dot\varphi\dot\theta\delta\varphi^2 + \frac{1}{f}\Big(W_{\theta\theta}\delta\theta + W_{\theta\varphi}\delta\varphi + \frac{1}{2}W_{\theta\theta\theta}\delta\theta^2 + W_{\theta\theta\varphi}\delta\varphi\delta\theta + \frac{1}{2}W_{\theta\varphi\varphi}\delta\varphi^2\Big) + \left(\frac{1}{f}\right)'\Big(W_\theta + W_{\theta\theta}\delta\theta + W_{\theta\varphi}\delta\varphi\Big)\delta\varphi + \frac{1}{2}\left(\frac{1}{f}\right)''W_\theta\delta\varphi^2 = 0\,. \tag{7.19}$$

Notice that many terms appear only because there is a non-canonical kinetic term. In particular, all the terms with derivatives of f would be null if the kinetic term of θ was canonical. The equations for the perturbations can be derived in different equivalent ways. One can perturb directly the equations of motion (7.8) and (7.9) up to the desired order. Alternatively, one can perturb the Lagrangian (7.2) and then deduce the equations of motion for the perturbations via the Euler-Lagrange equations. Although the previous equations do not seem to be covariant, one can show that indeed they are since they have the same form as (4.31) (e.g. see [91]).

7.2 Viable initial conditions for inflation

In this section, we will study the acceptable initial conditions for the fields that lead to an inflationary period lasting at least $50 \div 70$ e-folds. As in section 5.6, here we adopt the definition $dN = Hdt$ for the number of e-folds (see equation (4.10)). Initial conditions are given at $N = 0$ and inflation may start some time later. To study the inflationary dynamics, it is useful to rewrite background equations (7.12) and (7.13) with respect to the e-folds number N,

$$\varphi'' + \omega_\theta + (3-\varepsilon)\left(\varphi' + \frac{W_\varphi}{W}\right) = 0\,, \tag{7.20}$$

$$\theta'' + \omega_\varphi + (3-\varepsilon)\left(\theta' + \frac{1}{f}\frac{W_\theta}{W}\right) = 0\,, \tag{7.21}$$

$$H^2 = \frac{W}{3-\varepsilon}\,, \tag{7.22}$$

$$\varepsilon \equiv -\frac{\dot H}{H^2} = \frac{1}{2}\varphi'^2 + \frac{f}{2}\theta'^2, \tag{7.23}$$

[1]Hint: only equations (7.30) and (7.31) contain the complete fields.

where we have defined

$$\omega_\theta \equiv -\frac{f'}{2}\theta'^2, \tag{7.24}$$

$$\omega_\varphi \equiv \frac{f'}{f}\theta'\varphi', \tag{7.25}$$

and where the prime denotes the derivative with respect to N, but f' stands for $df/d\varphi$.

Referring to section 4.2, the background equations of motion in the slow-roll and slow-turn approximation reduce to (see equations (4.25))

$$\varphi' + \frac{W_\varphi}{W} = 0\,, \tag{7.26a}$$

$$\theta' + \frac{1}{f}\frac{W_\theta}{W} = 0\,, \tag{7.26b}$$

$$H^2 = \frac{W}{3}\,. \tag{7.26c}$$

Notice that in the second equation the potential for θ is suppressed by the function f that goes as $\exp(\sqrt{2/3}\varphi)$. If inflation occurs in the region $\varphi \gg 1$, the velocity θ' should be small during slow-roll unless the potential term compensates this exponential suppression. Later, as φ moves toward the minimum of the potential, the suppression is reduced and the velocity θ' can increase. Let us remember that inflation occurs for $\varphi \gg 1$ in single-field case. On the other hand, in multi-field case this condition can be relaxed since inflaton can move in more directions and then the aforementioned suppression can be ineffective. In the following chapter, we will underline this behaviour.

The presence of a second field makes the analysis harder than in section 5.6. In this section, we will study only a few instances for the potential. In the following chapter, we will study other possibilities.

First of all, let us suppose that $\varphi' \gg W_\varphi/W$ and $\theta' \gg W_\theta/(fW)$. In this limit, the background equations of motion (7.20) and (7.21) read

$$\varphi'' - \frac{f'}{2}\theta'^2 + (3-\varepsilon)\varphi' = 0\,, \tag{7.27a}$$

$$\theta'' + \frac{f'}{f}\theta'\varphi' + (3-\varepsilon)\theta' = 0\,. \tag{7.27b}$$

Hence, the dynamics of the system is determined only by the non-canonical kinetic term. This approximation is useful when we are dealing with sufficiently high initial velocities (so that the potential terms can be neglected). However, notice that during slow-roll the terms related to the potential are not negligible due to equations (7.26). The phase space diagram of this system of differential equations is represented in figure 7.1. The behaviour of the solutions is quite clear. If the velocities are sufficiently high that the terms W_φ/W and $W_\theta/(fW)$ can be neglected, then inflation usually does not occur because the fields accelerates and slow-roll cannot be reached. This acceleration is driven by the term ω_θ (7.24) which derives from the non-canonical kinetic term. In order to have inflation, the term ω_θ should be sufficiently small and should remain so.

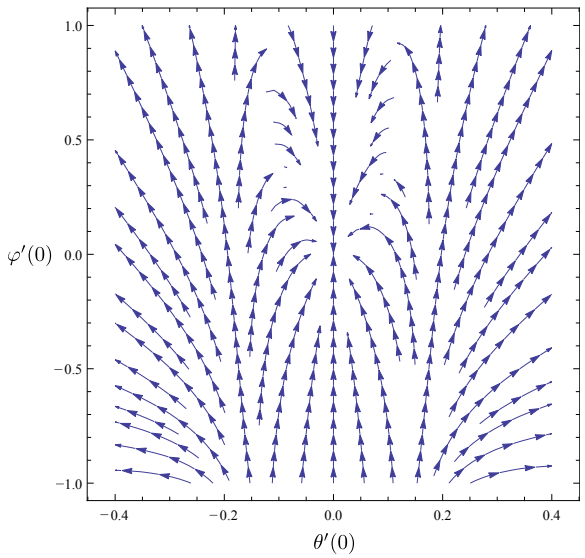

(a) $\varphi(0) = 6$, $f(\varphi(0)) \sim 200$. Notice the attractor behaviour of the system in the region $|\theta'| \lesssim 0.16$ and that inflation cannot occur in the region $|\theta'| \gtrsim 0.16$ since the fields accelerate and the slow-roll regime $\varepsilon \ll 1$ cannot be reached (notice the separatrix between these two behaviours).

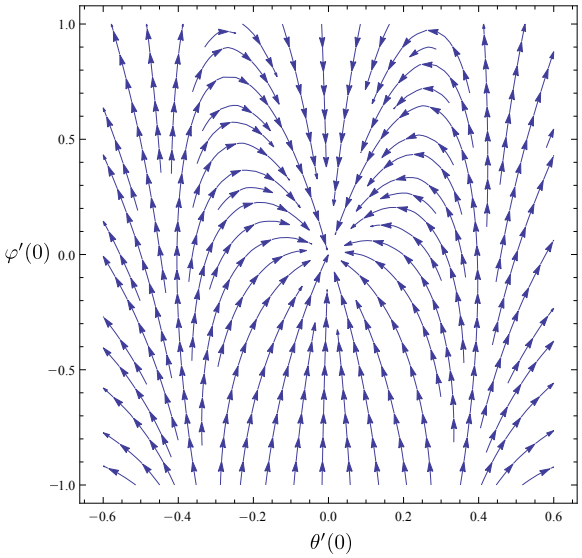

(b) $\varphi(0) = 4$, $f(\varphi(0)) \sim 36$. Notice that inflation can occur with a higher θ' than the left case.

Figure 7.1: Phase space diagrams for the system (7.27). Points represent initial velocities $\big(\theta'(0), \varphi'(0)\big)$ and vectors are accelerations $\big(\theta''(0), \varphi''(0)\big)$. These phase space diagrams are represented at a fixed value of $\varphi(0)$ and hence are reliable in a small neighbourhood of it (we should have represented a three dimensional plot with the additional coordinate $\varphi(0)$).

Note that, if f is an even function (as the function (7.3)), equations (7.27) are invariant under the transformations $\varphi \to -\varphi$ and $\theta \to -\theta$.

Consider equation (7.21). To begin our analysis, let us choose the simplest case $W_\theta = 0$. In this case, the equation of motion for θ coincides with (7.27b), i.e.

$$\theta'' + J\theta' = 0\,, \tag{7.28}$$

where we have defined

$$J\big(\varphi, \varphi', \theta'\big) \equiv 3 - \frac{1}{2}\varphi'^2 - \frac{f}{2}\theta'^2 + \frac{f'}{f}\varphi'. \tag{7.29}$$

The sign of the function J is fundamental for the behaviour of the system. If it is negative, θ accelerates and inflation will never occur since also φ accelerates (due to the term ω_θ (7.24) in (7.20)) and the slow-roll regime cannot be reached. On the other hand, if this term is positive, it acts like a viscous term and θ' is suppressed. Because of the previous considerations, the sign of the function J at $N = 0$ determines the initial dynamics of the system. If it is negative, inflation cannot start. However, notice that near $J = 0$ some caution must be used and only numerical analysis of the dynamics can distinguish whether inflation occurs. This function is represented in figure 7.2. During slow-roll the function J is certainly positive and hence θ' is

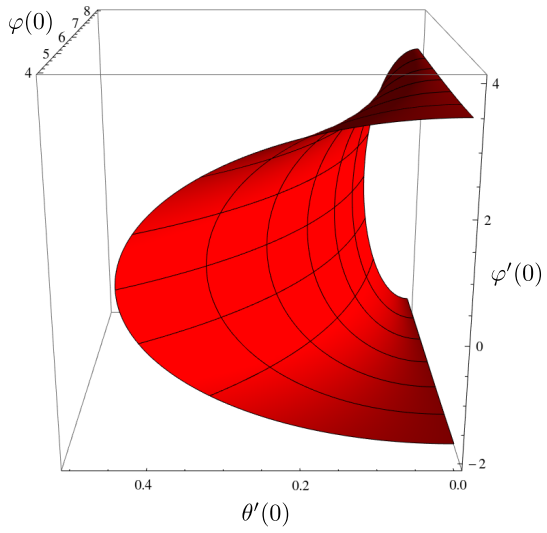

(a) Plot of the surface $J = 0$. Inflation occurs if initial conditions lies on the right of the red surface. Notice that $0.4 \gtrsim \theta'(0) \gtrsim -0.4$ (the plot is symmetric in $\theta'(0)$). In addition to this, notice that $4 \gtrsim \varphi'(0) \gtrsim -2$. However, $|\varphi'| < \sqrt{6}$ and hence there are practically no restrictions on the initial velocity $\varphi'(0)$ as opposed to $\theta'(0)$.

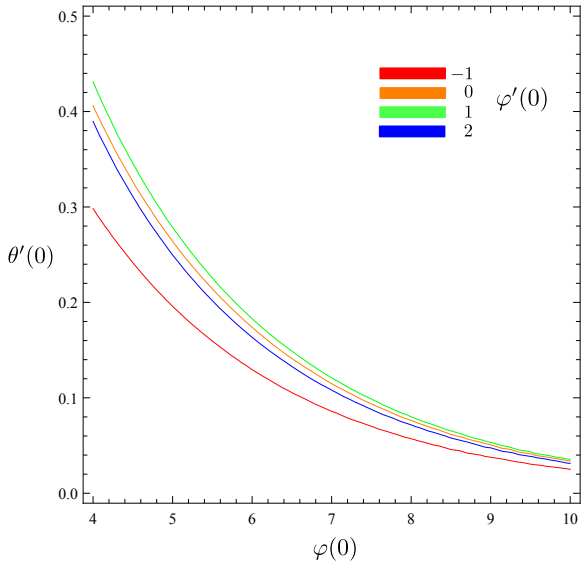

(b) Level curves of the left surface for some values of $\varphi'(0)$. Inflation occurs in the region under the curves. Notice that for large $\varphi(0)$ all the curves converges and hence $\varphi'(0)$ has no importance in the dynamics of the inflaton. On the other hand, for $\varphi(0) \gg 1$, $\theta'(0)$ should be very small otherwise the term ω_θ (7.24) becomes very large and dominates the dynamics of the system.

Figure 7.2: Study of the sign of the function J (7.29) evaluated at $N = 0$. Notice that $|\varphi'| < \sqrt{6}$ and $|\theta'| < \sqrt{6}$ due to equation (7.22).

suppressed (inflation approaches a nearly straight trajectory with small angular velocity θ').

Now, let us focus on equation (7.20) in order to understand what are the effects of the presence of the non-canonical kinetic term of θ. The additional term originating from the non-canonical kinetic term is ω_θ (7.24). Notice that it is always a negative term (f' is positive as well as θ'^2, obviously) and hence it induces a positive acceleration. Qualitatively, the dynamics of the field φ is very simple. If the term ω_θ is dominant, the field φ accelerates and inflation might be no more possible since also the field θ accelerates for the previous considerations. The remaining term $(3 - \varepsilon)\varphi'$ is like a viscous force and always reduce the speed ($3 - \varepsilon > 0$ due to equation (7.22)).

Some numerical calculations were performed in order to study the acceptable initial conditions. We studied the simple case of the potential $W(\varphi, \theta) = \tanh^2\left(\varphi/\sqrt{6}\right)$. The results are represented in figure 7.3 and they can be interpreted thanks to the previous analysis. Notice that inflation occurs only if θ' is sufficiently small from the beginning. However, the term ω_θ (7.24) could be of order unity at $N = 0$, as can be inferred from equation (7.14) and from figure 7.3. Notice that during slow-roll ω_θ is certainly small since it is a slow-roll parameter (ω_φ is also a slow-roll parameter, see section 7.4).

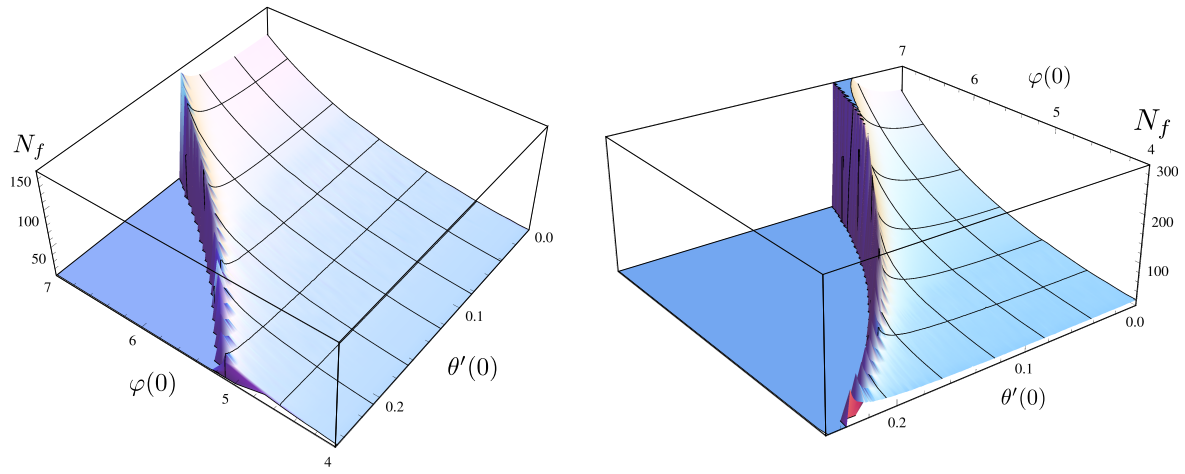

(a) $\varphi'(0) = 0$. (b) $\varphi'(0) = 2$.

Figure 7.3: Viability of initial conditions for the model with potential $W(\varphi, \theta) = \tanh^2\left(\varphi/\sqrt{6}\right)$. The graphs have the same x and y scales, but different z one. Let us focus on a fixed value of $\varphi(0)$. Increasing the initial velocity $\theta'(0)$ increases the number of e-folds N_f of inflation until they suddenly drop (inflation does not start). The same occurs increasing the initial position with $\theta'(0)$ fixed (unless $\theta'(0) \to 0$). In the region $\theta'(0) \to 0$, the fields follow a nearly straight trajectory and the field θ can practically be ignored (the solution is very well-approximated by the single-field one studied in section 5.6). The term ω_θ in (7.20) has the dominant effect on the inflationary region. Notice that increasing the initial velocity φ' reduces the region where inflation can occur; moreover, it increases the number of e-folds of inflation, keeping fixed the other initial conditions. Finally, note that the boundary of the inflationary region has the shape depicted in figure 7.2b.

Clearly, introducing a non-trivial potential for θ opens a Pandora's box. This makes a general study impossible since it can produce a multitude of different and peculiar landscapes. If the term $W_\theta/(fW)$ is negligible, we recover one of the previously studied cases. On the other hand, viable initial conditions are mainly determined by the term ω_θ in the background equation (7.20) and by the particular form of the potential. In the next chapter, we will analyse in detail two potentials.

Finally, let us make an observation. As we have seen, the background dynamics and the initial conditions are primarily affected by the term ω_θ in (7.20). The function f (7.3) has a first derivative positive for $\varphi > 0$. This constrains the possible initial conditions because the aforementioned term always increases the velocity φ' in the region $\varphi > 0$. On the other hand, nothing prevents us considering a different non-canonical kinetic term with $f' < 0$ for $\varphi > 0$. In this case, the considered term would suppress φ' helping the field to reach the attractor solution. However, $f > 0$ (because energy is always positive) and hence the term ω_φ in (7.21) can accelerate the field θ breaking the inflationary dynamics. In this case a more detailed study is necessary for the particular chosen function f.

7.3 Setup of *in-in* formalism

At first, we write the Hamiltonian associated with the Lagrangian (7.2). The conjugate momenta are

$$\pi_\varphi = \frac{\partial \mathcal{L}}{\partial \dot{\varphi}} = a^3 \dot{\varphi}, \tag{7.30a}$$

$$\pi_\theta = \frac{\partial \mathcal{L}}{\partial \dot{\theta}} = a^3 f(\varphi) \dot{\theta}, \tag{7.30b}$$

and thus the Hamiltonian is given by

$$\mathcal{H} = \frac{\pi_\varphi^2}{2a^3} + \frac{\pi_\theta^2}{2a^3 f} + \frac{a}{2}\left(\partial_i\varphi\partial_i\varphi + f\,\partial_i\theta\partial_i\theta\right) + a^3 W\,. \tag{7.31}$$

It is trivial to check that Hamilton equations of motion reproduce equations (7.8) and (7.9).

Following the *in-in* prescriptions, the fields and their conjugate momenta should be perturbed. Formally, the perturbed Hamiltonian can be written as

$$\mathcal{H} = \mathcal{H}^{(0)} + \sum_{i=1}^{+\infty} \delta\mathcal{H}^{(i)}, \tag{7.32}$$

where $\mathcal{H}^{(0)}$ is the background term and $\mathcal{H}^{(i)}$ contains terms of i-th order of the fields' perturbations. For our purposes, it is sufficient to consider terms up to third order. Through a straightforward calculation, the different contributions are given by

$$\mathcal{H}^{(0)} = \frac{\pi_\varphi^2}{2a^3} + \frac{\pi_\theta^2}{2a^3 f} + a^3 W\,, \tag{7.33}$$

$$\delta\mathcal{H}^{(1)} = \frac{\pi_\varphi}{a^3}\delta\pi_\varphi + \frac{\pi_\theta^2}{2a^3}\left(\frac{1}{f}\right)'\delta\varphi + \frac{\pi_\theta}{a^3}\left(\frac{1}{f}\right)\delta\pi_\theta + a^3\left(W_\varphi\delta\varphi + W_\theta\delta\theta\right), \tag{7.34}$$

$$\begin{aligned}\delta\mathcal{H}^{(2)} = {} & \frac{\delta\pi_\varphi^2}{2a^3} + \frac{\pi_\theta^2}{4a^3}\left(\frac{1}{f}\right)''\delta\varphi^2 + \frac{\pi_\theta}{a^3}\left(\frac{1}{f}\right)'\delta\varphi\delta\pi_\theta + \frac{1}{2a^3}\left(\frac{1}{f}\right)\delta\pi_\theta^2 \\ & + \frac{a}{2}\left((\partial_i\delta\varphi)^2 + f(\partial_i\delta\theta)^2\right) + a^3\left(\frac{1}{2}W_{\varphi\varphi}\delta\varphi^2 + W_{\varphi\theta}\delta\varphi\delta\theta + \frac{1}{2}W_{\theta\theta}\delta\theta^2\right),\end{aligned} \tag{7.35}$$

$$\begin{aligned}\delta\mathcal{H}^{(3)} = {} & \frac{\pi_\theta^2}{12a^3}\left(\frac{1}{f}\right)'''\delta\varphi^3 + \frac{\pi_\theta}{2a^3}\left(\frac{1}{f}\right)''\delta\pi_\theta\delta\varphi^2 + \frac{1}{2a^3}\left(\frac{1}{f}\right)'\delta\pi_\theta^2\delta\varphi + \frac{a}{2}f'\delta\varphi\left(\partial_i\delta\theta\right)^2 \\ & + \frac{a^3}{6}\left(W_{\varphi\varphi\varphi}\delta\varphi^3 + 3W_{\varphi\varphi\theta}\delta\varphi^2\delta\theta + 3W_{\varphi\theta\theta}\delta\varphi\delta\theta^2 + W_{\theta\theta\theta}\delta\theta^3\right).\end{aligned} \tag{7.36}$$

Obtaining equations (7.18) and (7.19) from this perturbed Hamiltonian is rather involved. We have indeed performed such a check, but we do not report here all the computations. Notice that one can neglect the linear terms in this calculation since they do not contribute to the equations for the fluctuations.

Notice that we have not considered the perturbations of the metric. The reason is that the calculations will be simpler without them. In addition to this, our main concern is studying the non-Gaussianities and, if they are produced through the interactions between the fields, the contributions from the perturbations of the metric are usually negligible.

The next step is the separation of the Hamiltonian into a kinetic part and an interaction part. After that, one can substitute the perturbations of the momenta with those of the fields via the relation

$$\dot{\delta\phi_I} = \frac{\partial \mathcal{H}^{(0)}}{\partial \delta\pi_I}\,. \tag{7.37}$$

The resulting terms are given by

$$\begin{aligned}
\mathcal{H}_0 &= \frac{a^3}{2}\dot{\delta\varphi}^2 + \frac{a^3 f^2\dot{\theta}^2}{4}\left(\frac{1}{f}\right)''\delta\varphi^2 + \frac{a^3 f}{2}\dot{\delta\theta}^2 + \frac{a}{2}\left((\partial_i\delta\varphi)^2 + f(\partial_i\delta\theta)^2\right) \\
&\quad + \frac{a^3}{2}\left(W_{\varphi\varphi}\delta\varphi^2 + W_{\theta\theta}\delta\theta^2\right), && \text{(7.38a)} \\
\mathcal{H}^{(2)}_{INT} &= -a^3 f'\dot{\theta}\delta\varphi\dot{\delta\theta} + a^3 W_{\varphi\theta}\delta\varphi\delta\theta && \text{(7.38b)} \\
&\equiv\ a^3 Z_1\delta\varphi\dot{\delta\theta} + a^3 Z_2\delta\varphi\delta\theta\,, \\
\mathcal{H}^{(3)}_{INT} &= \frac{a^3 f^2\dot{\theta}^2}{12}\left(\frac{1}{f}\right)'''\delta\varphi^3 + \frac{a^3 f^2\dot{\theta}}{2}\left(\frac{1}{f}\right)''\dot{\delta\theta}\delta\varphi^2 + \frac{a^3 f^2}{2}\left(\frac{1}{f}\right)'\dot{\delta\theta}^2\delta\varphi + \frac{a}{2}f'\delta\varphi(\partial_i\delta\theta)^2 \\
&\quad + \frac{a^3}{6}\left(W_{\varphi\varphi\varphi}\delta\varphi^3 + 3W_{\varphi\varphi\theta}\delta\varphi^2\delta\theta + 3W_{\varphi\theta\theta}\delta\varphi\delta\theta^2 + W_{\theta\theta\theta}\delta\theta^3\right) && \text{(7.38c)} \\
&\equiv\ a^3\Big[A_1\delta\varphi^3 + B_1\dot{\delta\theta}\delta\varphi^2 + C_1\big(\dot{\delta\theta}^2\delta\varphi - a^{-2}\delta\varphi(\partial_i\delta\theta)^2\big) \\
&\quad + A_2\delta\varphi^3 + B_2\delta\varphi^2\delta\theta + C_2\delta\varphi\delta\theta^2 + D\delta\theta^3\Big],
\end{aligned}$$

where we have defined the coupling constants Z_i, A_i, B_i, C_i, D. The term $\mathcal{H}_0$ is the kinematical part, $\mathcal{H}^{(2)}_{INT}$ and $\mathcal{H}^{(3)}_{INT}$ are respectively the second and third order interaction terms. All the fields are written in the interaction picture but, for brevity, we shall not employ any distinctive notation. Notice that there are derivatives of the field perturbation $\delta\theta$ in the interaction terms, as opposed to $\delta\varphi$. Furthermore, the connection with (6.7) and (6.8) is straightforward and hence we can rely on the results of the previous chapter.

Before proceeding, let us make some comments on the coupling constants (that indeed are not constant). The couplings can be divided into two classes, those which depend on f (related to the non-canonical kinetic term) and those which depend on the derivatives of the potential. The latter couple the field perturbations directly without derivatives. Their magnitude is constrained by the slow-roll conditions that require a sufficiently flat potential (at least along the direction of motion of the inflaton). The other terms, that depend on f, contain the background field velocity $\dot{\theta}$ except two of them. Let us remember that $\dot{\theta}/H$ should be small during inflation in order to have slow-roll (see section 7.2). Note that, if $\dot{\theta} = 0$, some of the couplings vanish. The coupling of the first term of $\mathcal{H}^{(2)}_{INT}$ goes as $f'\dot{\theta}$. Notice that in our model with f given by (7.3), we have $f \sim f' \sim f''$ and then the couplings of the first two term of $\mathcal{H}^{(3)}_{INT}$ behaves respectively as $f\dot{\theta}^2$ and $f\dot{\theta}$. We are left with two terms that does not depend on $\dot{\theta}$. The first one is $-\frac{a^3}{2}f'\dot{\delta\theta}^2\delta\varphi$ and its coupling behaves as f'. This is rather interesting since there are no tight constraints[2] on the derivatives of f. The coupling of the last term $\frac{a}{2}f'\delta\varphi(\partial_i\delta\theta)^2$ seems to behave as f', but

[2]We are reffering here to the constraints that derive from slow-roll conditions. For example, from the condition $\frac{1}{2}\dot{\varphi}^2 + \frac{f}{2}\dot{\theta}^2 \ll W$ it is clear that f can be large if $\dot{\theta}$ is sufficiently small. On the other hand, if f is small enough, $\dot{\theta}$ may be high (however $\ddot{\theta}$ should be small in order to have slow-roll).

the spatial derivatives should be kept in consideration. In fact, in Fourier space, the coupling goes as $f'k^2$ and on large scales (when f' is large) k is small and therefore one has to study the relative amplitude of the factors. For a generic function f the previous arguments should be reconsidered according to the specific expression of f (some terms with the derivatives might be enhanced or suppressed) and the velocity $\dot{\theta}$ might be very large[3].

The equations of motion for the free fields (in the interaction picture), following from the kinetic Hamiltonian (7.38a), are

$$\ddot{\delta\varphi} + 3H\dot{\delta\varphi} - \frac{1}{a^2}\nabla^2\delta\varphi + \frac{\dot{\theta}^2}{2}f^2\left(\frac{1}{f}\right)''\delta\varphi + W_{\varphi\varphi}\delta\varphi = 0\,, \tag{7.39}$$

$$\ddot{\delta\theta} + 3H\dot{\delta\theta} - \frac{1}{a^2}\nabla^2\delta\theta + \frac{f'}{f}\dot{\varphi}\dot{\delta\theta} + \frac{1}{f}W_{\theta\theta}\delta\theta = 0\,. \tag{7.40}$$

Notice that interactions between the perturbations are absent unlike in equations (7.18) and (7.19). The reason is that the previous equations derive from the free Hamiltonian and hence there are no interactions between the perturbations.

As previously done, we quantize the interaction picture fields as

$$\delta\varphi^I_{\mathbf{k}} = u_{\mathbf{k}}a_{\mathbf{k}} + u^*_{-\mathbf{k}}a^\dagger_{-\mathbf{k}}\,, \tag{7.41a}$$

$$\delta\theta^I_{\mathbf{k}} = v_{\mathbf{k}}b_{\mathbf{k}} + v^*_{-\mathbf{k}}b^\dagger_{-\mathbf{k}}\,, \tag{7.41b}$$

with the commutation relations (6.6). In order to solve these equations, we will suppose that expansion is quasi-de Sitter and thus we will adapt the techniques explained in section 1.5.2.

Let us start with the equation (7.39) for $\delta\varphi$, which is the simplest to solve. After having defined $q \equiv au$ and having switched to conformal time, these equation becomes

$$q'' - (\mathcal{H}^2 + \mathcal{H}')q + k^2q + a^2\left(\frac{f'^2}{f} - \frac{f''}{2}\right)\dot{\theta}^2q + a^2W_{\varphi\varphi}q = 0\,. \tag{7.42}$$

Let us define the following set of parameters,

$$\varepsilon = \frac{\varphi'^2 + f\theta'^2}{2\mathcal{H}^2} \equiv \varepsilon_\varphi + \varepsilon_\theta\,, \tag{7.43a}$$

$$\eta_\varphi \equiv \frac{a^2W_{\varphi\varphi}}{3\mathcal{H}^2}\,, \tag{7.43b}$$

$$\eta_\theta \equiv \frac{a^2W_{\theta\theta}}{3f\mathcal{H}^2}\,, \tag{7.43c}$$

$$\xi_\varphi \equiv \frac{f'\varphi'}{f\mathcal{H}} = \frac{f'}{f}\sqrt{2\varepsilon_\varphi}\,, \tag{7.43d}$$

$$\xi_\theta \equiv \frac{f'^2\theta'^2}{2f\mathcal{H}^2} = \frac{f'^2}{f^2}\varepsilon_\theta\,, \tag{7.43e}$$

$$\gamma_\theta \equiv \frac{f''\theta'^2}{2\mathcal{H}^2} = \frac{f''}{f}\varepsilon_\theta\,. \tag{7.43f}$$

In the next section, we will prove that all this parameters are actually slow-roll parameters for our model. For the moment, we are interested only in their definitions.

[3]See footnote 2.

Using equation (1.54)[4] and the previously defined parameters (7.43), equation (7.42) can be recast as

$$q'' + \left(k^2 - \frac{\nu^2 - \frac{1}{4}}{\tau^2}\right) q = 0\,, \tag{7.44}$$

where

$$\nu^2 = \frac{9}{4} + 3\varepsilon - 3\eta_\varphi + \gamma_\theta - 2\xi_\theta\,, \tag{7.45}$$

to first order the in slow-roll parameters. Notice that the non-canonical kinetic term is responsible for the correction $\gamma_\theta - 2\xi_\theta$. The last equation coincides in form with (1.57) and hence the solution is given by (1.64) (if ν is constant). Finally, the mode function u_k associated to $\delta\varphi$ is

$$u_k(\tau) = \frac{\sqrt{\pi}}{2} e^{i(\nu+\frac{1}{2})\frac{\pi}{2}} (-\tau)^{\frac{3}{2}} H\, H_\nu^{(1)}(-k\tau)\,. \tag{7.46}$$

Now, let us consider $\delta\theta$. Defining $p \equiv av$, equation (7.40) becomes

$$p'' + \frac{f'}{f}\varphi' p' + \left(k^2 - \left(\mathcal{H}' + \mathcal{H}^2\right) + \frac{a^2}{f} W_{\theta\theta} - \frac{f'}{f}\varphi'\mathcal{H}\right) p = 0\,. \tag{7.47}$$

The non-canonical kinetic term is responsible for the contribution $\frac{f'}{f}\varphi' p'$. Its presence spoils the standard strategy to obtain the mode functions we have followed so far. In order to proceed, we need to introduce the rescaled function

$$\tilde{p} \equiv \sqrt{f}\, p\,. \tag{7.48}$$

We do not write down all the calculations (apart for the non-trivial redefinition, they are similar to the former ones), but we are comforted to get once again the familiar result

$$\tilde{p}'' + \left(k^2 - \frac{\tilde{\nu}^2 - \frac{1}{4}}{\tau^2}\right) \tilde{p} = 0\,, \tag{7.49}$$

where now

$$\tilde{\nu}^2 = \frac{9}{4} + 3\varepsilon + \frac{f''}{f}\varepsilon - 3\eta_\theta + \frac{3}{2}\xi_\varphi + \frac{1}{2}\xi_\theta\,, \tag{7.50}$$

to first order in the slow-roll parameters. At the end, the mode function v_k has the form

$$v_k(\tau) = \frac{1}{\sqrt{f}} \frac{\sqrt{\pi}}{2} e^{i(\tilde{\nu}+\frac{1}{2})\frac{\pi}{2}} (-\tau)^{\frac{3}{2}} H\, H_{\tilde{\nu}}^{(1)}(-k\tau)\,. \tag{7.51}$$

Notice that the factor $1/\sqrt{f}$ is a suppression factor in our model since f is given by (7.3) and inflation occurs usually for $\varphi \gg 1$. In the following, we will analyse the consequences of this dependence.

[4]For consistency, we should keep only first-order terms in slow-roll parameters since equation (1.54) is a first-order expansion.

7.4 Non-canonical kinetic term and slow-roll

The standard definition of the slow-roll parameters (equations (1.28) and (1.29)) should be properly modified when there is a non-canonical kinetic term. In this section, we will prove that the parameters 7.43 are slow-roll parameters in the sense that they are small during slow-roll regime. The definitions 7.43 are adapted to our model. One can find definitions of slow-roll parameters similar to ours in [45, 95] since they study a non-canonical kinetic term analogous to ours. Since we will move back and forth from conformal time to cosmic time, the results of appendix A can be useful.

It is instructive to begin with a more general situation. Let us start with the multi-field action (4.1). We suppose that the field metric G_{IJ} is a generic function of the fields ϕ^I. The background equations of motion are (see equations (4.4) and (4.9))

$$\ddot{\phi}^I + \Gamma^I_{JK}\dot{\phi}^J\dot{\phi}^K + 3H\dot{\phi}^I + G^{IJ}W_{,J} = 0\,, \tag{7.52a}$$

$$H^2 = \frac{1}{3}\left(\frac{1}{2}G_{IJ}\dot{\phi}^I\dot{\phi}^J + W\right), \tag{7.52b}$$

$$\dot{H} = -\frac{1}{2}G_{IJ}\dot{\phi}^I\dot{\phi}^J. \tag{7.52c}$$

In order to have slow-roll inflation $\varepsilon \equiv -\dot{H}/H^2 \ll 1$, and hence the energy density of the universe should be dominated by the potential energy of the fields,

$$\frac{1}{2}G_{IJ}\dot{\phi}^I\dot{\phi}^J \ll W\,. \tag{7.53}$$

It is natural to define the slow-roll parameter

$$\varepsilon \equiv -\frac{\dot{H}}{H^2} = \frac{\mathcal{H}^2 - \mathcal{H}'}{\mathcal{H}^2} = \frac{G_{IJ}\phi^{I\prime}\phi^{J\prime}}{2\mathcal{H}^2}\,, \tag{7.54}$$

which quantifies the variation over time of H (remember that during inflation ε must be less than one, see chapter 1). Let us make a comment on the construction of the slow-roll parameters. These parameters are dimensionless and should be small. The first condition can be satisfied with appropriate powers of H. Indeed, the expansion rate H provides both a mass scale and a time scale, hence every time derivative should be paired with H^{-1} and also every field. The smallness condition can be obtained imposing constraints like (7.53).

Other constraints to impose are

$$|\ddot{\phi}^I| \ll 3H|\dot{\phi}^I|\,, \tag{7.55}$$

$$|\Gamma^I_{JK}\dot{\phi}^J\dot{\phi}^K| \ll 3H|\dot{\phi}^I|\,. \tag{7.56}$$

Using the first condition, it can be proven that

$$\eta_{IJ} \equiv \frac{1}{3}\frac{W_{,IK}G^{KJ}}{H^2} = \frac{a^2}{3}\frac{W_{,IK}G^{KJ}}{\mathcal{H}^2} \tag{7.57}$$

are slow-roll parameters (notice the analogy with (1.29)). Instead, from the second condition, one can define the slow-roll parameters

$$\Upsilon_I \equiv \frac{\Gamma^I_{JK}\phi^{J\prime}\phi^{K\prime}}{\mathcal{H}^2}\,. \tag{7.58}$$

Now, let us return to our model with the metric (7.4). The parameters (7.43a)-(7.43c) follows from the just mentioned definitions. Hence, they are small during slow-roll. We are left with the parameters (7.43d)-(7.43f). They are small during slow-roll because they can be rewritten in terms of ε_φ and ε_θ and in our model $f \sim f' \sim f''$. Notice that ξ_φ (7.43d) is only the square root of a slow-roll parameter in our model.

Let us comment the case of a generic function f. The slow-roll condition $\frac{1}{2}\dot{\varphi}^2 + \frac{f}{2}\dot{\theta}^2 \ll W$ does not forbid $\dot{\theta}$ to be large if f is sufficiently small. On the other hand, $\frac{f\theta'^2}{2\mathcal{H}^2} \ll 1$ and $\frac{f'\theta'^2}{2\mathcal{H}^2} \ll 1$ due to conditions (7.53) and (7.56), but there are no constraints on $\frac{f''\theta'^2}{2\mathcal{H}^2}$ that might be big. As an example, suppose that the trajectory is a circle in field space with constant radius $\varphi(0)$ (this circumstance can be obtained with a confining potential along the radial direction). Moreover, suppose that $f(\varphi) = (\varphi - \varphi(0))^2$. Notice that the velocity $\dot{\theta}$ is not limited by slow-roll conditions. Therefore $f(\varphi(0)) = f'(\varphi(0)) = 0$, but $f'' = 2$. Hence γ_θ is not a slow-roll parameter for this model[5].

7.5 Constant turn case

Our starting point is the two-field Lagrangian (7.1). Let us suppose that the background trajectory is a circle with fixed φ and constant angular velocity $\dot{\theta}$. We also assume that the potential depends only on φ (hence θ is massless). With all these assumptions, our model is analogous to Chen's quasi-single field [82] except for the presence in our model of a non-trivial coupling in the kinetic term. Inflation is driven by the field θ (inflaton), the second field φ (isocurvaton) produces the non-Gaussianities that are eventually transferred to the former field [72, 126].

We have supposed that the potential W is a function only of φ, neglecting the dependence on θ (in subsection (7.5.3) we will consider a potential W that depends on both φ and θ). This seems a drastic approximation at a first sight since θ should have a suitable potential in order to be the inflaton. However this approximation allows us to focus on the non-Gaussianities produced by the field φ and transferred to θ. Indeed, as we will see, the contributions to the bispectrum due to the dependence of the potential on θ should be subdominant due to the slow-roll conditions. Hence, for the moment we suppose that a suitable potential for θ was chosen but that its contributions to bispectrum can be neglected. A pictorial representation of a constant turn trajectory is given in figure 7.4.

This model relies on strict assumptions, but it is nevertheless instructive since the isocurvature perturbations can source the curvature ones if the trajectory is curved, see section 4.3. Then, if the isocurvaton produces non-Gaussian fluctuations, they can be transferred to the inflaton through interactions between the fields. The couplings between the fields depend on the potential and on the non-canonical kinetic term. The most important characteristic of this

[5] Many authors require that the field space is nearly flat and hence it has little curvature. With this assumption, one can show that ξ_φ, ξ_θ and γ_θ (defined in (7.43d)-(7.43f)) are indeed small. Let us stress the fact that this condition is independent from slow-roll and slow-turn conditions, but it can affects them. See for example the appendix of [91].

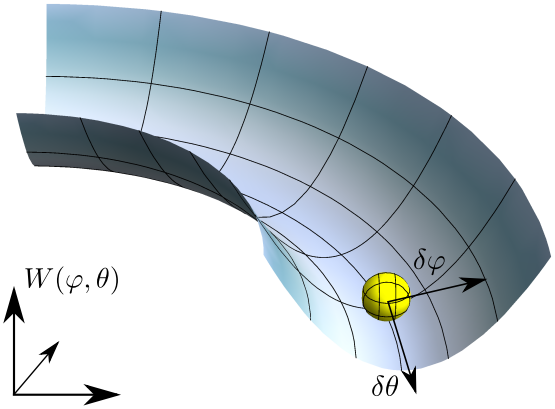

Figure 7.4: Example of constant turn trajectory. The field (the yellow ball) moves along a circle thanks to the particular form of the potential. The fluctuation $\delta\theta$ is related to the curvature perturbation of the inflaton field θ and $\delta\varphi$ to the isocurvature perturbation of the field φ.

model is that it can produce large non-Gaussianities [72, 82, 126] because the field φ is not subjected to the slow-roll conditions that usually constrain the magnitude of the couplings between the fields.

With the previous assumptions, the Hamiltonian (7.38) becomes

$$\mathcal{H}_0 = \frac{a^3}{2}\dot{\delta\varphi}^2 + \frac{a^3 f^2\dot\theta^2}{4}\left(\frac{1}{f}\right)''\delta\varphi^2 + \frac{a^3 f}{2}\dot{\delta\theta}^2 + \frac{a}{2}\left((\partial_i\delta\varphi)^2 + f(\partial_i\delta\theta)^2\right) + \frac{a^3}{2}W_{\varphi\varphi}\delta\varphi^2, \tag{7.59a}$$

$$\mathcal{H}^{(2)}_{INT} = -a^3 f'\dot\theta\delta\varphi\dot{\delta\theta}, \tag{7.59b}$$

$$\mathcal{H}^{(3)}_{INT} = \frac{a^3 f^2\dot\theta^2}{12}\left(\frac{1}{f}\right)'''\delta\varphi^3 + \frac{a^3 f^2\dot\theta}{2}\left(\frac{1}{f}\right)''\dot{\delta\theta}\delta\varphi^2 + \frac{a^3 f^2}{2}\left(\frac{1}{f}\right)'\dot{\delta\theta}^2\delta\varphi + \frac{a}{2}f'\delta\varphi(\partial_i\delta\theta)^2 + \frac{a^3}{6}W_{\varphi\varphi\varphi}\delta\varphi^3. \tag{7.59c}$$

It is worth noticing that, even if $\dot\theta = 0$, there are anyway interactions between the fields (but only at third order in perturbations) originating from the potential W and the non-canonical kinetic term. In the following, we will use the same definitions of equations (7.38) to characterize the different terms of the Hamiltonian. For example, $\mathcal{H}^{(3)}_{A_2} = a^3 W_{\varphi\varphi\varphi}\delta\varphi^3/6$.

Since θ is massless, $\tilde\nu = 3/2$ (see equation (7.50)). Therefore, the mode functions (7.46) and (7.51), respectively for the $\delta\varphi$ and $\delta\theta$ fluctuations, reduce to

$$u_k(\tau) = \frac{\sqrt{\pi}}{2}e^{i(\nu+\frac{1}{2})\frac{\pi}{2}}(-\tau)^{\frac{3}{2}}H\,H^{(1)}_\nu(-k\tau), \tag{7.60a}$$

$$v_k(\tau) = \frac{H}{\sqrt{2k^3}\sqrt{f}}(1+ik\tau)e^{-ik\tau}. \tag{7.60b}$$

Finally, since the trajectory is a circle, the curvature perturbation ζ can be written [82] as[6]

$$\zeta \simeq -\frac{H}{\dot{\theta}}\delta\theta\,. \tag{7.61}$$

Remember that we are not interested in the expectation value $\langle\delta\theta^2\rangle$, but rather in the expectation value of the curvature perturbation ζ. The reason is that (in single-field models of inflation) the curvature perturbation ζ is conserved on superhorizon scales and it is a gauge-invariant quantity unlike $\delta\theta$, as we have seen in chapter 2.

7.5.1 Power spectrum

At lowest order in the *in-in* expansion, the two-point correlation function is given by (6.13), that is

$$\begin{aligned}\left\langle\zeta^2(\tau)\right\rangle^{(0)} &= (2\pi)^3\delta^3(\mathbf{p}_1+\mathbf{p}_2)\frac{H^2}{\dot{\theta}^2}|v_{p_1}(\tau)|^2 \\ &= (2\pi)^3\delta^3(\mathbf{p}_1+\mathbf{p}_2)\frac{H^4}{2f\dot{\theta}^2\,p_1^3}(1+p_1^2\tau^2)\,.\end{aligned} \tag{7.62}$$

On super-horizon scales $-p_1\tau \ll 1$, the previous expression becomes

$$\left\langle\zeta^2(0)\right\rangle^{(0)} = (2\pi)^3\delta^3(\mathbf{p}_1+\mathbf{p}_2)\frac{H^4}{2f\dot{\theta}^2\,p_1^3}\,. \tag{7.63}$$

The lowest-order correction is given by the expression (6.19). Its contribution reads

$$\left\langle\zeta^2(t)\right\rangle^{(2)} = (2\pi)^3\delta^3(\mathbf{p}_1+\mathbf{p}_2)\frac{f'^2H^2}{f^2p_1^3}\mathcal{C}_T(\nu)\,, \tag{7.64}$$

where we have defined

$$\mathcal{C}_T(\nu) \equiv \frac{\pi}{4}\mathrm{Re}\left\{\int_0^\infty dx_1\int_{x_1}^\infty dx_2\left(\frac{e^{i(x_1-x_2)}}{\sqrt{x_1x_2}}H_\nu^{(1)}(x_1)H_\nu^{(2)}(x_2)-\frac{e^{-i(x_1+x_2)}}{\sqrt{x_1x_2}}H_\nu^{(1)}(x_1)H_\nu^{(2)}(x_2)\right)\right\}, \tag{7.65}$$

and $x \equiv -p_1\tau$. In the previous expression, we have considered the superhorizon limit. The factor $\mathcal{C}_T(\nu)$ is plotted in figure 7.5. The lowest integration limit is not zero, but one needs to impose a cutoff at

$$e^{N_*} = -\frac{1}{p_1\tau_f}\,, \tag{7.66}$$

where N_* is the number of e-folds before the end of inflation at which the considered scale p_1 leaves the horizon and τ_f is the end of inflation. More details about the numerical computation of these type of integrals can be found in appendix D.2. In the following, we will suppose that inflation ends at $\tau_f = 0$.

[6]The general expression of the curvature perturbation for the Lagrangian (7.1) is given by equation (8.13). Since the trajectory is a circle with fixed value of φ, the velocity $\dot{\varphi} = 0$ and then the adiabatic direction is parallel to $\delta\theta$.

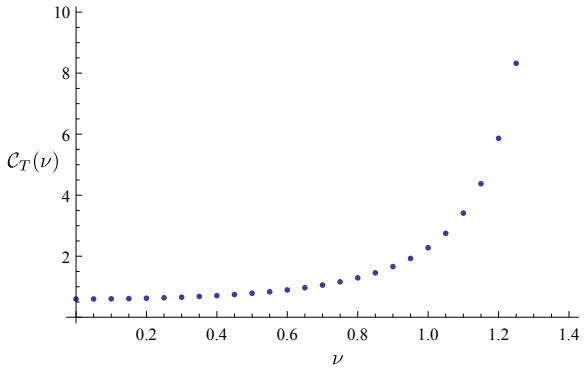

(a) $\mathcal{C}_T(\nu)$ for a scale that exits the horizon 50 e-folds before the end of inflation.

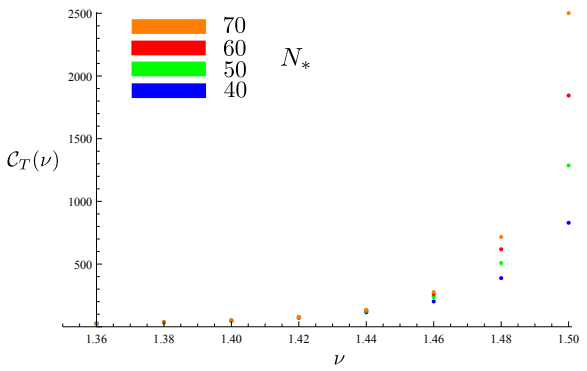

(b) $\mathcal{C}_T(\nu)$ for different scales that exit the horizon N_* e-folds before the end of inflation.

Figure 7.5: The factor $\mathcal{C}_T(\nu)$ defined in (7.65). For $\nu \ll 3/2$ the dependence on the scale is negligible, it becomes significant as $\nu \to 3/2$.

Summing up, the power spectrum (up to second order in the *in-in* expansion) is given by

$$\begin{aligned}\langle\zeta^2(t)\rangle &= \langle\zeta^2(t)\rangle^{(0)} + \langle\zeta^2(t)\rangle^{(2)} \\ &= (2\pi)^3\delta^3(\mathbf{p}_1+\mathbf{p}_2)\frac{(2\pi)^2}{2p_1^3}\left(\frac{H^4}{4\pi^2 f\dot\theta^2}+\frac{f'^2H^2}{2\pi^2 f^2}\mathcal{C}_T(\nu)\right),\end{aligned} \tag{7.67}$$

and the adimensional power spectrum (see the definition (4.72)) reads

$$\mathcal{P}_\zeta = \frac{H^4}{(2\pi\dot\theta)^2 f}\left[1+\frac{2f'^2}{f}\mathcal{C}_T(\nu)\left(\frac{\dot\theta^2}{H^2}\right)\right]. \tag{7.68}$$

Notice that

$$\frac{2f'^2}{f}\left(\frac{\dot\theta^2}{H^2}\right) = 2\xi_\theta\,, \tag{7.69}$$

where ξ_θ is defined in (7.43e). Therefore the correction to the adimensional power spectrum is of first order in the slow-roll parameters. This is fundamental in order for the theory to remain perturbative (by definition perturbations should be small). Another feature to notice is the dependence of $\mathcal{P}_\zeta$ on f^{-1}. In the constant turn case, this is like a normalization factor since φ is assumed constant.

7.5.2 Bispectrum

In this section, we will not compute carefully the different terms of section 6.3 since there are too many terms to consider. Rather, we prefer to estimate naively their contributions to the amplitude of f_{NL} and then calculate only the relevant ones.

As discussed in section 3.2, the definition of the non-linearity parameter f_{NL} is obtained considering the amplitude of the bispectrum in the equilateral configuration, i.e.

$$\langle\zeta(\mathbf{p}_1)\zeta(\mathbf{p}_2)\zeta(\mathbf{p}_3)\rangle \xrightarrow{p_1=p_2=p_3} (2\pi)^7\delta^3(\mathbf{p}_1+\mathbf{p}_2+\mathbf{p}_3)\mathcal{P}_\zeta^2\left(\frac{9}{10}f_{NL}\right)\frac{1}{p_1^6}\,. \tag{7.70}$$

The magnitude of f_{NL} can be estimated using Feynman rules. At each vertex is associated the corresponding adimensional coupling constant (it is convenient to work with adimensional constants since f_{NL} is dimensionless). The n-th order term (6.2) of the *in-in* expansion can be estimated as [82]

$$\langle\zeta^3\rangle^{(n)} \sim I\prod_i^n C_i\frac{\sqrt{f}\dot{\theta}}{H^2}\mathcal{P}_\zeta^2\frac{1}{p_1^6}\,, \tag{7.71}$$

where I denotes the integral term and C_i are the coupling constants. The integral term can be considered $I\sim\mathcal{O}(1)$ even in the limit $\nu\to 3/2$ [82]. Let us notice that the power spectrum (7.68) (at zeroth order) can be rewritten as

$$\mathcal{P}_\zeta = \frac{H^2}{8\pi^2\varepsilon_\theta}\,. \tag{7.72}$$

Finally, the amplitude of f_{NL} can be approximated as

$$f_{NL}\sim\prod_i^n C_i\frac{\sqrt{f}\dot{\theta}}{H^2}\,. \tag{7.73}$$

The lowest order non-vanishing contribution to the bispectrum is given by

$$\langle\delta\theta^3\rangle^{(2)} \supseteq \langle\delta\theta^3 H^{(2)}H^{(3)}_{C_1}\rangle\,. \tag{7.74}$$

The adimensional coupling constant of $H^{(2)}$ is $f'f^{-1/2}\dot{\theta}H^{-1}$, and that of $H^{(3)}_{C_1}$ is given by $f'f^{-1}H$. Then, it is simple to show that

$$\langle\zeta^3\rangle^{(2)}_{C_1} \sim \frac{f'^2}{f^2}\varepsilon_\theta\mathcal{P}_\zeta^2\frac{1}{p_1^6}\,. \tag{7.75}$$

We have introduced the notation $\langle\zeta^3\rangle^{(2)}_{C_1}$ that denotes the second order term in the expansion of the three-point correlator $\langle\zeta^3\rangle$ that contains the free vacuum expectation value $\langle 0|\,\zeta^3H^{(2)}H^{(3)}_{C_1}\,|0\rangle$ (see expansion (6.2)). In the following, we will use this shorthand notation to characterize the terms of the *in-in* expansion. We will consider only the connected diagrams of sections 6.2 and 6.3 and write down only the relevant couplings to identify the different terms (e.g. in the previous example we did not write the coupling Z_1 for $H^{(2)}$ since it was uniquely determined).

At third order ,

$$\langle\delta\theta^3\rangle^{(3)} \supseteq \langle\delta\theta^3 H^{(2)}H^{(2)}H^{(3)}_{B_1}\rangle\,, \tag{7.76}$$

since $H^{(3)}$ (7.59c) does not contain a $\delta\theta^3$ term (in the following subsection we will consider a massive inflaton field θ). Its contribution to the bispectrum is given by

$$\langle\zeta^3\rangle^{(3)}_{B_1} \sim \varepsilon_\theta^2\frac{f'}{f}\frac{2f'^3-ff'f''}{f^3}\mathcal{P}_\zeta^2\frac{1}{p_1^6}\,. \tag{7.77}$$

Finally, at fourth order we need to calculate terms like

$$\langle\delta\theta^3\rangle^{(4)} \supseteq \langle\delta\theta^3 H^{(2)}H^{(2)}H^{(2)}H^{(3)}\rangle\,, \tag{7.78}$$

where $H^{(3)} = H^{(3)}_A$ or $H^{(3)} = H^{(3)}_{C_1}$. The naive evaluations of these contributions are

$$\langle\zeta^3\rangle^{(4)}_{A_1} \sim \varepsilon_\theta^3 \frac{f'^3}{f^3}\left(\frac{6ff'f'' - 6f'^3 - f^2 f'''}{f^3}\right)\mathcal{P}_\zeta^2 \frac{1}{p_1^6}\,, \tag{7.79a}$$

$$\langle\zeta^3\rangle^{(4)}_{A_2} \sim \frac{W_{\varphi\varphi\varphi}}{H}\varepsilon_\theta^2 \frac{f'^3}{f^3}\mathcal{P}_\zeta^2 \frac{1}{p_1^6}\,, \tag{7.79b}$$

$$\langle\zeta^3\rangle^{(4)}_{C_1} \sim \varepsilon_\theta^2 \frac{f'^4}{f^4}\mathcal{P}_\zeta^2 \frac{1}{p_1^6}\,. \tag{7.79c}$$

All the previously estimated contributions are suppressed by the slow-roll parameters. In addition to this, notice that $f \sim f' \sim f''$ for the function (7.3) and hence the non-canonical kinetic term cannot affect the order of magnitude of f_{NL}. Chen [82] computes a term similar to $\langle\zeta^3\rangle^{(4)}_{A2}$ since it is the only term that can be enhanced thanks to $W_{\varphi\varphi\varphi}$ which is not suppressed by the slow-roll conditions (the field φ is not the inflaton). Since our model is very similar to that of Chen[7], the aforementioned term is the only one that can be enhanced for the same reason; all the other contributions are suppressed by the slow-roll parameters.

The diagrammatic representation of the term (7.79b) is given by the diagram (c) in figure 6.2 with the fields $\delta\varphi$ and $\delta\theta$ swapped. The full expression of the term (7.79b) in the commutator form is

$$\begin{aligned}\langle\zeta^3\rangle^{(4)}_{A_2} = &-12(2\pi)^3\delta^3(\mathbf{p}_1+\mathbf{p}_2+\mathbf{p}_3)\left(\frac{Hf'}{\dot\theta}\right)^3 v_{p_1}(0)v_{p_2}(0)v_{p_3}(0)\\ &\mathrm{Re}\Bigg\{\int_{-\infty}^0 d\tau_1\int_{-\infty}^{\tau_1}d\tau_2\int_{-\infty}^{\tau_2}d\tau_3\int_{-\infty}^{\tau_3}d\tau_4\prod_{i=1}^4\Big(a^3(\tau_i)\Big)\dot\theta^3\big(v'_{p_1}(\tau_1)-\text{c.c.}\big)\\ &\left(\frac{a(\tau_2)W_{\varphi\varphi\varphi}(\tau_2)}{6}A+\frac{a(\tau_3)W_{\varphi\varphi\varphi}(\tau_3)}{6}B+\frac{a(\tau_4)W_{\varphi\varphi\varphi}(\tau_4)}{6}C\right)\Bigg\}+5\,\text{perm}\,,\end{aligned} \tag{7.80}$$

where

$$\begin{aligned}A &= \big(u_{p_1}(\tau_1)u^*_{p_1}(\tau_2)-\text{c.c.}\big)\big(u_{p_3}(\tau_2)u^*_{p_3}(\tau_4)v'^*_{p_3}(\tau_4)-\text{c.c.}\big)u_{p_2}(\tau_2)u^*_{p_2}(\tau_3)v'^*_{p_2}(\tau_3)\,,\\ B &= \big(v'_{p_2}(\tau_2)-\text{c.c.}\big)\big(u^*_{p_1}(\tau_1)u^*_{p_2}(\tau_2)u_{p_1}(\tau_3)u_{p_2}(\tau_3)-\text{c.c.}\big)u_{p_3}(\tau_3)u^*_{p_3}(\tau_4)v'^*_{p_3}(\tau_4)\,,\\ C &= -\big(v'_{p_2}(\tau_2)-\text{c.c.}\big)\big(v'_{p_3}(\tau_3)-\text{c.c.}\big)u^*_{p_1}(\tau_1)u^*_{p_2}(\tau_2)u^*_{p_3}(\tau_3)u_{p_1}(\tau_4)u_{p_2}(\tau_4)u_{p_3}(\tau_4)\,.\end{aligned}$$

In order to calculate f_{NL}, we consider the equilateral limit $p_1 = p_2 = p_3 = p$ (see equation (7.70)). Using the mode functions 7.60, equation (7.80) becomes

$$\begin{aligned}\langle\zeta^3\rangle^{(4)}_{A_2} = (2\pi)^3\delta^3(\mathbf{p}_1+\mathbf{p}_2+\mathbf{p}_3)\frac{3\pi^3}{2^7}\frac{f'^3H^2}{f^3p^6}W_{\varphi\varphi\varphi}\,\mathrm{Re}\Bigg\{\int_0^{+\infty}dx_1\int_{x_1}^{+\infty}dx_2\int_{x_2}^{+\infty}dx_3\int_{x_3}^{+\infty}dx_4\\ \prod_{i=1}^4\left(\frac{1}{x_i^4}\right)\big(\tilde v'(x_1)-\text{c.c.}\big)\left(\frac{\tilde A}{x_2}+\frac{\tilde B}{x_3}+\frac{\tilde C}{x_4}\right)\Bigg\}\,,\end{aligned} \tag{7.81}$$

[7]The main difference is the presence in our model of a non-canonical kinetic term, but this does not alter significantly the results since for the function f (7.3) we have $f \sim f' \sim f''$. However, our treatment is general and can be generalized considering other possibilities for f.

where we have defined $x_i \equiv -p\tau_i$ and

$$\tilde{v}(x) \equiv (1-ix)e^{ix}, \tag{7.82a}$$

$$\tilde{u}(x) \equiv x^{\frac{3}{2}} H_\nu^{(1)}(x), \tag{7.82b}$$

$$\tilde{A} = \big(\tilde{u}(x_1)\tilde{u}^*(x_2) - \text{c.c.}\big)\big(\tilde{u}(x_2)\tilde{u}^*(x_4)\tilde{v}'^*(x_4) - \text{c.c.}\big)\tilde{u}(x_2)\tilde{u}^*(x_3)\tilde{v}'^*(x_3), \tag{7.82c}$$

$$\tilde{B} = (\tilde{v}'(x_2) - \text{c.c.})\big(\tilde{u}^*(x_1)\tilde{u}^*(x_2)\tilde{u}(x_3)\tilde{u}(x_3) - \text{c.c.}\big)\tilde{u}(x_3)\tilde{u}^*(x_4)\tilde{v}'^*(x_4), \tag{7.82d}$$

$$\tilde{C} = -(\tilde{v}'(x_2) - \text{c.c.})(\tilde{v}'(x_3) - \text{c.c.})\tilde{u}^*(x_1)\tilde{u}^*(x_2)\tilde{u}^*(x_3)\tilde{u}(x_4)\tilde{u}(x_4)\tilde{u}(x_4). \tag{7.82e}$$

Finally, using the definition (7.70) and the expression of the power spectrum (7.68), the contribution of the previous correlator to the parameter f_{NL} is given by

$$f_{NL}^{(4)} = \frac{5\pi^3}{3\cdot 2^6}\frac{f'^3}{f^3}\left(f\frac{\dot{\theta}^2}{H^2}\right)^2 \frac{W_{\varphi\varphi\varphi}}{H^2}\,\text{Re}\Bigg\{\int_0^{+\infty} dx_1 \int_{x_1}^{+\infty} dx_2 \int_{x_2}^{+\infty} dx_3 \int_{x_3}^{+\infty} dx_4 \prod_{i=1}^{4}\left(\frac{1}{x_i^4}\right)(\tilde{v}'(x_1) - \text{c.c.})\left(\frac{\tilde{A}}{x_2} + \frac{\tilde{B}}{x_3} + \frac{\tilde{C}}{x_4}\right)\Bigg\}. \tag{7.83}$$

Notice that $f_{NL}^{(4)}$ is proportional to the square of the slow-roll parameter ε_θ (7.43a). As we have already said, the amplitude can be increased thanks to the third derivative $W_{\varphi\varphi\varphi}$. Obviously, this enhancement depends on the particular form of the potential W. We postpone this discussion to section 7.5.4, where we are going to study the effects of the presence of the parameter α.

7.5.3 Generalizations

In this section, we will generalize the previous model introducing a potential for the inflaton θ. We will see that the new contributions to the power spectrum and the bispectrum are small since they are suppressed by the slow-roll conditions. Let us suppose that the potential is separable, $W(\varphi,\theta) = V(\varphi) + U(\theta)$. If the field θ is massive, the expression of the power spectrum (7.68) is slightly modified by the mass term $\frac{a^3}{2}W_{\theta\theta}\delta\theta^2$ in the Hamiltonian (7.38). The mode functions are given by (7.46) and (7.51). Now the power spectrum reads

$$\mathcal{P}_\zeta = \frac{H^4}{(2\pi\dot{\theta})^2 f}\left[1 + \frac{2f'^2}{f}\,\mathcal{C}_T(\nu,\tilde{\nu})\left(\frac{\dot{\theta}^2}{H^2}\right)\right], \tag{7.84}$$

where

$$\mathcal{C}_T(\nu,\tilde{\nu}) \equiv \frac{\pi^3}{4^3}\text{Re}\Bigg\{\int_0^\infty dx_1 \int_{x_1}^\infty dx_2 H_\nu^{(1)}(x_1)x_1^{-\frac{3}{2}}\frac{d}{dx_2}\left(x_2^{\frac{3}{2}}H_{\tilde{\nu}}^{(2)}(x_2)\right)H_\nu^{(2)}(x_2)x_2^{-\frac{3}{2}} \left[H_{\tilde{\nu}}^{(1)}(0)H_{\tilde{\nu}}^{(2)}(0)\frac{d}{dx_1}\left(x_1^{\frac{3}{2}}H_{\tilde{\nu}}^{(1)}(x_1)\right) - H_{\tilde{\nu}}^{(1)}(0)H_{\tilde{\nu}}^{(1)}(0)\frac{d}{dx_1}\left(x_1^{\frac{3}{2}}H_{\tilde{\nu}}^{(2)}(x_1)\right)\right]\Bigg\}. \tag{7.85}$$

The cubic Hamiltonian (7.59c) has the additional term

$$\mathcal{H}_D^{(3)} = \frac{a^3}{6}W_{\theta\theta\theta}\delta\theta^3. \tag{7.86}$$

New corrections arise for the bispectrum. At first order, the term

$$\langle \delta\theta^3 \rangle^{(1)} \supseteq \langle \delta\theta^3 H_D^{(3)} \rangle \tag{7.87}$$

constitutes a self-interaction of the field θ. As previously done, its contribution to the curvature perturbation can be approximated as

$$\langle \zeta^3 \rangle_D^{(1)} \sim \frac{W_{\theta\theta\theta}}{H} \sqrt{\varepsilon_\theta} f^{-\frac{3}{2}} \mathcal{P}_\zeta^2 \frac{1}{p_1^6} \,. \tag{7.88}$$

This contribution is negligible since $W_{\theta\theta\theta} H^{-1}$ should be small during slow-roll[8]. At second order, there are not new terms. Instead at third order, the term

$$\langle \delta\theta^3 \rangle^{(3)} \supseteq \langle \delta\theta^3 H_D^{(3)} H^{(2)} H^{(2)} \rangle \tag{7.89}$$

appears, and its contribution is given by

$$\langle \zeta^3 \rangle_D^{(3)} \sim \frac{W_{\theta\theta\theta}}{H} \frac{f'^2}{f^{\frac{7}{2}}} \varepsilon_\theta^{\frac{3}{2}} \mathcal{P}_\zeta^2 \frac{1}{p_1^6} \,. \tag{7.90}$$

However, this term cannot contribute significantly to the bispectrum for the same reason as the term $\langle \zeta^3 \rangle_D^{(1)}$. Therefore, the field θ can be considered massless with good approximation as long as the slow-roll conditions hold.

If f is a generic function, one can increase the ratio f'/f in order to produce large non-Gaussianities since the previously estimated corrections usually depend on this ratio. However, some caution must be used. Indeed, this ratio affects the first non-vanishing correction to the power spectrum (7.68) (or (7.84)), and hence we have to impose a constraint like

$$\frac{f'^2}{f^2} \varepsilon_\theta^2 \ll 1 \,. \tag{7.91}$$

In addition to this, since θ is the inflaton we should require that the slow-roll parameters in the definition of $\tilde{\nu}$ (7.50) are small. The latter condition implies that

$$\varepsilon_\theta \ll 1 \,, \tag{7.92a}$$

$$\frac{f''}{f} \varepsilon_\theta \ll 1 \,. \tag{7.92b}$$

These conditions prevent an enhancement of all the estimated contributions apart for (7.79a) and for the self-interaction terms (7.88) and (7.90). The latter terms can be enhanced if f is sufficiently small because they are proportional to inverse powers of f. The actual enhancement depends on the specific expression of f and thus we do not make a deeper analysis. However, notice that these two terms are suppressed by the slow-roll parameter ε_θ and also by the factor $W_{\theta\theta\theta}/H$ that should be small during inflation if θ drives it[9]. The term (7.79a) can be enhanced if $f''' f^2 f'^{-3} \gg 1$ thanks to the third derivative f''' which is not constrained by the slow-roll conditions. Again, the magnitude of this enhancement depends on the particular form of f.

[8] The third derivative of the potential is related to a second-order slow-roll parameter. As an example, in [6] it is defined the slow-roll parameter $\xi_V^2 \equiv V_\varphi V_{\varphi\varphi\varphi} / V^2$, where V is the potential of the inflaton.

[9] See footnote 8.

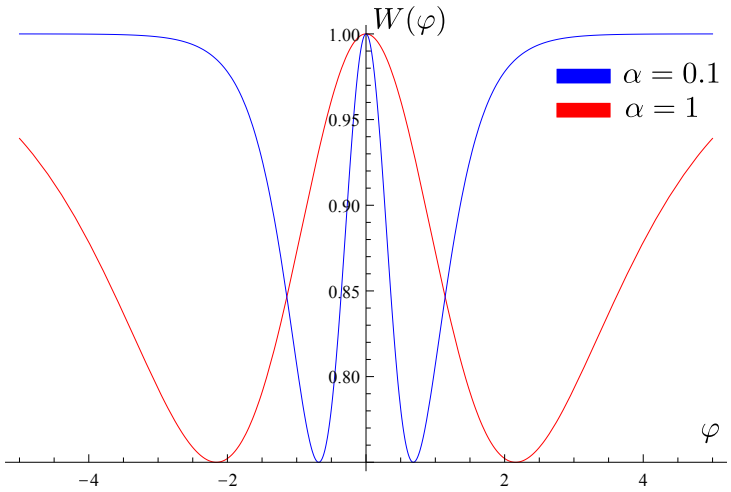

Figure 7.6: The double well potential (7.95). Notice that a little variation of α could make the potential more confining. For comparison, the third derivative of the potential with $\alpha = 1$ evaluated at the minima is $-0.15\, M_{Pl}$, that of the potential with $\alpha = 0.1$ is $-4.56\, M_{Pl}$.

7.5.4 The α parameter

Now, let us introduce the parameter α into the Lagrangian (7.1). This can be done simply replacing $\varphi/M_{Pl} \to \varphi/(\sqrt{\alpha}M_{Pl})$ into the function f and the potential W of Lagrangian (7.1). Can we produce large non-Gaussianities through the parameter α? This parameter can be introduced into the previous estimates noticing that each derivative with respect to φ corresponds to a factor $1/\sqrt{\alpha}$. This is clear after the introduction of a rescaled field $\phi \equiv \sqrt{\alpha}\varphi$. Obviously, α should be small if we want to enhance through it some of the previous contributions. However, there is a tight constraint deriving from the correction to the power spectrum (7.84). Since the correction should be small in order to preserve almost scale-invariance, we require

$$\frac{\varepsilon_\theta}{\alpha} \ll 1\,. \tag{7.93}$$

One can show that this condition prevents an enhancement of all the terms estimated in the previous two subsections apart for (7.79b). Indeed, this term can be estimated as

$$\langle\zeta^3\rangle^{(4)}_{A_2} \sim \frac{1}{\alpha}\frac{W_{\phi\phi\phi}}{H^2}\frac{\varepsilon_\theta^2}{\alpha^2}\frac{f'^3}{f^3}\mathcal{P}_\zeta^2\frac{1}{p_1^6}\,, \tag{7.94}$$

where we have supposed that the potential W has the same dependence of (7.1). This is rather interesting. We have obtained a term that can be enhanced through the parameter α as $\alpha \to 0$ since it scales as α^{-1}. Furthermore, the main contribution to the bispectrum comes from a single term.

Chen, in his paper [82], does not provide an explicit potential that could produce large non-Gaussianities since his main concern is to discuss a mechanism to produce non-Gaussianities and not a specific model. In the context of α-attractors, we have seen (equation (5.80)) that the potential depends on the hyperbolic tangent of φ. Remember we have supposed that the

trajectory is a circle in field space and hence we need a confining potential along the radial direction φ in order to satisfy the initial assumptions. One possibility is the potential

$$W(\varphi) = 1 - \tanh^2 \frac{\varphi}{\sqrt{6\alpha}} + \tanh^4 \frac{\varphi}{\sqrt{6\alpha}}\,, \tag{7.95}$$

where we have only given the dependence on φ with the assumption that a suitable potential for θ should be chosen in order to have inflation[10]. The previous example is a double well potential with minima at $\varphi_\pm \simeq \pm 2.2\sqrt{\alpha}$ and it is represented in figure 7.6. The third derivative of the potential evaluated at the minima is $W_{\varphi\varphi\varphi}(\varphi_\pm) \simeq -0.15\alpha^{-\frac{3}{2}}$. Notice that decreasing α makes the potential more confining and it increases the magnitude of non-Gaussianities enhancing the third derivative of the potential.

Finally, let us make a comment. In spite of the dependence on α^{-1}, the reader should not think that it is simple to obtain large non-Gaussianities. Indeed as $\alpha \to 0$, the slow-roll parameter $\varepsilon_\theta \to 0$ (due to the constraint (7.93)) and this can become a very stringent requirement on the potential of θ which should be accurately fine-tuned to be sufficiently flat in order to have $\varepsilon_\theta \to 0$.

7.6 Nearly single-field trajectory

Let us consider one of the simplest models that Lagrangian (7.1) can describe, namely the one with potential [102]

$$W(\varphi, \theta) = \tanh^2 \frac{\varphi}{\sqrt{6}}\,. \tag{7.96}$$

This potential is represented in figure 7.7a. We have already studied this model in section 5.6 for the single-field case and in section 7.2 examining initial conditions for the two-field case. We have seen that the angular velocity $\dot{\theta}/H \ll 1$ in order to have inflation. Hence we suppose that inflation is driven by the field φ which slowly rolls down the potential on a nearly straight trajectory[11]. We assume that the angular velocity $\dot{\theta}$ is small (with respect to H) and constant. We want to study whether it is possible to produce large non-Gaussianities, even if the background trajectory reduces to that of the single-field case, thanks to the non-canonical kinetic term of θ or to the introduction of the parameter α. Indeed, this is an interesting question since we know that for single-field inflation non-Gaussianities are of order of slow-roll parameters [66]. In fact our (background) trajectory is the same as in single-field case but it lives in a two dimensional field space. Inflation is driven by the field φ and θ does not contribute significantly to it since it has no potential energy and small kinetic energy.

Assuming that the trajectory is a straight line seems, at first sight, to be a restrictive assumption. However, for the type of models we are studying this is not the case. Indeed, the term

[10] Given the full dependence (5.80) of the potential term, one possibility for the potential of the inflaton θ could be $U(\theta) = (1 + \cos(\theta/\mu))$, where μ is a scale that determines the curvature of the potential. This potential is proper of natural inflation models [127, 128].

[11] We call "nearly straight" a trajectory with $\dot{\theta}/H \ll 1$ during slow-roll, which corresponds to $\theta' \ll 1$ using the notation of section 7.2.

ω_θ in the background equation (7.20) forces the velocity θ' to be small at least during slow-roll (see section 7.2). Furthermore, we have seen that in the limit $\varphi \gg 1$ the trajectories are nearly straight thanks to the suppression of the potential term in equation (7.21) due to the factor f^{-1} (f is defined in equation (7.3)). Therefore, this simple trajectory can be a good starting point to study the more general models described by the Lagrangian (7.1), as we will see in the following chapter.

The Hamiltonian (7.38) for this model coincides with (7.59). The first, second and third derivatives of the potential are respectively given by

$$W_\varphi = \sqrt{\frac{2}{3}}\frac{\sinh(\varphi/\sqrt{6})}{\cosh^3(\varphi/\sqrt{6})}\,, \tag{7.97a}$$

$$W_{\varphi\varphi} = \frac{1-2\sinh^2(\varphi/\sqrt{6})}{3\cosh^4(\varphi/\sqrt{6})}\,, \tag{7.97b}$$

$$W_{\varphi\varphi\varphi} = \frac{2}{3}\sqrt{\frac{2}{3}}\frac{\sinh(\varphi/\sqrt{6})(\sinh^2(\varphi/\sqrt{6})-2)}{\cosh^5(\varphi/\sqrt{6})}\,, \tag{7.97c}$$

and hence they behave as $\exp\bigl(-\sqrt{2/3}\,\varphi\bigr)$ in the limit $\varphi \gg 1$, i.e. the region where inflation occurs. Thanks to this, we can consider both $\delta\varphi$ and $\delta\theta$ as almost massless field ($\nu = \tilde{\nu} = 3/2$). Therefore, the mode functions (7.46) and (7.51) reduce to

$$u_k(\tau) = \frac{H}{\sqrt{2k^3}}(1+ik\tau)e^{-ik\tau}, \tag{7.98a}$$

$$v_k(\tau) = \frac{H}{\sqrt{2k^3}\sqrt{f}}(1+ik\tau)e^{-ik\tau}. \tag{7.98b}$$

Finally, since the trajectory is nearly straight, we can approximate the curvature perturbation ζ as[12]

$$\zeta \simeq -\frac{H}{\dot{\varphi}}\delta\varphi. \tag{7.99}$$

7.6.1 Power spectrum

At lowest order in the *in-in* expansion, the correlator $\langle\zeta^2\rangle$ is given by (6.13), that is

$$\begin{aligned}\langle\zeta^2(\tau)\rangle^{(0)} &= (2\pi)^3\delta^3(\mathbf{p}_1+\mathbf{p}_2)\frac{H^2}{\dot{\varphi}^2}|u_{p_1}(\tau)|^2 \\ &= (2\pi)^3\delta^3(\mathbf{p}_1+\mathbf{p}_2)\frac{H^4}{2p_1^3\dot{\varphi}^2}(1+p_1^2\tau^2).\end{aligned} \tag{7.100}$$

On super-horizon scales $-p_1\tau \ll 1$, the previous expression becomes

$$\langle\zeta^2(0)\rangle^{(0)} = (2\pi)^3\delta^3(\mathbf{p}_1+\mathbf{p}_2)\frac{H^4}{2p_1^3\dot{\varphi}^2}\,. \tag{7.101}$$

[12]The general expression of the curvature perturbation for the Lagrangian (7.1) is given by equation (8.13). Since the nearly straight trajectory is characterized by $\dot{\theta}/H \ll 1$, the adiabatic direction is approximately parallel to $\delta\varphi$.

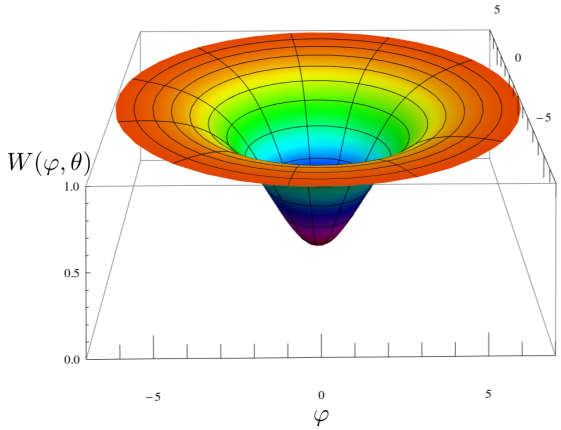

(a) The potential (7.96) $W(\varphi,\theta) = \tanh^2\left(\varphi/\sqrt{6}\right)$ represented in cylindrical coordinates.

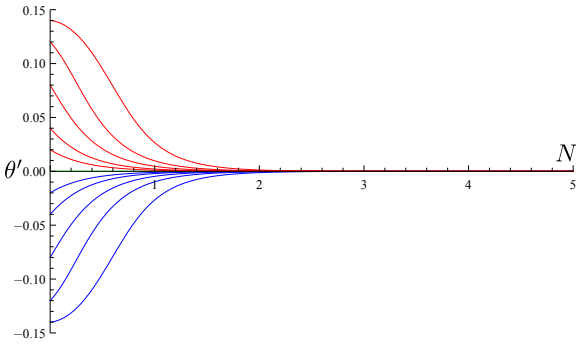

(b) The velocity θ' as a function of the number of e-folds N. In this plot, the same notation and conventions of section 7.2 are used. The initial conditions are $\varphi(0) = 6.5$ and $\varphi'(0) = 0$. Notice the suppression of the velocity θ'.

Figure 7.7

The next correction is given by expression (6.19), that is

$$\left\langle\zeta^2(\tau)\right\rangle^{(2)} = 4\frac{H^2}{\dot\varphi^2}\mathrm{Re}\left\{\int_{-\infty}^{\tau} d\tau_1 \int_{-\infty}^{\tau_1} d\tau_2 a^3(\tau_1)a^3(\tau_2)f'(\tau_1)f'(\tau_2)\dot\theta^2 \right.$$
$$\left.\left[|u_{p_1}(\tau)|^2 u_{p_1}(\tau_1)v'_{p_1}(\tau_1)u^*_{p_1}(\tau_2)v'^*_{p_1}(\tau_2) - u^2_{p_1}(\tau)u^*_{p_1}(\tau_1)v'_{p_1}(\tau_1)u^*_{p_1}(\tau_2)v'^*_{p_1}(\tau_2)\right]\right\}, \tag{7.102}$$

where we have omitted the factor $(2\pi)^3\delta^3(\mathbf{p}_1+\mathbf{p}_2)$. We compute this correction in appendix D.1 because the calculation has some subtleties and the result has little importance for what follows. At the end, the adimensional power spectrum is given by

$$\mathcal{P}_\zeta = \frac{H^4}{(2\pi\dot\varphi)^2}\left(1 + \mathcal{C}f\frac{\dot\theta^2}{H^2}\right), \tag{7.103}$$

where

$$\mathcal{C} \simeq \frac{1}{2}, \tag{7.104}$$

and where we have assumed $\dot\theta$, f' and f nearly constant for simplicity.

7.6.2 Bispectrum

Let us first estimate naively the amplitude of the different contributions of the terms in the expansion of $\langle\zeta^3\rangle$, following the strategy of the previous section. Now, the function $f(\varphi)$ is integrated over time, but we will neglect this fact and consider f and its derivatives constant during inflation (see equation (7.15)).

The lowest order non-vanishing term is given by

$$\langle \delta\varphi^3 \rangle^{(1)} \supseteq \langle \delta\varphi^3 H_A^{(3)} \rangle , \tag{7.105}$$

and its contributions to bispectrum are

$$\langle \zeta^3 \rangle^{(1)}_{A_1} \sim \frac{6ff'f'' - 6f'^3 - f^2 f'''}{f^3} \varepsilon_\theta \sqrt{\varepsilon_\varphi} \mathcal{P}_\zeta^2 \frac{1}{p^6} , \tag{7.106}$$

$$\langle \zeta^3 \rangle^{(1)}_{A_2} \sim \frac{W_{\varphi\varphi\varphi}}{H} \sqrt{\varepsilon_\varphi} \mathcal{P}_\zeta^2 \frac{1}{p^6} . \tag{7.107}$$

At second order, the correlator contains the term

$$\langle \delta\varphi^3 \rangle^{(2)} \supseteq \langle \delta\varphi^3 H_{B_1}^{(3)} H^{(2)} \rangle , \tag{7.108}$$

and its contribution can be estimated as

$$\langle \zeta^3 \rangle^{(2)}_{B_1} \sim \frac{2f'^3 - ff'f''}{f^3} \sqrt{\varepsilon_\varphi} \varepsilon_\theta \mathcal{P}_\zeta^2 \frac{1}{p^6} . \tag{7.109}$$

At third order, the correlator can be estimated as

$$\langle \delta\varphi^3 \rangle^{(3)} \supseteq \langle \delta\varphi^3 H^{(3)} H^{(2)} H^{(2)} \rangle , \tag{7.110}$$

where $H^{(3)} = H_A^{(3)}$ or $H^{(3)} = H_C^{(3)}$. The contributions of these terms are given by

$$\langle \zeta^3 \rangle^{(3)}_{A_1} \sim \frac{6ff'f'' - 6f'^3 - f^2 f'''}{f^3} \frac{f'^2}{f^2} \sqrt{\varepsilon_\varphi} \varepsilon_\theta^2 \mathcal{P}_\zeta^2 \frac{1}{p^6} , \tag{7.111a}$$

$$\langle \zeta^3 \rangle^{(3)}_{A_2} \sim \frac{W_{\varphi\varphi\varphi}}{H} \frac{f'^2}{f^2} \sqrt{\varepsilon_\varphi} \varepsilon_\theta \mathcal{P}_\zeta^2 \frac{1}{p^6} , \tag{7.111b}$$

$$\langle \zeta^3 \rangle^{(3)}_{C_1} \sim \frac{f'^3}{f^3} \sqrt{\varepsilon_\varphi} \varepsilon_\theta \mathcal{P}_\zeta^2 \frac{1}{p^6} . \tag{7.111c}$$

Finally, at fourth order,

$$\langle \delta\varphi^3 \rangle^{(4)} \supseteq \langle \delta\varphi^3 H_{B_1}^{(3)} H^{(2)} H^{(2)} H^{(2)} \rangle , \tag{7.112}$$

and we obtain the contribution

$$\langle \zeta^3 \rangle^{(4)}_{B_1} \sim \frac{2f'^2 - ff''}{f^2} \frac{f'^3}{f^3} \sqrt{\varepsilon_\varphi} \varepsilon_\theta^2 \mathcal{P}_\zeta^2 \frac{1}{p^6} . \tag{7.113}$$

Unfortunately, all these terms are suppressed by the slow-roll parameters. If $W_\theta = 0$ (e.g. the potential (7.96)), one can show that the main suppression comes from ε_θ during slow-roll due to previous considerations of section 7.2 (typically, $\varepsilon_\theta \lesssim 10^{-4}$ few e-folds after the beginning of inflation, see figure 7.7b). Since we are considering a nearly single-field trajectory, this result is not surprising. Notice that there is no enhancement thanks to the non-canonical kinetic term since $f \sim f' \sim f''$ for the function (7.3). We will discuss in section 7.6.4 the possibility of obtaining large non-Gaussianities changing the function f. For the moment, the only contribution that may be interesting is the self-interaction term $\langle \zeta^3 \rangle^{(1)}_{A_2}$, which is the least suppressed by the slow-roll parameters. Then, let us focus on it.

The explicit expression of the contribution $\langle\zeta^3\rangle^{(1)}_{A_2}$ (7.107) can be obtained from equation (6.21). The result is

$$\begin{aligned}\langle\zeta^3(\tau)\rangle^{(1)}_{A_2} &= 12\frac{H^3}{\dot\varphi^3}\,\mathrm{Im}\left\{u^*_{p_1}(\tau)u^*_{p_2}(\tau)u^*_{p_3}(\tau)\int_{-\infty}^{\tau}d\tau_1 a^4(\tau_1)\frac{W_{\varphi\varphi\varphi}}{6}u_{p_1}(\tau_1)u_{p_2}(\tau_1)u_{p_3}(\tau_1)\right\}\\ &= \frac{H^5}{4p_1^3p_2^3p_3^3\,\dot\varphi^3}\,\mathrm{Im}\left\{\int_{-\infty}^{\tau}d\tau_1\frac{1}{\tau_1^4}W_{\varphi\varphi\varphi}e^{-i\tau_1(p_1+p_2+p_3)}(1+ip_1\tau_1)(1+ip_2\tau_1)(1+ip_3\tau_1)\right\},\end{aligned} \tag{7.114}$$

where we have omitted the factor $(2\pi)^3\delta^3(\mathbf{p}_1+\mathbf{p}_2+\mathbf{p}_3)$. The previous expression in the equilateral limit ($p_1=p_2=p_3=p$) becomes

$$\begin{aligned}\langle\zeta^3(\tau)\rangle^{(1)}_{A_2} &= \frac{H^5}{4p^6\dot\varphi^3}\,\mathrm{Im}\left\{\int_0^{\infty}dx\frac{1}{x^4}W_{\varphi\varphi\varphi}e^{3ix}(1-ix)^3\right\}\\ &= \frac{(2\pi)^4}{4p^6}\frac{\dot\varphi}{H^3}\,\mathcal{P}_\zeta^2\,\mathrm{Im}\left\{\int_0^{\infty}dx\frac{1}{x^4}W_{\varphi\varphi\varphi}e^{3ix}(1-ix)^3\right\},\end{aligned} \tag{7.115}$$

where we have defined $x\equiv -p\tau$ and in the second line we have used the definition (7.103) of the adimensional power spectrum $\mathcal{P}_\zeta$. Appendix D.2 contains a detailed study of the last correlator. Here, we give only a rough estimate of its value. During inflation, $W_{\varphi\varphi\varphi}\sim 0.01$ can be considered a constant (as can be estimated by (7.97c)). The integral is of order ~ 100 and then non-Gaussianities are suppressed by $\sqrt{\varepsilon_\varphi}$. The value of f_{NL} estimated from the previous term is represented in figure 7.8a. Due to the attractor behaviour of the system, the aforementioned plot is quite representative of all possible trajectories in field space.

Hence, in this model it is impossible to obtain large non-Gaussianities. On the other hand, this model is too bare and we would not have expected any surprise. In the following sections, we will refine the model producing more interesting results.

7.6.3 The α parameter

Reintroducing the parameter α into the previously estimated contributions, one can show that some terms are enhanced if α is sufficiently small. Remember that in order to introduce the α parameter one should substitute $\varphi/M_{Pl}\to\varphi/(\sqrt{\alpha}M_{Pl})$ into the non-canonical kinetic term of θ and into the potential W of Lagrangian (7.1). Again, the parameter α enters in the correction to the power spectrum (7.103) leading to the constraint (7.93) (this fact is not evident from equation (7.103), one should refer to its full expression in appendix D.1). As $\alpha\to 0$, this implies a very tight constraint on the initial velocity $\dot\theta$. This constraint can be satisfied reducing the initial angular velocity $\dot\theta$, but practically we reduce to single-field case and we would not expect large non-Gaussianities.

With the introduction of α, the function f (7.3) becomes

$$f(\varphi)\equiv 6\sinh^2\frac{\varphi}{\sqrt{6\alpha}}\,, \tag{7.116}$$

and this affects the background dynamics through the term $\omega_\theta = -\frac{f'}{2}\theta'^2$ into the background equation (7.20). Defining $\phi = \sqrt{\alpha}\varphi$, the term ω_θ scales as $\alpha^{-1/2}$. Remember that this term should be small in order to have inflation, hence as $\alpha \to 0$ the inflationary region shrinks and the initial velocity $\theta'(0) \to 0$ (see section 7.2 and figure 7.3). At the end, reducing α makes the trajectory a straight line in field space. Notice that this behaviour is insensitive of the the form of the potential, it depends only on the non-trivial field space metric.

Let us consider the general potential

$$W(\varphi) = \tanh^{2l}\frac{\varphi}{\sqrt{6\alpha}}\,. \tag{7.117}$$

Let us see that in order to produce large non-Gaussianities, α should be small. In the limit $\alpha \ll 1$ and during slow-roll, one can show from equation (7.26a) that the velocity φ' scales roughly as

$$\varphi' \propto \sqrt{\alpha}\,. \tag{7.118}$$

Thanks to the previous scaling property (7.118) and to (7.93), it is simple to show that, for the potential (7.117), the only terms that can be enhanced through α are the self-interaction term $\langle\zeta^3\rangle^{(1)}_{A_2}$ (7.115) and the third-order correction $\langle\zeta^3\rangle^{(3)}_{A_2}$ (7.111b). Both scale roughly as $1/\alpha$ and hence they can be enhanced as $\alpha \to 0$. However, this estimate in not accurate and a more detailed study of the background dynamics is necessary. The term $\langle\zeta^3\rangle^{(3)}_{A_2}$ is suppressed by the slow-roll parameter ε_θ in addition to $\sqrt{\varepsilon_\varphi}$ and hence we focus on the other term for the moment.

Using the definition (3.12), we get

$$f_{NL}^{(1)} \equiv \frac{5}{18}\frac{\dot\varphi}{H^3}\,\mathrm{Im}\left\{\int_0^\infty dx \frac{1}{x^4} W_{\varphi\varphi\varphi} e^{3ix}(1-ix)^3\right\}, \tag{7.119}$$

where

$$W_{\varphi\varphi\varphi} = \sqrt{\frac{2^3}{3^3\alpha^3}}\, l\,\tanh^{2l}\left(\frac{\varphi}{\sqrt{6\alpha}}\right)\cosh^{-3}\left(\frac{2\varphi}{\sqrt{6\alpha}}\right)\left[3+8l^2-12l\cosh\left(\frac{2\varphi}{\sqrt{6\alpha}}\right)+\cosh\left(\frac{4\varphi}{\sqrt{6\alpha}}\right)\right]. \tag{7.120}$$

Note the suppression factor $\cosh^{-3}$ which is partially compensated by the terms in square brackets. The magnitude of $f_{NL}^{(1)}$ depends on l linearly and one can show that φ' does not depend on l in the limit $l \gg 1$. Hence, it will be simple to account for its contribution. Therefore, we provide only plots for $l = 1$. The parameter $f_{NL}^{(1)}$ is represented in figure 7.8 for different values of α. At a fixed value of α and during slow-roll, φ' is nearly the same for all initial positions due to the attractor behaviour (see figure 5.7a) and hence we represent the value of $f_{NL}^{(1)}$ as a function of the scale only for one trajectory. Notice that f_{NL} should scale as $1/\alpha$. However, passing from α to $\alpha/10$ increases the magnitude of $f_{NL}^{(1)}$ only by a factor of ~ 3. The third derivative factor $W_{\varphi\varphi\varphi}$ is responsible for this suppression.

Some considerations are in order. First, the second field θ does not participate actively to inflation. Notice that we could have obtained large non-Gaussianities through α even in a pure single-field case. Indeed, the self-interaction term has the same form as (7.114) since the second field cannot modify the self-interaction at first order. However (at least in a real single-field

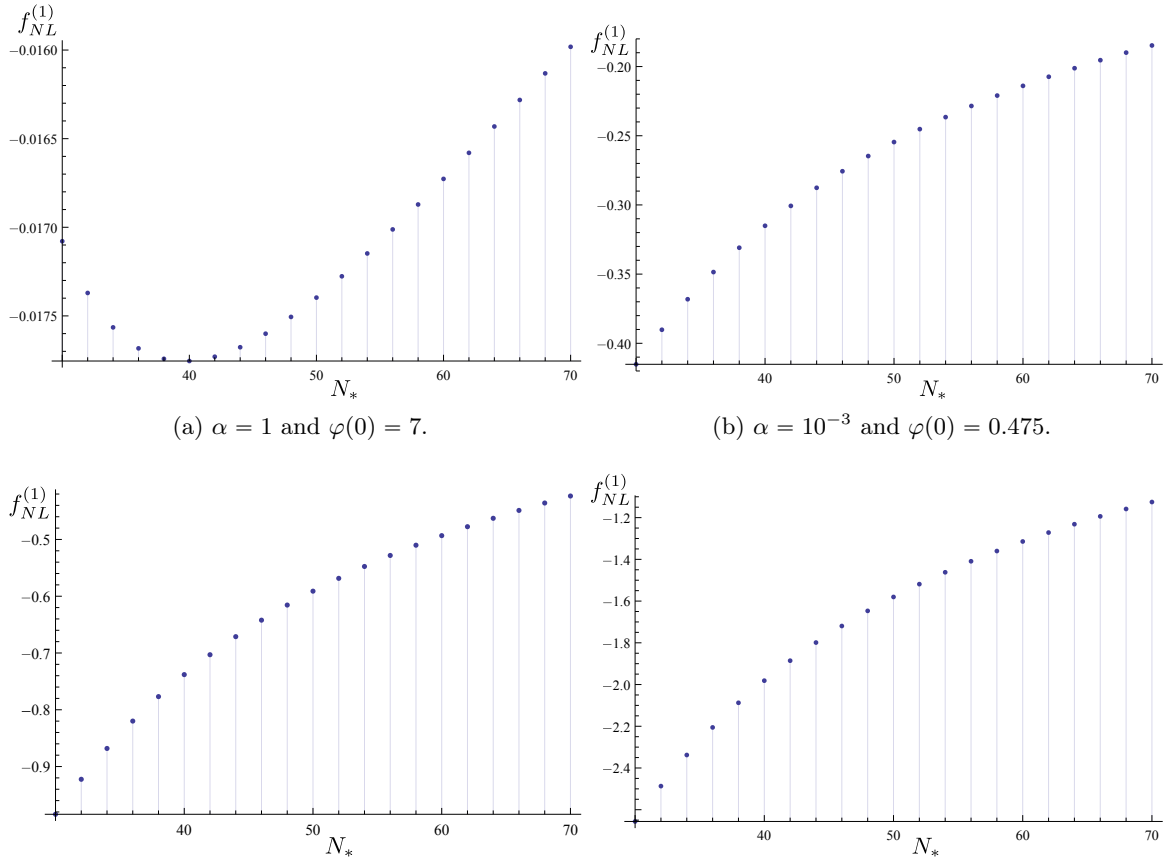

(a) $\alpha = 1$ and $\varphi(0) = 7$.

(b) $\alpha = 10^{-3}$ and $\varphi(0) = 0.475$.

(c) $\alpha = 10^{-4}$ and $\varphi(0) = 0.185$.

(d) $\alpha = 10^{-5}$ and $\varphi(0) = 0.066$.

Figure 7.8: Estimations of $f_{NL}^{(1)}$ (7.119) for the potential $W(\varphi) = \tanh^2\left(\varphi/\sqrt{6\alpha}\right)$ for different values of α. In all simulations, $\varphi'(0) = 0$. N_* is the number of e-folds until the end of inflation at which the considered scale crosses the horizon. In particular, notice the modulation due to $W_{\varphi\varphi\varphi}$ comparing these plots with figure D.1a.

case) this enhancement is spurious since we have not considered the perturbations of the metric. Including these perturbations, one can show that the self-interaction term is perfectly balanced by a term dependent on the metric perturbations [40, 66]. This result is somewhat comforting since otherwise one could produce large non-Gaussianities simply rescaling the coupling constant of the self-interaction even in the single-field case. This suggests that also in the two-field case considered the full computation should include the metric perturbations.

Therefore, this calculation can be thought as an instructive example. Indeed, we have seen that the expected enhancement $1/\alpha$ does not coincide with the effective enhancement due to the shift of the inflationary region caused by the variation of α. Due to this shift, the third derivative of the potential becomes a suppression factor and the effective enhancement is less than $1/\sqrt{\alpha}$.

Now, let us focus on the third-order term (7.111b). This term constitutes a correction of the self-interaction term due to the presence of the second field (see diagram (b) of figure 6.2). Notice that the coupling constant of this interaction between φ and θ is $f'/f\sqrt{\varepsilon_\theta}$. The term (7.111b)

is explicitly given by

$$\begin{aligned}\langle\zeta^3\rangle^{(3)}_{A_2} =& -(2\pi)^3\delta^3(\mathbf{p}_1+\mathbf{p}_2+\mathbf{p}_3)\frac{H^3}{\dot\varphi^3}2u_{p_1}(0)u_{p_2}(0)u_{p_3}(0)\\ &\mathrm{Im}\bigg\{\int_{-\infty}^0 d\tau_1\int_{-\infty}^0 d\tau_2\int_{-\infty}^{\tau_2}d\tau_3\dot\theta^2\prod_{i=1}^3\big(a^3(\tau_i)f'(\tau_i)\big)\sum_{j=1}^3\bigg(a(\tau_j)\frac{W_{\varphi\varphi\varphi}(\tau_j)}{f'(\tau_j)}\mathcal{A}_j\bigg)-\\ &\int_{-\infty}^0 d\tau_1\int_{-\infty}^{\tau_1} d\tau_2\int_{-\infty}^{\tau_2}d\tau_3\dot\theta^2\prod_{i=1}^3\big(a^3(\tau_i)f'(\tau_i)\big)\sum_{j=1}^3\bigg(a(\tau_j)\frac{W_{\varphi\varphi\varphi}(\tau_j)}{f'(\tau_j)}\mathcal{B}_j\bigg)+5\,\mathrm{perm}\bigg\},\end{aligned} \tag{7.121}$$

where

$$\mathcal{A}_1 = 2u_{p_1}(\tau_1)u_{p_2}(\tau_1)u_{p_3}(\tau_1)u^*_{p_3}(\tau_2)v'_{p_3}(\tau_2)u^*_{p_3}(\tau_3)v'^*_{p_3}(\tau_3), \tag{7.122a}$$

$$\mathcal{A}_2 = u_{p_3}(\tau_1)v'_{p_3}(\tau_1)u^*_{p_1}(\tau_2)u^*_{p_2}(\tau_2)u^*_{p_3}(\tau_3)v'^*_{p_3}(\tau_3)\big(u_{p_3}(\tau_2)+\text{c.c.}\big), \tag{7.122b}$$

$$\mathcal{A}_3 = u_{p_3}(\tau_1)v'_{p_3}(\tau_1)v'^*_{p_3}(\tau_2)u^*_{p_1}(\tau_3)u^*_{p_2}(\tau_3)u^*_{p_3}(\tau_3)\big(u_{p_3}(\tau_2)+\text{c.c.}\big), \tag{7.122c}$$

$$\mathcal{B}_1 = 2u^*_{p_1}(\tau_1)u^*_{p_2}(\tau_1)u_{p_3}(\tau_1)u^*_{p_3}(\tau_2)v'_{p_3}(\tau_2)u^*_{p_3}(\tau_3)v'_{p_3}(\tau_3), \tag{7.122d}$$

$$\mathcal{B}_2 = v'_{p_3}(\tau_1)u^*_{p_1}(\tau_2)u^*_{p_2}(\tau_2)u^*_{p_3}(\tau_3)v'^*_{p_3}(\tau_3)\big(u^*_{p_3}(\tau_1)u_{p_3}(\tau_2)+\text{c.c.}\big), \tag{7.122e}$$

$$\mathcal{B}_3 = v'_{p_3}(\tau_1)v'^*_{p_3}(\tau_2)u^*_{p_1}(\tau_3)u^*_{p_2}(\tau_3)u^*_{p_3}(\tau_3)\big(u^*_{p_3}(\tau_1)u_{p_3}(\tau_2)+\text{c.c.}\big). \tag{7.122f}$$

In the equilateral limit, the previous expression becomes

$$\langle\zeta^3\rangle^{(3)}_{A_2} = \frac{3}{2^3}(2\pi)^3\delta^3(\mathbf{p}_1+\mathbf{p}_2+\mathbf{p}_3)\frac{H^3}{\dot\varphi^3}\frac{H^2}{p^6}\mathcal{I}, \tag{7.123}$$

where we have defined $x_i \equiv -p\tau_i$ and

$$\begin{aligned}\mathcal{I} =& \mathrm{Im}\bigg\{\int_0^{+\infty}dx_1\int_0^{+\infty}dx_2\int_{x_2}^{+\infty}dx_3\frac{\dot\theta^2}{H^2}\prod_{i=1}^3\bigg(\frac{f'(x_i)}{x_i^3}\bigg)\sum_{j=1}^3\bigg(\frac{1}{x_j}\frac{W_{\varphi\varphi\varphi}(x_j)}{Hf'(x_j)}\mathcal{A}_j\bigg)\\ &-\int_0^{+\infty}dx_1\int_{x_1}^{+\infty}dx_2\int_{x_2}^{+\infty}dx_3\frac{\dot\theta^2}{H^2}\prod_{i=1}^3\bigg(\frac{f'(x_i)}{x_i^3}\bigg)\sum_{j=1}^3\bigg(\frac{1}{x_j}\frac{W_{\varphi\varphi\varphi}(x_j)}{Hf'(x_j)}\mathcal{B}_j\bigg)\bigg\},\end{aligned} \tag{7.124a}$$

$$\tilde u(x) \equiv (1-ix)e^{ix}, \tag{7.124b}$$

$$\tilde v(x) \equiv \frac{1}{\sqrt{f(x)}}(1-ix)e^{ix}, \tag{7.124c}$$

$$\tilde{\mathcal{A}}_1 = 2\tilde u_p(x_1)\tilde u_p(x_1)\tilde u_p(x_1)\tilde u^*_p(x_2)\tilde v'_p(x_2)\tilde u^*_p(x_3)\tilde v'^*_p(x_3), \tag{7.124d}$$

$$\tilde{\mathcal{A}}_2 = \tilde u_p(x_1)\tilde v'_p(x_1)\tilde u^*_p(x_2)\tilde u^*_p(x_2)\tilde u^*_p(x_3)\tilde v'^*_p(x_3)\big(\tilde u_p(x_2)+\text{c.c.}\big), \tag{7.124e}$$

$$\tilde{\mathcal{A}}_3 = \tilde u_p(x_1)\tilde v'_p(x_1)\tilde v'^*_p(x_2)\tilde u^*_p(x_3)\tilde u^*_p(x_3)\tilde u^*_p(x_3)\big(\tilde u_p(x_2)+\text{c.c.}\big), \tag{7.124f}$$

$$\tilde{\mathcal{B}}_1 = 2\tilde u^*_p(x_1)\tilde u^*_p(x_1)\tilde u_p(x_1)\tilde u^*_p(x_2)\tilde v'_p(x_2)\tilde u^*_p(x_3)\tilde v'_p(x_3), \tag{7.124g}$$

$$\tilde{\mathcal{B}}_2 = \tilde v'_p(x_1)\tilde u^*_p(x_2)\tilde u^*_p(x_2)\tilde u^*_p(x_3)\tilde v'^*_p(x_3)\big(\tilde u^*_p(x_1)\tilde u_p(x_2)+\text{c.c.}\big), \tag{7.124h}$$

$$\tilde{\mathcal{B}}_3 = \tilde v'_p(x_1)\tilde v'^*_p(x_2)\tilde u^*_p(x_3)\tilde u^*_p(x_3)\tilde u^*_p(x_3)\big(\tilde u^*_p(x_1)\tilde u_p(x_2)+\text{c.c.}\big). \tag{7.124i}$$

Finally, the contribution of (7.111b) to f_{NL} (7.70) is given by

$$f^{(3)}_{NL} = \frac{5}{48}\frac{\dot\varphi}{H^2}\mathcal{I}. \tag{7.125}$$

If the potential W is given by (7.117), we would expect an enhancement of order α^{-1} due to (7.120). However, as we have seen in the previous calculation of $\langle\zeta^3(\tau)\rangle^{(1)}$, the effective enhancement is lower than this. Nonetheless, this term constitutes an interaction between the fields and it can be enhanced through the parameter α. In this case, the non-Gaussianities can become large because the field space is not one dimensional and the existence of the second field is necessary. In addition to this, notice that the enhancement is possible only if the function f has the dependence (7.116) on α. If f did not depend on α, we would not be able to enhance the term $\langle\zeta^3\rangle^{(3)}_{A_2}$.

7.6.4 Generalizations

Let us study under which conditions f could produce large non-Gaussianities even if the background trajectory is nearly indistinguishable from that of single-field case. Notice that many of the previously estimated contributions contain the ratio f'/f, and then a possibility to enhance the previous terms is to increase this ratio. Since we suppose that φ is the inflaton, we should verify that at least the slow-roll parameters in the definition of ν (7.45) are small. This fact leads to the conditions

$$\varepsilon_\theta \ll 1\,, \tag{7.126a}$$

$$\frac{f'^2}{f^2}\varepsilon_\theta \ll 1\,, \tag{7.126b}$$

$$\frac{f''}{f}\varepsilon_\theta \ll 1\,. \tag{7.126c}$$

The first of these conditions implies that the trajectory should be nearly a straight line since θ' should be small. Notice that if $\theta' \equiv 0$ many of the estimated contributions vanish since some of the couplings of the interactions in the Hamiltonian (7.38) depend on θ'.

Consider the terms (7.109) and (7.111c). Their contributions have the same magnitude and they can be approximated as

$$\langle\zeta^3\rangle^{(3)} \sim \frac{f'^3}{f^3}\sqrt{\varepsilon_\varphi}\varepsilon_\theta\mathcal{P}_\zeta^2\frac{1}{p^6}\,. \tag{7.127}$$

Notice that this term can be enhanced if the ratio f'/f is sufficiently large. The slow-roll parameters are usually of order $10^{-3} \div 10^{-1}$. We suppose that ε_φ and $\xi_\theta = f'^2 f^{-2}\varepsilon_\theta$ are of this order of magnitude. Hence, the slow-roll parameters suppress this amplitude by a factor $10^{-\frac{9}{2}} \div 10^{-\frac{3}{2}}$. To compensate this, the ratio f'/f should satisfy

$$\frac{f'}{f} \sim 10^{\frac{3}{2}} \div 10^{\frac{9}{2}}\,. \tag{7.128}$$

This is a rather tight condition since it forces the function f to have a nearly exponential behaviour. Indeed, assume that f'/f is a constant, then the previous condition becomes

$$f \propto e^{A\varphi}, \tag{7.129}$$

where $A \sim 30 \div 30 \cdot 10^3$. Remember that one has to integrate over the whole background trajectory. If we want to produce large non-Gaussianities, we need to require that previous

Couplings	Z_2B_1	Z_2B_2	Z_1B_1	$Z_2Z_2A_1$
f_{NL}	$\frac{W_{\varphi\theta}}{H^2}\frac{f'^2}{f^{5/2}}\sqrt{\varepsilon_\theta}\sqrt{\varepsilon_\varphi}$	$\frac{W_{\varphi\theta}}{H^2}\frac{W_{\varphi\varphi\theta}}{H}\frac{1}{f}\sqrt{\varepsilon_\varphi}$	$\frac{W_{\varphi\varphi\theta}}{H}\frac{f'}{f^{3/2}}\sqrt{\varepsilon_\theta}\sqrt{\varepsilon_\varphi}$	$\frac{W^2_{\varphi\theta}}{H^4}\frac{f'^3}{f^3}\frac{1}{f}\varepsilon_\theta\sqrt{\varepsilon_\varphi}$
Couplings	$Z_2Z_2A_2$	$Z_2Z_1A_1$	$Z_2Z_1A_2$	$Z_2Z_2C_1$
f_{NL}	$\frac{W^2_{\varphi\theta}}{H^4}\frac{W_{\varphi\varphi\varphi}}{H}\frac{1}{f}\sqrt{\varepsilon_\varphi}$	$\frac{W_{\varphi\theta}}{H^2}\frac{f'^4}{f^4}\frac{1}{\sqrt{f}}\varepsilon_\theta^{3/2}\sqrt{\varepsilon_\varphi}$	$\frac{W_{\varphi\theta}}{H^2}\frac{W_{\varphi\varphi\varphi}}{H}\frac{f'}{f^{3/2}}\sqrt{\varepsilon_\theta}\sqrt{\varepsilon_\varphi}$	$\frac{W^2_{\varphi\theta}}{H^4}\frac{f'}{f}\frac{1}{f}\sqrt{\varepsilon_\varphi}$
Couplings	$Z_2Z_2C_2$	$Z_2Z_1C_1$	$Z_2Z_1C_2$	$Z_1Z_1Z_1B_1$
f_{NL}	$\frac{W^2_{\varphi\theta}}{H^4}\frac{W_{\varphi\theta\theta}}{H}\frac{1}{f^2}\sqrt{\varepsilon_\varphi}$	$\frac{W_{\varphi\theta}}{H^2}\frac{f'^2}{f^2}\frac{1}{\sqrt{f}}\sqrt{\varepsilon_\theta}\sqrt{\varepsilon_\varphi}$	$\frac{W_{\varphi\theta}}{H^2}\frac{W_{\varphi\theta\theta}}{H}\frac{f'}{f^{5/2}}\sqrt{\varepsilon_\theta}\sqrt{\varepsilon_\varphi}$	$\frac{f'^5}{f^5}\varepsilon_\theta^2\sqrt{\varepsilon_\varphi}$
Couplings	$Z_1Z_1Z_2D_1$	$Z_1Z_2Z_2B_1$	$Z_2Z_2Z_2B_2$	$Z_2Z_2Z_2D_1$
f_{NL}	$\frac{W_{\theta\theta\theta}}{H}\frac{W_{\varphi\theta}}{H^2}\frac{f'^2}{f^4}\varepsilon_\theta\sqrt{\varepsilon_\varphi}$	$\frac{W^2_{\varphi\theta}}{H^4}\frac{f'^3}{f^3}\frac{1}{f}\varepsilon_\theta\sqrt{\varepsilon_\varphi}$	$\frac{W_{\varphi\varphi\theta}}{H}\frac{W^3_{\varphi\theta}}{H^6}\frac{1}{f^2}\sqrt{\varepsilon_\varphi}$	$\frac{W_{\theta\theta\theta}}{H}\frac{W^3_{\varphi\theta}}{H^6}\frac{1}{f^3}\sqrt{\varepsilon_\varphi}$

Table 7.1: Contribution to f_{NL} for different terms of the expansion of bispectrum using the *in-in* formalism. The coupling Z, A, B, C, D are defined in equation (7.38). The first entry Z_2B_1 should be interpreted as the contribution of the correlator $\langle\zeta^3 H^{(2)}_{Z_2} H^{(3)}_{B_1}\rangle$ to the nonlinearity parameter f_{NL}. We have reported all the terms up to third order and some terms at fourth order.

condition is satisfied for a sufficiently long period during inflation. In addition to this, the ratio f'/f enters into the background equation of motion (7.21) and it can break the slow-roll regime accelerating the field θ.

Notice that the third derivative f''' is not constrained by (7.126). Hence, a function with $f'''/f \gg 1$ can enhance some of the previous terms, e.g. the contribution (7.106) or (7.111a). This is a viable way to obtain large non-Gaussianities for a nearly straight trajectory. Obviously, the function f should be chosen properly (but the field space metric is usually fixed *a priori* for a given model and we can modify only the potential term, as in our example). To sum up, if we want to build a model with Lagrangian (7.2) that can produce large non-Gaussianities with a nearly straight trajectory, we should consider a function f with a high third derivative.

7.6.5 Massive isocurvaton

Let us suppose that the potential W depends on both φ and θ. The Hamiltonian has the general expression (7.38). The new contributions to f_{NL} due to the dependence on θ are estimated in table 7.1.

Notice that there are terms that do not contain the slow-roll parameter ε_θ. All these terms contain the coupling Z_2 and the corresponding Hamiltonian terms describe an interaction between $\delta\varphi$ and $\delta\theta$ mediated by the potential W. In addition to this, notice that many of the terms are multiplied by an inverse power of f. For the function (7.3) these are suppression factors, but for another metric these could be enhancement factor even if the ratio f'/f is of order unity. For example one can consider an exponential function like $\exp(-\varphi)$. Moreover, all

the terms with coupling A_1 contain the third derivative f''' and hence they can be enhanced with an appropriate function f, as it was discussed in the previous subsection.

If we introduce the parameter α, some additional terms which can be enhanced appear. For example, the terms $Z_2 Z_2 A_2$ and $Z_2 Z_2 Z_2 B_2$ scale as α^{-2} and hence large enhancement are possible. Obviously, the introduction of a potential for θ can alter significantly the dynamics of the system and the trajectory could not be any more nearly straight. These terms can nonetheless increase f_{NL} after a rotation of the basis $(\delta\varphi, \delta\theta)$ into that of the curvature and isocurvature perturbations, see section 4.3.

Finally, let us sum up our analysis. If we suppose that the dependence of W on (φ, θ) is given by (5.80), then terms that contains W_φ are suppressed by $\exp\bigl(-\sqrt{2/3}\varphi\bigr)$. Therefore, it is very difficult to produce large non-Gaussianities if the trajectory is nearly straight and we consider a model like (7.96). However, thanks to the parameter α one can produce observable non-Gaussianities even in a model where there is a nearly single-field background trajectory thanks to the term $\langle\zeta^3\rangle^{(3)}_{A_2}$ (7.111b) (or other terms if the potential W depends on both φ and θ). It is worth noticing that this enhancement relies on two facts. First, the parameter α enters into the potential W and into the non-canonical kinetic term f of θ. Secondly, the parameter α is not simply a rescale of the field φ. This type of enhancement is one of the main results we have obtained in this chapter. If we let f be a generic function and consider an appropriate potential W, we can obtain the production of large non-Gaussianities even if the trajectory is practically of single-field type through interactions between the fields (in particular thanks to the third derivative f''' that is not directly constrained by the slow-roll conditions).

Chapter 8

Two two-field models

> "The effort to understand the Universe is one of the very few things that lifts human life a little above the level of farce, and gives it some of the grace of tragedy."
>
> Steven Weinberg

In this chapter we will study more complex possibilities than that considered in the previous one. In particular, we will start again from Lagrangian (5.77), but we will introduce an explicit potential for the field θ. We will study two models.

In section 8.1, we will analyse the background dynamics of these models. In the following two sections 8.2 and 8.3, we will focus on the predictions of these models, in particular the power spectrum and the bispectrum. We will set up the *in-in* formalism, but we will not proceed further in the computations. For the second model, we will obtain estimates of f_{NL} using the δN formalism (see section 3.4).

8.1 Model setting and background dynamics

In this chapter, we will write the equations with respect to the number of e-folds N, defined as in equation (4.10). Initial conditions are given at $N = 0$.

Before setting the models and studying the background dynamics, let us deduce an useful equation. The trajectory of the field can be parametrized as $\theta = \theta(\varphi)$. Therefore, we can write

$$\theta' = -\frac{1}{f}\frac{W_\theta}{W}, \tag{8.1a}$$

$$\frac{d\theta}{d\varphi}\varphi' = -\frac{d\theta}{d\varphi}\frac{W_\varphi}{W}, \tag{8.1b}$$

where the prime denotes the derivative with respect to the number of e-folds N and we have made use of the slow-roll equations (7.26). Therefore, we get

$$\frac{d\theta}{d\varphi} = \frac{1}{f}\frac{W_\theta}{W_\varphi}, \tag{8.2}$$

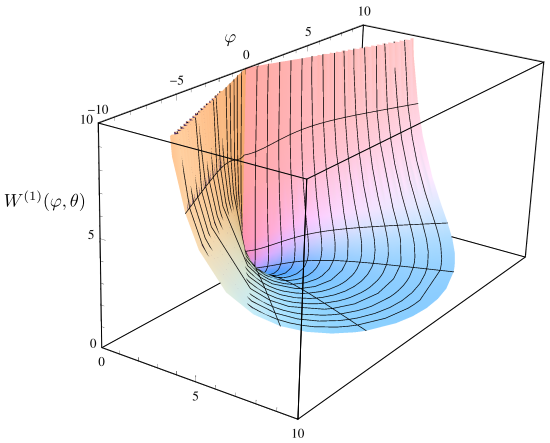

(a) Potential $W^{(1)}(\varphi,\theta) = \tanh^2 \frac{\varphi}{\sqrt{6}} + \tan^2\theta$ represented using cylindrical coordinates.

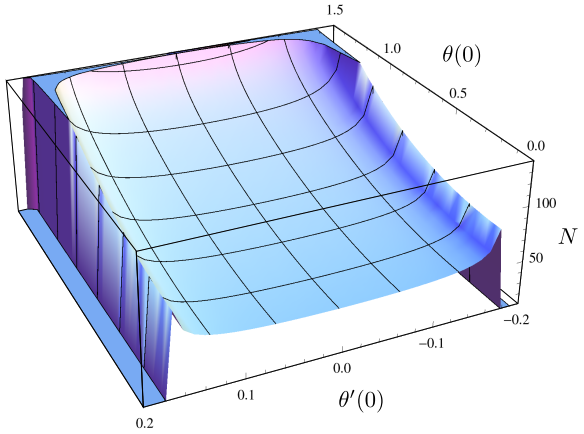

(b) Initial conditions that lead to inflation for $\varphi(0) = 6$ and $\varphi'(0) = 0$. Notice that for $|\theta'(0)| \gtrsim 0.16$ inflation does not occur. This is the critical value that can be inferred from figure 7.2b.

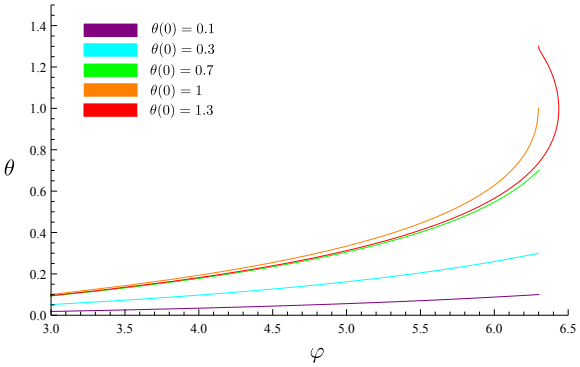

(c) Different trajectories for $\varphi(0) = 6.3$ with $\varphi'(0) = 0$ and $\theta'(0) = 0$. Notice the different regimes for $\theta \to 0$ and $\theta \to \frac{\pi}{2}$.

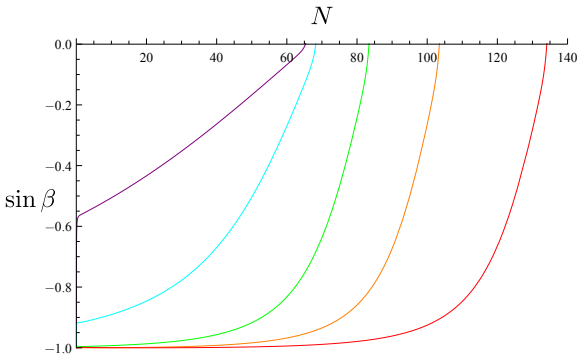

(d) $\sin\beta$ (8.17). Different trajectories for $\varphi(0) = 6.3$, $\varphi'(0) = 0$ and $\theta'(0) = 0$. The colors of the trajectories are the same as those in the left picture.

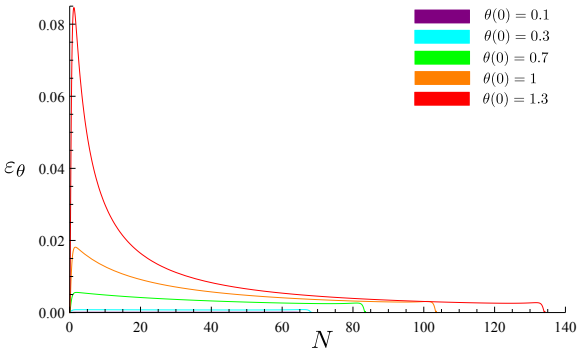

(e) ε_θ (7.43a). Notice that $\varepsilon_\theta \gg \varepsilon_\varphi$ during slow-roll, but at the end of inflation ε_θ is suppressed unlike ε_φ.

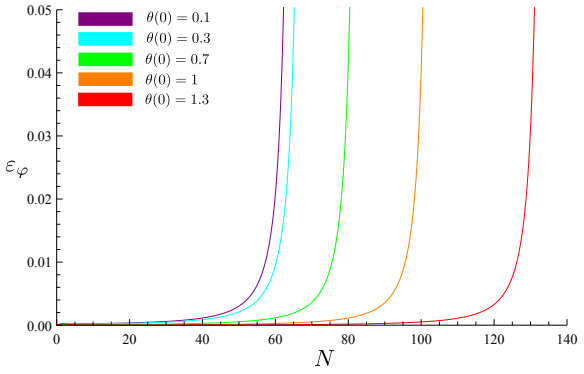

(f) ε_φ (7.43a). During slow-roll $\varepsilon_\varphi \sim 2 \cdot 10^{-4}$ for all trajectories. Notice that inflation ends for the different trajectories at different value of N.

Figure 8.1: Dynamics of the model with potential $W^{(1)}(\varphi,\theta) = \tanh^2\left(\varphi/\sqrt{6}\right) + \tan^2\theta$. The figures (c)-(f) refer to the same five trajectories.

which holds during slow-roll. In the limit $\varphi \gg 1$, we get $d\theta/d\varphi \simeq 0$ (since f (7.3) grows exponentially in this limit) and hence the trajectory is effectively nearly straight in this region (unless W_φ or W_θ have an exponential behaviour that compensates that of f).

8.1.1 First model

Let us start from the explicit dependence of the potential $W(\varphi,\theta)$ of Lagrangian (5.77). First, suppose we want a separable potential like $W^{(1)}(\varphi,\theta) = V(\varphi) + U(\theta)$. Notice that, if we need a potential that depends only on θ, we should consider $U = U(\tan\theta)$. Thus, let us assume $U(\tan\theta) = m^2\tan^2\theta$, where m^2 is a parameter that reduces to the mass of θ in the limit $\theta \to 0$ (in the following, we will refer to it as the mass of the field θ). In addition to this, we suppose that the potential for φ is $V(\varphi) = \tanh^2\left(\varphi/\sqrt{6}\right)$. Finally, the full potential is given by

$$W^{(1)}(\varphi,\theta) = \tanh^2\frac{\varphi}{\sqrt{6}} + m^2\tan^2\theta\,, \tag{8.3}$$

and it is represented in figure 8.1a for $m^2 = 1$.

The background equations (7.20) and (7.21) become respectively

$$\varphi'' - \frac{f'}{2}\theta'^2 + (3-\varepsilon)\left(\varphi' + \sqrt{\frac{2}{3}}\frac{\tanh(\varphi/\sqrt{6})}{\cosh^2(\varphi/\sqrt{6})\left(\tanh^2\varphi/\sqrt{6} + m^2\tan^2\theta\right)}\right) = 0\,, \tag{8.4a}$$

$$\theta'' + \frac{f'}{f}\theta'\varphi' + (3-\varepsilon)\left(\theta' + \frac{1}{f}\frac{2m^2\tan\theta}{\cos^2\theta\left(\tanh^2\varphi/\sqrt{6} + m^2\tan^2\theta\right)}\right) = 0\,. \tag{8.4b}$$

We should study two regimes. If $\theta \sim 0$ the trajectories are nearly straight because $\tan\theta$ is small. Then, the dynamics of the system is similar to that studied in section 7.2. The second regime is $\theta \to \pm\frac{\pi}{2}$, but we will consider only $\theta \to \frac{\pi}{2}$ since the potential is symmetric. In this regime, the potential affects the background dynamics and the trajectories are curved. In figure 8.1c some trajectories are represented (others are represented in figures E.1c and E.1d in appendix E). Notice the different regimes described earlier.

In the limits $\theta \to \frac{\pi}{2}$ and $\varphi \gg 1$, the background equation (8.4b) reads

$$\theta'' + \theta'\varphi' + (3-\varepsilon)\left(\theta' + \frac{2}{f}\frac{1}{\tan\theta}\right) \simeq 0\,. \tag{8.5}$$

During slow-roll, the previous equation becomes

$$\theta' \simeq -\frac{2}{f}\frac{1}{\tan\theta}\,, \tag{8.6}$$

and then the velocity θ' is suppressed due to the presence of f^{-1}, but it is enhanced thanks to the tangent factor. If the initial position $\theta(0) \to \frac{\pi}{2}$, the field θ rolls down the potential slowly due to the suppression factor f^{-1}. When the suppression is no more efficient, i.e. when $\varphi \sim \sqrt{6}$, the field θ reaches the minimum of its potential rapidly since the flattening of the derivative term $W_\theta^{(1)}/W^{(1)}$ due to f vanishes.

During the slow-roll regime, equation (8.2) becomes

$$\frac{d\theta}{d\varphi} = \frac{1}{f}\frac{W_\theta}{W_\varphi} = \frac{m^2}{\sqrt{6}}\left(\coth\frac{\varphi}{\sqrt{6}}\right)^3\frac{\sin\theta}{\cos^3\theta}\,. \tag{8.7}$$

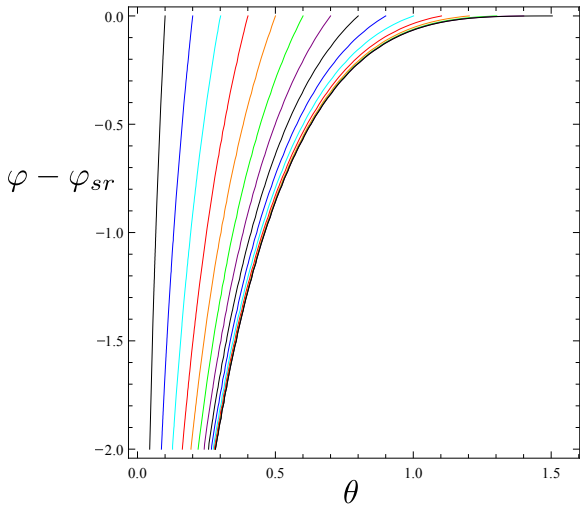

(a) $m^2 = 1$. Notice the different behaviour of the trajectories for $\theta \lesssim 0.5$ and $\theta \gtrsim 0.5$.

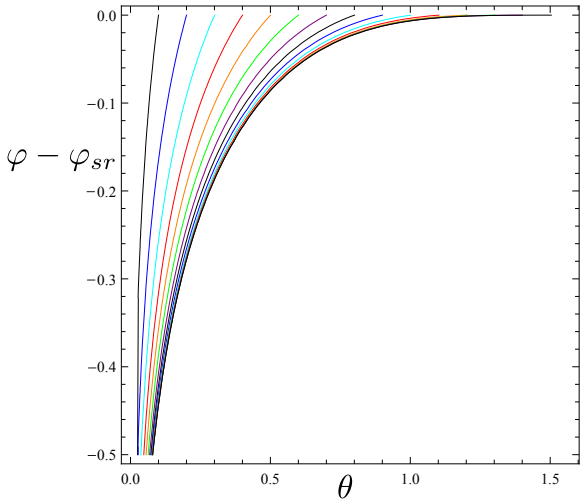

(b) $m^2 = 10$. Increasing the value of m focuses the trajectories.

Figure 8.2: Representation of the trajectories during slow-roll described by equation (8.8). The subscript "sr" denotes that the fields are evaluated during the slow-roll period. Notice the different scales adopted for the axis $\varphi - \varphi_{sr}$ in these plots.

In the limit $\varphi \gg 1$, $\coth\left(\varphi/\sqrt{6}\right) \to 1$ and we suppose it is a constant. After having integrated the previous equation, we obtain the solution

$$\frac{1}{4}\Big(\cos(2\theta) - \cos(2\theta_{sr})\Big) + \ln\frac{\sin\theta}{\sin\theta_{sr}} = \frac{m^2}{\sqrt{6}}\Big(\varphi - \varphi_{sr}\Big), \tag{8.8}$$

where φ_{sr} and θ_{sr} are evaluated after the beginning of inflation during the slow-roll regime. During slow-roll, the field excursion of φ sufficient to produce $50 \div 70$ e-folds of inflation is of order unity (e.g. see figure 5.6a) and that of θ is less than $\frac{\pi}{2}$ due to the form of the potential. The behaviour of the trajectories is represented in figure 8.2 for $m^2 = 1$ and $m^2 = 10$. Notice the two aforementioned regimes for $\theta \to 0$ and $\theta \to \frac{\pi}{2}$. Varying the value of m^2 is equivalent to rescale the field φ (at least during slow-roll) as can be seen from equation (8.8). Then, increasing the value of m results in the fact that θ tends to zero with a lower field excursion $\varphi - \varphi(0)$. Practically, this means that the parameter m focuses the trajectories. The reason is that, increasing m steepens the potential $U(\theta)$ and hence the field θ reaches its minimum faster.

The slow-roll parameters ε_θ and ε_φ, defined in equation (7.43a), are represented respectively in figures 8.1e and 8.1f for different trajectories. Notice that $\varepsilon_\theta \gg \varepsilon_\varphi$ if the initial position $\theta(0) \gtrsim 1$. Furthermore, note the suppression of ε_θ during the latest e-folds of inflation. This suppression is due to the presence of the factor f^{-1} into (8.7). Indeed, as φ is reaching the minimum of its potential, the function f becomes of order unity and the field θ can accelerate towards the minimum of its potential. However, this acceleration is compensated by the viscous terms into (8.4b) and the field θ practically comes to rest at the minimum. The main constraints on the viable initial conditions come again from the term $-f'\theta'^2/2$ into equation (8.4a) as can be seen in figure 8.1b (compare also with figures E.1a and E.1b in appendix E).

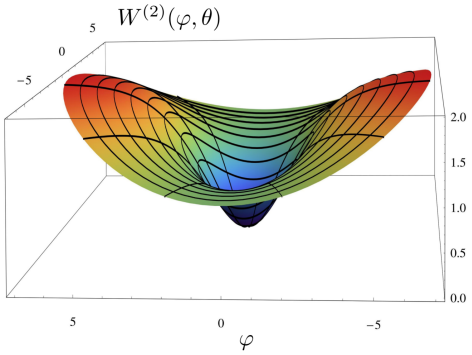

(a) Potential $W^{(2)}(\varphi,\theta) = \big(1+\sin^2\theta\big)\tanh^2\frac{\varphi}{\sqrt{6}}$ represented using cylindrical coordinates.

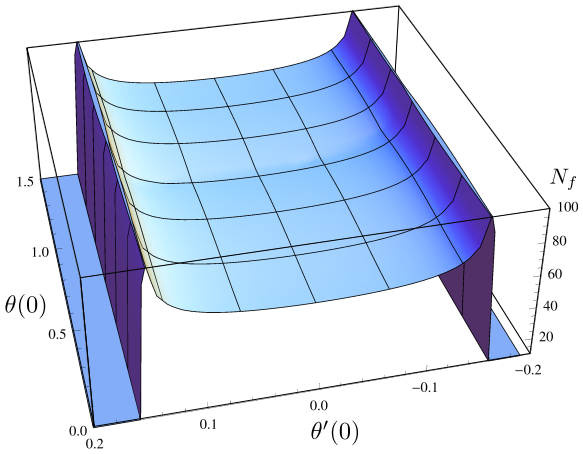

(b) Number of e-folds of inflation for $\varphi(0) = 6.3$ and $\varphi'(0) = 0$. Notice that for $|\theta'(0)| \gtrsim 0.16$ inflation does not occur.

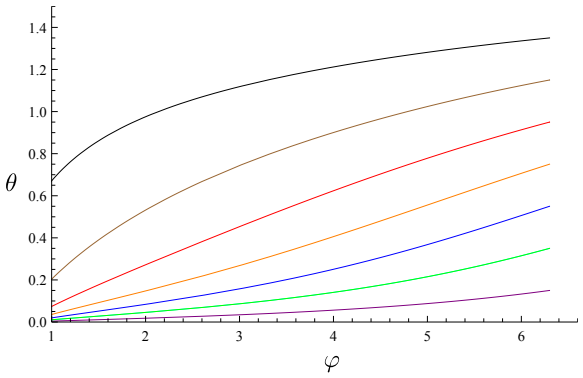

(c) Different trajectories for $\varphi(0) = 6.3$, $\varphi'(0) = 0$ and $\theta'(0) = 0$. Inflation starts immediately.

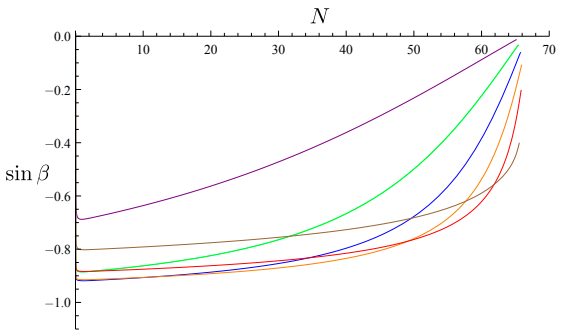

(d) $\sin\beta$ (8.17). Same trajectories as those shown in figure (d) with the same colors.

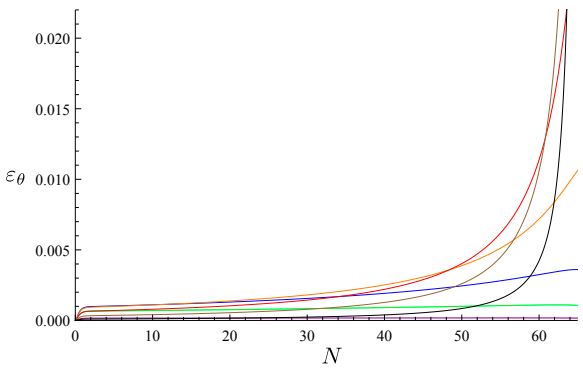

(e) ε_θ (7.43a). During slow-roll $\varepsilon_\theta \sim 2\cdot 10^{-3}$. Same trajectories as those shown in figure (d) with the same colors.

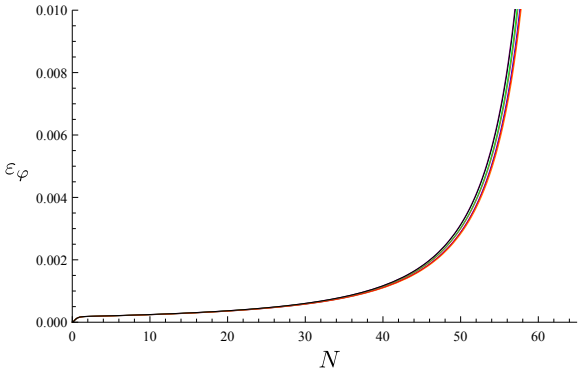

(f) ε_φ (7.43a). Same trajectories as those shown in figure (d) with the same colors. Inflation ends for the shown trajectories at $N_f \simeq 67$. During slow-roll, $\varepsilon_\varphi \sim 2\cdot 10^{-4}$ for the depicted trajectories.

Figure 8.3: Dynamics of the model $W^{(2)}(\varphi,\theta) = \big(1+\sin^2\theta\big)\tanh^2\big(\varphi/\sqrt{6}\big)$. Compare this plots with those for the model $W^{(1)}$ in figure 8.1.

8.1.2 Second model

Let us start again from the Lagrangian (5.77) and consider another potential $W(\varphi,\theta)$ (5.80) which depends on both the fields. The simple potential $\tanh^2\frac{\varphi}{\sqrt{6}}\sin^2(\theta)$ is not interesting. Indeed, when the inflaton reaches one of the valleys $\theta = k\pi$, with k integer, inflation ends. However, the inflaton usually reaches those regions in a few e-folds leading to an early end of inflation. For this reason, we will consider a different potential with a well defined minimum. One possibility is the potential

$$W^{(2)}(\varphi,\theta) = \tanh^2\frac{\varphi}{\sqrt{6}} + M^2\tanh^2\frac{\varphi}{\sqrt{6}}\sin^2\theta\,, \tag{8.9}$$

where M^2 is a parameter introduced for studying the relative contributions of the two terms. The potential is represented in figure 8.3a for $M^2 = 1$.

The model-dependent terms of the background equations (7.20) and (7.21) are given by

$$\frac{W^{(2)}_\varphi}{W^{(2)}} = \sqrt{\frac{2}{3}}\frac{1}{\cosh(\varphi/\sqrt{6})\sinh(\varphi/\sqrt{6})}\,, \tag{8.10a}$$

$$\frac{1}{f}\frac{W^{(2)}_\theta}{W^{(2)}} = \frac{M^2\sin(2\theta)}{6\sinh^2(\varphi/\sqrt{6})(1+M^2\sin^2\theta)}\,. \tag{8.10b}$$

In the limit $\varphi \gg 1$, we can rely on the analysis made in section 7.2 since the sine function is limited and the term $W^{(2)}_\theta/(W^{(2)}f)$ is suppressed by the factor f^{-1}. This suppression is almost insensitive of the position of the field θ. Hence, for this model we do not expect two well defined regimes as in the previous one. Obviously, if θ starts near a minimum of $\sin^2(\theta)$, i.e. $\theta \simeq k\pi$ with k integer, then the background trajectory is nearly straight. In this case, we can rely on the analysis and results of section 7.6. The behaviour of the trajectories is represented in figure 8.3c. One can compare those represented trajectories with those in figures E.2c and E.2e in appendix E. Note that a non-null initial velocity $\theta'(0)$ has little impact on the trajectory followed by the fields.

During the slow-roll regime, equation (8.2) becomes

$$\frac{d\theta}{d\varphi} = \frac{M^2}{2\sqrt{6}}\frac{\sin 2\theta}{1+M^2\sin^2\theta}\coth\frac{\varphi}{\sqrt{6}}\,, \tag{8.11}$$

which can be integrated (in the limit $\varphi \gg 1$, $\coth\frac{\varphi}{\sqrt{6}} \to 1$), and the final result is

$$\left[\ln\left(\frac{\sin\theta}{\sin\theta_{sr}}\right) - (M^2+1)\ln\left(\frac{\cos\theta}{\cos\theta_{sr}}\right)\right] = \frac{M^2}{\sqrt{6}}\Big(\varphi-\varphi_{sr}\Big), \tag{8.12}$$

where φ_{sr} and θ_{sr} are evaluated during the slow-roll regime. During slow-roll, the field excursion of φ sufficient to produce $50 \div 70$ e-folds of inflation is of order unity (e.g. see figure 5.6a) and that of θ is less than $\pi/2$ due to the form of the potential. In figure 8.4 some trajectories are represented for $M^2 = 1$ and $M^2 = 10$. Notice that the trajectories are nearly straight in the case $M^2 = 1$, but they are not in the case $M^2 = 10$. The reason is that in the latter there exist an attractor solution at $\theta = k\pi$, with k integer. Considerations about the variation of M are similar to that explained after equation (8.8).

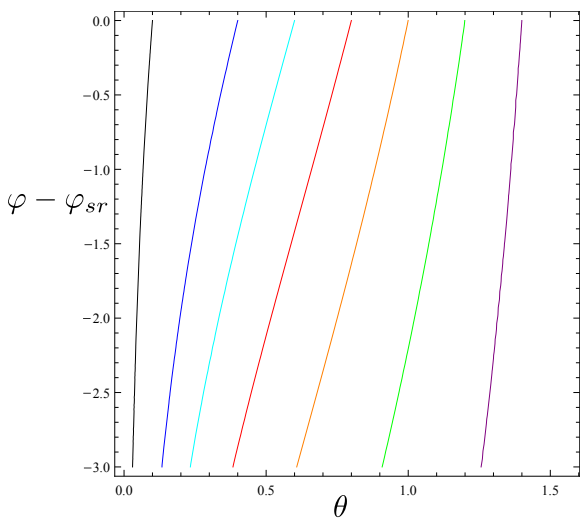

(a) $M^2 = 1$. Notice that the trajectories are nearly straight.

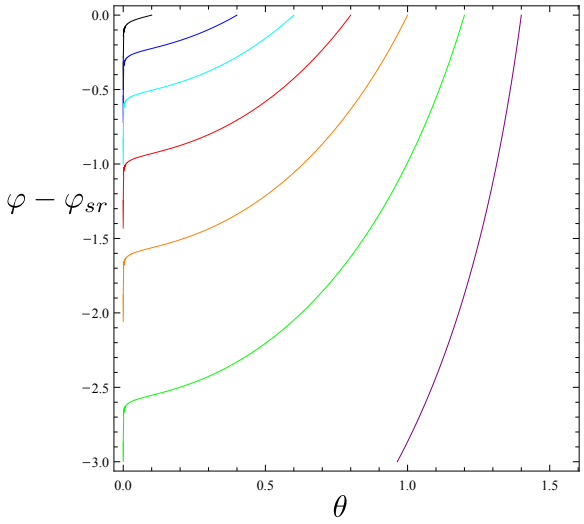

(b) $M^2 = 10$. Notice the effects of the variation of M^2 making a comparison with the plot on the left.

Figure 8.4: Representation of the trajectories during slow-roll using equation (8.12). The subscript "sr" denotes that the fields are evaluated during the slow-roll period. When $\varphi - \varphi_{sr} = 0$, the field θ is in the position θ_{sr}. Compare these plots with those of figure 8.2.

The considerations made for the previous case about ε_φ apply also for this model as can be seen in figure 8.3f. However, the slow-roll parameter ε_θ is not suppressed at the end of inflation like in the previous case (at least for $M^2 = 1$). Another difference is that for the model $W^{(2)}$ inflation lasts nearly for the same number of e-folds regardless of $\theta(0)$ as opposed to the model $W^{(1)}$ (compare figures 8.1f and 8.3f).

In figures 8.3b, E.2a and E.2b we report some further numerical examples useful for understanding the viable initial conditions that lead to inflation. The comments are similar to those of the previous model and we do not repeat them.

8.2 First model

The Hamiltonian of this model (and hence the couplings) can be read off from the expression (7.38) neglecting the terms that contain mixed derivatives of the potential. Before computing the power spectrum, we need to rotate the basis of perturbations $\delta\varphi$ and $\delta\theta$ into that of the curvature and isocurvature perturbations. The curvature perturbation is given by [95]

$$\zeta = -\frac{H}{\dot{\sigma}}\delta\sigma\,, \tag{8.13}$$

where

$$\delta\sigma \equiv \cos\beta\,\delta\varphi + \sin\beta\,\sqrt{f}\delta\theta\,, \tag{8.14}$$

$$\dot{\sigma} \equiv \sqrt{\dot{\varphi}^2 + f\dot{\theta}^2}\,, \tag{8.15}$$

$$\cos\beta = \frac{\dot{\varphi}}{\dot{\sigma}}\,, \tag{8.16}$$

$$\sin\beta = \frac{\sqrt{f}\dot{\theta}}{\dot{\sigma}}\,. \tag{8.17}$$

If we know the mode functions u and v of respectively $\delta\varphi$ and $\delta\theta$, we can "rotate" them in order to obtain the mode function of $\delta\sigma$. In order to simplify the analysis, we will consider the mode functions of massless fields, i.e. equations (7.98). This approximation is a good starting point thanks to the smallness of the slow-roll parameters in these models, see for example figures 8.1e and 8.1f (however a more detailed analysis is necessary since there are other slow-roll parameters (7.43)).

8.2.1 Power spectrum

At lowest order in the *in-in* expansion, the two-point correlation function is given by equation (6.13), i.e.

$$\langle\delta\sigma^2\rangle^{(0)} = (2\pi)^3\delta^3(\mathbf{p}_1+\mathbf{p}_2)\left(\cos^2\beta\,|u_{p_1}(t)|^2 + \sin^2\beta\,f\,|v_{p_1}(t)|^2\right). \tag{8.18}$$

Thanks to the definition (8.13), we get

$$\langle\zeta^2\rangle^{(0)} = (2\pi)^3\delta^3(\mathbf{p}_1+\mathbf{p}_2)\frac{H^2}{\dot{\sigma}^2}\left(\cos^2\beta\,|u_{p_1}(t)|^2 + \sin^2\beta\,f\,|v_{p_1}(t)|^2\right). \tag{8.19}$$

Using the expressions of the mode functions (7.98) and the definition of the adimensional power spectrum (1.69), we obtain

$$\mathcal{P}_\zeta^{(0)} = \frac{H^4}{4\pi^2\dot{\sigma}^2}\,, \tag{8.20}$$

where we have considered the superhorizon limit. Notice that this contribution is similar to the single-field one (1.73) with the difference that $\dot{\sigma}$ is the generalized velocity (8.15).

The next non-vanishing order of the two-point correlator is given by

$$\begin{aligned}
\langle\zeta^2\rangle^{(2)} &= \langle\frac{H^2}{\dot{\sigma}^2}\delta\sigma^2\rangle = \langle\frac{H^2}{\dot{\sigma}^2}\left(\cos^2\beta\,\delta\varphi^2 + \sin^2\beta\,f\,\delta\theta^2\right)\rangle \\
&= (2\pi)^3\delta^3(\mathbf{p}_1+\mathbf{p}_2)4\frac{H^2}{\dot{\sigma}^2}\,\mathrm{Re}\Bigg\{\int_{-\infty}^{\tau}d\tau_1\int_{-\infty}^{\tau_1}d\tau_2\,a^2(\tau_1)a^2(\tau_2)\,f'(\varphi(\tau_1))f'(\varphi(\tau_2))\,\theta'(\tau_1)\theta'(\tau_2) \\
&\quad\Bigg[\cos^2\beta\,v'_{p_1}(\tau_1)u^*_{p_1}(\tau_2)v'^*_{p_1}(\tau_2)\Big(|u_{p_1}(\tau)|^2u_{p_1}(\tau_1) - u^2_{p_1}(\tau)u^*_{p_1}(\tau_1)\Big) \\
&\quad + \sin^2\beta\,f\,v'_{p_1}(\tau_1)u^*_{p_1}(\tau_2)v'^*_{p_1}(\tau_2)\Big(|v_{p_1}(\tau)|^2u_{p_1}(\tau_1) - v^2_{p_1}(\tau)u^*_{p_1}(\tau_1)\Big)\Bigg]\Bigg\}.
\end{aligned} \tag{8.21}$$

We are not going to calculate this correction. Let us only notice that this correction is small if ε_θ is small as in the case of section 7.6 (see also the appendix D.1). The reason is that the coupling Z_1 of the interaction between $\delta\varphi$ and $\delta\theta$ into the Hamiltonian 7.38 depends on $\dot{\theta}$.

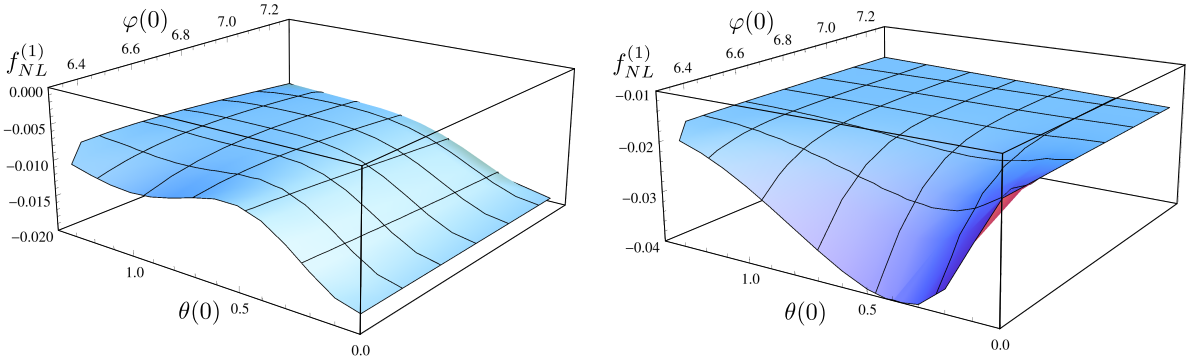

(a) $m^2 = 1$. (b) $m^2 = 10$.

Figure 8.5: Contribution $f_{NL}^{(1)}$ (8.25) for the model $W^{(1)}$ (8.3). The parameter $f_{NL}^{(1)}$ is evaluated for a scale that crosses the horizon 50 e-folds before the end of inflation. The initial velocities are $\varphi'(0) = 0$ and $\theta'(0) = 0$.

8.2.2 Bispectrum

The first-order non-null term in the expansion of the three-point correlation function reads

$$\begin{aligned}\langle\zeta^3(\tau)\rangle^{(1)} &= -\frac{H^3}{\dot\sigma^3}\Big(\langle\cos^3\beta\,\delta\varphi^3\rangle^{(1)} + \langle\sin^3\beta\, f^{\frac{3}{2}}\,\delta\theta^3\rangle^{(1)}\Big)\\ &= 2(2\pi)^3\delta^3(\mathbf{p}_1+\mathbf{p}_2+\mathbf{p}_3)\frac{H^3}{\dot\sigma^3}\\ &\quad \mathrm{Im}\Big\{u_{p_1}^*(\tau)u_{p_2}^*(\tau)u_{p_3}^*(\tau)\int_{-\infty}^{\tau}d\tau_1\,a^4(\tau_1)\mathcal{A}(\tau_1)\cos^3\beta\,u_{p_1}(\tau_1)u_{p_2}(\tau_1)u_{p_3}(\tau_1)\\ &\quad + v_{p_1}^*(\tau)v_{p_2}^*(\tau)v_{p_3}^*(\tau)\int_{-\infty}^{\tau}d\tau_1\,a^4(\tau_1)W_{\theta\theta\theta}(\tau_1)\sin^3\beta\, f^{\frac{3}{2}}\,v_{p_1}(\tau_1)v_{p_2}(\tau_1)v_{p_3}(\tau_1)\Big\},\end{aligned} \tag{8.22}$$

where we have defined

$$\mathcal{A}(\tau) \equiv W^{(1)}_{\varphi\varphi\varphi}(\tau) + \frac{f^2(\varphi(\tau))}{2a^2(\tau)}\left(\frac{1}{f}\right)'''\theta'^2(\tau). \tag{8.23}$$

In the equilateral limit $p_1 = p_2 = p_3 = p$, the previous contribution becomes

$$\begin{aligned}\langle\zeta^3(\tau)\rangle^{(1)} &= 2(2\pi)^3\delta^3(\mathbf{p}_1+\mathbf{p}_2+\mathbf{p}_3)\frac{H^3}{\dot\sigma^3}\mathrm{Im}\Big\{\Big(u_p^*(\tau)\Big)^3\int_{-\infty}^{\tau}d\tau_1\,a^4(\tau_1)\mathcal{A}(\tau_1)\cos^3\beta\Big(u_p(\tau_1)\Big)^3\\ &\quad + \Big(v_p^*(\tau)\Big)^3\int_{-\infty}^{\tau}d\tau_1\,a^4(\tau_1)W_{\theta\theta\theta}\sin^3\beta\, f^{\frac{3}{2}}\Big(v_p(\tau_1)\Big)^3\Big\}.\end{aligned} \tag{8.24}$$

Using the mode functions (7.98), the power spectrum (8.20) and the definition of f_{NL} (7.70), it can be derived the expression (valid on superhorizon scales)

$$f_{NL}^{(1)} = \frac{5}{18}\frac{\dot{\sigma}}{H^3}\mathrm{Im}\left\{\int_0^\infty dx\,\frac{1}{x^4}\left(\mathcal{A}(x)\cos^3\beta + f^{-\frac{3}{2}}W_{\theta\theta\theta}\sin^3\beta\right)e^{3ix}(1-ix)^3\right\}, \tag{8.25}$$

where $x \equiv -p\tau$. The third derivatives of the potential (8.3) are given by

$$W_{\varphi\varphi\varphi}^{(1)} = \frac{2}{3}\sqrt{\frac{2}{3}}\frac{\sinh(\varphi/\sqrt{6})}{\cosh^5(\varphi/\sqrt{6})}\left(\sinh^2\frac{\varphi}{\sqrt{6}} - 2\right), \tag{8.26}$$

$$W_{\theta\theta\theta}^{(1)} = 8m^2\frac{\sin\theta}{\cos^5\theta}\left(2+\sin^2\theta\right). \tag{8.27}$$

The contribution $f_{NL}^{(1)}$ is represented in figure 8.5 for different trajectories. Reintroducing the parameter α can enhance the contribution of $\langle\delta\varphi^3\rangle$ to the bispectrum, but not that of $\langle\delta\theta^3\rangle$. The contribution (8.25) is quite similar to (7.119), and then we expect an analogous behaviour.

The second-order term of the expansion of the three-point correlation function in the equilateral limit ($p_1 = p_2 = p_3 = p$) is given by

$$\langle\zeta^3(\tau)\rangle^{(2)} \equiv (2\pi)^3\delta^3(\mathbf{p}_1+\mathbf{p}_2+\mathbf{p}_3)\left(\langle\zeta^3(\tau)\rangle_1^{(2)} + \langle\zeta^3(\tau)\rangle_2^{(2)}\right), \tag{8.28}$$

where

$$\begin{aligned}\langle\zeta^3(\tau)\rangle_1^{(2)} \equiv -24\frac{H^3}{\dot{\sigma}^3}\mathrm{Re}\Bigg\{&\int_{-\infty}^{\tau}d\tau_1\int_{-\infty}^{\tau_1}d\tau_2\,a^3(\tau_1)a^3(\tau_2)B_1(\tau_1)Z(\tau_2)\cos^3\beta\,v_p'(\tau_1)v_p'^*(\tau_2)\\ &\Big(u_p^*(\tau)u_p^*(\tau)u_p(\tau)u_p(\tau_1)u_p(\tau_1)u_p^*(\tau_2) + u_p(\tau)u_p(\tau)u_p^*(\tau)u_p^*(\tau_2)u_p^*(\tau_2)u_p(\tau_1)\\ &- u_p(\tau)u_p(\tau)u_p(\tau)u_p^*(\tau_2)u_p^*(\tau_2)u_p^*(\tau_1) - u_p(\tau)u_p(\tau)u_p(\tau)u_p^*(\tau_1)u_p^*(\tau_1)u_p^*(\tau_2)\Big)\Bigg\},\end{aligned} \tag{8.29}$$

$$\begin{aligned}\langle\zeta^3(\tau)\rangle_2^{(2)} \equiv -24\frac{H^3}{\dot{\sigma}^3}\mathrm{Re}\Bigg\{&\int_{-\infty}^{\tau}d\tau_1\int_{-\infty}^{\tau_1}d\tau_2\,a^3(\tau_1)a^3(\tau_2)B_2(\tau_1)Z(\tau_2)\sin^3\beta\,f^{\frac{3}{2}}u_p(\tau_1)u_p^*(\tau_2)\\ &\Big(v_p^*(\tau)v_p^*(\tau)v_p(\tau)v_p'(\tau_1)v_p'(\tau_1)v_p'^*(\tau_2) + v_p(\tau)v_p(\tau)v_p^*(\tau)v_p'^*(\tau_2)v_p'^*(\tau_2)v_p'(\tau_1)\\ &- v_p(\tau)v_p(\tau)v_p(\tau)v_p'^*(\tau_2)v_p'^*(\tau_2)v_p'^*(\tau_1) - v_p(\tau)v_p(\tau)v_p(\tau)v_p'^*(\tau_1)v_p'^*(\tau_1)v_p'^*(\tau_2)\Big)\Bigg\},\end{aligned} \tag{8.30}$$

$$Z(\tau) \equiv -f'(\varphi(\tau))a^{-1}(\tau)\theta'(\tau), \tag{8.31}$$

$$B_1(\tau) \equiv \frac{2f'^2 - f''f}{2f}, \tag{8.32}$$

$$B_2(\tau) \equiv -\frac{1}{2}f'. \tag{8.33}$$

We are not going to give an explicit expression for the contribution of the previous term to f_{NL} (this can be nonetheless derived from (8.28) as previously done) since we are not going to compute numerically this contribution.

8.3 Second model

The Hamiltonian of the model with potential $W^{(2)}$ (8.9) is given by (7.38), where all terms should be considered. In order to study this model, we are going to apply the δN formalism, discussed in section 3.4, because using the *in-in* formalism is rather tough in this case.

Before applying the δN formalism, let us discuss what are the corrections that should be considered into the terms of the *in-in* expansion computed in the previous section. We suppose that the mode functions (7.98) are those proper of massless fields. At zeroth order, the power spectrum is given by equation (8.20). The next non-vanishing correction of the *in-in* expansion is similar to equation (8.21). However, in this case, we should consider both the interaction Hamiltonian terms $\mathcal{H}^{(2)}_{Z_1}$ and $\mathcal{H}^{(2)}_{Z_2}$ defined in (7.38). The contribution (8.21) accounts only for the interaction between the fields described by $\mathcal{H}^{(2)}_{Z_1}$. One should modify properly the expression (8.21) in order to take care of the second possible interaction. For what concerns the bispectrum, at first order, the parameter f_{NL} has the same expression of (8.25) with the redefinition

$$\mathcal{A}(\tau) \equiv W^{(2)}_{\varphi\varphi\varphi}(\tau) + \frac{f^2(\varphi(\tau))}{2a^2(\tau)} \left(\frac{1}{f}\right)''' \theta'^2(\tau). \tag{8.34}$$

The higher order contributions to the bispectrum are more complex to write down due to the presence of many couplings between the fields.

Finally, we have seen in section 8.1 that the trajectories are nearly straight for this model and hence we can rely on the analysis of section 7.6. Notice that the terms of the *in-in* expansion that contains derivative of the potential with respect to θ cannot enhance significantly the amount of non-Gaussianity since the derivatives of the sine functions are limited. Hence, we do not expect that this model can produce large non-Gaussianities.

8.3.1 f_{NL} estimated via the δN formalism

In this subsection (and in the figures therein) we define the number of e-folds N as in equation (4.10). Initial conditions are given at $N = 0$ and the prime denotes the derivative with respect to N.

As we have said, the *in-in* formalism is rather involved to employ; however, since the trajectories are nearly straight, the results of section 8.1 constitute a good starting point for a deeper analysis. Thus, for this model we prefer to apply the δN formalism, discussed in section 3.4. We rely on the analysis and the formulae derived by K. Choi, L. M. H. Hall and C. van de Bruck [75], since they studied a Lagrangian similar to (7.1). In particular, we adapt equation (4.10) to our non-canonical kinetic term. This choice allows us to estimate the magnitude of local non-Gaussianities produced during the superhorizon evolution of the perturbations.

Let us focus on figures 8.6. In this figures, some numerical results are shown for different values of M^2. The fields start from rest and inflation starts immediately in the region considered. We choose null initial velocities since their effect on the estimations of f_{NL} is marginal if inflation occurs. The initial velocity φ' has practically no effect on the inflationary dynamics because

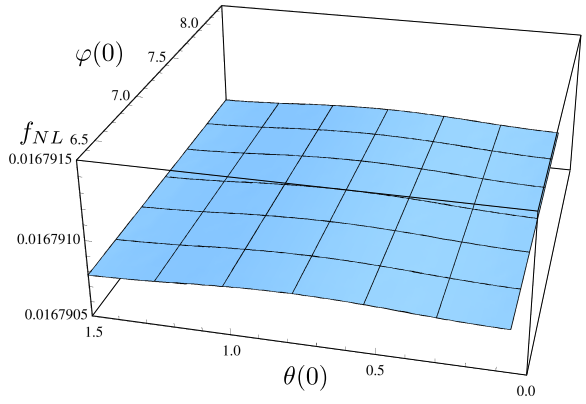

(a) f_{NL} for $M^2 = 0.01$.

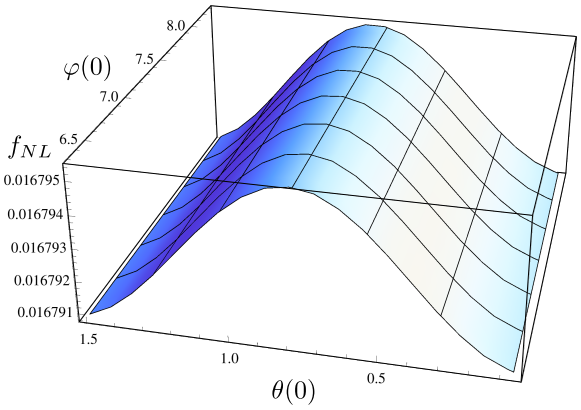

(b) f_{NL} for $M^2 = 0.1$.

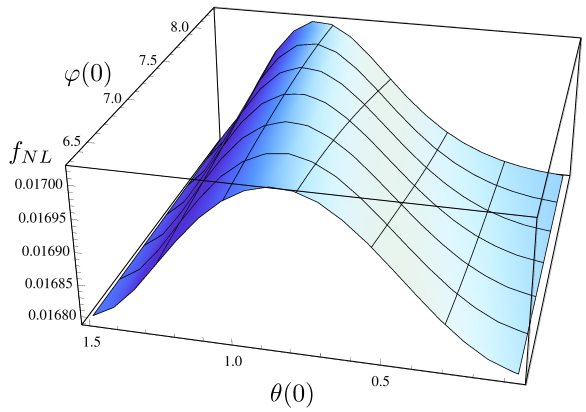

(c) f_{NL} for $M^2 = 1$.

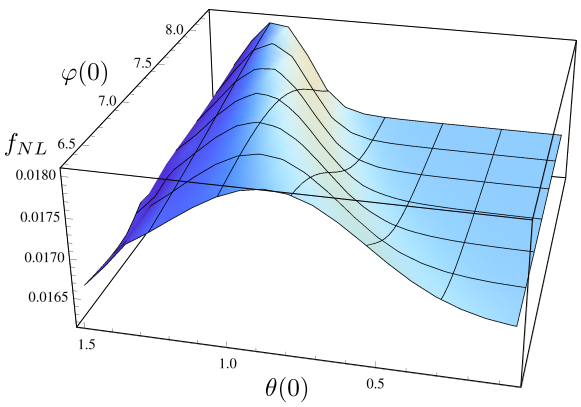

(d) f_{NL} for $M^2 = 5$.

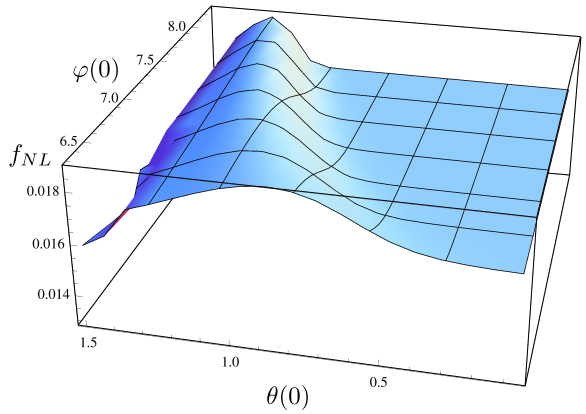

(e) f_{NL} for $M^2 = 10$.

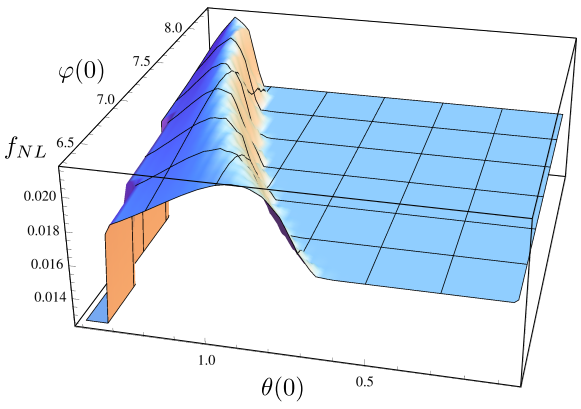

(f) f_{NL} for $M^2 = 50$.

Figure 8.6: f_{NL} for the model $W^{(2)}(\varphi,\theta) = \left(1 + M^2 \sin^2\theta\right)\tanh^2\left(\varphi/\sqrt{6}\right)$ estimated via the δN formalism for different initial configurations of the fields. All simulations share the same initial conditions, $\varphi'(0) = 0$ and $\theta'(0) = 0$. The value of f_{NL} is computed for a scale that exits the horizon 50 e-folds before the end of inflation.

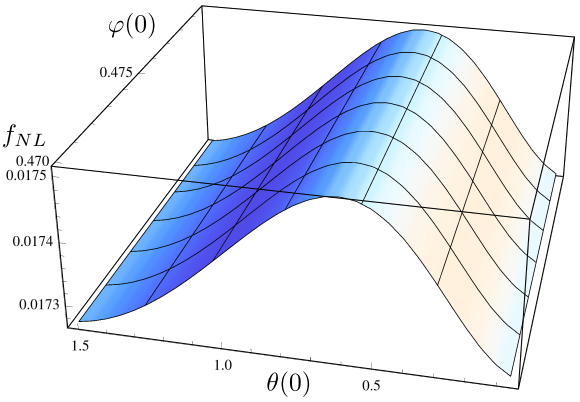

(a) f_{NL} for $\alpha = 10^{-3}$ and $M^2 = 1$. $\varphi'(0) = 0$ and $\theta'(0) = 0$.

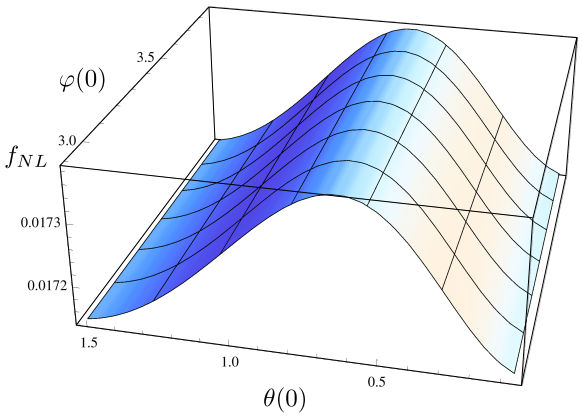

(b) f_{NL} for $\alpha = 10^{-1}$ and $M^2 = 1$. $\varphi'(0) = 0$ and $\theta'(0) = 0$.

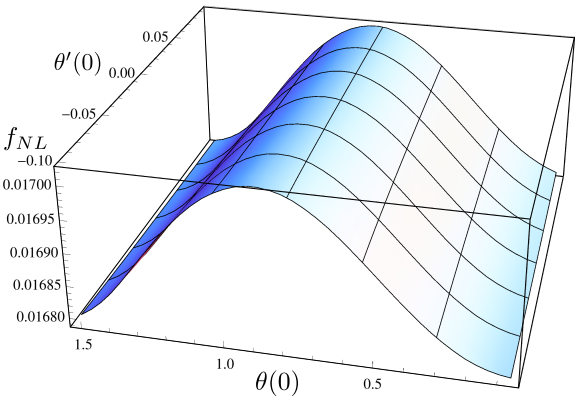

(c) f_{NL} for $\alpha = 1$ and $M^2 = 1$. $\varphi(0) = 6.3$ and $\varphi'(0) = 0$. Notice the little dependence on $\theta'(0)$.

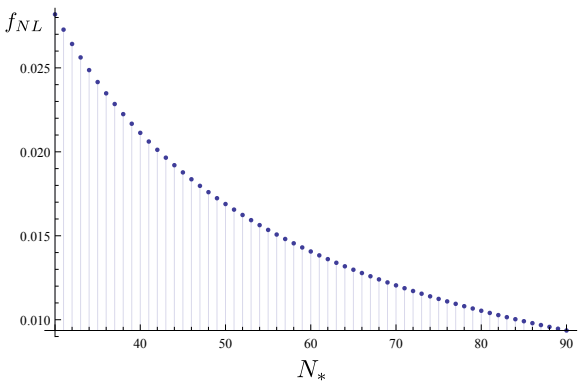

(d) f_{NL} for $\alpha = 10^{-1}$, $M^2 = 1$, $\varphi(0) = 7$, $\theta(0) = 1.3$, $\varphi'(0) = 0$ and $\theta'(0) = 0$ as a function of the scale. N_* is the number of e-folds from the end of inflation at which the scale crosses the horizon.

Figure 8.7: f_{NL} for the model $W^{(2)}(\varphi, \theta) = \left(1 + M^2 \sin^2(\theta)\right) \tanh^2\left(\varphi/\sqrt{6\alpha}\right)$ estimated using the δN formalism. The value of f_{NL} is computed for a scale that exits the horizon 50 e-folds before the end of inflation apart in figure (d) in which it is shown its scale dependence.

it is suppressed in a few e-folds before reaching the slow-roll regime (see sections 5.6 and 7.2). Conversely, the initial velocity θ' affects mainly the viable initial conditions and only slightly the inflationary trajectory (remember that inflation occurs only if $\theta'(0) \ll 1$). Therefore, considering the fields initially at rest is a good approximation. See figures E.2c and E.2e in appendix E for the effects on the trajectories of a non-null initial velocity.

In figure 8.6c it is shown the $M^2 = 1$ case. Notice that the value of f_{NL} is nearly constant in the represented region (the percentage difference is less than 2%). Increasing the value of M has little effect on the magnitude of f_{NL} as it is shown in the following figures 8.6d-8.6f. Notice that in the figures 8.6d-8.6f a flat region appears starting from the upper right corner. The value of

f_{NL} flattens increasing M because the slope of the potential for θ increases and hence the field reaches faster the attractor solution $\theta = 0$.

In figures 8.6a and 8.6b the case $M^2 = 0.01$ and $M^2 = 0.1$ are respectively shown. Again, the magnitude of f_{NL} is nearly constant in the depicted region. If $M^2 = 0.01$, the potential $W^{(2)}$ is very close to be flat. Hence, we can suppose that this plot represents the amount of local non-Gaussianities produced by the case of section 7.6.

To sum up, varying M is not possible to enhance the nonlinearity parameter f_{NL}. It can be proven that the magnitude of f_{NL} is of order $\sqrt{\varepsilon_\varphi}$ evaluated at the horizon crossing for our model. Indeed, this factor gives the most important contribution to the expression of f_{NL} (4.10) in [75].

We can introduce the parameter α into the potential $W^{(2)}$ (8.9) and into the function f as previously done. However, varying α does not help to increase the amount of f_{NL} as can be seen in figures 8.7a and 8.7b. Hence, at least on superhorizon scales and for local non-Gaussianities, the parameter α cannot enhance f_{NL}.

The plot 8.7c shows the dependence of f_{NL} on the initial position $\theta(0)$ and the initial velocity $\theta'(0)$. Notice that there is no dependence on $\theta'(0)$. Hence, a non-null initial velocity $\theta'(0)$ affects the initial conditions but not the predictions for non-Gaussianity. In figure 8.7d, the dependence of f_{NL} on the scale considered is depicted for a given trajectory.

Let us briefly comment the previous results. The analysis made is not conclusive. We have shown that it is not possible to produce large local non-Gaussianities in the context of this model relying on the δN formalism. On the other hand, this does not forbid the possibility that large non-Gaussianities could be produced when the full *in-in* computation is performed. However, at least in the case $M^2 \lesssim 1$, we do not expect important differences with the results of section 7.6 since we have seen in section 8.1 that the trajectories are nearly straight.

Summary and outlook

In this thesis, we analysed different inflationary models and tried to answer different questions. Since from the first chapter, we pointed out that inflation is currently an active area of research. In particular, the so-called α-attractor models [103, 112] were born only recently but, as we discussed, they posses some interesting features. Our main concern was to study the two-field models described by the Lagrangian (5.77). In particular, we studied under which conditions large (which corresponds to f_{NL} of order unity or greater) non-Gaussianities can be generated. Studying multi-field models is a really hard task. In particular, if the field space metric is non-trivial. Throughout the chapters, we developed the necessary tools to fully face this study.

The most important results of this work are the following.

In chapter 5, we studied the α-attractors models. In section 5.4 we explained why the predictions of these models do not practically depend on the particular form of the potential. Then, in section 5.6, we focused on the dynamics of the single-field T-models. We studied the initial conditions that lead to an inflationary epoch. We saw that it is not difficult to obtain an inflationary period that lasts for at least $50 \div 70$ e-folds. Indeed, if the scalar field starts from a position sufficiently distant from the minimum of the potential, inflation occurs regardless of its initial velocity. The reason is that the form of the potential of T-models is appropriate for inflation since it possesses a sufficiently flat plateau.

Subsequently, we focused on the two-field α-attractor models described by Lagrangian (5.77). A first analysis of the background dynamics was performed in section 7.2. We concentrated especially on the behaviour of the system in the region where inflation is most likely to occur. The most stringent condition to satisfy in order to have inflation is that the initial velocity of the angular field θ should be small. We estimated the magnitude of this smallness using both an analytical approximation and numerical results.

In section 7.3, we applied the *in-in* formalism to the more general Lagrangian (7.2). We derived the expressions of the free and the interaction Hamiltonians considering the perturbations of the fields up to third order. Furthermore, we solved the equations for the free mode functions for the fields' perturbations.

In section 7.5, we considered a simple curved trajectory in field space following [82]. In this section, we built an interesting model. Indeed, we showed that large primordial non-Gaussianities can be generated in this case thanks to the α parameter (see equations 7.83 and 7.94). These non-Gaussianities are produced by an interaction term between the fields (corresponding to a transfer of non-Gaussianities from the isocurvature to the adiabatic mode perturbations), while we proved that other contributions should be negligible.

In section 7.6, we studied another example of trajectory, a nearly straight one. As we saw,

this type of trajectory is representative (at least in certain regions of the field space and under some assumptions) of the behaviour of the fields described via Lagrangian (5.77). Also in this case we obtained large non-Gaussianities varying the parameter α thanks to interactions between the fields. The noticeable fact is that large non-Gaussianities are produced even if the trajectory is almost straight and the second field does not participate actively to inflation (but its presence is nonetheless fundamental for this enhancement). In addition to this, we proved that it is possible to produce large non-Gaussianities considering a model different to (5.77) if the third derivative of the function f, defined in equation (7.2), is high.

Finally, in chapter 8, we analysed two specific models described by the Lagrangian (5.77). We discussed in detail their background dynamics and we began to apply the *in-in* formalism in order to study the power spectrum and the bispectrum. Finally, we used the δN formalism to estimate the amplitude (i.e. the nonlinearity parameter f_{NL}) of primordial local non-Gaussianities for one of the aforementioned models (see figures 8.6). We showed that it is not possible to generate large local non-Gaussianities in the latter model. In addition to this, we showed numerically that it is not possible to enhance the parameter f_{NL} thanks to the α parameter (see figures 8.7).

Obviously, a lot of work remains to do, even in the examples and models discussed in the previous chapters. One of the things that can be improved is the inclusion of the metric perturbations in the computations of primordial non-Gaussianity. In fact we did not consider them, taking into account only the perturbations of the fields. One of the reasons underneath this choice is that it is simpler to do calculations without considering the perturbations of the metric. However, one of our main concerns was the possibility to obtain large non-Gaussianities; if they are produced through interactions of the fields, then the contribution given by the metric perturbations is usually subdominant. Furthermore, section 7.5 should be integrated with a suitable potential that could lead to an inflationary epoch. We mentioned a possibility, but we did not investigate it. Finally, one can study different models from those proposed in chapter 8. In particular, we focused on two simple examples that do not exhaust all the possibilities described by the dependence (5.80) of the potential.

The main goal of a master thesis is to learn new notions and tools in order to deal with different problems and try to find solutions. The author believes that this thesis certainly accomplish this goal. The original parts of this work are the considerations about the universality behaviour of α-attractor models (section 5.4), the study of the acceptable initial conditions for T-Models (section 5.6), the majority part of chapter 7 and chapter 8.

Appendix A

Conformal time

Conformal time is defined as

$$d\tau \equiv \frac{dt}{a(t)}\,, \tag{A.1}$$

where t is the cosmic time and $a(t)$ is the scale factor (see the line element (1.6)). The flat FRW metric rewritten with respect to conformal time reads

$$ds^2 = a^2(\tau)\left(-d\tau^2 + dx^i dx^i\right). \tag{A.2}$$

Let $f(t) = f(t(\tau))$ be a generic function of time, we denote with an overdot ($\dot{f}$) the derivative with respect to t and with a prime (f') that with respect to τ. The expansion rate rewritten in terms of conformal time is given by

$$\mathcal{H} = \frac{a'}{a}. \tag{A.3}$$

We omit to write the arguments of the functions because they can easily argued.

Directly from the definition of conformal time, we can derive some useful relations between cosmological time quantities and conformal time ones:

$$\dot{f} = \frac{f'}{a}, \tag{A.4}$$

$$\ddot{f} = \frac{1}{a^2}\left(f'' - \mathcal{H}f'\right), \tag{A.5}$$

$$f' = a\dot{f}, \tag{A.6}$$

$$f'' = a^2\left(\ddot{f} + H\dot{f}\right), \tag{A.7}$$

$$H = \frac{\mathcal{H}}{a}, \tag{A.8}$$

$$\dot{H} = \frac{1}{a^2}\left(\mathcal{H}' - \mathcal{H}^2\right), \tag{A.9}$$

$$\mathcal{H} = aH\,, \tag{A.10}$$

$$\mathcal{H}' = a^2\left(\dot{H} + H^2\right). \tag{A.11}$$

Thanks to the previous equalities, Friedmann equations (1.8) can be rewritten as

$$\mathcal{H}' = -\frac{4\pi G a}{3}(\rho + 3P)\,, \tag{A.12a}$$

$$\mathcal{H}^2 = \frac{8\pi G a^2}{3}\rho - K\,, \tag{A.12b}$$

and the continuity equation (1.10) as

$$\rho' + 3\mathcal{H}(\rho + P) = 0\,. \tag{A.13}$$

Appendix B

Conformal transformations

A conformal transformation is a local transformation of the metric

$$g_{\mu\nu}(x) \mapsto \widetilde{g}_{\mu\nu} = \Omega^2(x) g_{\mu\nu}(x). \tag{B.1}$$

A simple example is provided by the flat FRW metric (1.6) rewritten in terms of conformal time that can be obtained through a conformal transformation ($\Omega^2(x) \equiv a^2(\tau)$) starting from Minkowski metric. A conformal transformation affects the lengths of spacelike and timelike intervals, but it leaves the light cones unchanged. Hence, causal structure is preserved. A theory is conformally invariant if the form of its action is preserved under conformal transformations.

Performing a conformal transformation has the following results in a four dimensional spacetime[1]

$$\widetilde{g}^{\mu\nu} = \Omega^{-2} g^{\mu\nu}, \tag{B.2}$$

$$\sqrt{-\widetilde{g}} = \Omega^4 \sqrt{-g}, \tag{B.3}$$

$$\widetilde{\Gamma}^{\mu}_{\nu\rho} = \Gamma^{\mu}_{\nu\rho} + \Omega^{-1} \left(\delta^{\mu}_{\rho} \partial_{\nu} \Omega + \delta^{\mu}_{\nu} \partial_{\rho} \Omega - g_{\nu\rho} \partial^{\mu} \Omega \right), \tag{B.4}$$

$$\widetilde{R}_{\mu\nu} = R_{\mu\nu} - \Omega^{-1} \left(g_{\mu\nu} \nabla_{\alpha} \nabla^{\alpha} \Omega + 2 \nabla_{\mu} \nabla_{\nu} \Omega \right) - \Omega^{-2} \left(g_{\mu\nu} \nabla_{\alpha} \Omega \nabla^{\alpha} \Omega - 4 \nabla_{\mu} \Omega \nabla_{\nu} \Omega \right), \tag{B.5}$$

$$\widetilde{R} = \Omega^{-2} \left(R - \frac{6}{\Omega} \nabla_{\alpha} \nabla^{\alpha} \Omega \right) = \Omega^{-2} \left(R - \frac{12 \, \Box \sqrt{\Omega}}{\sqrt{\Omega}} - \frac{3 g^{\mu\nu} \nabla_{\mu} \Omega \nabla_{\nu} \Omega}{\Omega^2} \right). \tag{B.6}$$

The Weyl tensor and null geodesics are conformally invariant. The conservation equation $\nabla^{\mu} T_{\mu\nu} = 0$ for a symmetric stress-energy tensor $T_{\mu\nu}$ is conformally invariant if the trace $T^{\mu}{}_{\mu}$ vanishes. The Klein-Gordon equation $\Box \phi = 0$ for a scalar field ϕ is not conformally invariant, but its generalization

$$\Box \phi - \frac{R}{6} \phi = 0 \tag{B.7}$$

is conformally invariant. The last equation can be obtained introducing a coupling term between the field ϕ and the Ricci scalar R into the action for the scalar field. Notice that the transformation

$$g_{\mu\nu}(x) \mapsto \widetilde{g}_{\mu\nu} = \Omega^2(\phi(x)) \, g_{\mu\nu}(x) \tag{B.8}$$

is a particular type of conformal ones (this type of conformal transformation is used in chapter 5).

[1] Indeed, there is a dependence on the dimension of spacetime in the listed formulas because of the presence of contracted Kronecker deltas. We neglect this dependence and consider only the four-dimensional case.

In general, conformal transformations are not diffeomorphisms of the manifold and the rescaled metric $\widetilde{g}_{\mu\nu}$ is not simply the metric $g_{\mu\nu}$ rewritten in another coordinate system. In fact, these two metrics describe different gravitational fields and, possibly, distinct physical phenomena (referring to the previous example, it is obvious that Minkowsi space and flat FRW are physically different). Then, a bunch of questions rises naturally. In which frame should a theory be formulated? Are Einstein frame and Jordan frame equivalent? Given a theory, what are the conformal transformations that leave it unchanged? For a meticulous review on conformal transformation, the interested reader is referred to [129, 130]. For other information and discussions about the frame issue, the reader can give a look at [131–133].

Appendix C

A brief introduction to CMB

The Cosmic Microwave Background (CMB) is a thermal radiation originated 380 000 years after the Big Bang at the time of *recombination*. The CMB was produced when electrons combined with protons to form neutral hydrogen. This epoch is oddly called recombination even if any combination had never happened before that time. After recombination the Universe became transparent to radiation and photons could free stream without practically interacting with any particle. Therefore, we can say that the CMB constitutes the oldest photograph ever taken. Although previously predicted, the CMB was discovered by chance only in 1964 by A. Penzias and R. Wilson, two American radio astronomers.

The physical mechanism that produced the CMB is rather simple. At early times, the Universe was expanding and cooling down. The main components were baryons, i.e. protons and electrons[1] and photons. All these species were in thermal equilibrium thanks to Compton (at high energies) and Thomson scattering (at lower energy) and to Coulomb interaction between electrons and protons. Photons interact mainly with electrons since the cross section $\sigma \propto m^{-1}$, where m is the mass of the particles involved. The components are said to be tight coupled as long as interactions are efficient. Mathematically, if Γ denotes the interaction rate, the tight coupling condition is $\Gamma > H$. When $\Gamma = H$, the components decouple and, after this, the interactions become inefficient so that the components are no more in thermal equilibrium (their temperatures evolve independently). During recombination, the number density of free electrons quickly drops and so does the rate of scatterings between photons and electrons. Photons decoupled from baryons at a temperature of $\sim 0.1\,\mathrm{eV}$. After recombination, photons can free stream and can reach us undisturbed. Indeed, observing CMB is like viewing the surface of last scattering.

As the name suggests, the CMB has a black body spectrum at a temperature $T_0 = 2.725\,\mathrm{K}$, which corresponds to photons with a wavelength in the microwave region (remember that after recombination the temperature of photons $T \propto a^{-1}$). If we were able to see such long radiation wavelengths, the night sky would appear bright[2] and with the same shade in every direction. If we could increase our eyes resolution, we would be able to distinguish little anisotropies of order $\Delta T/T_0 \sim 10^{-5}$. During 70's cosmologists were first surprised by the isotropy of the

[1] Electrons are not baryons. They are leptons. However, in cosmologists' jargon, electrons and protons are both baryons. Let us conclude this footnote with a related dumb fact. Astronomers call metals all the elements on the periodic table apart for hydrogen and helium.

[2] The reader maybe remembers Olbers' 18^{th}-century paradox.

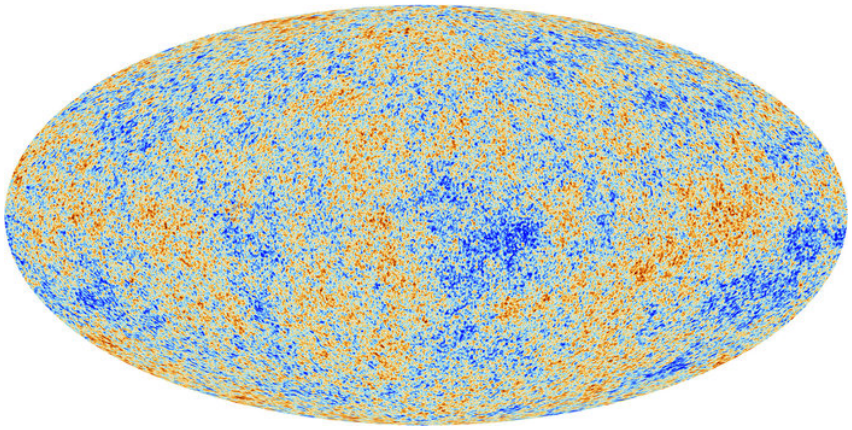

Figure C.1: CMB radiation as seen by *Planck* satellite. If one could turn off the Sun, stars and galaxies and could see infra-red frequencies, he would observe this sky. Picture taken from the ESA's website.

CMB, later their attention was captured by these small fluctuations so heavily that they have become our first source of information about the Universe. These fluctuations are the seeds of structure formation in the Universe. As we have seen in chapter 1, inflation can give birth to such perturbations and hence the CMB carries the imprints of the oldest studied physical phenomenon. These small fluctuations are depicted in figure C.1.

At recombination, the pressure of photons breaks down and they "photograph" the energy density fluctuations. Honestly, photons reach us after having been red or blueshifted due to the gravitational potential Φ they have encountered during their propagation. Hence, matter fluctuations became temperature anisotropies that reflect the matter distribution at the epoch of recombination. These anisotropies are described through the dimensionless ratio $(\Delta T/T_0)_*$, where the subscript "$*$" denotes the time of decoupling. The fluctuations measured at present epoch are given by

$$\frac{\Delta T}{T_0} = \left(\frac{\Delta T}{T}\right)_* + \Phi\,. \tag{C.1}$$

Since the CMB anisotropies are projected on the sky, it is convenient to work in spherical coordinates or with their momentum space transform, spherical harmonics. The temperature contrast seen by an observer can be written as

$$\Theta(\theta,\phi) \equiv \frac{\Delta T}{T_0}(\theta,\phi) = \sum Y_l^m(\theta,\phi) a_{lm}\,, \tag{C.2}$$

where the sum runs over the multipole number $l = 0, 1, 2, \ldots$ and $m = -l, \ldots, l$. The spherical harmonics constitute an orthonormal basis and then the coefficients of the expansion read

$$a_{lm} = \int Y_l^{m*}\,\Theta\, d\Omega\,. \tag{C.3}$$

The CMB anisotropy is due to the primordial perturbations, and therefore it reflects their (nearly) Gaussian nature. The coefficients a_{lm} are also (nearly) Gaussian since they are obtained from perturbations through linear equations [21]. Furthermore, their expectation value

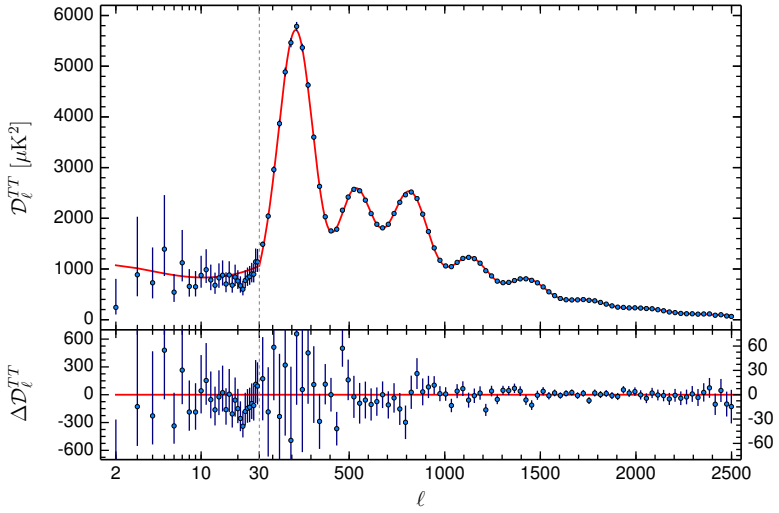

Figure C.2: The CMB peaks measured by *Planck*. $\mathcal{D}_l^{TT} \equiv l(l+1)C_l$. Blue dots are experimental data and the red line is the best-fit interpolating curve based on the ΛCDM theoretical prediction. Residuals with respect to this model are shown in the lower panel. Notice the three regimes (Sachs-Wolfe plateau, acoustic oscillations and Silk damping) described in the main text. The error bars correspond to $\pm 1\sigma$ uncertainties. Picture taken from [5].

$\langle a_{lm} \rangle = 0$ since they represent a deviation form the average temperature. The variance $\langle |a_{lm}|^2 \rangle$ characterizes the statistical properties of the fluctuations. Due to isotropy, the variance depends only on l and not on m. The variance of the coefficients a_{lm} is given by

$$\langle a_{lm} a^*_{l'm'} \rangle = \delta_{ll'} \delta_{mm'} C_l \,, \tag{C.4}$$

where C_l is related to the expansion into multipoles of the variance of the temperature fluctuations through

$$\langle \Theta^2 \rangle = \sum_l \frac{2l+1}{4\pi} C_l P_l(\cos\theta) \,, \tag{C.5}$$

where P_l are the Legendre polynomials. The function C_l is called the angular power spectrum of the CMB.

The CMB angular bispectrum is defined as

$$B^{m_1 m_2 m_3}_{l_1 l_2 l_3} = \langle a_{l_1 m_1} a_{l_2 m_2} a_{l_3 m_3} \rangle \,. \tag{C.6}$$

If we assume that the angular bispectrum satisfies statistical isotropy, the three-point function can be factorized as

$$\langle a_{l_1 m_1} a_{l_2 m_2} a_{l_3 m_3} \rangle = \mathcal{G}^{m_1 m_2 m_3}_{l_1 l_2 l_3} b_{l_1 l_2 l_3} \,, \tag{C.7}$$

where $b_{l_1 l_2 l_3}$ is called reduced bispectrum and

$$\mathcal{G}^{m_1 m_2 m_3}_{l_1 l_2 l_3} \equiv \int d\Omega \, Y^{m_1}_{l_1} \, Y^{m_2}_{l_2} \, Y^{m_3}_{l_3} \tag{C.8}$$

is the so-called Gaunt integral. The triplets (l_1, l_2, l_3) satisfy the triangle inequality condition, $|l_i - l_j| \leqslant l_k \leqslant l_i + l_j$ for all permutations of the indices, and the sum $l_1 + l_2 + l_3$ should be even for invariance under parity of the correlator.

The angular power spectrum of the CMB is represented in figure C.2. As can be seen, there are three regions originating from different underneath physical phenomena.

- **Sachs-Wolfe plateau** The largest scale ($l \lesssim 100$) are not affected by the interactions between photons and baryons since they re-enter the horizon after recombination. The main effect responsible for the temperature fluctuations is the Sachs-Wolfe effect. In order to describe it, let us work in the Newtonian gauge. In this gauge, the Bardeen potential Φ (2.64) completely characterizes scalar fluctuations. During matter domination (that is at the time of last scattering) and on large scales, the potential Φ is related to the curvature perturbation $\mathcal{R}$ (2.69) through
$$\Phi = \frac{3}{5}\mathcal{R}. \tag{C.9}$$
It can be shown that the observed temperature anisotropy is given by
$$\Theta(\theta, \phi) \equiv \frac{\Phi_*}{3}. \tag{C.10}$$
On such scales, the perturbations are nearly scale-invariant.

- **Acoustic oscillations** On the median scales ($100 \lesssim l \lesssim 800$) we observe the characteristic peak structure of the CMB. The physical mechanism that originates these peaks is the following. The baryons tend to fall into the wells of the gravitational potential but these tendency to create overdensities is balanced by the photon pressure during tight coupling regime. Indeed, photons tend to erase anisotropies and baryons to create them. These two effects compete and create acoustic oscillations that are imprinted on the CMB when the scales leave the horizon. In fact, perturbations on such scales freezes after the horizon crossing. Therefore, they keep track of the oscillations of the photon-baryon fluid. The acoustic oscillations propagate with the speed of sound $c_s \simeq 1/\sqrt{3}$ (this is a way to see that they cannot affect very large scales).

- **Silk damping** On the smallest scales, the tendency of photons to erase anisotropies is the dominant effect. On such scales, fluctuations are washed away and they vanish as the scale reduces.

How are the perturbations produced by inflation related to those of the CMB? Long story short, the inflaton's perturbations $\delta\varphi$ became curvature perturbations $\mathcal{R}$ after inflaton's decay and then they affected the matter distribution as an effective gravitational potential Φ. The curvature perturbations affect the matter distribution through Einstein equations. Finally, overdense regions grow thanks to the gravitational attraction and, eventually, give birth to structures like galaxies and clusters.

The CMB is an endless source of precious information about the early universe. Many cosmological parameters can be measured studying CMB [5]. The position (angular scale) of the

first peak determines the spatial curvature of the universe K (see equation (1.4)). The ratio between the magnitudes of the odd peaks and the even ones determines the baryon density. The third peak can be used to get information about the dark matter density. The locations of the peaks also give valuable information about the nature of the primordial density perturbations (i.e. if they are adiabatic or entropic). Observations are consistent with the primordial density perturbations being completely adiabatic (this strongly support the inflationary mechanism among others for perturbations production). Moreover, thanks to CMB cosmologists can investigate inflation and its properties [6]. In table 1.1, the latest *Planck* measurements of the cosmological and inflationary parameters are listed. All these can be measured from the pattern of anisotropies of the CMB.

Appendix D

Some explicit calculations

D.1 Equation (7.103)

In this section, we will derive the expression (7.103) for the power spectrum in the nearly single-field case. The power spectrum (7.103) can be obtained from equation (7.102), that is

$$\langle\zeta^2(t)\rangle^{(2)} = 4\frac{H^2}{\dot{\varphi}^2}\mathrm{Re}\Bigg\{\int_{-\infty}^{\tau}d\tau_1\int_{-\infty}^{\tau_1}d\tau_2 a^3(\tau_1)a^3(\tau_2)f'(\tau_1)f'(\tau_2)\dot{\theta}^2 \\ \Big[|u_{p_1}(\tau)|^2u_{p_1}(\tau_1)v'_{p_1}(\tau_1)u^*_{p_1}(\tau_2)v'^*_{p_1}(\tau_2) - u^2_{p_1}(\tau)u^*_{p_1}(\tau_1)v'_{p_1}(\tau_1)u^*_{p_1}(\tau_2)v'^*_{p_1}(\tau_2)\Big]\Bigg\}, \tag{D.1}$$

where we have omitted the factor $(2\pi)^3\delta^3(\mathbf{p}_1+\mathbf{p}_2)$ and where we have considered the velocity $\dot{\theta}$ constant. The mode functions are given by (7.98) and then, neglecting terms that vanish on superhorizon scales,

$$\langle\zeta^2(t)\rangle^{(2)} = 4\frac{H^2}{\dot{\varphi}^2}\mathrm{Re}\Bigg\{\int_{-\infty}^{\tau}d\tau_1\int_{-\infty}^{\tau_1}d\tau_2\frac{1}{\tau_1^3\tau_2^3}f'(\tau_1)f'(\tau_2)\frac{\dot{\theta}^2}{(2p_1^3)^3}\frac{d}{d\tau_1}\left(\frac{1}{\sqrt{f}}(1+ip_1\tau_1)e^{-ip_1\tau_1}\right)e^{ip_1\tau_2} \\ (1-ip_1\tau_2)\frac{d}{d\tau_2}\left(\frac{1}{\sqrt{f}}(1-ip_1\tau_2)e^{ip_1\tau_2}\right)\Big[(1+ip_1\tau_1)e^{-ip_1\tau_1}-(1-ip_1\tau_1)e^{ip_1\tau_1}\Big]\Bigg\}. \tag{D.2}$$

These integrations are rather complicated due to the presence of the function $f(\varphi(\tau))$. In fact, one needs to integrate over all the inflationary background trajectory. The derivatives are similar and the first is given by

$$\frac{d}{d\tau_1}\left(\frac{1}{\sqrt{f}}(1+ip_1\tau_1)e^{-ip_1\tau_1}\right) = \left(\frac{p_1^2\tau_1}{\sqrt{f}}-\frac{f'\varphi'}{2f^{\frac{3}{2}}}(1+ip_1\tau_1)\right)e^{-ip_1\tau_1}. \tag{D.3}$$

The previous integrals become

$$\langle\zeta^2(t)\rangle^{(2)} = 4\frac{H^2}{\dot{\varphi}^2}\frac{1}{(2p_1^3)^3}\mathrm{Re}\Bigg\{\int_{-\infty}^{\tau}d\tau_1\int_{-\infty}^{\tau_1}d\tau_2\frac{1}{\tau_1^3\tau_2^3}f'(\tau_1)f'(\tau_2)\dot{\theta}^2 \\ \left(\frac{p_1^2\tau_1}{\sqrt{f}}-\frac{f'\varphi'(\tau_1)}{2f^{\frac{3}{2}}}(1+ip_1\tau_1)\right)(1-ip_1\tau_2)\left(\frac{p_1^2\tau_2}{\sqrt{f}}-\frac{f'\varphi'(\tau_2)}{2f^{\frac{3}{2}}}(1-ip_1\tau_2)\right) \\ e^{ip_1(2\tau_2-\tau_1)}\Big[(1+ip_1\tau_1)e^{-ip_1\tau_1}-(1-ip_1\tau_1)e^{ip_1\tau_1}\Big]\Bigg\}. \tag{D.4}$$

Let us evaluate the magnitude of the final result. We expect this to be small (of order of slow-roll parameters) since it is a higher order correction to the power spectrum. We have assumed that $\dot{\theta}$ is constant but, for the moment, let us reintroduce its time dependence. The integrand goes as

$$\begin{aligned}
&\sim \dot{\theta}(\tau_1)\sqrt{f(\tau_1)}\frac{f'(\tau_1)}{f(\tau_1)}\left(p_1 - \frac{f'(\tau_1)}{f(\tau_1)}\varphi'(\tau_1)\right)\dot{\theta}(\tau_2)\sqrt{f(\tau_2)}\frac{f'(\tau_2)}{f(\tau_2)}\left(p_1 - \frac{f'(\tau_2)}{f(\tau_2)}\varphi'(\tau_2)\right)\\
&\sim \sqrt{\varepsilon_\theta(\tau_1)}\frac{f'(\tau_1)}{f(\tau_1)}\left(p_1 - \mathcal{H}\xi_\varphi\right)\sqrt{\varepsilon_\theta(\tau_2)}\frac{f'(\tau_2)}{f(\tau_2)}\left(p_1 - \mathcal{H}\xi_\varphi\right),
\end{aligned} \tag{D.5}$$

where we have neglected all irrelevant factors and used the definitions (7.43). Notice that

$$\frac{f'}{f} = \sqrt{\frac{2}{3}}\coth\frac{\varphi}{\sqrt{6}} \tag{D.6}$$

is $\mathcal{O}(1)$ during slow-roll and diverges exponentially as $\varphi \to 0$. On the other hand, we have seen in section 5.6 that inflation ends when $\varphi \sim \sqrt{6}$ and then we should not be worried about. Hence, we need to integrate factors of order of slow-roll parameters.

The correlator we started with becomes

$$\begin{aligned}
\left\langle\zeta^2(t)\right\rangle^{(2)} = \frac{H^2}{\dot{\varphi}^2}\frac{\dot{\theta}^2}{(2p_1^3)}\mathrm{Re}\Bigg\{\int_x^\infty dx_1\int_{x_1}^\infty dx_2\frac{f'(x_1)f'(x_2)}{\sqrt{f(x_1)}\sqrt{f(x_2)}}\frac{(1+ix_2)e^{-i(2x_2-x_1)}}{x_1^2x_2^2}\\
\Big[(1-ix_1)e^{ix_1} - (1+ix_1)e^{-ix_1}\Big]\Bigg\},
\end{aligned} \tag{D.7}$$

where we have neglected the higher order terms in slow-roll parameters and we have defined $x \equiv -p_1\tau$. Computing such an integral is a rather time consuming task. Its value depends on the trajectory of the inflaton (indeed this dependence is small due to the attractor behaviour of our system) and on the scale considered. We are not going to compute the previous integral for different trajectories. Rather, we prefer to make some additional assumptions and to roughly estimate its value. Since the slow-roll parameter ε 7.43a and its variation during time are small during slow-roll, we can consider f nearly constant[1] and then

$$\left\langle\zeta^2(t)\right\rangle^{(2)} = \frac{H^2}{\dot{\varphi}^2}\frac{2}{3}\frac{f\dot{\theta}^2}{(2p_1^3)}\mathrm{Re}\Bigg\{\int_x^\infty dx_1\int_{x_1}^\infty dx_2\frac{(1+ix_2)e^{-i(2x_2-x_1)}}{x_1^2x_2^2}\Big[(1-ix_1)e^{ix_1} - (1+ix_1)e^{-ix_1}\Big]\Bigg\}, \tag{D.8}$$

where we have considered $f'/f = 1$ thanks to (D.6). One can show that the previous integral is not divergent even in the limit $x \to 0$ and its value is ~ 0.65.

Finally, the second order correction to the power spectrum for a nearly straight trajectory can be estimated (thanks to all the previous assumptions) as

$$\mathcal{P}_\zeta^{(2)} \simeq \frac{H^4}{(2\pi\dot{\varphi})^2}\,\frac{f}{2}\frac{\dot{\theta}^2}{H^2}\,. \tag{D.9}$$

[1]The main contribution to integrals like (D.7) comes near the time of horizon crossing and when the considered scale is superhorizon. In fact, when the scale is well within the horizon, the mode functions have an oscillatory behaviour and their contribution to the integral is averaged to zero. Hence, considering the function f as constant can be a good starting point if it does not vary significantly during the time of horizon crossing.

D.2 Equation (7.115)

In this section, we will analyse equation (7.115) and give some useful suggestions to calculate *in-in* integrals.

Let us start with the integral factor of (7.115), that is

$$\mathcal{I} \equiv \mathrm{Im}\left\{\int_0^\infty dx \frac{1}{x^4} e^{3ix}(1-ix)^3\right\}. \tag{D.10}$$

Remember that $x \equiv -k\tau$. The lower integration limit is not zero. Practically, it should be taken at the time of the end of inflation. If we consider a scale k that exit the horizon N_* e-folds before the end of inflation and assume de Sitter expansion,

$$e^{N_*} = -\frac{1}{k\tau_f} \equiv \frac{1}{x_f}\,, \tag{D.11}$$

where τ_f is the end of inflation. Notice that the scale k exits the horizon at $x = 1$. Furthermore, one can show that

$$e^{N_*-N_f} = -\frac{1}{k\tau_i} \equiv \frac{1}{x_i}\,, \tag{D.12}$$

where N_f are the total number of e-folds of inflation which begins at τ_i. If inflation lasts $N_f = 60$ e-folds and a scale exits the horizon at $N_* = 50$ e-folds, then $x_i = e^{10}$ and $x_f = e^{-50}$ (it can be helpful to look at figure 1.1). Hence, the integral depends on the scale considered and it can be rewritten as

$$\mathcal{I}(k) = \mathrm{Im}\left\{\int_{x_f}^\infty dx \frac{1}{x^4} e^{3ix}(1-ix)^3\right\}, \tag{D.13}$$

where $x_f = x_f(k)$. In order to compute this integral numerically, one should introduce a cutoff scale[2] (for example $x_c = 2$) and rewrite the integral in the form

$$\mathcal{I}(k) = \frac{1}{2i}\int_{x_f}^{x_c} dx \frac{1}{x^4}\Big(e^{3ix}(1-ix)^3 - e^{-3ix}(1+ix)^3\Big) + \mathrm{Im}\left\{\int_{x_c}^\infty dx \frac{1}{x^4} e^{3ix}(1-ix)^3\right\}. \tag{D.14}$$

It is convenient to calculate the superhorizon evolution in the commutator form (in this manner divergent terms cancel during the numerical integration) and the subhorizon in the factorized form. In addition, one usually performs a Wick rotation in the subhorizon term to make it converge faster (otherwise the integrand is oscillating and numerically it is expensive to integrate till infinity). More details about these techniques are given in [82]. Finally, the integral $\mathcal{I}(k)$ is represented in figure D.1a as a function of N_*. We notice that previous integral can be solved analytically (even if the equilateral limit is not considered) and it can be proven that it diverges as $\ln(x_f)$ [134].

If the field φ is not massless, its mode function is given by (7.46) and the integral now becomes

$$\mathcal{I}_\nu(k) = \frac{\pi^3}{2^3}\mathrm{Im}\left\{\big[x_i^{3/2} H_\nu^{(2)}(x_i)\big]^3 \int_{x_f}^\infty dx\sqrt{x}\big[H_\nu^{(1)}(x)\big]^3\right\}, \tag{D.15}$$

[2]The result of the integration depends a little on the cutoff. For the integral (D.14) there are variations of order 0.5% if x_c varies from 1 to 100. Here, we are not interested in discussing this issue.

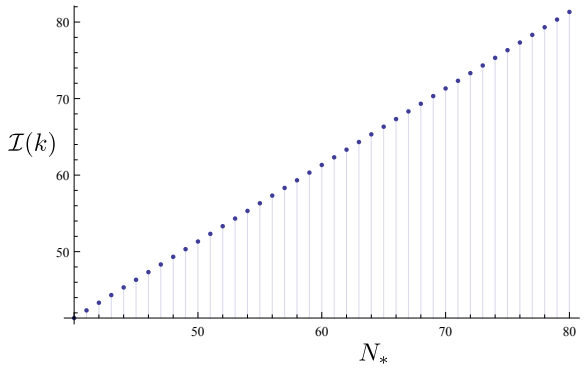

(a) Numerical evaluation of integral $\mathcal{I}(k)$. N_* corresponds to the number of e-folds from the end of inflation at which the considered scale crosses the horizon. Notice the linear dependence.

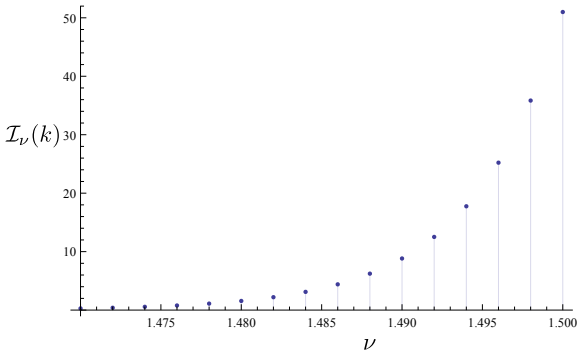

(b) Numerical evaluation of integral $\mathcal{I}_\nu(k)$ for $N_* = 50$. Notice the exponential suppression as ν departs from 3/2.

Figure D.1: Numerical evaluation of integral $\mathcal{I}(k)$ (D.14) and $\mathcal{I}_\nu(k)$ (D.15).

where the multiplicative factor has been chosen in order that $\mathcal{I}_\nu(k)$ has the same normalization as $\mathcal{I}(k)$ for $\nu = 3/2$. The integral $\mathcal{I}_\nu(k)$ is depicted in figure D.1b as a function of ν. Notice the suppression for small deviations of ν from 3/2. This behaviour can be explained via the asymptotic expansion (1.60).

Finally, let us come back to our original concern: computing the integral (7.115). Once the attractor solution is reached, the dynamics of different trajectories are nearly the same (the attractor solution is reached in a few e-folds, e.g. see figures 5.6b and 7.7b). In particular, raising the initial position $\varphi(0)$ increases the number of e-folds of inflation, but the integral (7.115) is practically not affected. Indeed, if we fix a scale that crosses the horizon N_* e-folds before the end of inflation, the additional e-folds are of subhorizon evolution and this has little importance in the final result. Hence, the value of f_{NL} has a tiny dependence on initial conditions as it can be shown through numerical calculations. Therefore, we will study only the dependence of f_{NL} on the scale considered. The final results are represented in figure (7.8a).

Appendix E

Additional plots

E.1 First model of chapter 8

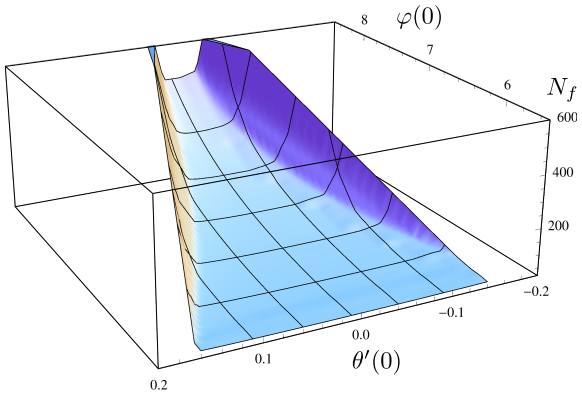

(a) Number of e-folds of inflation N_f for the initial conditions $\varphi'(0) = 0$ and $\theta(0) = 0.5$ with $m^2 = 1$.

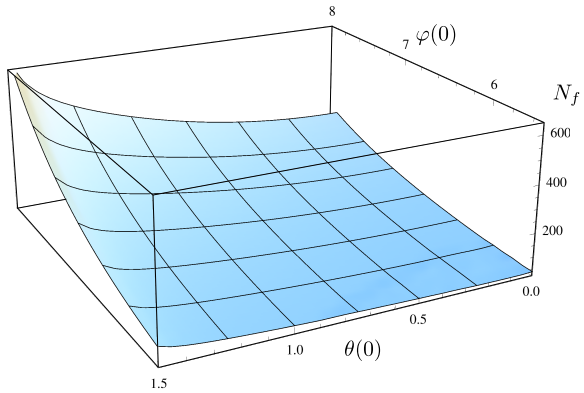

(b) Number of e-folds of inflation N_f for the initial conditions $\varphi'(0) = 0$ and $\theta'(0) = 0$ with $m^2 = 1$.

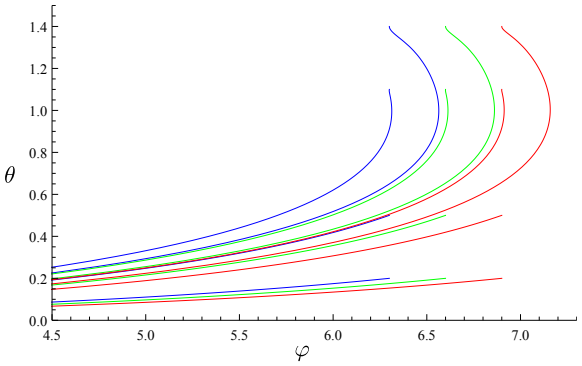

(c) Different trajectories for $m^2 = 1$, $\varphi'(0) = 0$ and $\theta'(0) = 0$. Blue trajectories start from $\varphi(0) = 6.3$, green ones from $\varphi(0) = 6.6$ and red ones from $\varphi(0) = 6.9$.

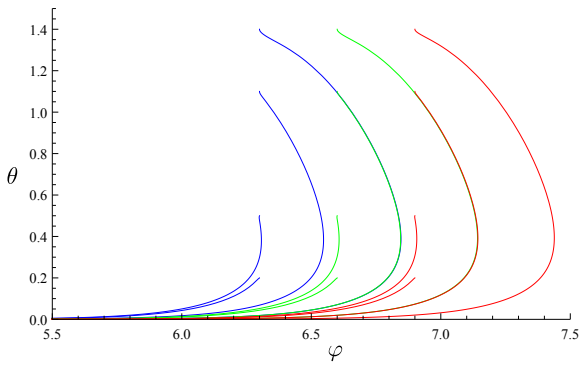

(d) Different trajectories for $m^2 = 10$, $\varphi'(0) = 0$ and $\theta'(0) = 0$. Blue trajectories start from $\varphi(0) = 6.3$, green ones from $\varphi(0) = 6.6$ and red ones from $\varphi(0) = 6.9$.

Figure E.1: Dynamics of the model (5.77) with potential $W^{(1)}(\varphi, \theta) = \tanh^2 \frac{\varphi}{\sqrt{6}} + m^2 \tan^2 \theta$ analysed in section 8.1.1. The conventions and notations used in these plots are the same as those of section 8.1.

E.2 Second model of chapter 8

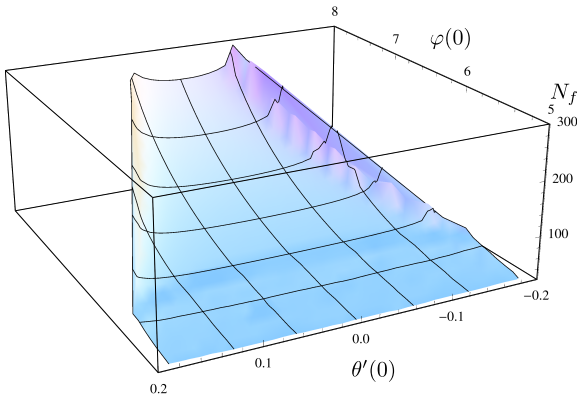

(a) Number of e-folds of inflation N_f for the initial conditions $\varphi'(0) = 0$ and $\theta(0) = 1$ with $M^2 = 1$.

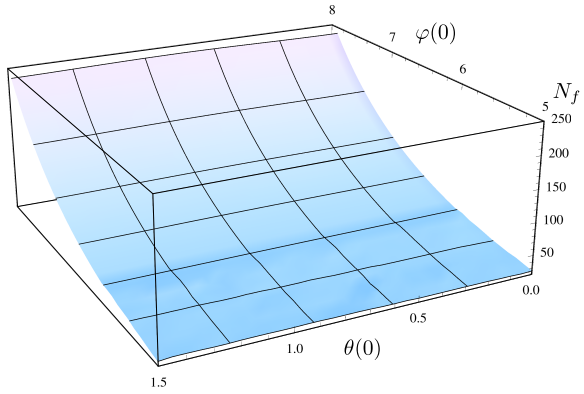

(b) Number of e-folds of inflation N_f for the initial conditions $\varphi'(0) = 0$ and $\theta'(0) = 0$ with $M^2 = 1$.

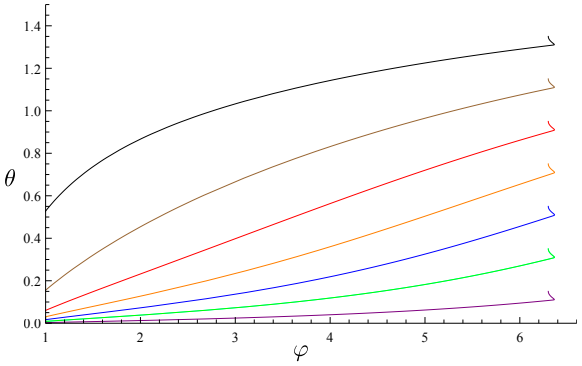

(c) Different trajectories for $\varphi(0) = 6.3$, $\varphi'(0) = 0$ and $\theta'(0) = -0.1$. For all trajectories inflation ends at $N_f \sim 65$.

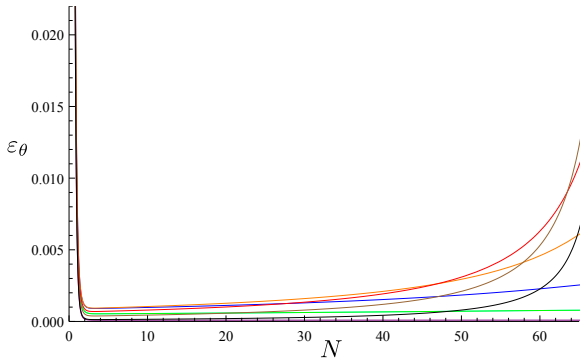

(d) ε_θ for $\varphi(0) = 6.3$, $\varphi'(0) = 0$ and $\theta'(0) = -0.1$. Notice the initial suppression of ε_θ and the attractor solution.

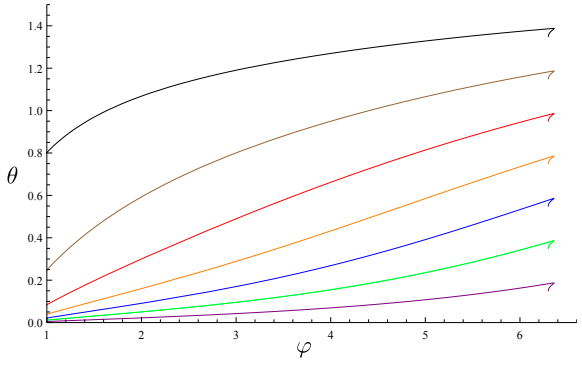

(e) Different trajectories for $\varphi(0) = 6.3$, $\varphi'(0) = 0$ and $\theta'(0) = 0.1$. For all trajectories inflation ends at $N_f \sim 65$.

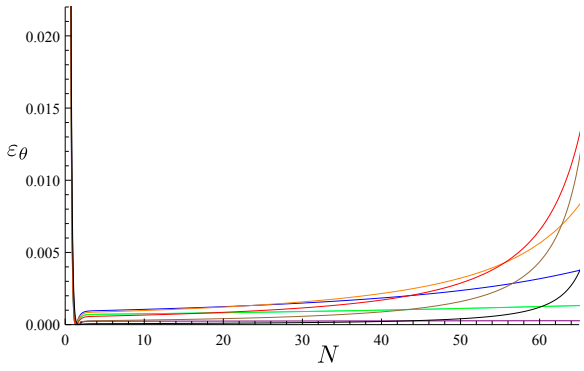

(f) ε_θ for $\varphi(0) = 6.3$, $\varphi'(0) = 0$ and $\theta'(0) = 0.1$. Notice the initial suppression of ε_θ and the attractor solution.

Figure E.2: Dynamics of the model (5.77) with potential $W^{(2)}(\varphi, \theta) = \left(1 + M^2 \sin^2\theta\right)\tanh^2 \frac{\varphi}{\sqrt{6}}$ analysed in section 8.1.2. Compare the pairs of plots E.2c-E.2d and E.2e-E.2f with 8.3c-8.3e.

Bibliography

[1] A. Liddle and D. Lyth, *Cosmological Inflation and Large-Scale Structure*. Cambridge University Press, 2000.

[2] E. W. Kolb and M. S. Turner, "The Early Universe", *Front. Phys.*, vol. 69, pp. 1–547, 1990.

[3] A. R. Liddle, "An Introduction to cosmological inflation", in *Proceedings, Summer School in High-energy physics and cosmology*, pp. 260–295, 1999.

[4] D. Langlois, "Lectures on inflation and cosmological perturbations", *Lect. Notes Phys.*, vol. 800, pp. 1–57, 2010.

[5] P. A. R. Ade *et al.*, "Planck 2015 results. XIII. Cosmological parameters", 2015.

[6] P. A. R. Ade *et al.*, "Planck 2015 results. XX. Constraints on inflation", 2015.

[7] A. H. Guth, "Inflationary universe: A possible solution to the horizon and flatness problems", *Phys. Rev. D*, vol. 23, pp. 347–356, Jan 1981.

[8] R. Brout, F. Englert, and E. Gunzig, "The Creation of the Universe as a Quantum Phenomenon", *Annals Phys.*, vol. 115, p. 78, 1978.

[9] A. A. Starobinsky, "A New Type of Isotropic Cosmological Models Without Singularity", *Phys. Lett.*, vol. B91, pp. 99–102, 1980.

[10] K. Sato, "First Order Phase Transition of a Vacuum and Expansion of the Universe", *Mon. Not. Roy. Astron. Soc.*, vol. 195, pp. 467–479, 1981.

[11] A. D. Linde, "A New Inflationary Universe Scenario: A Possible Solution of the Horizon, Flatness, Homogeneity, Isotropy and Primordial Monopole Problems", *Phys. Lett.*, vol. B108, pp. 389–393, 1982.

[12] A. Albrecht and P. J. Steinhardt, "Cosmology for Grand Unified Theories with Radiatively Induced Symmetry Breaking", *Phys. Rev. Lett.*, vol. 48, pp. 1220–1223, 1982.

[13] A. D. Linde, "Chaotic Inflation", *Phys. Lett.*, vol. B129, pp. 177–181, 1983.

[14] P. A. R. Ade *et al.*, "Joint Analysis of BICEP2/Keck Array and Planck Data", *Phys. Rev. Lett.*, vol. 114, p. 101301, 2015.

[15] A. Linde, "Inflationary Cosmology after Planck 2013", in *Proceedings, 100th Les Houches Summer School: Post-Planck Cosmology*, pp. 231–316, 2015.

[16] K. A. Malik and D. Wands, "Cosmological perturbations", *Phys. Rept.*, vol. 475, pp. 1–51, 2009.

[17] M. S. Turner, "Coherent scalar-field oscillations in an expanding universe", *Phys. Rev. D*, vol. 28, pp. 1243–1247, Sep 1983.

[18] J. H. Traschen and R. H. Brandenberger, "Particle Production During Out-of-equilibrium Phase Transitions", *Phys. Rev.*, vol. D42, pp. 2491–2504, 1990.

[19] Y. Shtanov, J. H. Traschen, and R. H. Brandenberger, "Universe reheating after inflation", *Phys. Rev.*, vol. D51, pp. 5438–5455, 1995.

[20] L. Kofman, A. D. Linde, and A. A. Starobinsky, "Towards the theory of reheating after inflation", *Phys. Rev.*, vol. D56, pp. 3258–3295, 1997.

[21] S. Dodelson, *Modern cosmology*. San Diego, CA: Academic Press, 2003.

[22] A. R. Liddle and S. M. Leach, "How long before the end of inflation were observable perturbations produced?", *Phys. Rev.*, vol. D68, p. 103503, 2003.

[23] E. R. Harrison, "Fluctuations at the threshold of classical cosmology", *Phys. Rev.*, vol. D1, pp. 2726–2730, 1970.

[24] Ya. B. Zeldovich, "A Hypothesis, unifying the structure and the entropy of the universe", *Mon. Not. Roy. Astron. Soc.*, vol. 160, pp. 1P–3P, 1972.

[25] L. Pilo, A. Riotto, and A. Zaffaroni, "On the amount of gravitational waves from inflation", *Phys. Rev. Lett.*, vol. 92, p. 201303, 2004.

[26] P. A. R. Ade *et al.*, "Improved Constraints on Cosmology and Foregrounds from BICEP2 and Keck Array Cosmic Microwave Background Data with Inclusion of 95 GHz Band", *Phys. Rev. Lett.*, vol. 116, p. 031302, 2016.

[27] S. Dodelson, W. H. Kinney, and E. W. Kolb, "Cosmic microwave background measurements can discriminate among inflation models", *Phys. Rev.*, vol. D56, pp. 3207–3215, 1997.

[28] F. Lucchin and S. Matarrese, "Power-law inflation", *Phys. Rev. D*, vol. 32, pp. 1316–1322, Sep 1985.

[29] A. Vilenkin, "Classical and Quantum Cosmology of the Starobinsky Inflationary Model", *Phys. Rev.*, vol. D32, p. 2511, 1985.

[30] J. Ellis, D. V. Nanopoulos, and K. A. Olive, "No-Scale Supergravity Realization of the Starobinsky Model of Inflation", *Phys. Rev. Lett.*, vol. 111, p. 111301, 2013. [Erratum: Phys. Rev. Lett.111,no.12,129902(2013)].

[31] F. Farakos, A. Kehagias, and A. Riotto, "On the Starobinsky Model of Inflation from Supergravity", *Nucl. Phys.*, vol. B876, pp. 187–200, 2013.

[32] S. Ferrara, R. Kallosh, and A. Van Proeyen, "On the Supersymmetric Completion of $R+R^2$ Gravity and Cosmology", *JHEP*, vol. 11, p. 134, 2013.

[33] R. Kallosh and A. Linde, "Superconformal generalization of the chaotic inflation model $\frac{\lambda}{4}\phi^4 - \frac{\xi}{2}\phi^2 R$", *JCAP*, vol. 1306, p. 027, 2013.

[34] B. Whitt, "Fourth Order Gravity as General Relativity Plus Matter", *Phys. Lett.*, vol. B145, pp. 176–178, 1984.

[35] V. F. Mukhanov, H. A. Feldman, and R. H. Brandenberger, "Theory of cosmological perturbations. Part 1. Classical perturbations. Part 2. Quantum theory of perturbations. Part 3. Extensions", *Phys. Rept.*, vol. 215, pp. 203–333, 1992.

[36] H. Kodama and M. Sasaki, "Cosmological Perturbation Theory", *Prog. Theor. Phys. Suppl.*, vol. 78, pp. 1–166, 1984.

[37] J. M. Bardeen, "Gauge-invariant cosmological perturbations", *Phys. Rev. D*, vol. 22, pp. 1882–1905, Oct 1980.

[38] M. Bruni, S. Matarrese, S. Mollerach, and S. Sonego, "Perturbations of space-time: Gauge transformations and gauge invariance at second order and beyond", *Class. Quant. Grav.*, vol. 14, pp. 2585–2606, 1997.

[39] E. D. Stewart and D. H. Lyth, "A More accurate analytic calculation of the spectrum of cosmological perturbations produced during inflation", *Phys. Lett.*, vol. B302, pp. 171–175, 1993.

[40] V. Acquaviva, N. Bartolo, S. Matarrese, and A. Riotto, "Second order cosmological perturbations from inflation", *Nucl. Phys.*, vol. B667, pp. 119–148, 2003.

[41] D. Langlois and S. Renaux-Petel, "Perturbations in generalized multi-field inflation", *JCAP*, vol. 0804, p. 017, 2008.

[42] D. Wands, "Multiple field inflation", *Lect. Notes Phys.*, vol. 738, pp. 275–304, 2008.

[43] K. A. Malik and D. Wands, "Adiabatic and entropy perturbations with interacting fluids and fields", *JCAP*, vol. 0502, p. 007, 2005.

[44] D. H. Lyth, C. Ungarelli, and D. Wands, "The Primordial density perturbation in the curvaton scenario", *Phys. Rev.*, vol. D67, p. 023503, 2003.

[45] Z. Lalak, D. Langlois, S. Pokorski, and K. Turzynski, "Curvature and isocurvature perturbations in two-field inflation", *JCAP*, vol. 0707, p. 014, 2007.

[46] J. M. Bardeen, "Gauge Invariant Cosmological Perturbations", *Phys. Rev.*, vol. D22, pp. 1882–1905, 1980.

[47] S. Weinberg, "Quantum contributions to cosmological correlations", *Phys. Rev.*, vol. D72, p. 043514, 2005.

[48] P. A. R. Ade *et al.*, "Planck 2015 results. XVII. Constraints on primordial non-Gaussianity", 2015.

[49] N. Bartolo, E. Komatsu, S. Matarrese, and A. Riotto, "Non-Gaussianity from inflation: Theory and observations", *Phys. Rept.*, vol. 402, pp. 103–266, 2004.

[50] X. Chen, "Primordial Non-Gaussianities from Inflation Models", *Adv. Astron.*, vol. 2010, p. 638979, 2010.

[51] M. E. Peskin and D. V. Schroeder, *An introduction to quantum field theory*. Advanced book program, Boulder (Colo.): Westview Press Reading (Mass.), 1995. Autre tirage : 1997.

[52] P. A. R. Ade *et al.*, "Planck 2013 Results. XXIV. Constraints on primordial non-Gaussianity", *Astron. Astrophys.*, vol. 571, p. A24, 2014.

[53] T. Falk, R. Rangarajan, and M. Srednicki, "The Angular dependence of the three point correlation function of the cosmic microwave background radiation as predicted by inflationary cosmologies", *Astrophys. J.*, vol. 403, p. L1, 1993.

[54] L. Verde, L.-M. Wang, A. Heavens, and M. Kamionkowski, "Large scale structure, the cosmic microwave background, and primordial non-gaussianity", *Mon. Not. Roy. Astron. Soc.*, vol. 313, pp. L141–L147, 2000.

[55] H. M. Hodges, G. R. Blumenthal, L. A. Kofman, and J. R. Primack, "Nonstandard Primordial Fluctuations From a Polynomial Inflaton Potential", *Nucl. Phys.*, vol. B335, pp. 197–220, 1990.

[56] D. S. Salopek and J. R. Bond, "Nonlinear evolution of long wavelength metric fluctuations in inflationary models", *Phys. Rev.*, vol. D42, pp. 3936–3962, 1990.

[57] J. S. Schwinger, "Brownian motion of a quantum oscillator", *J. Math. Phys.*, vol. 2, pp. 407–432, 1961.

[58] L. V. Keldysh, "Diagram technique for nonequilibrium processes", *Zh. Eksp. Teor. Fiz.*, vol. 47, pp. 1515–1527, 1964. [Sov. Phys. JETP20,1018(1965)].

[59] R. D. Jordan, "Effective Field Equations for Expectation Values", *Phys. Rev.*, vol. D33, pp. 444–454, 1986.

[60] M. Sasaki and E. D. Stewart, "A General analytic formula for the spectral index of the density perturbations produced during inflation", *Prog. Theor. Phys.*, vol. 95, pp. 71–78, 1996.

[61] D. H. Lyth, K. A. Malik, and M. Sasaki, "A General proof of the conservation of the curvature perturbation", *JCAP*, vol. 0505, p. 004, 2005.

[62] D. H. Lyth and Y. Rodriguez, "The Inflationary prediction for primordial non-Gaussianity", *Phys. Rev. Lett.*, vol. 95, p. 121302, 2005.

[63] D. Wands, K. A. Malik, D. H. Lyth, and A. R. Liddle, "A New approach to the evolution of cosmological perturbations on large scales", *Phys. Rev.*, vol. D62, p. 043527, 2000.

[64] A. Gangui and J. Martin, "Cosmic microwave background bispectrum and slow roll inflation", *Mon. Not. Roy. Astron. Soc.*, vol. 313, p. 323, 2000.

[65] M. Liguori, E. Sefusatti, J. R. Fergusson, and E. P. S. Shellard, "Primordial non-Gaussianity and Bispectrum Measurements in the Cosmic Microwave Background and Large-Scale Structure", *Adv. Astron.*, vol. 2010, p. 980523, 2010.

[66] J. M. Maldacena, "Non-Gaussian features of primordial fluctuations in single field inflationary models", *JHEP*, vol. 05, p. 013, 2003.

[67] X. Chen, M.-x. Huang, S. Kachru, and G. Shiu, "Observational signatures and non-Gaussianities of general single field inflation", *JCAP*, vol. 0701, p. 002, 2007.

[68] X. Chen, R. Easther, and E. A. Lim, "Large Non-Gaussianities in Single Field Inflation", *JCAP*, vol. 0706, p. 023, 2007.

[69] D. Langlois, S. Renaux-Petel, D. A. Steer, and T. Tanaka, "Primordial fluctuations and non-Gaussianities in multi-field DBI inflation", *Phys. Rev. Lett.*, vol. 101, p. 061301, 2008.

[70] D. Langlois, S. Renaux-Petel, D. A. Steer, and T. Tanaka, "Primordial perturbations and non-Gaussianities in DBI and general multi-field inflation", *Phys. Rev.*, vol. D78, p. 063523, 2008.

[71] F. Arroja, S. Mizuno, and K. Koyama, "Non-gaussianity from the bispectrum in general multiple field inflation", *JCAP*, vol. 0808, p. 015, 2008.

[72] N. Bartolo, S. Matarrese, and A. Riotto, "Nongaussianity from inflation", *Phys. Rev.*, vol. D65, p. 103505, 2002.

[73] F. Vernizzi and D. Wands, "Non-gaussianities in two-field inflation", *JCAP*, vol. 0605, p. 019, 2006.

[74] C. T. Byrnes, K.-Y. Choi, and L. M. H. Hall, "Conditions for large non-Gaussianity in two-field slow-roll inflation", *JCAP*, vol. 0810, p. 008, 2008.

[75] K.-Y. Choi, L. M. H. Hall, and C. van de Bruck, "Spectral Running and Non-Gaussianity from Slow-Roll Inflation in Generalised Two-Field Models", *JCAP*, vol. 0702, p. 029, 2007.

[76] G. I. Rigopoulos, E. P. S. Shellard, and B. J. W. van Tent, "Quantitative bispectra from multifield inflation", *Phys. Rev.*, vol. D76, p. 083512, 2007.

[77] S. Yokoyama, T. Suyama, and T. Tanaka, "Primordial Non-Gaussianity in Multi-Scalar Slow-Roll Inflation", *JCAP*, vol. 0707, p. 013, 2007.

[78] S. Yokoyama, T. Suyama, and T. Tanaka, "Primordial Non-Gaussianity in Multi-Scalar Inflation", *Phys. Rev.*, vol. D77, p. 083511, 2008.

[79] S. Mollerach, "Isocurvature Baryon Perturbations and Inflation", *Phys. Rev.*, vol. D42, pp. 313–325, 1990.

[80] A. D. Linde and V. F. Mukhanov, "Nongaussian isocurvature perturbations from inflation", *Phys. Rev.*, vol. D56, pp. R535–R539, 1997.

[81] D. H. Lyth and D. Wands, "Generating the curvature perturbation without an inflaton", *Phys. Lett.*, vol. B524, pp. 5–14, 2002.

[82] X. Chen and Y. Wang, "Quasi-Single Field Inflation and Non-Gaussianities", *JCAP*, vol. 1004, p. 027, 2010.

[83] D. Babich, P. Creminelli, and M. Zaldarriaga, "The Shape of non-Gaussianities", *JCAP*, vol. 0408, p. 009, 2004.

[84] L. Senatore, K. M. Smith, and M. Zaldarriaga, "Non-Gaussianities in Single Field Inflation and their Optimal Limits from the WMAP 5-year Data", *JCAP*, vol. 1001, p. 028, 2010.

[85] N. Barnaby and J. M. Cline, "Predictions for Nongaussianity from Nonlocal Inflation", *JCAP*, vol. 0806, p. 030, 2008.

[86] X. Chen, H. Firouzjahi, M. H. Namjoo, and M. Sasaki, "A Single Field Inflation Model with Large Local Non-Gaussianity", *Europhys. Lett.*, vol. 102, p. 59001, 2013.

[87] P. Creminelli and M. Zaldarriaga, "Single field consistency relation for the 3-point function", *JCAP*, vol. 0410, p. 006, 2004.

[88] J. Lahiri and G. Bhattacharya, "Perturbative analysis of multiple-field cosmological inflation", *Annals Phys.*, vol. 321, pp. 999–1023, 2006.

[89] C. M. Peterson and M. Tegmark, "Testing Two-Field Inflation", *Phys. Rev.*, vol. D83, p. 023522, 2011.

[90] C. M. Peterson and M. Tegmark, "Non-Gaussianity in Two-Field Inflation", *Phys. Rev.*, vol. D84, p. 023520, 2011.

[91] T. T. Nakamura and E. D. Stewart, "The Spectrum of cosmological perturbations produced by a multicomponent inflaton to second order in the slow roll approximation", *Phys. Lett.*, vol. B381, pp. 413–419, 1996.

[92] C. Gordon, D. Wands, B. A. Bassett, and R. Maartens, "Adiabatic and entropy perturbations from inflation", *Phys. Rev.*, vol. D63, p. 023506, 2001.

[93] D. Wands, N. Bartolo, S. Matarrese, and A. Riotto, "An Observational test of two-field inflation", *Phys. Rev.*, vol. D66, p. 043520, 2002.

[94] J. White, M. Minamitsuji, and M. Sasaki, "Non-linear curvature perturbation in multi-field inflation models with non-minimal coupling", *JCAP*, vol. 1309, p. 015, 2013.

[95] C. van de Bruck and M. Robinson, "Power Spectra beyond the Slow Roll Approximation in Theories with Non-Canonical Kinetic Terms", *JCAP*, vol. 1408, p. 024, 2014.

[96] D. Seery and J. E. Lidsey, "Primordial non-Gaussianities from multiple-field inflation", *JCAP*, vol. 0509, p. 011, 2005.

[97] I. Zaballa, Y. Rodriguez, and D. H. Lyth, "Higher order contributions to the primordial non-Gaussianity", *JCAP*, vol. 0606, p. 013, 2006.

[98] J. Elliston, D. Seery, and R. Tavakol, "The inflationary bispectrum with curved field-space", *JCAP*, vol. 1211, p. 060, 2012.

[99] M. Sasaki and T. Tanaka, "Superhorizon scale dynamics of multiscalar inflation", *Prog. Theor. Phys.*, vol. 99, pp. 763–782, 1998.

[100] R. Kallosh and A. Linde, "Superconformal generalizations of the Starobinsky model", *JCAP*, vol. 1306, p. 028, 2013.

[101] R. Kallosh and A. Linde, "Universality Class in Conformal Inflation", *JCAP*, vol. 1307, p. 002, 2013.

[102] R. Kallosh and A. Linde, "Multi-field Conformal Cosmological Attractors", *JCAP*, vol. 1312, p. 006, 2013.

[103] S. Ferrara, R. Kallosh, A. Linde, and M. Porrati, "Minimal Supergravity Models of Inflation", *Phys. Rev.*, vol. D88, no. 8, p. 085038, 2013.

[104] J. Ellis, D. V. Nanopoulos, and K. A. Olive, "Starobinsky-like Inflationary Models as Avatars of No-Scale Supergravity", *JCAP*, vol. 1310, p. 009, 2013.

[105] M. Yamaguchi, "Supergravity based inflation models: a review", *Class. Quant. Grav.*, vol. 28, p. 103001, 2011.

[106] G. Dall'Agata and F. Zwirner, "On sgoldstino-less supergravity models of inflation", *JHEP*, vol. 12, p. 172, 2014.

[107] A. Ceresole, G. Dall'Agata, S. Ferrara, M. Trigiante, and A. Van Proeyen, "A search for an $\mathcal{N} = 2$ inflaton potential", *Fortsch. Phys.*, vol. 62, pp. 584–606, 2014.

[108] A. Sagnotti and S. Ferrara, "Supersymmetry and Inflation", *PoS*, vol. PLANCK2015, p. 113, 2015.

[109] P. A. R. Ade *et al.*, "Planck 2013 results. XXII. Constraints on inflation", *Astron. Astrophys.*, vol. 571, p. A22, 2014.

[110] C. L. Bennett, D. Larson, J. L. Weiland, N. Jarosik, G. Hinshaw, N. Odegard, K. M. Smith, R. S. Hill, B. Gold, M. Halpern, E. Komatsu, M. R. Nolta, L. Page, D. N. Spergel, E. Wollack, J. Dunkley, A. Kogut, M. Limon, S. S. Meyer, G. S. Tucker, and E. L. Wright, "Nine-year wilkinson microwave anisotropy probe (wmap) observations: Final maps and results", *The Astrophysical Journal Supplement Series*, vol. 208, no. 2, p. 20, 2013.

[111] F. L. Bezrukov and M. Shaposhnikov, "The Standard Model Higgs boson as the inflaton", *Phys. Lett.*, vol. B659, pp. 703–706, 2008.

[112] R. Kallosh, A. Linde, and D. Roest, "Superconformal Inflationary α-Attractors", *JHEP*, vol. 11, p. 198, 2013.

[113] R. Kallosh, A. Linde, and D. Roest, "Universal Attractor for Inflation at Strong Coupling", *Phys. Rev. Lett.*, vol. 112, no. 1, p. 011303, 2014.

[114] G. F. Giudice and H. M. Lee, "Starobinsky-like inflation from induced gravity", *Phys. Lett.*, vol. B733, pp. 58–62, 2014.

[115] C. Pallis, "Linking Starobinsky-Type Inflation in no-Scale Supergravity to MSSM", *JCAP*, vol. 1404, p. 024, 2014.

[116] R. Kallosh, A. Linde, and D. Roest, "Large field inflation and double α-attractors", *JHEP*, vol. 08, p. 052, 2014.

[117] R. Kallosh, A. Linde, and D. Roest, "The double attractor behavior of induced inflation", *JHEP*, vol. 09, p. 062, 2014.

[118] B. Mosk and J. P. van der Schaar, "Chaotic inflation limits for non-minimal models with a Starobinsky attractor", *JCAP*, vol. 1412, no. 12, p. 022, 2014.

[119] M. Dias, J. Frazer, and D. Seery, "Computing observables in curved multifield models of inflation—A guide (with code) to the transport method", *JCAP*, vol. 1512, no. 12, p. 030, 2015.

[120] A. A. Starobinsky, "The Perturbation Spectrum Evolving from a Nonsingular Initially De-Sitter Cosmology and the Microwave Background Anisotropy", *Sov. Astron. Lett.*, vol. 9, p. 302, 1983.

[121] L. A. Kofman, A. D. Linde, and A. A. Starobinsky, "Inflationary Universe Generated by the Combined Action of a Scalar Field and Gravitational Vacuum Polarization", *Phys. Lett.*, vol. B157, pp. 361–367, 1985.

[122] D. S. Salopek, J. R. Bond, and J. M. Bardeen, "Designing Density Fluctuation Spectra in Inflation", *Phys. Rev.*, vol. D40, p. 1753, 1989.

[123] T. Terada, "Generalized Pole Inflation: Hilltop, Natural, and Chaotic Inflationary Attractors", 2016.

[124] M. Galante, R. Kallosh, A. Linde, and D. Roest, "Unity of Cosmological Inflation Attractors", *Phys. Rev. Lett.*, vol. 114, no. 14, p. 141302, 2015.

[125] B. J. Broy, M. Galante, D. Roest, and A. Westphal, "Pole inflation — Shift symmetry and universal corrections", *JHEP*, vol. 12, p. 149, 2015.

[126] N. Bartolo, S. Matarrese, and A. Riotto, "Oscillations during inflation and cosmological density perturbations", *Phys. Rev.*, vol. D64, p. 083514, 2001.

[127] K. Freese, J. A. Frieman, and A. V. Olinto, "Natural inflation with pseudo - Nambu-Goldstone bosons", *Phys. Rev. Lett.*, vol. 65, pp. 3233–3236, 1990.

[128] F. C. Adams, J. R. Bond, K. Freese, J. A. Frieman, and A. V. Olinto, "Natural inflation: Particle physics models, power law spectra for large scale structure, and constraints from COBE", *Phys. Rev.*, vol. D47, pp. 426–455, 1993.

[129] V. Faraoni, E. Gunzig, and P. Nardone, "Conformal transformations in classical gravitational theories and in cosmology", *Fund. Cosmic Phys.*, vol. 20, p. 121, 1999.

[130] R. Catena, M. Pietroni, and L. Scarabello, "Local transformations of units in scalar-tensor cosmology", *J. Phys.*, vol. A40, pp. 6883–6888, 2007.

[131] V. Faraoni and E. Gunzig, "Einstein frame or Jordan frame?", *Int. J. Theor. Phys.*, vol. 38, pp. 217–225, 1999.

[132] G. Magnano and L. M. Sokolowski, "On physical equivalence between nonlinear gravity theories and a general relativistic selfgravitating scalar field", *Phys. Rev.*, vol. D50, pp. 5039–5059, 1994.

[133] S. Capozziello and M. De Laurentis, "Extended Theories of Gravity", *Phys. Rept.*, vol. 509, pp. 167–321, 2011.

[134] F. Bernardeau, T. Brunier, and J.-P. Uzan, "High order correlation functions for self interacting scalar field in de Sitter space", *Phys. Rev.*, vol. D69, p. 063520, 2004.